

AD-A066 193

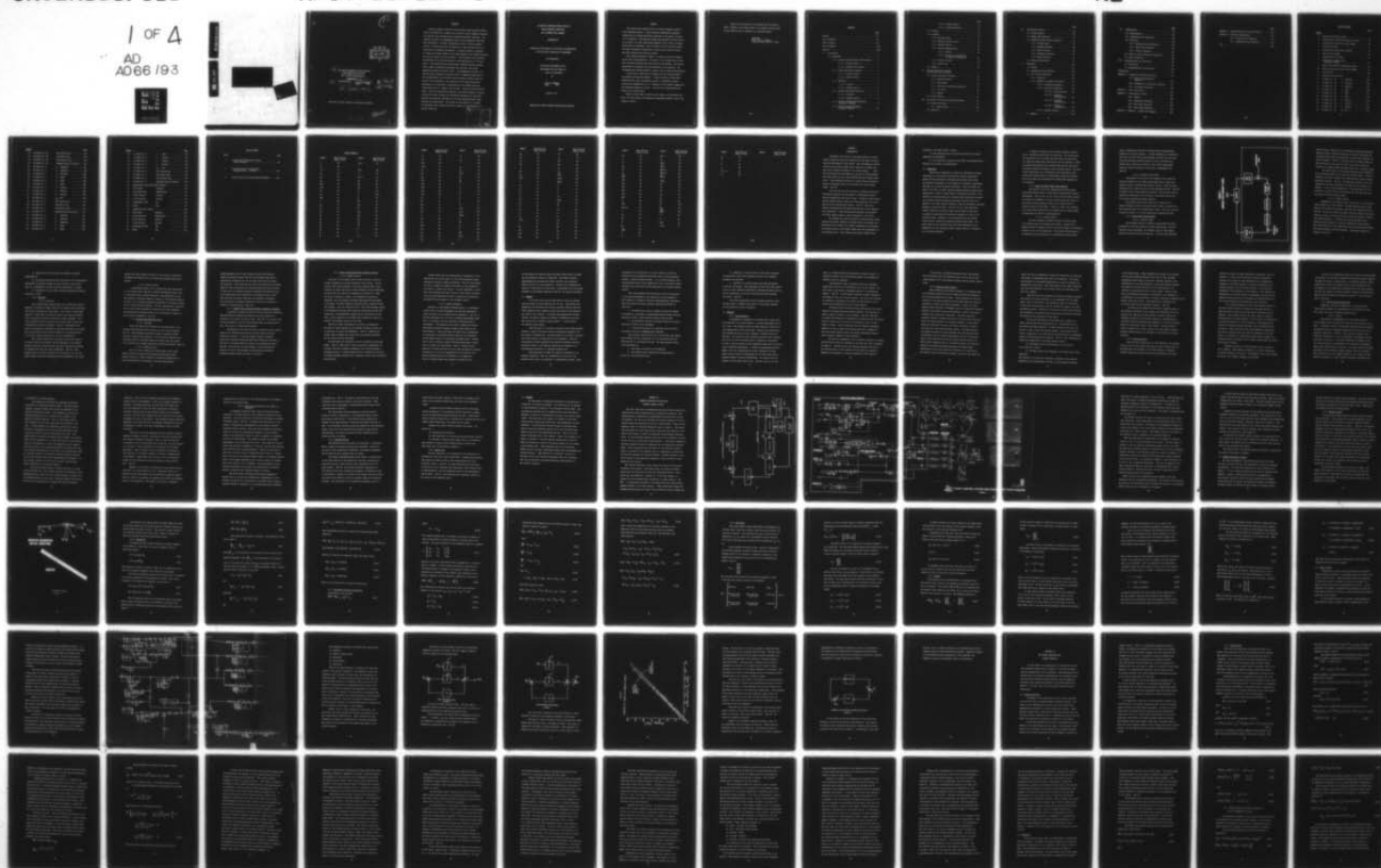
AIR FORCE INST OF TECH WRIGHT-PATTERSON AFB OHIO SCH--ETC F/G 1/3
AN ADAPTIVE CONTROLLER WHICH DISPLAYS HUMAN OPERATOR LIMITATION--ETC(U)
NOV 78 E K LINDBERG
AFIT/DS/EE/78-1

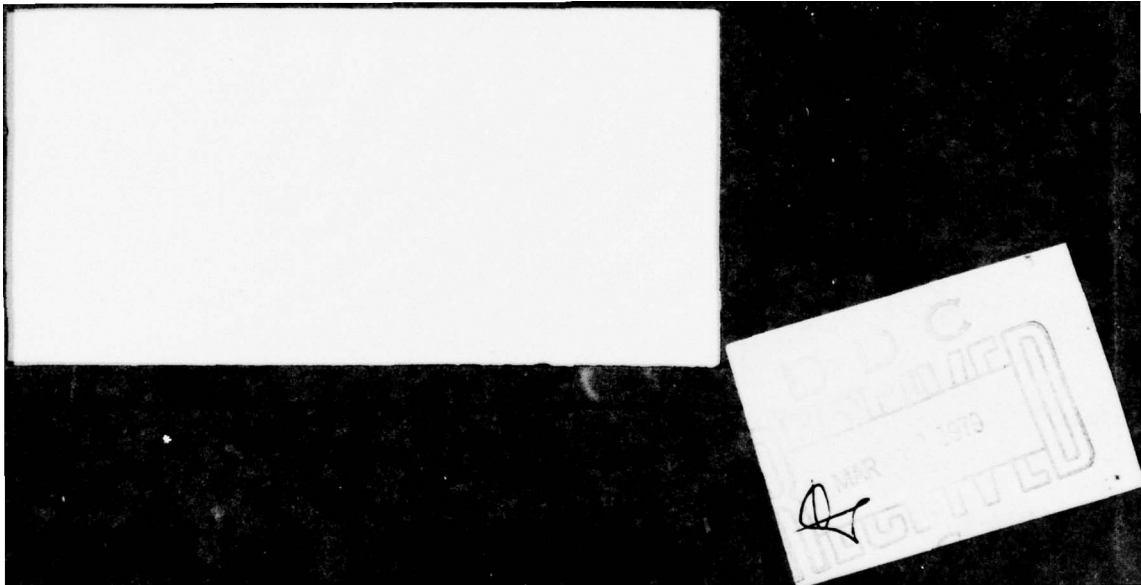
UNCLASSIFIED

NL

1 OF 4

AD
A066 193





1

DDC
RECEIVED
MAR 22 1979
C

6

AN ADAPTIVE CONTROLLER WHICH DISPLAYS
HUMAN OPERATOR LIMITATIONS
FOR A FIGHTER TYPE AIRCRAFT.

DISSERTATION

10

14

AFIT/DS/EE/78-1

Eric K. Lindberg
Major USAF

11

Nov-78

12

305p.

9

Doctoral thesis,

Approved for public release; distribution unlimited.

012225

79 03 19 022

B

Abstract

3	1. Position <input checked="" type="checkbox"/>	DISTRICT HEADQUARTERS DISTRICT OFFICE DISTRICT HEADQUARTERS DISTRICT OFFICE	SPECIAL SPECIAL
4	2. Position <input type="checkbox"/>		
5	3. Position <input type="checkbox"/>		
6	4. Position <input type="checkbox"/>		

**AN ADAPTIVE CONTROLLER WHICH DISPLAYS
HUMAN OPERATOR LIMITATIONS
FOR A FIGHTER TYPE AIRCRAFT**

DISSERTATION

**Presented to the Faculty of the School of Engineering
of the Air Force Institute of Technology**

Air University

**in Partial Fulfillment of the
Requirements for the Degree of
Doctor of Philosophy**

by

**Eric K. Lindberg
Major USAF**

November 1978

Approved for public release; distribution unlimited

Preface

The present pilot modeling effort is heavily weighted toward an axis decoupling approach. This decoupling considerably simplifies computation by allowing significant reduction in the number of states to be considered. Unfortunately during many maneuvers in state-of-the-art aircraft, the state decoupling assumption is not valid, so another method must be considered. Also the advent of the fly-by-wire system has added considerable flexibility to aircraft which cannot be mathematically predicted from present systems.

This research developed a method to address the pilots response during these varied maneuvers. The intent of the research was to show that the method developed was both useful and practicable. The results demonstrated the usability and practicability of the approach. The recommendations indicate methods to improve each of these characteristics.

I would like to thank Peter S. Maybeck for the continued support and guidance through the research. I would also like to thank Major Thomas Moriarty, Capt John MacBain, and Mr. F. Barfield for their interest and suggestions, Mr. R. O. Anderson for his helpful suggestions and background additions, and Ms. J. Wood for her interpretation and typing of the dissertation.

Finally I would like to thank my wife, Claire, and sons Kenny and Hans, for their support and frequent and sometimes untimely trips to the computer facility.

Copies of the program can be requested from the address below. Release of the digital model of the fighter aircraft used in this research will be handled on an individual basis.

AFFDL/FXM
Major Eric K. Lindberg
Wright-Patterson AFB, OH 45433

Contents

	Page
Preface	ii
List of Figures	ix
List of Tables	xii
List of Symbols	xiii
Abstract	xviii
I. Introduction	1
1.1 Background	2
1.1.1 Linear and Quasi-Linear Time-Invariant. . .	3
1.1.1.1 Crossover Model.	3
1.1.1.2 Optimal Control Model.	4
1.1.2 Linear Time-Varying Systems	4
1.1.2.1 Crossover Model.	4
1.1.2.2 Optimal Control.	6
1.1.3 Nonlinear	7
1.1.3.1 Crossover	7
1.1.3.2 Optimal Control.	8
1.1.4 Multiple-Input/Multiple-Output.	8
1.1.4.1 Crossover	8
1.1.4.2 Optimal Control.	8
1.1.5 Systems Involving Non-Stationary Stochastic Processes	9
1.1.6 Optimal Estimation/Optimal Stochastic Control.	10

	Page
1.1.6.1 Optimal Control	10
1.1.6.2 Optimal Estimation	11
1.2 Problem.	12
1.3 Approach	14
1.3.1 Decision Theory	14
1.3.2 Nonlinear System Control.	16
1.3.3 Decision Process	18
1.3.4 Decision Implementation.	20
1.3.4.1 Control.	20
1.3.4.2 Restricted Attention and Its Impact on Estimation	23
1.3.5 Decision Process.	24
1.3.6 Control Lag	25
1.4 Summary.	26
II. Aircraft Equations of Motion and Aircraft Control System	27
2.1 Aircraft Equations of Motion	31
2.1.1 Reference System.	32
2.1.2 Derivations	33
2.1.3 Rotational Acceleration Equations	36
2.1.4 The Forces.	40
2.1.5 Moments	42
2.2 Control System	46
III. The Optimal Controller and Optimal Estimator.	56
3.1 Optimal Controller	56
3.1.1 Control Gains	58
3.2 Estimation	70

	Page
IV. The Decision Process	81
4.1 Decision Theory	83
4.2 Higher Order Decisions	84
4.3 Bayesian Decision Function Approach	87
4.3.1 Decision Space	87
4.3.2 Possible Decisions	88
4.3.3 Payoff Function.	88
4.3.4 Probability Function	90
4.3.5 Payoff Functions	91
4.4 Decision Realizations	92
V. Simulation	105
5.1 General	105
5.2 Longitudinal Axis Simulation	105
5.3 Full Aircraft Simulation	109
5.3.1 Trajectory	110
5.3.2 Analysis of Parameter Variations	113
5.3.2.1 Estimation Parameters	114
5.3.2.2 Controller Parameters	116
5.3.2.2.1 General Results.	116
5.3.2.2.2 R_2 Matrix Determination	119
5.3.2.2.3 R_3 Matrix Determination	122
5.3.2.2.4 P_1 Matrix Determination	123
5.3.2.3 Decision Process.	124
5.4 Summary	125

	Page
VI. Demonstration	127
6.1 Implementation	127
6.2 Longitudinal Axis Simulation	130
6.3 Validation	137
6.3.1 Decision Process Validation	140
6.3.2 Error State Validation	143
6.3.3 Control Validation	149
6.4 Angle of Attack Information Degradation	150
6.5 Model Flexibility	152
VII. Recommendations and Conclusions.	162
7.1 Conclusions	162
7.2 Recommendations and Extensions.	166
Bibliography	171
Appendix 1: Computation Methodology Outline.	177
A1.1 State Transition Matrix Generator	179
A1.2 Propagation of the Riccati Equation.	181
A1.3 The System Computation	182
Appendix 2: Error State Plots.	185
Appendix 3: Linearization Process.	229
A3.1 General.	229
A3.2 Aerodynamics Equations	231
A3.3 Euler Angle Equations.	238
A3.4 Total System Equations	239
Appendix 4: Example: P_1 Matrix Not Diagonal	248

	Page
Appendix 5: Longitudinal Axis Simulation Results	252
Appendix 6: Parameter Specification	265
A6.1 Total Aircraft Simulation	265
A6.2 Longitudinal Axis Simulation	274
Vita	280

List of Figures

<u>Figure</u>		Page
1	General Pilot/Aircraft Model	5
2	Pilot/Aircraft System With Decision Process	28
3	Flight Control Functional Block Diagram	29
4	Coordinate Systems	33
5	Flight Control System Block Diagram	48
6	Rate Gyro Error Model	50
7	Accelerometer Error Model	51
8	Comparison of α Sensor with Inertially Sensed α	52
9	General Pilot/Aircraft System with Noises	54
10	Decision Process Functional Block Diagram	82
11	Decision Tree	88
12	Probability Determination	95
13	35 Alpha S.D. .09 P (Rad/sec)	187
14	36 Alpha S.D. .09 Q (Rad/sec)	188
15	37 Alpha S.D. .09 R (Rad/sec)	189
16	38 Alpha S.D. .09 ϕ (Rad)	190
17	39 Alpha S.D. .09 θ (Rad)	191
18	40 Alpha S.D. .09 ψ (Rad)	192
19	41 Alpha S.D. .09 U (Ft/sec)	193
20	42 Alpha S.D. .09 V (Ft/sec)	194
21	43 Alpha S.D. .09 W (Ft/sec)	195
22	46 Alpha S.D. .09 S_z (Ft).	196

<u>Figure</u>			<u>Page</u>
23	U1 Alpha S.D. .09	Roll Control LB_F	197
24	U2 Alpha S.D. .09	Yaw Control LB_F	198
25	U3 Alpha S.D. .09	Pitch Control LB_F	199
26	U4 Alpha S.D. .09	Airspeed Control LB Thrust. . .	200
27	35 Alpha S.D. 1.	P (Rad/sec)	201
28	36 Alpha S.D. 1.	Q (Rad/sec)	202
29	37 Alpha S.D. 1.	R (Rad/sec)	203
30	38 Alpha S.D. 1.	ϕ (Rad)	204
31	39 Alpha S.D. 1.	θ (Rad)	205
32	40 Alpha S.D. 1.	ψ (Rad)	206
33	41 Alpha S.D. 1.	U (Ft/sec)	207
34	42 Alpha S.D. 1.	V (Ft/sec)	208
35	43 Alpha S.D. 1.	W (Ft/sec)	209
36	46 Alpha S.D. 1.	S_Z (Ft)	210
37	U1 Alpha S.D. 1.	Roll Control LB_F	211
38	U2 Alpha S.D. 1.	Yaw Control LB_F	212
39	U3 Alpha S.D. 1.	Pitch Control LB_F	213
40	U4 Alpha S.D. 1.	Airspeed Control LB Thrust. . .	214
41	35 Alpha S.D. 3.	P (Rad/sec)	215
42	36 Alpha S.D. 3.	Q (Rad/sec)	216
43	37 Alpha S.D. 3.	R (Rad/sec)	217
44	38 Alpha S.D. 3.	ϕ (Rad)	218
45	39 Alpha S.D. 3.	θ (Rad)	219

<u>Figure</u>				Page
46	40 Alpha S.D. 3.	ψ	(Rad)	220
47	41 Alpha S.D. 3.	U	(Ft/sec)	221
48	42 Alpha S.D. 3.	V	(Ft/sec)	222
49	43 Alpha S.D. 3.	W	(Ft/sec)	223
50	46 Alpha S.D. 3.	S_Z	(Ft)	224
51	U1 Alpha S.D. 3.	Roll Control LB_F	225
52	U2 Alpha S.D. 3.	Yaw Control LB_F	226
53	U3 Alpha S.D. 3.	Pitch Control LB_F	227
54	U4 Alpha S.D. 3.	Airspeed Control LB Thrust.	228
55	Longitudinal Axis System Block Diagram		251
56	Pitch Angle	(Radians)	252
57	Pitch Angle Rate	(Radians/sec)	253
58	X Axis Velocity	(Ft/sec)	254
59	Y Axis Velocity	(Ft/sec)	255
60	Longitudinal Stick	LB_F	256
61	Thrust	LB_F	257
62	Applied Decision Channel		258
63	Pitch Angle	(Radians)	259
64	Pitch Angle Rate	(Radians/sec)	260
65	X Axis Velocity	(Ft/sec)	261
66	Y Axis Velocity	(Ft/sec)	262
67	Longitudinal Stick	LB_F	263
68	Thrust	LB_F	264

List of Tables

Table		Page
1	Initial Payoff Function for Lying Within Threshold	99
2	Payoff Function for Lying Within Threshold After .5 Seconds.	101
3	Payoff Function for Lying Outside Threshold	102

List of Symbols

Symbol	Page First Defined or Used	Symbol	Page First Defined or Used
A	89	C(t)	71
a.	89		
\dot{A}	77	D(t)	58
A _L	79	d	72
A _n	79	E (•)	72
A _N	48	E _X	40
AOA	48	E _Y	40
A(t)	58	E _Z	40
AY	48	F	59
_B	35	\bar{f}	229
B(t)	58	\bar{F}	34
C	40	$\Delta\bar{F}$	34
C _D	42	FI3	48
C _l	43	\bar{F}_O	34
C _L	42	F _{ox}	36
C _m	43	F _{oy}	36
C _n	43	F _{oz}	36
C _y	42	F _x	36
F _y	36	\dot{H}	74
\bar{F}_y	36	\bar{H}	34
g	40	I	37
\bar{g}	40	I..	37

Symbol	Page First Defined or Used	Symbol	Page First Defined or Used
I_G	35	I_I	34
GC	48	i_B	36
GI3	48	J	58
$G(t)$	71	$J_{..}$	37
G_x	40	\bar{j}_B	36
G_y	40	$K(t)$	72
G_z	40	K_A	48
G22	48	\bar{k}_B	36
G23	48	L	42
G30	48	$L_.$	91
G51	48	L_S	43
G52	48	m	34
$H_.$	37	M	42
\bar{M}	34	P	35
$\Delta\bar{M}$	34	$\cdot P$	77
\bar{M}_O	34	$p(t)$	59
M_5	43	$p(\cdot)$	90
N	42	PITCA	48
N4	48	$P_.$	74
N5	48	PR	48
N13	48	P_1	58
N_5	43	Q	35
N_1	50	QCI	48
N_2	50	$Q(t)$	72
N_3	51	R	35

Symbol	Page First Defined or Used	Symbol	Page First Defined or Used
N_4	51	R^+	90
N_5	51	\dot{R}	77
N_7	54	RC	48
N_8	54	RR	48
\dot{O}	34	R_1	59
R_2	58	u_{1j}	89
R_3	58	$\bar{U}(t)$	58
$R(t)$	72	$\bar{U}_o(t)$	28
S	41	$\delta\bar{u}(t)$	28
S_x	45	V	35
S_y	45	\bar{V}	34
S_z	45	\bar{v}	71
\dot{T}	45	V_T	41
\bar{T}_B	43	V_{TAS}	60
T_x	42	V_W	33
T_y	42	\dot{V}	77
T_z	42	δV	61
t_f	58	W	35
t_o	58	\bar{w}	71
$u^o(t)$	59	$W6$	48
U	35	$W7$	48
δU	61	$W8$	48
$W11$	48	x_2	50
$W12$	48	x_3	51
$W13$	48	x_4	51

Symbol	Page First Defined or Used	Symbol	Page First Defined or Used
δW	61	$\bar{x}(t)$	28
X	33	\bar{x}_0	58
X^\bullet	48	$\bar{x}_0(t)$	28
X_B	33	$\bar{\delta x}(t)$	28
X_G	33	$\bar{\delta x}(t-\tau)$	28
X_S	33	$\hat{\bar{\delta x}}(t-\tau)$	28
$XN8$	48	$\hat{\bar{\delta x}}(t)$	28
$XP2$	48	Y_{AWR}	48
$XP3$	48	Y_B	33
$X3P$	48	Y_G	33
$X3Q$	48	Y_S	33
$X4E$	48	Z_B	33
$X8E$	48	Z_G	33
x_1	50	Z_S	33
$\bar{z}(t)$	58	\bar{W}	229
$\bar{\delta}_z(t-\tau)$	29	\bar{W}_{GB}	35
α	33	$\frac{\partial(\cdot)}{\partial(\cdot)}$	230
α_N	50	\cdot_0	58
α_0	48	(\cdot)	35
β	61	d/dt	34
β_n	51	$\cdot(t^+)$	73
δ_{LEF}	48		
θ	40		
θ_\bullet	87		

Symbol	Page First Defined or Used
ξ_1	72
ρ	41
Σ	34
ϕ	40
$\Phi (\cdot, \cdot)$	73
ψ	40

Symbol	Page First Defined or Used
--------	----------------------------

CHAPTER I

INTRODUCTION

Knowledge of the effect of the human operator in a man/machine system has long been recognized as a key aspect in evaluating the performance of that system. When considering the pilot/aircraft system, Wilbur Wright said, "Inability to balance and steer still confronts students of the flying problem. . . . When this one feature has been worked out, the age of flying machines will have arrived, for all other difficulties are of minor importance." This statement was given in a speech before the Western Society of Engineers about two years before the first powered flight. (Ref 53)

Until the 1940's, when the theory of feedback control had sufficiently evolved, the only means for evaluating the pilot/aircraft compatibility was actual flight. During the 1940's Tustin applied feedback control theory with some extensions to the pilot portion of the pilot/aircraft system. (Ref 53) Since then, numerous investigations have added sophistication to his original pilot description. This sophistication generally has broadened the flight regime capable of being considered by this theory.

By combining the previous research in pilot/aircraft system analysis with recent advances in decision theory and optimal estimation and control theory, the research presented in this dissertation opens portions of the flight regime that were inaccessible to the existing theory. This research specifically reaches those

portions of the flight regime in which:

- 1) The nonlinearities in the motion equations and control equations are significant.

- 2) The stochastic processes in the model that mathematically describe the aircraft are nonstationary.

1.1 BACKGROUND

Since Tustin formulated the theory for addressing the human operating on a quasi-linear time-invariant system, considerable effort has been dedicated to extending and refining this theory. An excellent bibliography of this research is included in Agardograph 188 (Ref 53), written by McRuer and Krendel. Until the 1960's the bulk of the effort in human operator modeling addressed single-input/single-output, linear or quasi-linear, time-invariant systems. This research is characterized by the crossover model identified by McRuer. In the 1960's optimal estimation and optimal control theory were applied to the human operator problem by numerous individuals including Kleinman, Levison and Baron. (Ref 38, 39, 47) This application closely followed the crossover model and was shown in many cases to produce a human operator description comparable to that of the crossover model. Subsequent to the introduction of the optimal control model, research has continued along parallel paths. The path chosen by each researcher has often been determined by the adaptability of the particular model, optimal control or crossover, to the problem addressed.

To amplify the goals of this research, previous research can be conveniently partitioned by system type. The system types are categorized into (1) linear and quasi-linear time-invariant, (2) linear and quasi-linear time-varying, and (3) nonlinear. These are single-input/single-output systems admitting only wide-sense stationary stochastic processes, unless otherwise stated. Two additional subdivisions can be considered, multi-input/multi-output systems and systems driven by nonstationary stochastic processes, and in fact these are specifically the subdivisions addressed in this research.

1.1.1 Linear and Quasi-Linear Time-Invariant

The majority of the work completed has involved single-input/single-output linear or quasi-linear time-invariant aircraft descriptions. (Ref 38, 39, 47, 53) This is true to such an extent that McRuer has commented, "For most practical concerns related to pilot/vehicle system analysis, there are no further critical research issues for this model." (Ref 53, p. 865) For clarification, quasi-linear systems refer to systems that use linear models to approximate the effects of nonlinearities.

1.1.1.1 Crossover Model

The above statement by McRuer referred to efforts using the crossover model in the single loop context. Another way to summarize McRuer's comments is that the crossover model is an effective predictive tool in this application. The crossover model refers to an empirically derived procedure for determining the pilot model,

given a compensatory task and a transfer function representation assumed for the plant dynamics. It takes advantage of the empirical fact that the pilot will provide dynamics that will force the open loop pilot/aircraft transfer function to have a 20 decibel per decade slope at Bode plot crossover, and a stable phase margin.

Again, an excellent reference of this work is Agardograph 188.

(Ref 53)

1.1.1.2 Optimal Control Model

The majority of the work in the optimal control model has also been directed at the single-input/single-output linear time-invariant system, yielding some pertinent results. These have been obtained both in fixed wing and in rotary wing applications. (Ref 39)

In optimal control human operator literature, care has been taken to display the equivalence of the results of the optimal control and the crossover approaches whenever possible.

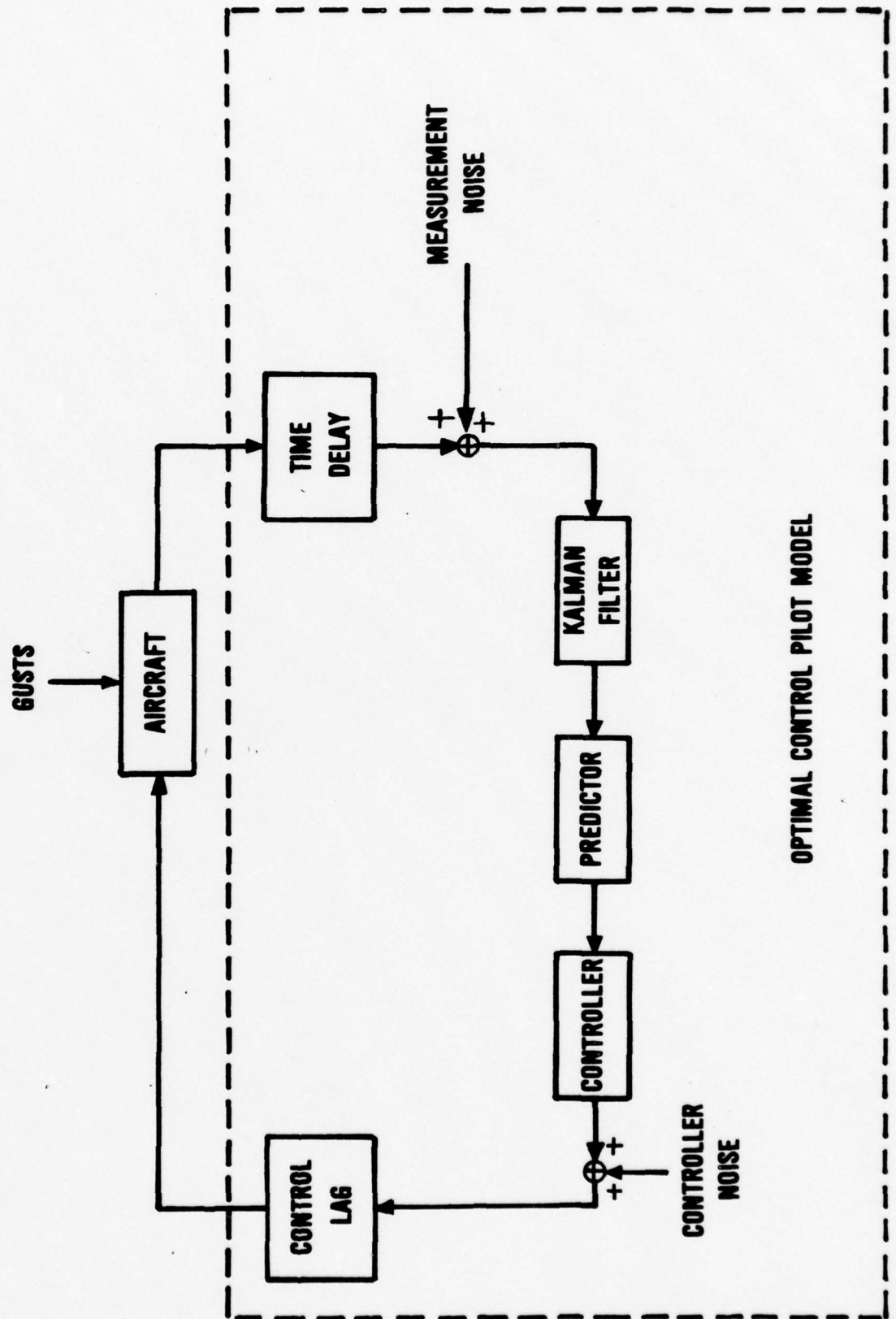
The optimal control pilot model uses a combination of optimal estimation theory and optimal control theory to replace the pilot mathematically in the man/aircraft system. The basic structure is given by Figure 1; it is well amplified by Kleinman (Ref 39).

1.1.2 Linear Time-Varying Systems

1.1.2.1 Crossover Model

The available research is severely limited when the system controlled by the human operator is linear time-varying. From the crossover model methodology, two different types of time-varying system descriptions have been researched. The first type addressed

FIGURE 1
GENERAL PILOT/AIRCRAFT MODEL



was the class of systems that instantaneously changed descriptions. Elkind and Miller considered this type of system by switching the controlled system from one description to another and recording the pilot's response. (Ref 24) They then used the crossover model as the description of the pilot for each of the above systems and described the change between crossover models with a transient model.

The second type of time-varying system previously addressed by the crossover model is the slowly time-varying system. Moriarty addressed this type of system in his dissertation by using a quasi-stationary approach. (Ref 55) Intervals were selected so that the variation of the system parameters was small for the interval considered. As this allowed assumptions of time invariance over that interval to be good, the pilot description for each interval could be attained from the crossover model.

1.1.2.2 Optimal Control

Extensions of the optimal control pilot model to time-varying system dynamics have been limited. The most pertinent work to date involved the problem of tracking an aircraft from a ground-based gun. (Ref 40) The gun was allowed two manual controls, azimuth control and elevation control, and the gun/aircraft system was allowed to display time-varying dynamics. To address the problem, Kleinman took a quasi-stationary approach, in that he considered the plant dynamic form time-invariant at each computation time and solved the estimation and control problems with those dynamics. Assumptions inherent in Kleinman's work are:

1) Controls for both elevation and azimuth are applied simultaneously.

2) The system description over any interval is the mathematical description the operator assumes for that system for future time. That is, no knowledge of future trajectory alterations is assumed.

3) Attention to the two tasks, azimuth pointing and elevation pointing, is equal.

1.1.3 Nonlinear

1.1.3.1 Crossover

The crossover model approach makes use of describing function analysis, as detailed by McRuer (Ref 53), to address system nonlinearities such as thresholds and time delays. This allows a quasi-linear system or a system that is linear but takes into account nonlinearities in predicting statistics applicable to pilot responses. This type of analysis has been used since the initial work of Tustin and is described by McRuer and Krendel. (Ref 52) Unfortunately the types of nonlinearities addressed by describing functions are limited, and the describing function theory outputs are only approximations to the actual outputs generated by the true nonlinearities.

The crossover model type of analysis has also been applied by Pollard (Ref 58) and Onstatt (Ref 56) separately to the general aircraft equations of motion before the usual linearization detailed by Blakelock and others has been accomplished. (Ref 12) Their approach does not actually account for the portions of the aircraft flight regime in which the nonlinearities are significant, but rather

assumes that these regions are short in time and that a linearized uncoupled-type analysis will not diverge unacceptably during those periods.

1.1.3.2 Optimal Control

A describing function type of analysis has also been applied to the optimal control approach to address nonlinearities that occur in the aircraft-pilot system description. The analysis has so far been limited to nonlinear elements in inputs to the aircraft equations of motion, or in nonlinear properties attributed to the pilots' perception of current aircraft displays. (Ref 39) Specifically, nonlinearities in the aircraft equations of motion have not been considered. The nonlinearities referenced above will be identified in Chapter II and are given in Blakelock. (Ref 12)

1.1.4 Multiple-Input/Multiple-Output

1.1.4.1 Crossover

McRuer and Krendel have extended the crossover model to the multiple-input/multiple-output system by the use of block diagrams. (Ref 52) These diagrams described the modes of analysis possible using the crossover model approach. Little practical experience has been gained with the crossover model in the multi-loop case because of the difficulty in finding unique pilot describing functions. (Ref 52)

1.1.4.2 Optimal Control

Some of the most recent work in the optimal control model approach has been concerned with multiple-input/multiple-output systems, because of current interests in multiloop problems and the direct applicability of this model to the multi-loop problem.

Though Kleinman's work on gun tracking involves both multiple-inputs and multiple-outputs (Ref 40), his multiple input work is qualified by addressing only the two input case where the inputs are decoupled. Other than this the recent work involving the optimal model has been accomplished in single-input/multiple-output systems. In this case, an attention allocation algorithm that specifies some of the measurement noise parameters in the Kalman filter is used. This attention allocation algorithm was developed by observing that the effect of parameter variance in the filter is similar to variance in human attention. (Ref. 40)

1.1.5 Systems Involving Non-Stationary Stochastic Processes

A stationary stochastic process is one in which the probability laws governing the mechanism producing the process remain time-invariant as the process evolves in time. (Ref 54) On the other hand if these probability laws are time-varying during the process evolution, the process is termed non-stationary.

The majority of the work in both the crossover and the optimal control pilot modeling task has been oriented toward stationary stochastic processes. In the gun tracker research, Kleinman's quasi-static approach allowed non-stationary stochastic processes in the input to the human operator portion of the operator/gun model. (Ref 40) This work has not been extended to the pilot/aircraft problem, nor has it been extended to non-stationary stochastic processes arising outside the input to the pilot.

1.1.6 Optimal Estimation/Optimal Stochastic Control

1.1.6.1 Optimal Control

The basis for the optimal control model referred to above is optimal estimation and optimal stochastic control theory. The portions of that theory pertinent to the pilot modeling task of this research are stated and proven in many references, such as Kwakernaak and Sivan (Ref 39); they will be addressed in Chapter III. When the plant in question is linear, the optimization criterion is quadratic, and the stochastic processes associated with the system are Gaussian, the Linear Quadratic Gaussian theory, hereafter called LQG, applies. (see, for instance, Ref 8) This theory strongly relies on the separation theorem, which basically states that with the LQG constraints, the deterministic optimal control gain matrix for any time t_1 can be applied to the optimal state estimate for time t_1 to arrive at the optimal control for that time.

When any of these constraints are violated, the separation principal no longer applies, and the optimal stochastic control can be nonlinear, as proven by Witsenhausen. (Ref 75) Numerous sub-optimal control schemes have evolved when the problems considered did not satisfy the LQG constraints.

One such case is in team theory control considered by Chong and Athans. (Ref 17) This type of control assumes two independent controllers, each with a separate information set and each applying a continuous control. A linear optimal control is assumed in this case, but Chong and Athans observed that a nonlinear control could conceivably perform better.

Another method that has compromised the "optimality" of the solution but has proven useful, is the forced separation scheme addressed by Farison, Graham, and Sheldon. (Ref 26) This method, at time t_1 , applies the optimal state gains to the estimates of the states, to compute the control. In their experiment, a 20-run Monte Carlo analysis was used to arrive at the salient conclusion that the forced separation was able to stabilize the system and performed well with respect to the "optimal" control.

1.1.6.2 Optimal Estimation

Optimality in the maximum likelihood sense of an estimation procedure with variable measurement sets has been addressed by Jaffer and Gupta, and by Ackerson and Fu separately. (Ref 35, 1) Variable measurement sets are sets of physical measurements available to the system, each set containing a different group of measurements. This approach can be used to display the varying measurements available through the human visual system to the human operator. Jaffer and Gupta have shown that by propagating the appropriate non-Gaussian density functions, the estimation scheme remains optimal in the maximum likelihood sense. Ackerson and Fu used an alternate scheme involving growing memory requirements to address the same problem. (Ref 1) Because the propagation of density functions is not an easy procedure and requires integration for at best an approximation of the function, and because growing memory is not desirable for a lengthy problem, an alternate method was proposed by Ackerson and Fu.

In this method the computer memory necessary remains fixed in length but the estimation process is suboptimal. This method involves approximating the non-Gaussian density function with a Gaussian density function for the propagation. Ackerson and Fu examined the effects of this method and found that it approximated well the optimal estimates in the maximum likelihood sense for the systems considered.

1.2 PROBLEM

Up to this point care has been taken to point out methods used when specific LQG assumptions were not met. Identifying these assumptions and detailing the previous successful methods used when these assumptions were invoked, provide the basis for the mechanization used in this research. To specify this mechanization further, consider the general problem of providing a mathematical structure that can be used to replace a human operator. In this context, two important goals emerge.

The first goal is to provide a structure with enough parameter freedom to specify the desired operator performance adequately over the region of consideration. The second goal is to provide a structure that allows physical interpretation of the parameters. With the correspondence between parameters and physical properties detailed, altering an aspect of the physical system can be translated to a corresponding alteration of a specified parameter set.

With these goals in mind, the concept of optimality is of secondary importance. That is, optimization is only one of the vehicles which result in a solution to a mathematical problem. When

optimization is not practical, as in this research, extracting portions from the optimization procedure used in similar problems, presents a logical alternate method. It is stressed, however, that the extractions used in this research are a set of previously tested techniques that were found to have application in the human operator context.

With this background and these goals in mind, the specifics of the problem addressed in this research can now be presented. That problem is to design a controller displaying human limitations that will extend the present nonlinear pilot/aircraft model in three ways:

1. The model will be able to handle the entire six degree of freedom set of nonlinear, multiple-input/multiple-output aircraft equations of motion, along with the aircraft control system.
2. Non-stationary stochastic processes driving the aircraft equations of motion can be considered.
3. A decision process will be formulated that will allow the model to account for changing pilot dynamics.

This decision process will be set in the natural time domain, which presents the best opportunity for its correlation with, and interpretation of, the physical system. The human operator limitations considered are:

1. Time delay in perception of information.
2. Lag between control computation and application to account for the neuromuscular lag.

3. Inability to attend visually to more than one channel of information at any time (channels are pitch, roll, heading, airspeed, and altitude).

4. Inability to control actively more than one channel at any one time margin. The requirement for the first three limitations has been discussed extensively by Kleinman and Baron (Ref 3), and the requirement for the last limitation has been discussed by Levison. (Ref 12)

From these limitations a need for another analytical tool, decision theory, is apparent and facets of that theory pertinent to the problem will now be considered.

1.3 APPROACH

1.3.1 Decision Theory

To implement the assumption of limited direct visual attention available to the human operator, a variable measurement set is to be used. This approach allows the human operator to make one of five observations at each time instant. Because five alternatives are available and only one can be sampled, a decision process is necessary. Two decision routes considered previously were examined. The first, the work of Ackerson and Fu, considered a measurement at time t_1 with the origin of that measurement known only to be one of a set of possible measurements. A number was associated with each member of the set representing the apriori probability of that member actually being the measurement, and the output then being a weighted average of possible measurements. The second route considered is the decision theory route. (Ref 70) That is, at each

time t_1 , a decision based upon some preset criteria is made. To attempt to address this type decision process, the discipline of decision theory was examined.

Four different types of decision theory are considered potentially fruitful for incorporation into the pilot model. The first type is the dynamic programming approach, as developed by Sandell. (Ref 65) In this method a decision is made according to an analysis of the cost of that decision. The cost of the decision is evaluated by propagating the effects of that decision to the final time and analyzing the cost of those effects.

The second type of decision process explored was the utility function or Bayesian decision function approach. This approach is given in depth in Chapter 4 and in Tummala. (Ref 70) Basically, it requires specification of probabilities associated with the various states of nature and a cost for the occurrence of each of those states of nature. This is different from the dynamic programming approach, in that it makes the decision based upon a judgment of past and present behavior, while the dynamic programming approach uses an apriori judgment of future behavior.

The other two approaches, the cue theoretic approach of Pollard, (Ref 58) and the fuzzy set approach of Jain (Ref 36), will be expanded in Chapter 4. Portions of the cue theoretic approach were used in the decision model of this research, and the fuzzy set concept is suggested as an approach to certain extensions of this research.

At this point, alternative approaches have been examined for the decision task, the estimation task, and the control task: tasks necessary due to the problem statement and the problem limitations.

1.3.2 Nonlinear System Control

When considering the problem statement, it is apparent that two troublesome properties must be addressed before any definition of the problem approach can be made. These properties are the nonlinearity of the system equations and the large number of equations necessary to satisfy that problem statement. To date, the only general method available for feedback control of large-scale nonlinear systems is the method of small perturbations. (Ref 8) This method is based upon a given state trajectory. The state trajectory necessary involves a nominal time history of each of the states that enter the system equations in a nonlinear fashion. As the system states are stochastic in nature, the actual trajectory of each of the states will vary from this given nominal. The small perturbation method provides the control designer with some assurance that if deviations from the nominal remain small, that is if the higher-order terms associated with both the control and the state in the Taylor series expansion used in the method are small, the equations derived by the small perturbation approach will remain valid. Satisfaction of the first objective of Section 1.2 is qualified by the method of small perturbations. However, since the only inputs and

states that can be considered are inputs and states that are perturbations about a prespecified input and state trajectory, this limits the generality of the problems addressed to a class of problems with prespecified trajectories. This limit should not be overly constraining, since many maneuvers such as barrel rolls and cloverleaves fall into this category.

The only restriction imposed by the small perturbation approach that affects the second objective is the requirement for the higher order terms to remain small. The stochastic nature of the problem, in this case non-stationary, does not preclude the usage of the small perturbation method. Therefore, as long as the control system devised can accommodate the general linear time-varying perturbation equations, the problem can be approached in this manner.

As the small perturbation system model will in general be linear time-varying when nonlinearities are a consideration in the full-order non-linear equations, the model chosen for the pilot must be able to admit linear time-varying systems. Using optimal control theory, computation of the time-varying controller gains is accomplished using the time-varying Riccati equation. (Ref 44) This implementation implies two assumptions in the human operator context:

- 1) The human operator has knowledge of the trajectory the aircraft will follow.

- 2) The human operator has knowledge of the final time of that trajectory.

Also inherent in the LQG type controller considered is the quadratic assumption on the optimization criteria, and the Gaussian assumption

on the problem noise. These assumptions are argued in the optimal control pilot modelling literature (Ref 38, 39, 40), and these assumptions will be made in this work. Therefore because of the applicability of the LQG assumptions to the human operator problem, and because of the LQG controller's direct application, it is selected as the controller form for this problem. When the time delay in information perception is considered, as in limitation 1, an adaptation of the LQG problem to include a predictor in addition to the Kalman filter must be made. This adaptation is frequently used in optimal control pilot modelling literature. (Ref 39)

At this point an adapted LQG controller, adapted because of the nonlinear time delay in the problem, was specified as the basic structure for modeling the human operator, primarily because the framework provided by the controller appears to correspond well to the physical system and because the mathematics of the LQG controller admit the time-varying nature of the problem. The basic LQG controller requires only a linear system as the name implies; however, practical simplifications are available if the system is also time-invariant.

1.3.3 Decision Process

With the above framework set for the controller, the question of how to deal with the aspect that only one active control and only one observation are available to the human operator, is analyzed. Consider employing a decision process versus employing no decision

process to account for these limitations, limitations 3 and 4 of Section 1.2. With no active decision process, as applied by Ackerson and Fu (Ref 1), these limitations on the mathematics translate to the human operator as an apriori knowledge of the attention pattern or of the control pattern, or as an apriori knowledge of the probability of such patterns. This requires pre-specification of the time history of measurement matrices and observation noise matrices in the estimator and prespecification of the control-weighting matrix histories in the controller.

If no apriori knowledge of the future attention pattern or the future control pattern is assumed for the human operator, a decision process using only past and present information must be employed. That decision process can output either an attention position and/or a control position, or it can output a probability of an attention position or a control position. This mechanization entails two parallel decision processes, one on attention and one on control. Since this dual nature could lengthen the simulation, and since no empirical data were found to substantiate this dual nature or to amplify on a distinction between these processes, one decision process was assumed, and its output provided both the control and attention decision.

Attention position or control position refers to one of a set of channels. Each channel is defined by a specific observation or control available to the pilot. The channels used in this research are pitch, roll, heading, airspeed, and altitude.

As none of the approaches allows the solution to remain optimal in any sense, the decision to implement the discrete decision approach was made based upon its similarities to the physical problem. These similarities include the features that no future information need be assumed by this mathematical representation of the human operator, and that the concept of discrete decisions translates to visual movements between instruments and physical attention to controls available to the pilot.

1.3.4 The Decision Implementation

Employing a controller adapted with a decision process opens numerous avenues for implementation of the decision in both the control task and the attention specification.

1.3.4.1 Control

The avenues of implementation for the control decision in the optimal control context have received little attention in the past. As mentioned earlier, one possible implementation was explored by Chong and Athans by allowing continuous control from each of two different controllers. (Ref 17) Each controller, however, had a different information set, with no crossfeed of information from one controller to the next. As the human controller is assumed to have one visual processor, the assumption of no crossfeed of information used by this approach does not pertain. The basic concept of multiple controllers used by Chong and Athans, however, does have relevance. This relevance lies in the assumed limitation that a human can only control one channel at a time; therefore, multiple controllers must

be available to the human operator.

Two concepts were explored for implementing different controllers via varying gain matrix values. The first concept requires a decision process that outputs the probability of a particular decision occurring. This probability could then be applied mathematically to a reference set of weights in the quadratic criterion equation. (Ref 44) This would produce a set of weights for each time, based upon the situation at that time. If these weights were considered constant until time t_f and used in propagating the Riccati equation backward in time, a control gain matrix could be computed for each time. This method appears to satisfy the desired physical appeal, but necessitates on-line computation of a control gain matrix at each discrete time, as the parameters, in this case weightings, would change at each time because of the changing probability associated with them. For a problem containing only a few states, this mechanization would be attractive because the new Riccati equation solution necessary at each time interval would not be computationally infeasible. For this problem, however, the 63-state state space used precludes online computation of the Riccati equation.

The second concept requires a definite decision to be made at each decision time. This concept uses only five different control weighting matrices, while the first concept implies a different control weighting matrix at each time. Using this method, control gain matrices can be precomputed by assuming five separate weighting

conditions. Each of the five weighting conditions would emphasize control on one of the channels: pitch, roll, heading, airspeed, or altitude. The decision process can then choose the channel that is to be controlled, so that the control gain matrix coinciding with that discrete time and that discrete channel can be accessed and used. This use, then, assumes that this control will be exerted throughout the rest of the problem. This assumption appears physically appealing in that what the pilot is presently controlling is what he is planning to control, as he has no knowledge of future aircraft excursions.

The matrix of control weightings for each individual channel emphasis is chosen to reflect a variation in the pilot neuromuscular time constant described by Kleinman. (Ref 3) When the attention is assumed to be on the particular mode in question, the time constant is .1 seconds, a value considered to be indicative of peak human performance. When the operator is not attending to the channel, a time constant of .2 seconds is assumed, to reflect a degraded mode of performance. These values fall in the 0.1 to 0.4 second range assumed for the neuromuscular lag time constant in most previous work. (Ref 46)

Because of its ability to calculate the control gain matrices "off-line", the second method was used. Computation time is at a premium, and when the problem can be modularized by separate computation of a facet of the problem, the approach that allows that modularization is very appealing. This method is then used to implement

limitation four of Section 1.2, the limited ability of the human to control a multi-input system.

1.3.4.2 Restricted Attention and its Impact on Estimation

To implement limitation three, that of restricted visual attention of the human operator, three different possibilities were evaluated. The first method was an extension of Kleinman's attention allocation scheme. (Ref 39) By adding a decision process to this scheme, a probabilistic representation of the specific attention decisions could be derived. This could then be applied by multiplication or by some other mathematical approach to the covariance values of the observation noises to create an emphasis or deemphasis on any or all observations. For example, consider two possible measurements, one of pitch and one of roll. Also assume the decision process had produced a probability of 70% that roll was being measured and of 30% that pitch was being measured. Assume that the noise on pitch and roll had as a base a standard deviation value of 1 degree. Then at the time of the decision process output, the standard deviation value of the assumed (Gaussian) noise on pitch could be 1.2 degrees and on roll could be, say, .8 degrees. That would generate a more accurate measurement on roll which was identified by the decision process as being the most important channel to measure.

The second method evaluated was the method suggested by Ackerson and Fu, in which the probabilistic representation of the decision was applied by an alteration of the Kalman filter corrector equations instead of applying it to the observation noise covariance

as Kleinman had. (Ref 1) The specific alterations took the form of additive terms and are detailed in the above reference. These terms were used to approximate a non-Gaussian density function with a Gaussian density function.

The third method evaluated employed a discrete decision process to choose a realization of the observation matrix for the next discrete time interval. This method actually simulates the movement of the human operator's visual and non-visual attention in time. As the discrete decision process was required for the controller chosen, and as the third representation presented a good physical interpretation, the specific observation matrix implementation of limitation three was chosen.

1.3.5 Decision Process

The decision process now needs to be specified. As mentioned above, a number of decision processes were considered. Because of the need for the computational feasibility, the dynamic programming and the Ackerson and Fu approach were not chosen.

The dynamic programming method would involve a consideration of the future effects of each decision at each time a decision was required, and then a choice would be made considering the cost of these effects. (Ref 65) This requires multiple integrations of the system at each time a decision is necessary, to evaluate the cost of the decision. Because of the size of the system, this type of decision process was deemed too costly in computer usage for the purpose required. Also this method is not physically appealing in that it

would require the human operator to have apriori knowledge of the effect of his decision through time, and this is not considered likely.

A decision process based on Ackerson and Fu's work would involve propagation of a non-Gaussian density function or propagation of an approximating Gaussian density function. Either would require extensive computation; as computation is critical because of the already large problem size, this method was not chosen.

Instead, the utility function approach was chosen. Its assets are:

- 1) Computational feasibility
- 2) Easy adaptation to the discrete decision process required
- 3) Provides a structure which adapts well to the empirical data available on human decision making during a control task.

(This aspect will be discussed in Chapter V.)

1.3.6 Control Lag

The last limitation to be considered is the limitation of a neuromuscular lag in the control application. Kleinman has addressed this problem by adding a state to the system equation for each individual control. (Ref 39) By proper application of this state, a control lag can be simulated which duplicates a time constant found by experimentation to be the approximate value of the neuromuscular time constant. (Ref 3) This limitation was referred to earlier in the choice of the weighting values.

1.4 SUMMARY

At this point the suboptimal realization of the LQG type of controller to be used is specified. The controller will be applied to the perturbation equations of the nonlinear aircraft model. The perturbation equations will be augmented with states described by Kleinman to allow for a neuromuscular time lag in the control application. The controller will consist of 5 optimal (in the least squares sense) control gain matrix sets, each generated by the LQG synthesis. It will have one decision process as discussed above which at each time iteration chooses one of the five control gain matrices and one of five observation matrices. Each of the five choices accentuates one of the channels: pitch, roll, heading, airspeed, or altitude. A utility function approach will be used to make the decision as to which of the above channels is to be chosen at any decision time. This formulation then can theoretically address each of the pilot limitations assumed while accomplishing the problem objective. This objective is to provide a structure to describe a pilot in an aircraft environment which can be modelled well only by explicitly including substantial nonlinearities in the nominal trajectory.

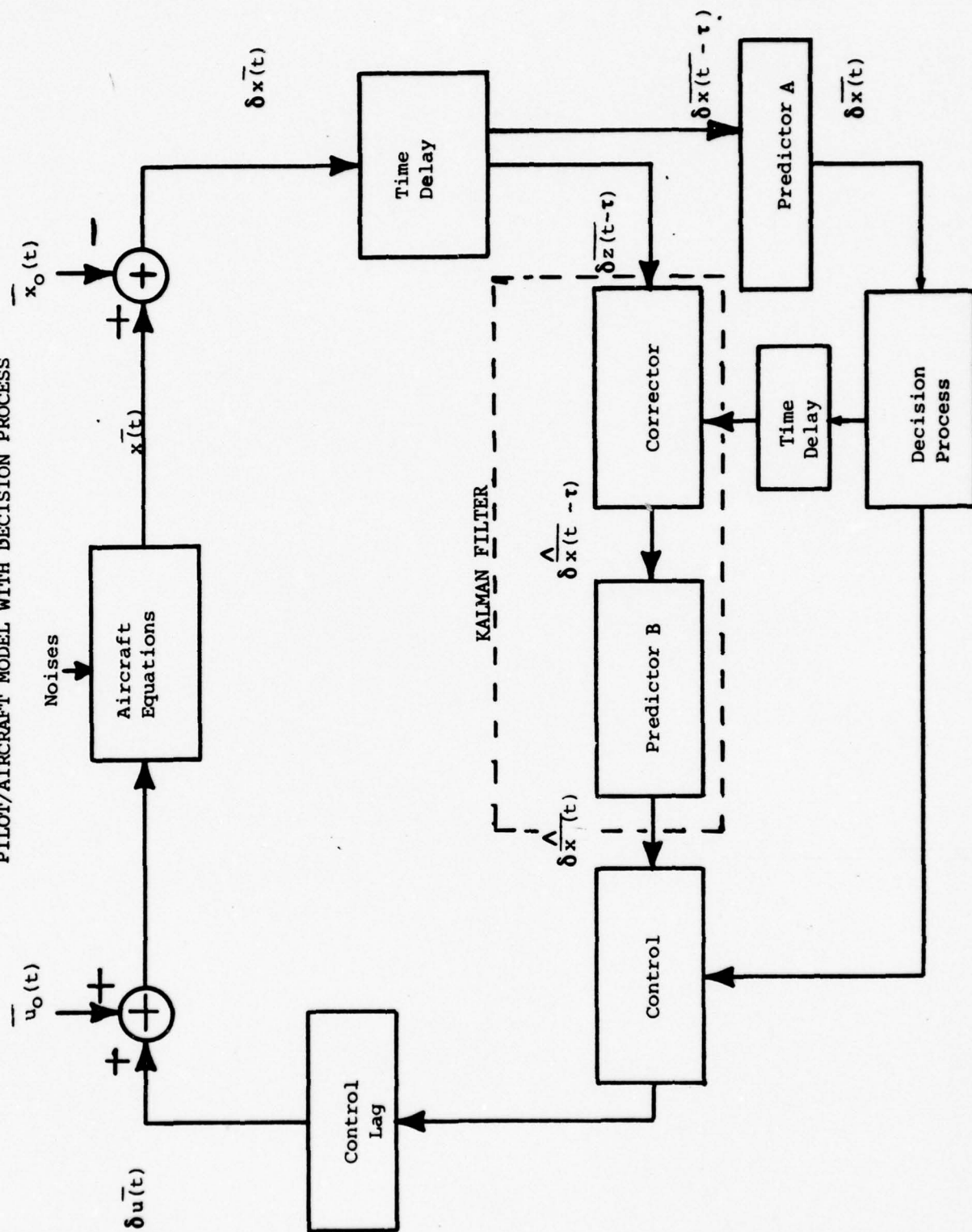
CHAPTER III

AIRCRAFT EQUATIONS OF MOTION AND AIRCRAFT CONTROL SYSTEM

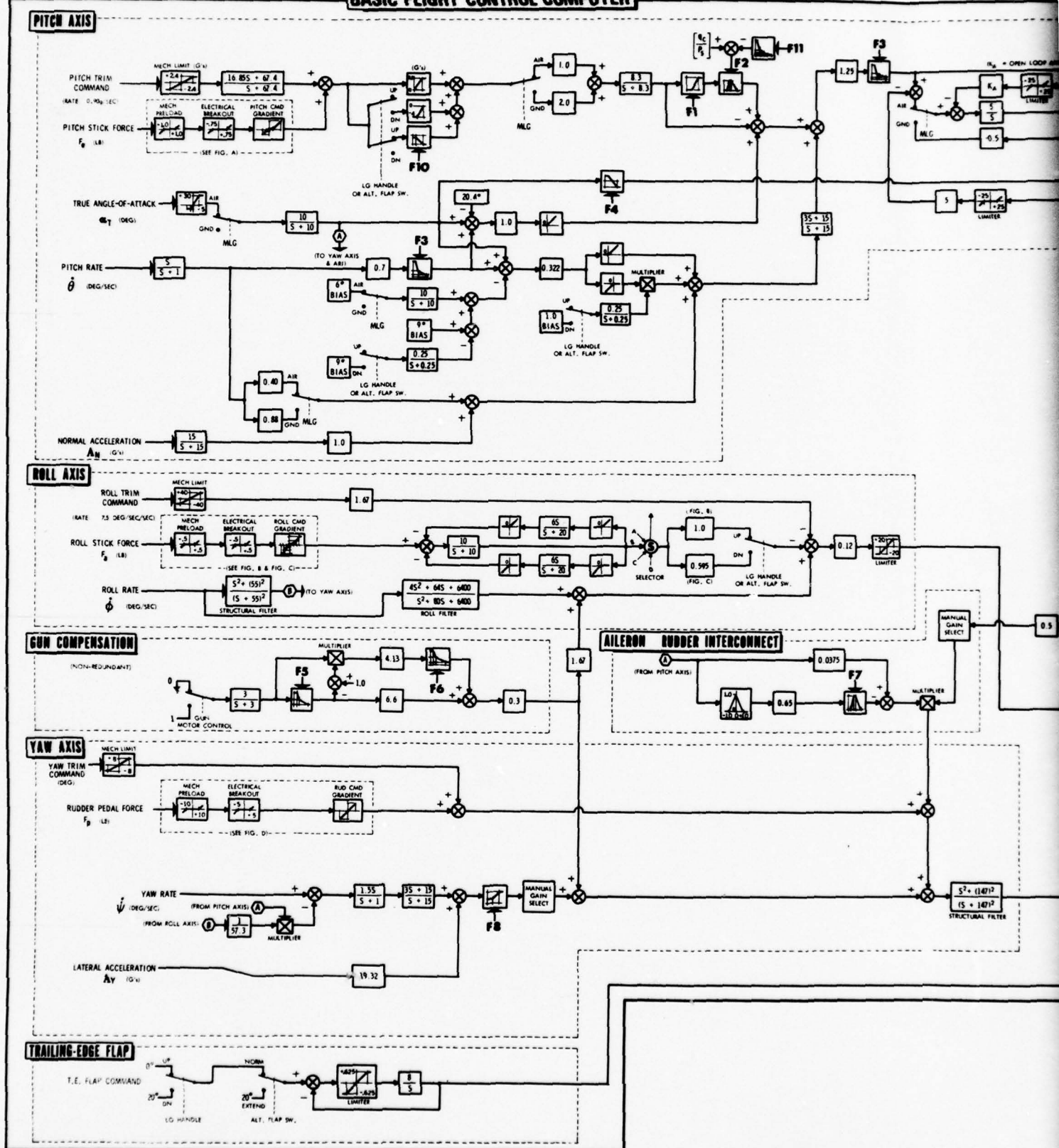
The first step taken in synthesizing the pilot/aircraft system is to identify the aircraft mathematically as completely as possible. This identification is simplified by subdividing the aircraft into two sets of equations. The first set describes the aircraft equations of motion, and the second set describes the aircraft control system. These two sets combine to make the "Aircraft Equations" block of Figure 2. This figure also identifies the other major areas of this work, and reference can be made to this figure to clarify the synthesis process between functional areas. In the succeeding chapters each block will be explained in detail, as will its tie to other blocks, when necessary. This chapter expands the "Aircraft Equations" block by considering the two subdivisions detailed above. Before proceeding with the details of the "Aircraft Equation" block, an overview of the schematic will be accomplished, starting with the aircraft equations and working clockwise. Detailed analysis of each block is given in the appropriate chapters so only an overview is presented here for clarity.

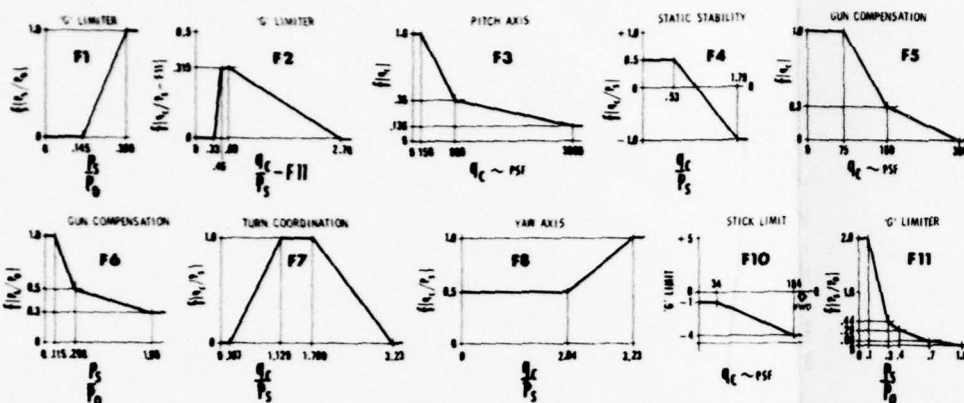
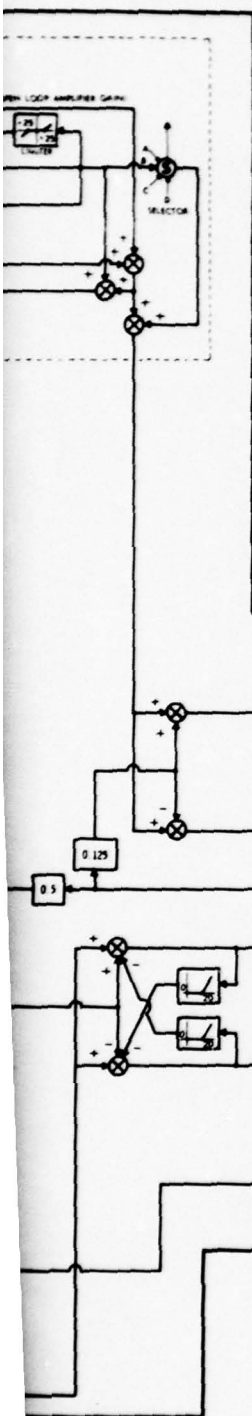
The "Aircraft Equations" block outputs the states of the aircraft including control system. From these states, the nominal trajectory states $x_0(t)$ are subtracted to yield the perturbation states. These states are then delayed by τ seconds ($\tau = .2$ for this example) to account for the processing delay attributed to a human operator. The $\delta \tilde{z}(t - \tau)$ observations available to the Kalman Filter are observations, assumed available to the human operator. These observations change with changing decisions which are input from the decision process, through the

FIGURE 2
PILOT/AIRCRAFT MODEL WITH DECISION PROCESS



BASIC FLIGHT CONTROL COMPUTER





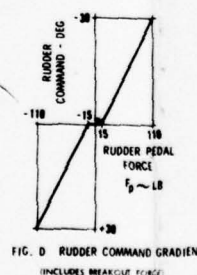
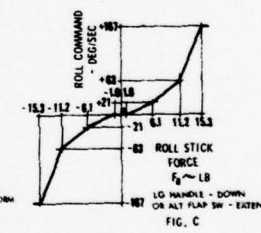
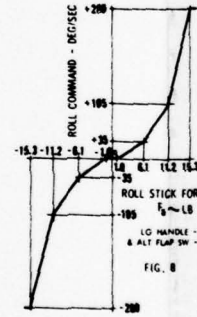
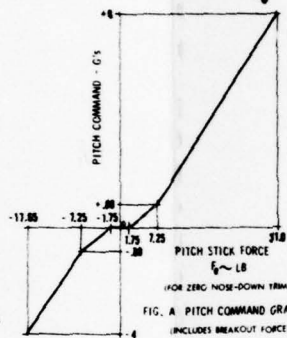
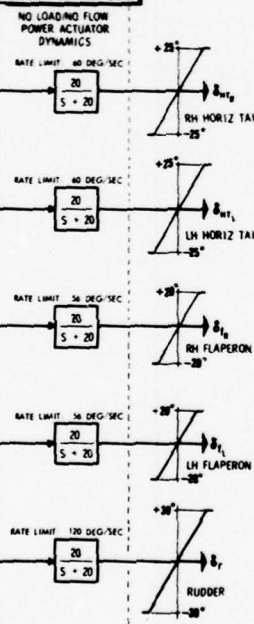
- P_1 = STATIC PRESSURE FOR GIVEN PRESSURE ALTITUDE
- P_2 = STATIC PRESSURE AT SEA LEVEL (29.9213 in. Hg STD)
- P_3 = TOTAL PRESSURE
- P_4 = IMPACT PRESSURE $(P_3 - P_2)$
- M = MACH NUMBER (V / a)

STANDBY GAINS

$Q_c = 800 \text{ psi}$ 324 psi when LG handle is DOWN or ALT FLAP SW is EXTEND
 $P_2 = 2116 \text{ psi}$

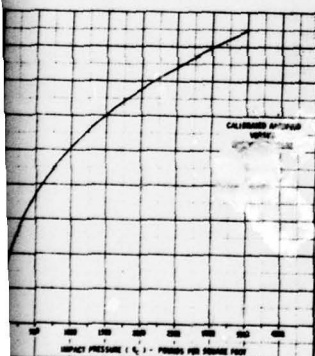
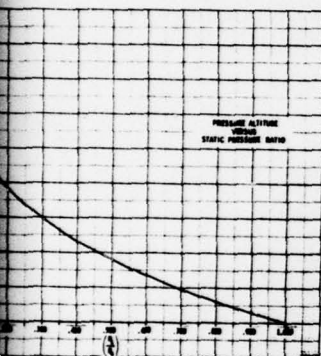
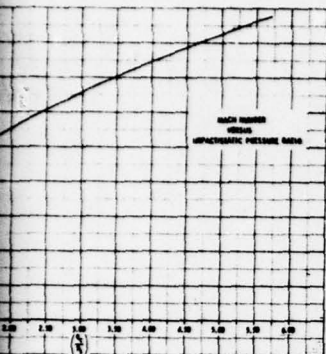
COMMAND SERVOS

POWER ACTUATORS



FLIGHT CONTROL SYSTEM FUNCTION

FIGURE 3



031076:CCB/RRG/WCW
031076:CCB/RRG/WCW
031076:CCB/RRG/WCW
031076:CCB/RRG/WCW
031076:CCB/RRG/WCW
031076:CCB/RRG/WCW
031076:CCB/RRG/WCW
031076:CCB/RRG/WCW
031076:CCB/RRG/WCW
031076:CCB/RRG/WCW

031076:CCB/RRG/WCW

AL BLOCK DIAGRAM

time delay for proper sequencing, to the corrector. Those decisions are made on the basis of threshold information provided by the mean and covariance propagation inherent in "Predictor A". The full state is assumed available for observations of the decision process since only thresholds are used from this information. This aspect is discussed later and in chapter IV.

The decision process also inputs a decision into the control which then identifies a control gain matrix for the appropriate time, to correspond with that decision. This aspect is also explained in Chapter IV. A lag is then applied to the control which accounts for the neuromuscular lag assumed for a human operator. The nominal control is then added to the computed control and applied to the aircraft equations.

With this explanation as background, it is necessary to elaborate further on some of the unique aspects of the model. The first aspect to consider is the two different observations output from the time delay.

The observation entering Predictor A represents the full state information assumed available to the decision process as a result of scanning. The observation entering the corrector is the observation assumed available to the control process. As explained in Chapter 4, this observation can be one of a set of possible observations. This set is composed of possible observations which the controller could emphasize while flying a specific maneuver. Exactly which one of the set is specified by the decision process input to the corrector.

There is also a set of possible controls composed of the same channels as the set of possible observations. The decision process affects the control in the same manner that it affects the corrector, by specifying which of this set is to be applied to the system.

At this point the inputs to the decision process and corrector, and outputs from the decision process have been discussed. These are the major elements which are unique to this model. The other elements which will be discussed briefly are shown in Figure 1 as traditional elements in this process.

Predictor B and the corrector are the elements of the Kalman Filter assumed available to provide state estimates. The next block, the control, is a set of control gain matrices, each individual matrix emphasizing one of the possible channels, referred to above and in Chapter V. The application of the state estimate to the control gain matrix specifies the control. This control is then put through a lag to simulate the neuromuscular lag attributed to human operators.

At this point the nominal control is added to the perturbation control to arrive at the total control applied in the aircraft equations. In like fashion, the nominal states are subtracted from the state values to arrive at the perturbed state values.

This Figure details the modelling process and provides cohesion when the separate functions are examined.

2.1 AIRCRAFT EQUATIONS OF MOTION

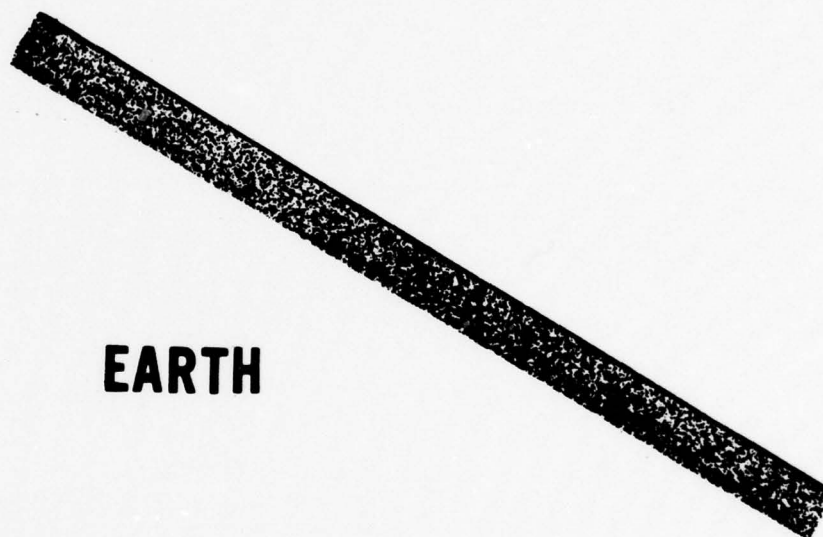
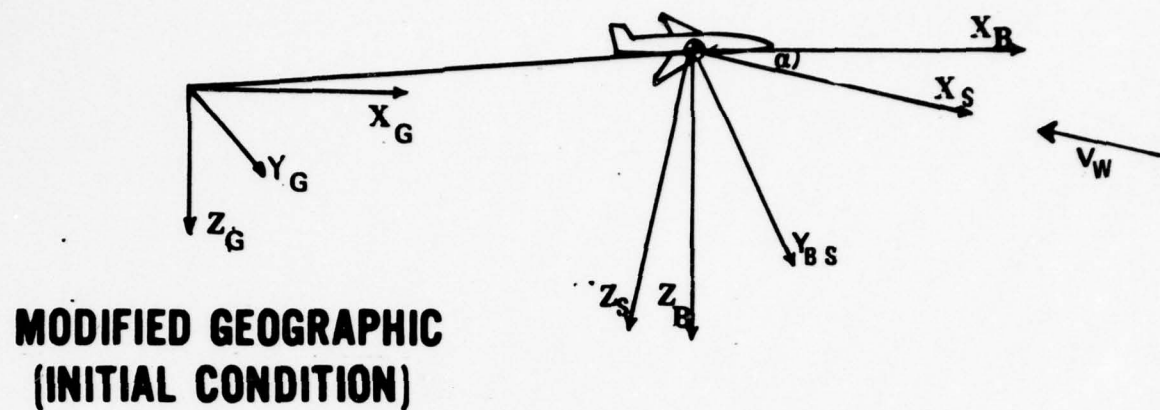
The basic development of the aircraft equations will be much the same as Pollard (Ref 58), with diversions to accent the difference in approaches. The controller equations will then be derived from Figure 3. It can be easily seen that the two sets are integrally tied together. However, a definite division can be accomplished, as the controller equation's inputs are pilot controls and instrument-sensed values and its outputs are deflections, whereas the equations of motion display the reaction of the aircraft to the given control

surface deflection or engine operating position. One point that should be made is that some of the inputs are instrument-sensed quantities and therefore susceptible to the usual sensor errors. Those errors are modeled and will be discussed later.

2.1.1 Reference System

To specify the problem adequately, three coordinate systems will be employed. These systems are a modified geographic system, the body system, and the stability system, as labeled in flight control literature and portrayed in Figure 4. (Ref 12) The modified geographic frame is a frame employed especially for the short time duration trajectories considered in this problem. The origin remains fixed with respect to the earth at the initial condition of the problem. The X_G direction of the modified geographic frame is along the initial heading of the aircraft and remains fixed with respect to earth at that heading. The Z_G direction is pointed along the gravity vector and the Y_G direction makes up a right-handed orthonormal system. The axis system is earth-fixed and therefore not purely inertial; however, for the small time interval considered for this problem, at most ten seconds, the assumption will be made that this is essentially an inertial system.

The next system considered is the body axis system. The origin of the system is at the center of gravity of the aircraft, the X_B direction is positioned out the nose of the aircraft, the Y_B axis is out the right wing, and the Z_B axis is directed out the underside of the fuselage.



COORDINATE SYSTEMS

FIGURE 4

The stability axis system retains the same origin and Y axis as the body system, but the X_S and Z_S axes are rotated in the X_B, Z_B plane through the angle of attack. The positive rotation direction is a positive rotation about the Y_B axis. Figure 4 displays the three axis systems at some time after problem start.

2.1.2 Derivations

The genesis for the aircraft equations of motion, assuming the aircraft is a rigid body, is the set of Newton's Laws for forces and moments:

$$\Sigma \bar{F} = d/dt [m \bar{v}]_I \quad (2-1)$$

$$\Sigma \bar{M} = d/dt [\bar{H}]_I \quad (2-2)$$

The subscript I denotes an inertial frame that, as stated previously, will be the modified geographic axis system for this problem.

The forces and moments acting on the aircraft will be considered to be either equilibrium or perturbational in nature. This can be portrayed by the expansion of Equations (2-1) and (2-2).

$$\Sigma \bar{F} = \Sigma \bar{F}_0 + \Sigma \Delta \bar{F} = d/dt [m \bar{v}]_I \quad (2-3)$$

$$\Sigma \bar{M} = \Sigma \bar{M}_0 + \Sigma \Delta \bar{M} = d/dt [\bar{H}]_I \quad (2-4)$$

The "0" subscript refers to the equilibrium forces and moments. Also, as short time periods are to be considered, the mass of the aircraft will be considered constant so that Equations (2-3) and (2-4) reduce to

$$\Sigma \Delta \bar{F} + \Sigma \bar{F}_0 = m \frac{d}{dt} \bar{V} \Big|_G \quad (2-5)$$

$$\Sigma \Delta \bar{M} + \Sigma \bar{M}_0 = \frac{d}{dt} \bar{H} \Big|_G \quad (2-6)$$

Now, employing the theorem of Coriolis, the derivative of \bar{V} in the G frame is

$$\frac{d\bar{V}}{dt} \Big|_G = \frac{d\bar{V}}{dt} \Big|_B + \bar{\omega}_{GB} \times \bar{V} \quad (2-7)$$

where $\frac{d\bar{V}}{dt} \Big|_G$ is the derivative of the velocity vector as seen in the

modified geographic frame, $\frac{d\bar{V}}{dt} \Big|_B$ is the derivative of the velocity

vector in the body axis system, and $\bar{\omega}_{GB}$ is the angular velocity of the body frame with respect to the modified geographic frame. Expressing \bar{V} in terms of body axes, we now have

$$\bar{V} \Big|_B = \hat{i}_B U + \hat{j}_B V + \hat{k}_B W \quad (2-8)$$

and

$$\bar{\omega}_{GB} \Big|_B = \hat{i}_B P + \hat{j}_B Q + \hat{k}_B R \quad (2-9)$$

Therefore,

$$\frac{d}{dt} \bar{V} \Big|_B = \hat{i}_B \dot{U} + \hat{j}_B \dot{V} + \hat{k}_B \dot{W} \quad (2-10)$$

and

$$\bar{\omega}_{GB} \times \bar{V} \Big|_B = (WQ-VR) \hat{i}_B + (UR-WP) \hat{j}_B + (VP-UQ) \hat{k}_B \quad (2-11)$$

Now, expressing the forces in terms of the inertial axis system generates

$$\begin{aligned} \Sigma \Delta \bar{F} + \Sigma \bar{F}_0 &= \hat{i}_B \Sigma F_x + \hat{j}_B \Sigma F_y + \hat{k}_B \Sigma F_z + \hat{i}_B \Sigma F_{ox} + \hat{j}_B \Sigma F_{oy} + \hat{k}_B \Sigma F_{oz} = \\ \hat{i}_B m (\dot{U}+WQ-VR) &+ \hat{j}_B m (\dot{V}+UR-WP) + \hat{k}_B m (\dot{W}+VP-UQ) \end{aligned} \quad (2-12)$$

Writing the equations by components yields the final results:

$$\Sigma \Delta F_x + \Sigma F_{ox} = m (\dot{U}+WQ-VR) \quad (2-13)$$

$$\Sigma \Delta F_y + \Sigma F_{oy} = m (\dot{V}+UR-WP) \quad (2-14)$$

$$\Sigma \Delta F_z + \Sigma F_{oz} = m (\dot{W}+VP-UQ) \quad (2-15)$$

which are the equations for the linear accelerations.

2.1.3 Rotational Acceleration Equations

Considering now the equation

$$[\Sigma \Delta \bar{M} + \Sigma \bar{M}_0] \Big|_G = \frac{d}{dt} \bar{H} \Big|_G \quad (2-6)$$

where

$$\bar{H} = I \bar{\omega}_{GB} \quad (2-16)$$

\bar{H} is angular momentum and I is defined as the matrix of moments of inertia and products of inertia relative to the body axis of the aircraft. The sign convention for the individual moments is standard.

$$I = \begin{bmatrix} I_{xx} & -J_{yx} & -J_{zx} \\ -J_{xy} & I_{yy} & -J_{zy} \\ -J_{xz} & -J_{yz} & I_{zz} \end{bmatrix} \quad (2-17)$$

Because of the short time duration under consideration, a constant I matrix is assumed. As fuel burnoff and munition expenditure are the primary sources of changes in the equation I matrix, and no munitions are considered for the problem, this assumption is considered reasonable, and the equation is simplified to that below.

$$\left[\Sigma \Delta \bar{M} + \Sigma \bar{M}_0 \right] \Big|_G = I \frac{d}{dt} \bar{\omega}_{GB} \Big|_G = \frac{dH}{dt} \Big|_G \quad (2-18)$$

Now considering the aircraft body axis XZ plane as the plane of symmetry of the aircraft, $J_{xy} = J_{yz} = J_{yx} = J_{zy} = 0$, and

$$H_x = P I_{xx} - R J_{zx} \quad (2-19)$$

$$H_y = Q I_{yy} \quad (2-20)$$

$$H_z = R I_{zz} - P J_{zx} \quad (2-21)$$

Introducing these equations into the original equation, (2-18), and using the theorem of Coriolis

$$\left[\Sigma \bar{M}_O + \Sigma \Delta \bar{M} \right] \Big|_B = \frac{d\bar{H}}{dt} \Big|_B + \omega_{GB} \times \bar{H} \Big|_B \quad (2-22)$$

then

$$\frac{dH_x}{dt} = \dot{P} I_{xx} - \dot{R} J_{xz} \quad (2-23)$$

$$\frac{dH_y}{dt} = \dot{Q} I_{yy} \quad (2-24)$$

$$\frac{dH_z}{dt} = \dot{R} I_{zz} - \dot{P} J_{zx} \quad (2-25)$$

≅ ✓

and

$$\bar{\omega}_{GB} \times \bar{H} \Big|_B \quad (2-26)$$

$$= \hat{i} (QH_z - RH_y) + \hat{j} (RH_x - PH_z) + \hat{k} (PH_y - QH_x) \quad (2-27)$$

Separating equations yields

$$\Sigma \Delta M_x + \Sigma M_{Ox} = \dot{P} I_{xx} - \dot{R} J_{xz} + QR (I_{zz} - I_{yy}) - PQ J_{xz} \quad (2-28)$$

$$\Sigma \Delta M_y + \Sigma M_{Oy} = \dot{Q} I_{yy} + PR (I_{xx} - I_{zz}) + P^2 J_{xz} - R^2 J_{zx} \quad (2-29)$$

$$\Sigma \Delta M_z + \Sigma M_{oz} = \dot{R} I_{zz} - \dot{P} J_{xz} + PQ (I_{yy} - I_{xx}) + QR J_{zx} \quad (2-30)$$

Now to obtain the standard form for the above equations, solve Equation (2-30) for \dot{R} and substitute into the first equation. Then similarly solve Equation (2-28) for \dot{P} and substitute into third equation.

$$\begin{aligned} \Sigma \Delta M_x + \Sigma M_{ox} + (J_{xz} / I_{zz}) (\Sigma \Delta M_{oz} + \Sigma \Delta M_z) = \\ \dot{P} I_{xx} + QR (I_{zz} - I_{yy}) - PQ J_{xz} - \dot{P} J_{xz}^2 / I_{zz} + \\ PQ (I_{yy} - I_{xx}) J_{xz} / I_{zz} + QR J_{xz} J_{zx} / I_{zz} \end{aligned} \quad (2-31)$$

$$\Sigma \Delta M_y + \Sigma \Delta M_{oy} = \dot{Q} I_{yy} + PR (I_{xx} - I_{zz}) + P^2 J_{xz} - R^2 J_{zx} \quad (2-32)$$

$$\begin{aligned} \Sigma \Delta M_z + \Sigma M_{oz} + (J_{xz} / I_{xx}) (\Sigma \Delta M_x + \Sigma \Delta M_{ox}) = \\ \dot{R} I_{zz} + PQ (I_{yy} - I_{xx}) + QR J_{zx} + \dot{R} J_{xz}^2 / I_{xx} - \\ QR (I_{zz} - I_{yy}) J_{xz} / I_{xx} + PQ J_{xz}^2 / I_{xx} \end{aligned} \quad (2-33)$$

2.1.4 The Forces

The forces summed to make $\Sigma \Delta \bar{F}$ and $\Sigma \bar{F}_0$ are considered to be of three types, those due to thrust, those due to the airflow, and those due to gravity. The resolved forces due to thrust will be labelled E_x , E_y , E_z , those due to aerodynamics will be labelled X , Y , and Z , and those due to gravity will be labelled G_x , G_y , and G_z .

First consider the gravity terms. Gravity is expressed in the modified geographic coordinate system along the Z direction. Assuming gravity to be constant, a reasonable assumption in the limited time considered, the gravity vector in the modified geographic frame is

$$\bar{g} \big|_G = \begin{bmatrix} 0 \\ 0 \\ g \end{bmatrix}$$

The direction cosine matrix from the modified geographic system to the body axis system is given by the following

$$C_G^B = \begin{bmatrix} \cos\theta \cos\psi & \cos\theta \sin\psi & -\sin\theta \\ \sin\phi \sin\theta \cos\psi & \sin\phi \sin\theta \sin\psi & \sin\phi \cos\theta \\ -\cos\phi \sin\psi & +\cos\phi \cos\psi & \\ \cos\phi \sin\theta \cos\psi & \cos\phi \sin\theta \sin\psi & \cos\phi \cos\theta \\ +\sin\phi \sin\psi & -\sin\phi \cos\psi & \end{bmatrix} \quad (2-34)$$

where ϕ , θ , and ψ are Euler angles as defined in Blakelock (Ref 12).

Multiplying by the transformation matrix gives $C_G^B \bar{g} |_G$ where

$\bar{g} |_B$ is:

$$\bar{g} |_B = C_G^B \bar{g} |_G = \begin{bmatrix} -g \sin\theta \\ g \cos\theta \sin\phi \\ g \cos\theta \cos\phi \end{bmatrix} \quad (2-35)$$

The thrust vector E is a function of the engine alignment in the airframe. For the single-engine fighter-type aircraft used in this model it is assumed that the engine is mounted directly along the x axis of the body frame, so that the thrust vector is given by

$$E_B = \begin{bmatrix} E_x \\ 0 \\ 0 \end{bmatrix} \quad (2-36)$$

The last consideration is the set of aerodynamic forces resolved into the X_B , Y_B , Z_B components. These forces are indirectly determined from wind tunnel tests and displayed in the stability axis system. The wind tunnel results yield the coefficients of lift, yaw, and drag, and a representation of the relation of these terms to the corresponding forces is given by equations (2-37) through (2-39).

$$X_S = -\rho V_T^2 S C_D/2 \quad (2-37)$$

$$Y_S = \rho V_T^2 S C_Y/2 \quad (2-38)$$

$$Z_S = -\rho V_T^2 S C_L/2 \quad (2-39)$$

In these equations ρ is the air density at the flight condition specified, V_T is the velocity of the aircraft relative to the air mass and S is the aircraft reference area.

Transforming into body axis using the rotation through the angle of attack yields the following equations to specify the forces in the body frame, assuming nominal $B = 0$.

$$X_B = X_S \cos \alpha - Z_S \sin \alpha \quad (2-40)$$

$$Y_B = Y_S \quad (2-41)$$

$$Z_B = X_S \sin \alpha + Z_S \cos \alpha \quad (2-42)$$

To implement these equations, expressions are given for C_L , C_D , and C_Y in tabular form, derived empirically from wind tunnel tests for the particular aircraft considered.

2.1.5 Moments

The equations for the specification of the moments about the vehicle center of mass in the appropriate coordinate frame will now be considered. The resolved $\Sigma \Delta \bar{M}$ and $\Sigma \bar{M}_O$ will be decomposed into two moments; those induced by the thrust, T_x , T_y , and T_z , and those induced by the airflow, L , M , and N . The resulting equation is:

$$\Sigma \Delta \bar{M} \Big|_B + \Sigma \bar{M}_O \Big|_B = \begin{bmatrix} L \\ M \\ N \end{bmatrix}_B + \begin{bmatrix} T_x \\ T_y \\ T_z \end{bmatrix}_B \quad (2-43)$$

As the aircraft's engine is aligned with the X_B axis and the center of mass is assumed to lie on this axis, the moment vector is essentially

$$\bar{T}_B = \begin{bmatrix} 0 \\ 0 \\ 0 \end{bmatrix}_B \quad (2-44)$$

As with the forces, the moments are computed in the stability axis system. Using the aerodynamic equations relating the coefficients of the moments to the moments

$$L_S = \rho V_T^2 S b C_l / 2 \quad (2-45)$$

$$M_S = \rho V_T^2 \bar{c} S C_m / 2 \quad (2-46)$$

$$N_S = \rho V_T^2 b S C_n / 2 \quad (2-47)$$

where ρ is the air density, V_T is the velocity of the aircraft relative to the air mass, b is the aircraft wing span, and \bar{c} is the wing aerodynamic chord. As with the forces, C_l , C_m , and C_n are determined from tables which were computed by wind tunnel tests.

At this point we have six equations which can be solved for \dot{U} , \dot{V} , \dot{W} , \dot{P} , \dot{Q} , and \dot{R} , given by equations (2-13), (2-14), (2-15), (2-31), (2-32), and (2-33). We next need to determine equations for Euler angles ϕ , θ , and ψ , where ϕ is the roll angle, θ is the pitch angle, and ψ is the angle between magnetic north and the aircraft

heading. We also need expressions for S_x , S_y , and S_z , the distances traveled in the modified geographic coordinate system.

As P, Q, and R are angular rates expressed in the body axis system, a relationship must be derived relating ϕ , θ , and ψ to P, Q, and R. To understand that relationship consider each Euler angular rate expressed in its respective coordinate system. First examine heading angular rate:

$$\begin{bmatrix} 0 \\ 0 \\ \dot{\psi} \end{bmatrix}_G$$

Upon rotation using the transformation matrix specified in equation (2-34), the contribution by $\dot{\psi}$ to P is $-\dot{\psi}\sin\theta$; to Q is $\dot{\psi}\cos\phi\cos\theta$; and to R is $\dot{\psi}\cos\phi\sin\theta$. Now $\dot{\theta}$ is expressed in the intermediate coordinate system and, when rotated to the body axis, the contribution to Q is $\dot{\theta}\cos\phi$ and to R is $-\dot{\theta}\sin\phi$. Collecting terms produces

$$P = \dot{\phi} - \dot{\psi}\sin\theta \quad (2-48)$$

$$Q = \dot{\theta}\cos\phi + \dot{\psi}\cos\theta\sin\phi \quad (2-49)$$

$$R = -\dot{\theta}\sin\phi + \dot{\psi}\cos\theta\cos\phi \quad (2-50)$$

It should be mentioned that this realization was chosen because, for this problem, selection could be made on the trajectory.

That control was used because the above equations, (2-48), (2-49), and (2-50) have indeterminate points when solved for $\dot{\phi}$, $\dot{\theta}$ and $\dot{\psi}$ at

$Q = 90^\circ$. If the indeterminate points presented a problem the four-parameter quaternion method would have been used, since, though it is a bit more complex, it resolves the indeterminate point problem.

The last equations needed are the equations for the displacement of the aircraft from its position at the initial time. These equations are given in the body axis by

$$\dot{s}_x|_B = U + \text{wind}_x \quad (2-51)$$

$$\dot{s}_y|_B = V + \text{wind}_y \quad (2-52)$$

$$\dot{s}_z|_B = W + \text{wind}_z \quad (2-53)$$

where wind_x , wind_y , and wind_z are the wind velocities resolved in the body X_B , Y_B , and Z_B axis system. Unfortunately this is not a particularly usable form, as the needed displacement is from the modified geographic system to the body center of gravity. Therefore

$$\begin{bmatrix} \dot{s}_x \\ \dot{s}_y \\ \dot{s}_z \end{bmatrix}_G = C_B^G \begin{bmatrix} \dot{s}_x \\ \dot{s}_y \\ \dot{s}_z \end{bmatrix}_B \quad (2-54)$$

where the direction cosine C_B^G is equal to $(C_G^B)^T$, which was specified in equation (2-40). The equations thus derived are

$$\begin{aligned}\dot{S}_x &= U \cos\theta \cos\psi + V(-\cos\phi \sin\psi + \sin\phi \sin\theta \cos\psi) \\ &\quad + W (\sin\phi \sin\psi + \cos\phi \sin\theta \cos\psi) + \text{wind}_x\end{aligned}\quad (2-55)$$

$$\begin{aligned}\dot{S}_y &= U \cos\theta \sin\psi + V (\cos\phi \cos\psi + \sin\phi \sin\theta \sin\psi) \\ &\quad + W (-\sin\phi \cos\psi + \cos\phi \sin\theta \sin\psi) + \text{wind}_y\end{aligned}\quad (2-56)$$

$$\begin{aligned}\dot{S}_z &= U (-\sin\theta) + V \sin\phi \cos\theta + W \cos\theta \cos\phi \\ &\quad + \text{wind}_z\end{aligned}\quad (2-57)$$

With these twelve equations the aerodynamics of the aircraft are adequately specified for the problem.

2.2 Control System

Historically, aircraft control systems have incorporated numerous mechanical devices in the linkage between the control stick and the control surface. These mechanical devices were designed to allow the aircraft to respond to a control stick input in a manner that was both safe and comfortable for the pilot. As time progressed the linkage was augmented with hydraulics to allow the force levels required of the pilot to remain constant while aircraft speed and size increased.

In the present generation of aircraft, heavy emphasis has been placed on aircraft response. This is demonstrated by some

current airframes which display relaxed aerodynamic stability. To allow for the margin of safety required in the pilot/aircraft system, these relaxed aerodynamic stability airframes are equipped with stability augmentation control systems. The inner loop control systems allow the system controlled by the pilot to have the same stability characteristics as other systems with dynamically stable airframes.

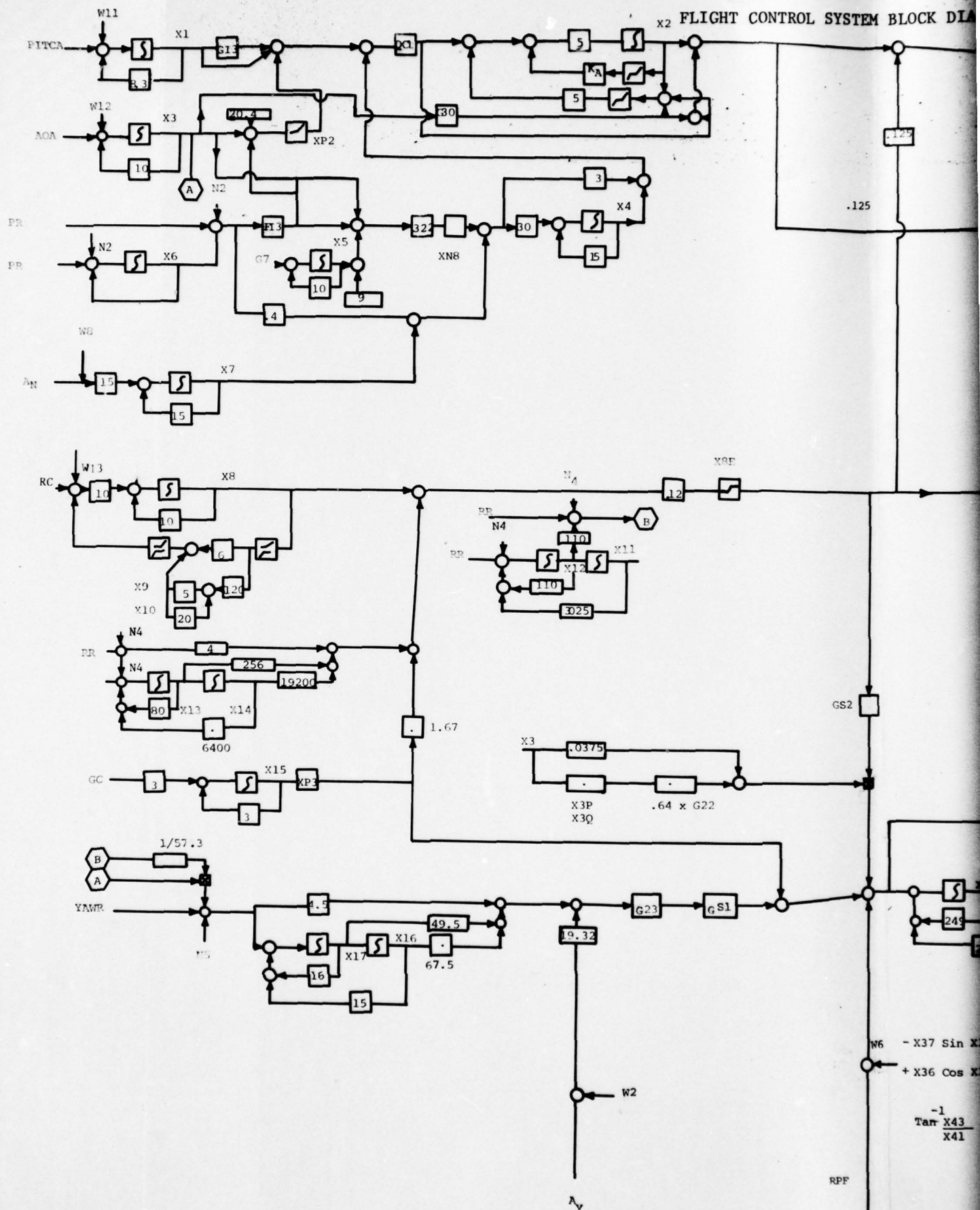
The inner loop control referenced above has been provided in many ways, the latest of which is the fly-by-wire system. A current fly-by-wire system is referenced in Figure 3, with the corresponding system block diagram given in Figure 5. The gain schedules have not been labeled because of possible proprietary problems. This is considered a general model, as most fly-by-wire systems investigated feed back pitch, yaw, and roll rates, angle of attack, and lateral and normal accelerations.

Before this control system could be implemented, an accurate model of the above aircraft and its environment, complete with sensors and actuators consistent with the earlier assumptions in Chapter II had to be derived. This total model could then be implemented on a digital computer.

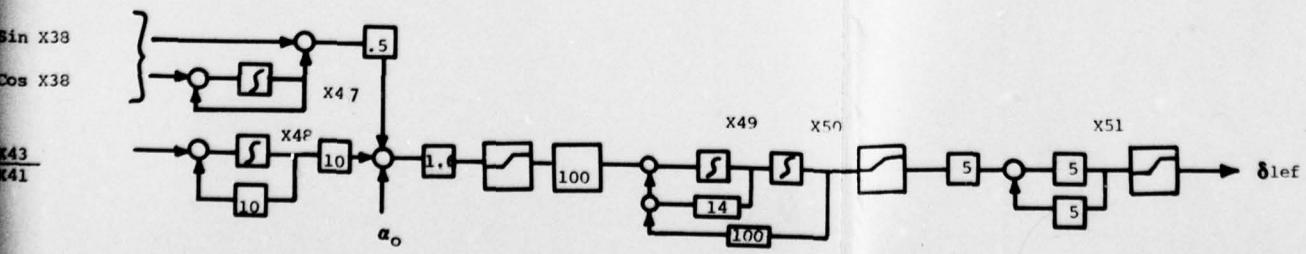
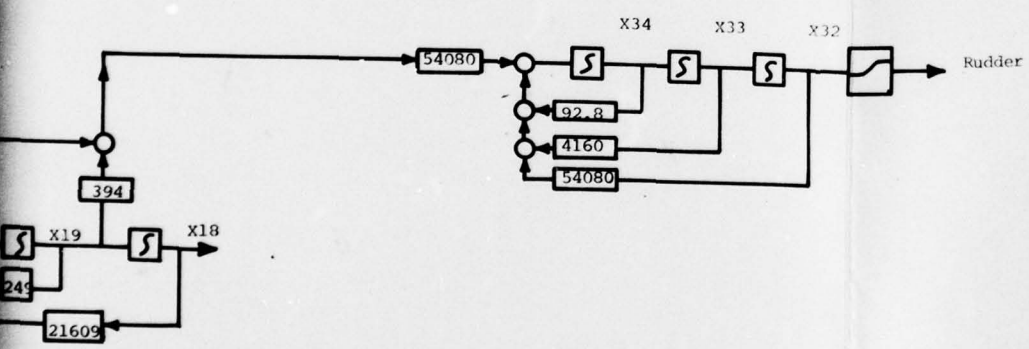
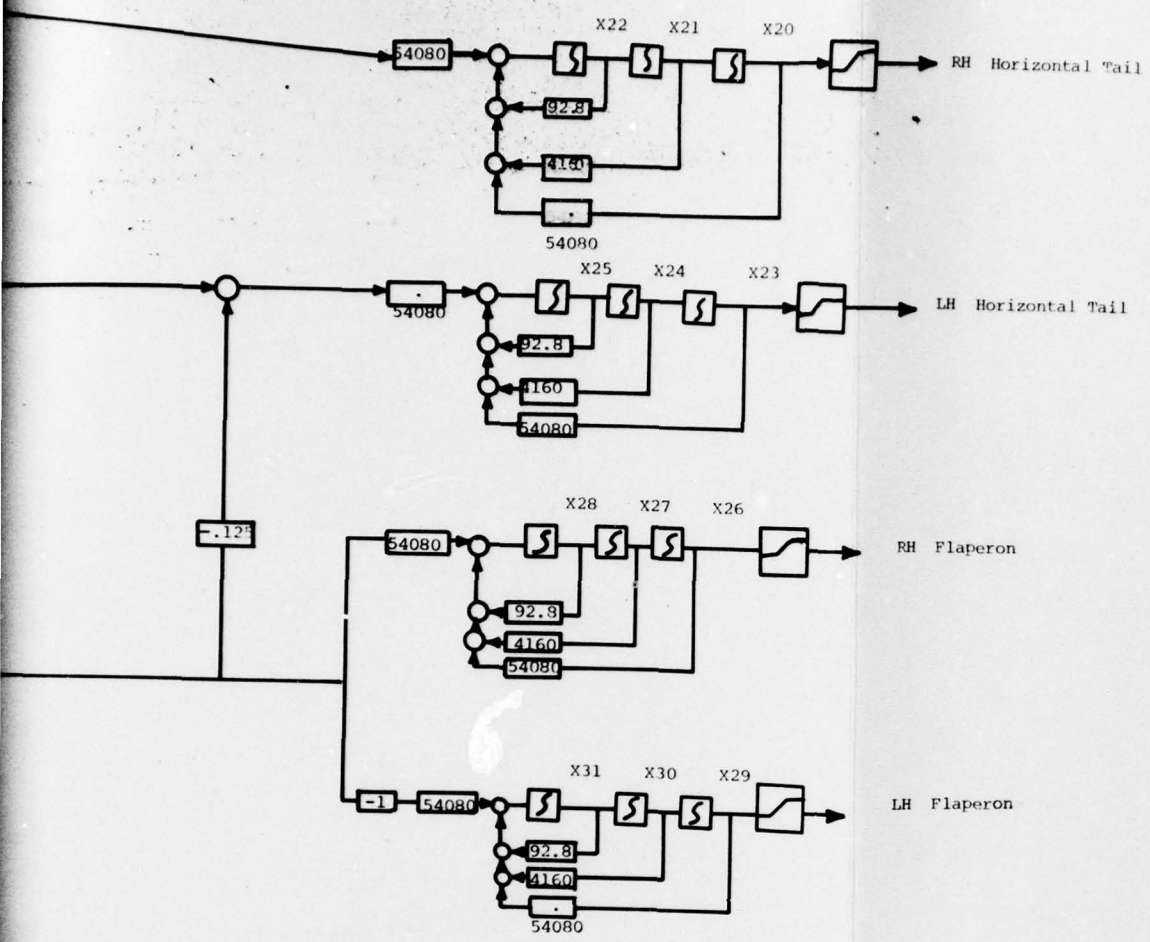
To provide for statistical accuracy of the model, possible sources of errors in the control system and in the equations of motion were identified. Once identified, these sources of error were modeled as accurately as possible using white Gaussian noises and "shaped" (time-correlated) Gaussian noises, with the noise statistics obtained from specifications for the components.

FIGURE 5

FLIGHT CONTROL SYSTEM BLOCK DIA



DIAGRAM



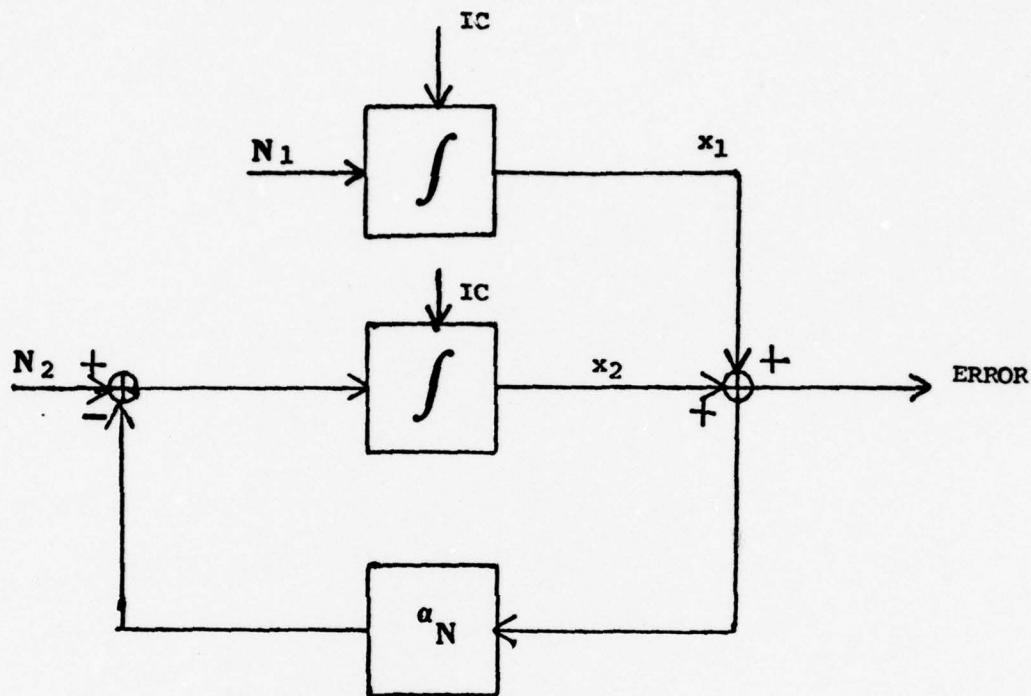
The components considered as possible error sources were

- 1) actuators
- 2) angle of attack sensors
- 3) gyroscopes
- 4) accelerometers
- 5) multipliers

This set was chosen because it influences the inner loop control of the aircraft considered. The components, such as the altimeter, which influence the outer loop, were considered in a different manner. This was necessary because the outer loop contains the human operator, so cumulative errors, the error in the operator's interpretation of a measurement and the error in the device used to obtain and display that measurement to the pilot, must be considered. Because of the difficulty in differentiating these errors, an aggregate error which accounted for both the above errors was considered. This error was modeled through both the decision process of Chapter IV and the Kalman filter of Chapter III, and is explained in more depth in those chapters.

Another source of error considered is wind gusts. The appropriate statistical models for wind gusts were taken from Air Force Specification 8785B (Ref 16). Light turbulence was used throughout the problem as representative of the gust environment most likely to be encountered in the maneuvering regions of the aircraft dynamics.

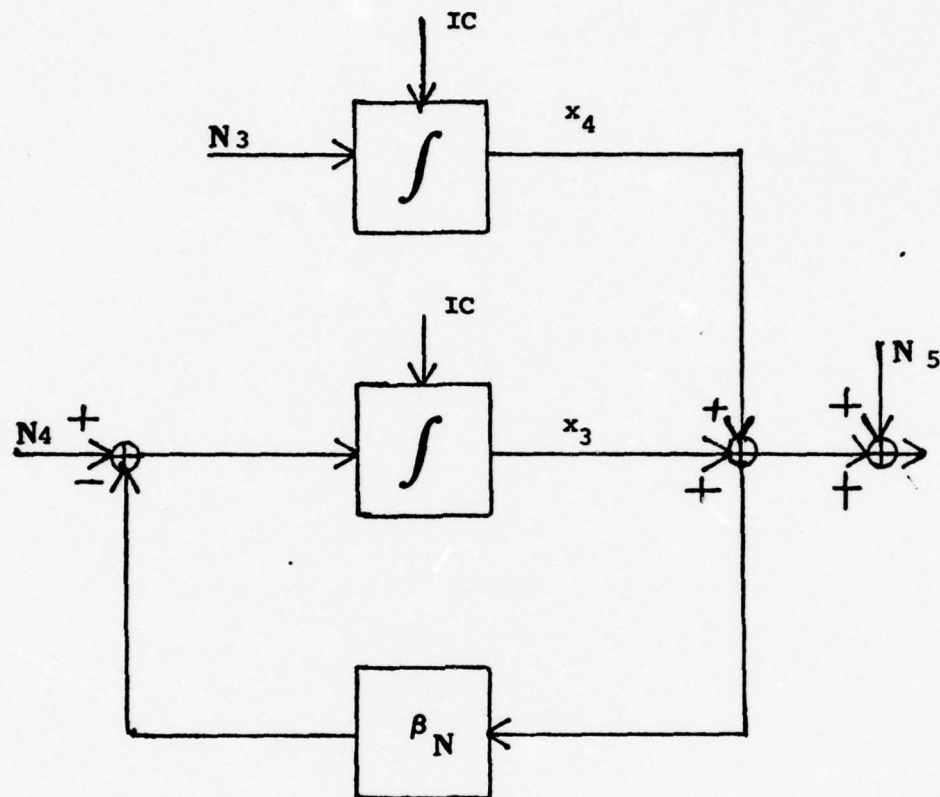
The form of the error models for many of the individual components is given in Britting. (Ref 13) Figure 6 displays the error models for the rate gyroscopes.



RATE GYRO ERROR MODEL
FIGURE 6

N_1 and N_2 are white Gaussian noises. The bias term x_1 represents varying conditions encountered from turn on to turn on, or nonrepeatability, and x_2 represents gyroscopic drift.

The accelerometer error model taken from Maybeck is given in Figure 7. In Figure 7, N_3 , N_4 , and N_5 are white Gaussian noises, x_3 represents an exponentially correlated error component, and x_4 represents accelerometer bias. (Ref 50)



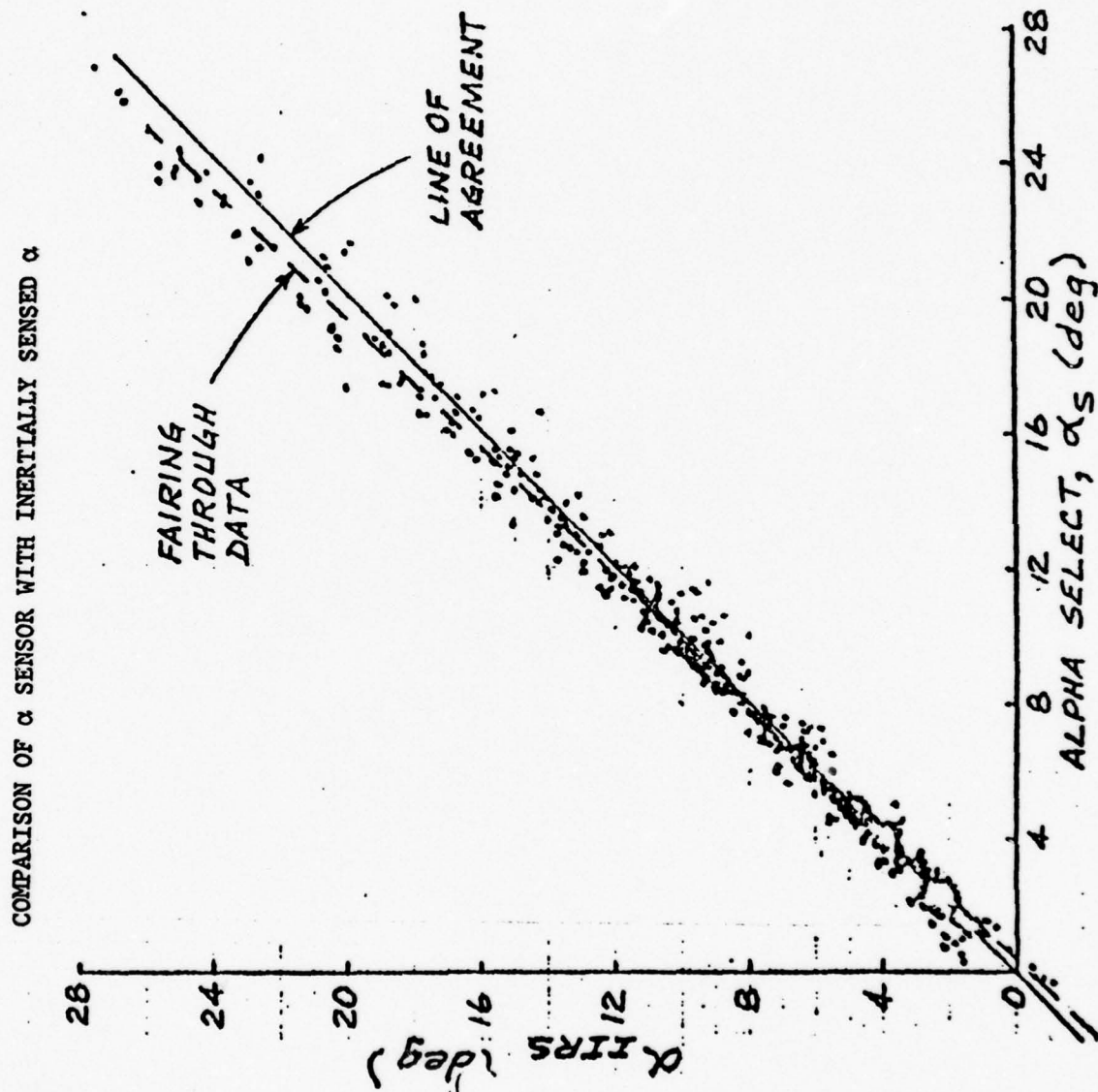
ACCELEROMETER ERROR MODEL

FIGURE 7

One error model represented by the above figures is mathematically included for each physical instrument in the system.

The angle of attack instrument error is represented by simply adding white Gaussian noise to the angle of attack. This noise is dependent on the angle of attack realization. This dependence is assumed from Figure 8 which gives data on a current angle of attack

Figure 8



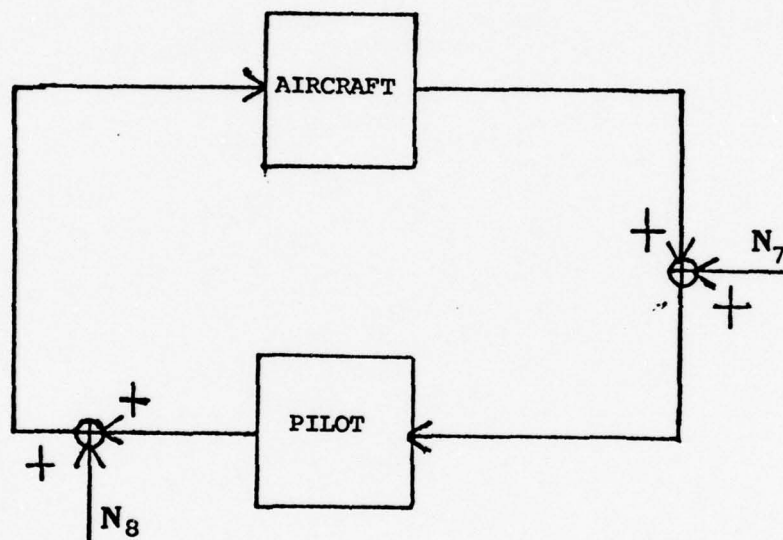
system. The solid line, or "line of agreement", represents angle of attack computed via an onboard inertial system. The dots represent measurements from the actual angle of attack instrument, and the "fairing through data" line represents a smoothed average of these data points. From this chart, assuming that the inertial information is precise, it is apparent that as angle of attack increases, the accuracy of the sensed information is decreased. This was taken into account in the modeling process by allowing the noise strength term to be a function of angle of attack.

The last two error sources, the actuators and the multipliers, were next considered. Using current specifications written for each of these instruments, it was determined that the error sources each instrument introduces to the system were insignificant. That determination was made because at the normal operation signal levels, the signal to noise ratio was so high that when considered with the second or third place accuracy of the aircraft coefficients, effects from these noises were negligible.

The above error sources are identified in the aircraft equations of motion or the aircraft control system. When the pilot is added to the system, other noise sources appear. (Ref 39) The noises are displayed in Figure 9.

Figure 9 is an extremely simplified diagram to show the two predominant noises attributed to the pilot. These noises are observation noise, N_7 and remnant N_8 . The observation noise is assumed white and Gaussian and is attributed to the pilot's imperfect

comprehension of information presented to him by his instruments. The remnant noise is assumed white and Gaussian and uncorrelated with the observation noise, and is attributed to the pilot's inability to position his control input device precisely.



GENERAL PILOT/AIRCRAFT SYSTEM WITH NOISES

FIGURE 9

At this point the aircraft equations of motion have been specified, as well as the control system equations. The coupling of these two sets of equations with their respective error sources constitutes the model block on Figure 2. As mentioned in the intro-

duction, this is a highly nonlinear set of equations which will be analyzed using the small perturbation technique. Appendix 3 details the linearization process necessary for this technique, and Appendix 6 details the parameters used in the simulation.

CHAPTER III

THE OPTIMAL CONTROLLER AND OPTIMAL ESTIMATOR

In this chapter the mechanization of the specific control and estimation methods chosen in Chapter I to portray the human operator mathematically will be specified. This specification will include both the functional representations of the optimal control and the optimal estimation methods employed, and the adaptation techniques which apply those methods to the problem specified in Chapter I. For this task, first the optimal controller will be investigated.

3.1 Optimal Controller

In Appendix 3 the linearization of the aircraft equations is carried out about an assumed nominal operating condition. The output of the linearization is an $A(t)$ and a $B(t)$ matrix which mathematically represents a current fighter-type aircraft. These matrices coupled with a linearized $C(t)$ provide a partial basis for the LQG controller addressed earlier. Unfortunately, due to the time delay, the system when assembled as in Figure 1, is not linear.

As the LQG assumptions are not met, the separation principle inherent in the LQG solution does not apply. This principle states simply that the optimal control problem and the optimal estimation problem can be solved separately and then recombined to produce the

optimal control. (Ref 8) An alternative suggested by Farison, Graham, and Sheldon and evaluated by Ku and Athans can be applied. (Ref 26, 45) That alternative suggests that, even though the LQG assumptions are not met, the problem can still be separated into two problems, the control problem and the estimation problem. After each problem is solved separately, the state estimates are combined with the control gains to arrive at a control for the system. Because of its computational feasibility and its proven success in previous problems, this "forced separation" philosophy was chosen as the control theory basis for the pilot.

A second reason for the forced separation philosophy choice is the size and the complexity of the system being considered. For this problem, each of these factors requires a computational burden large enough that if any route investigated other than forced separation were taken, the amount of computation involved could make the problem intractable.

It is important to note that a forced separation controller was chosen because it is the most tractable as well as the most flexible method available for large linearized systems. The ideal controller would, given the general aircraft equations and the assumed human limitations, solve for a control which when applied to the aircraft equations, would control the aircraft through a specific maneuver. This maneuver would be the result of some type of decision process. Since this type of general control is not tractable with current control methods, only the simplified control methods suggested above were considered.

3.1.1 Control Gains

Since the forced separation philosophy was chosen, the Kalman filter equations and the controller gains must be computed. The computation of the control gain time history will first be considered. For the perturbation case under consideration, the optimal control gains can be computed using the optimal linear regulator format defined in optimal control literature. (Ref 35, 44) The chosen optimal linear regulator requires the control gains to drive the regulated states or linear combinations of states to zero.

The mechanization of the regulator was chosen to be of the continuous form while the mechanization of the estimator, shown later, was chosen to be of the discrete form. This difference in representation allowed some streamlining of the computer model, an aspect that will be discussed later. A rigorous definition of the linear optimal regulator problem can be stated in the following manner:

Consider the linear time-varying system modelled by

$$\dot{\bar{x}}(t) = A(t) \bar{x}(t) + B(t) \bar{u}(t) \quad (3-1)$$

where

$$\bar{x}(t_0) = \bar{x}_0 \quad (3-2)$$

with

$$\bar{z}(t) = D(t) \bar{x}(t) \quad (3-3)$$

Consider also the quadratic performance criterion

$$J = \bar{x}^T(t_f) P_1 \bar{x}(t_f) + \int_{t_0}^{t_f} [\bar{z}^T(t) R_3(t) \bar{z}(t) + \bar{u}^T(t) R_2(t) \bar{u}(t)] dt \quad (3-4)$$

where P_1 is a nonnegative definite symmetric matrix and $R_3(t)$ and $R_2(t)$ are positive definite symmetric matrices for $t_0 \leq t \leq t_f$. Then

the problem of determining the input $\bar{u}^0(t)$, $t_0 \leq t \leq t_f$, for which the criterion is minimal, is called the deterministic linear optimal regulator problem. (ref 44)

The optimal feedback for the deterministic optimal linear regulator problem is generated by the linear control law

$$\bar{u}^0(t) = -F^0(t) \bar{x}^0(t) \quad (3-5)$$

where

$$F^0(t) = R_2^{-1}(t) B^T(t) P(t) \quad (3-6)$$

Here the symmetric nonnegative definite matrix $P(t)$ satisfies the matrix Riccati equation

$$\dot{P}(t) = -R_1(t) + P(t) B(t) R_2^{-1}(t) B^T(t) P(t) - P(t) A(t) - A^T(t) P(t) \quad (3-7)$$

with the terminal condition

$$P(t_f) = P_1 \quad (3-8)$$

and where

$$R_1(t) = D^T(t) R_3(t) D(t) \quad (3-9)$$

The optimal cost to complete the control process from time t is:

$$x^{oT}(t_1) P_1 x^o(t_1) + \int_t^{t_1} [x^{oT}(\tau) R_1(\tau) x^o(\tau) + u^{oT}(\tau) R_2(\tau) u^o(\tau)] d\tau$$

$$x^{oT}(t) P(t) x^o(t) \quad t \leq t_f \quad (3-10)$$

Therefore, by applying forced separation, the controller gain matrix $F^0(t)$ can be determined by Equation (3-6) and applied using Equation (3-5) to obtain the optimal control at time t .

Examining Equations (3-1) to (3-10), it is apparent that though $A(t)$ and $B(t)$ are already specified, $R_3(t)$, $D(t)$, P_1 , and $R_2(t)$ are still free. It therefore becomes necessary either to specify each matrix functionally or to define the use of each matrix numerically. The purpose of this specification is to allow users of the research to understand how each value of each matrix is determined so that a translation of this method to other problems can be achieved. When a numerical value is involved, a general procedure to obtain that value is given, and when a functional representation is involved, such as in $D(t)$, the reason for that selection is outlined.

Consider first $D(t)$. This is the matrix from Equation (3-3) that relates the states to the controlled variables. As the variables to be controlled are already specified as altitude, airspeed, pitch angle, roll angle, and heading it is only necessary to relate these individual quantities to the system states to define the $D(t)$ matrix. For this purpose, pitch angle, roll angle, and altitude are states, so there is a one-to-one relationship for those three controlled variables with system states.

Next consider airspeed, V_{TAS}

$$V_{TAS} = (U^2 + V^2 + W^2)^{\frac{1}{2}} \quad (3-11)$$

The perturbation of Equation (3-11) about a nominal becomes

$$\delta A_S = [U_o^2 + V_o^2 + W_o^2]^{-1/2} [U_o \delta U + V_o \delta V + W_o \delta W] \quad (3-12)$$

where the "o" notation refers to the nominal trajectory value.

The last equation necessary is the equation for yaw angle or

$$\beta = \sin^{-1} \frac{V}{(U^2 + V^2 + W^2)^{1/2}} \quad (3-13)$$

which results in the perturbation equation

$$\begin{aligned} \delta \beta = & \left[\frac{1}{(U_o^2 + V_o^2 + W_o^2)^{1/2}} - \frac{V_o^2}{(U_o^2 + V_o^2 + W_o^2)^{3/2}} \right] \delta V \\ & - \frac{W_o V_o}{(U_o^2 + V_o^2 + W_o^2)^{3/2}} \delta W \\ & - \frac{U_o V_o}{(U_o^2 + V_o^2 + W_o^2)^{3/2}} \delta U \end{aligned} \quad (3-14)$$

The four equations discussed above specify the D(t) matrix.

At this point the matrices that can be specified algebraically are functionally represented; the three remaining matrices for the controller contain system parameters. Those system parameter matrices are the P_1 , R_3 , and R_2 matrices. These matrices represent the Riccati initial condition weighting matrix, the weighting matrix on variables of interest, and the control weighting matrix. Of these matrices, the P_1 matrix value effects are defined first. It must be stressed that since the Riccati Equation solution runs backward in problem time, the initial value matrix, P_1 , for the Riccati Equation actually effects control at the final problem time. This definition involves two aspects of the Riccati equation: the first is that the final value of the Riccati equation is not based on its initial conditions, P_1 , and the second is that, as the Riccati solution is directly related to the control, a high value in a P_1 diagonal term will force a large value of control to be associated with that position during the initial transient phase. That control will emphasize driving the state associated with that particular P_1 matrix value to its desired position. Therefore, using the above insights, the steady state value of the Riccati solution can be computed once the R_2 and R_3 matrices are set. By examining this solution, and determining whether the operator is emphasizing or deemphasizing a particular state in the final phases of a maneuver, the desired P_1 can be determined by increasing the particular steady state value of its associated component if

emphasis is desired and by decreasing the steady state value of its associated component if deemphasis is desired. Using this method the parameters of the controller can be examined for the periods for which they are a factor, that is, the R_2 and R_3 matrices are important in the early real-time stages of problem time or steady state stages of Riccati solution time for a trajectory, and the P_1 matrix is important in the final real-time stage of the trajectory.

This observation was used to develop the methodology to determine the controller parameters numerically. That methodology is explained as follows: the early maneuver control is "tuned" by adjusting the R_1 and R_2 matrices, and the control for the last portion of the maneuver is "tuned" by adjusting the P_1 matrix. "Tuned" refers to a systematic alteration of problem parameters, accomplished to effect overall problem performance in a predetermined manner. This tuning must take into account hard limits on aircraft controls which are represented by setting the weights so that the state limits are not reached. The limits on state were chosen for the "tuning" because the states account for the aircraft controls, throttle movement, aileron, rudder, and elevator, which display the hard limits. The problem controls are the human controls such as stick force or rudder force. Since the aircraft control system interprets these forces up to the force required for maximum surface deflection, and then disregards any excess force, it is very possible for a pilot to exert more force than is necessary for the maximum control deflection. Therefore it was felt that limits on state were more appropriate.

A philosophy for selection of the numerical P_1 matrix values has already been given. The actual selection was done through consideration of a combination of flight experience of the author and AFM 51-37 flight guidelines for permissible maneuver performance, as well as realistic control magnitudes which account for the "hard limits" on control.

One interesting aspect concerning the selection of P_1 matrix values surfaced during value specification for this problem. That aspect, which concerns selecting zero values in specific positions in the P_1 matrix, is detailed in Appendix 4.

The consideration of a final time is inherent in using the P_1 matrix, as its terms are a function of the squares of the individual state values at the final time. This concept of a finite final time is new to the human operator framework. Previous work has considered steady state solutions to Equation (3-7) to specify the control gains. These steady state solutions have always been applied to the realization of the $A(t)$ matrix at the time in question for control, and therefore a knowledge of the future trajectory is not assumed. Kleinman uses this technique in the Vulcan gun problem because the $A(t)$ matrix specifies the evader, and it is realistic to assume that the gun operator does not know, apriori, the trajectory to be flown by the evader. (Ref 40)

In the pilot/aircraft context, many maneuver trajectories are in fact known. Some of these - cloverleaves, Immelmans, barrel rolls, etc. - are practiced by pilots repeatedly for precision. For each

of the above maneuvers, maneuver terminating instruction as per AFM 51-37 is to maintain straight and level flight.

Using the above information, the pilot's control was assumed to have a finite final time, the time when the pilot would return to straight and level flight. A second consideration at this point is the time-invariant versus the time-varying realization of the Riccati equation. By assuming a final time and using the time-varying realization of the Riccati equation it is possible for the human operator to alter his dynamics to account for future changes in the aircraft dynamics. Repeated accomplishment of a specific maneuver would allow for this apriori knowledge of changing aircraft dynamics. Therefore, using this approach, the control philosophy of the pilot was assumed to be based upon a knowledge of trajectory until that final time. This physical interpretation translated directly into the control philosophy specified by Equations (3-1) to (3-19). It is observed that the above assumptions imply a partitioning of each flight into two regions. The first region is that region in which the aircraft perturbation equations are time-invariant or at worst slowly time-varying. The second region, the region discussed in this work, is the region in which the aircraft perturbation equations are acting in a rapidly time-varying fashion. One situation that will force this occurrence is when nonlinearities in the general aircraft equations are predominant. For the maneuvers to which those nonlinearities apply, it is assumed the pilot has an apriori knowledge of both the trajectory and the associated final time.

The final specifications necessary are for the $R_2(t)$ and the $R_3(t)$ matrices. These matrices are respectively the control weighting matrix and the controlled variable weighting matrix. These matrices are assumed diagonal in this work, as is done in most practicable optimal control problems. Examination of quadratic cost optimal control literature gives an indication of what can be expected by varying the individual diagonal values in each matrix. (Ref 3, 44, 54) An outline of that discussion is detailed below, and these insights are used to specify the tuning process used to determine the R_2 and R_3 matrices.

Consider first the R_2 matrix. An increase in the diagonal value of this control weighting matrix associated with a particular control will have the effect of reducing the amount of that control used at that time, since greater penalty is assigned to applied control values in the cost function. Using this relationship, the limit on control available to the human operator can be regulated with these values.

The effect of varying the diagonal value associated with each controlled variable also can be explained in a physically meaningful manner. The higher the weighting value associated with each state, the less excursion from zero that state is allowed. Unfortunately, as these values have interactive effects, a change in one diagonal value of either matrix often has more effect than just a commensurate change in the related control or related controlled variable.

Considering the above background, the major aspect of the control for this problem can be addressed. That aspect is: how to implement the quadratic cost optimal control, assuming that active

control is available to the pilot in only one of the control variables. To answer this question, the existence of a decision process that produces the control variable the human operator has specified for attention for the next time interval is assumed. This decision process will be explained in the next chapter.

Once the decision process has output the control variable for the next time interval, it is desirable for the computed control gain matrix $F^o(t)$ to use this information to accentuate control for the selected control variable. To do this, the cause/effect relationship of the weighting matrices is used. First, the relationship is specified between the aircraft controls available to the pilot and the controlled variables. This linkage is made so that it is possible to respond to increased control variable weighting with the appropriate controls. Four controls are considered in this problem. Those controls are fore and aft control stick movement to control pitch, left and right control stick movement to control roll, throttle movement, and rudder movement. Their respective linkages are

- a) pitch - fore/aft stick movement
- b) roll - left/right stick movement
- c) heading - rudder
- d) airspeed - throttle
- e) altitude - throttle and fore/aft stick movement

It is important to note that the heading will be controlled by rudder rather than by the aileron. This is because with the small corrections desired, it is not feasible to use aileron.

It is apparent that the altitude control variable links to two controls. This presents no problem, since by the control weighting

change philosophy detailed above, the weightings will be decreased on both controls and increased on the altitude state variable to allow for better altitude control.

Therefore, in general, to accomplish the accentuated control on the controlled variable specified by the decision process, the controlled state variable weighting will be increased and the associated control weighting will be decreased, while the remaining weightings stay constant. To this point, the only time addressed has been the time of the decision. However, when Equation (3-7) is examined, it can be seen that the weighting matrices $R_2(t)$ and $R_3(t)$ are required to be specified from the present time until the end of the problem. Earlier in this chapter a similar problem was addressed to determine how to use the $A(t)$ matrix. It was argued that the pilot had an idea of the trajectory to be flown, mathematically resulting in a time-varying $A(t)$ matrix. Using a comparable physical argument, it was decided that the values for $R_2(t)$ and $R_3(t)$ could be considered constant in time, from current time until the final time, for each control variable/control set. Specifically, the physical interpretation is that, though the pilot has an idea of the trajectory for a time interval, he does not have any idea of the random trajectory perturbations he is to experience for that time interval. Therefore, as the decision process reacts to error states, it is logical to assume that the specific control the pilot is accentuating now is the control he anticipates accentuating until the end of the problem. That allows Equation (3-7) to be solved backward in time from Equation (3-8), using constant values for R_2 and R_3 .

Another asset, precomputation, is realized by prespecifying five specific R_2 , R_3 matrix sets, each of the five corresponding to a particular control variable emphasis. With the matrices pre-specified, Equation (3-7) is precomputable from the terminal condition P_1 . Therefore, precomputing this equation five times, each time with the specific R_2 and R_3 matrix set identified for each control variable, and applying the result to Equation (3-6) produces five sets of F^0 time histories. Therefore when the decision process identifies a specific control application, the specific F^0 history corresponding to that application is accessed. Once the proper set is accessed, the decision time is considered and the particular $F^0(t)$ evaluated for that time. The control block of Figure 1 is therefore specified by a control gain matrix.

The last aspect of the control process to be considered is the realizations of the individual values of the R_2 and R_3 matrices. This also considers the control lag block of Figure 1. By introducing an added state for each control and setting the time derivative of that state equal to the control, Kleinman was able to include two favorable properties in the human operator problem. The first was that weighting could now be considered on control rates, an aspect felt pertinent for human control. The second was that data is available for the neuromuscular lag of the human operator. This data indicates that the lag has a time constant of between .1 and .4 seconds. (Ref 4,42) By using this extra state, the appropriate R_2 weighting can be related to the neuromuscular time constant, so that

one of the problem parameters is specified. Therefore, by selecting two desired neuromuscular time constants, one for when the pilot is attending to the specific control and one for when he is not attending to that specific control, the R_2 matrix is specified. Unfortunately, because of the interaction of R_2 and R_3 , this involves a trial and error process to realize the desired neuromuscular time constant. The trial and error process used was to vary the appropriate elements of the R_2 matrix one at a time until the desired neuromuscular time constant was achieved. The R_2 elements were varied in succession with no earlier element repeat until all elements had been set. Repeated iterations through the R_2 terms were anticipated because of element coupling. After all elements had been set, it was planned that any elements driven to an unacceptable value by succeeding element changes would be reconsidered. In practice this process was not needed, as the element coupling contributed to, at worst, the second significant figure of each neuromuscular time constant. Therefore, after one computation cycle the R_2 matrix values were set.

3.2 Estimation

In the control section above, the methodology for determining $F^0(t)$ was defined. To complete the control computation for perturbation states from Equation 3.5, an estimation of the vector $\delta \bar{x}$ must be made. The determination of this vector has taken two forms in optimal control pilot modeling. The first method, used in most steady state tasks, assumes that the time delay is negligible and therefore

does not assume a time delay for the pilot model. The second method, the method applied in this research, assumes the time delay is critical to the problem, making a Kalman filter necessary. This last assumption is made because the transitory nature of the problem and a highly maneuvering trajectory requires a high pilot workload. This workload requirement should force the .2 second time delay usually assumed for information processing, to be an essential part of the problem. (Ref 39)

The approach taken to define the estimation process will be the same as the approach taken to define the control problem. First the equations for the Kalman filter will be stated, and then an explanation given of how each element of the equations was realized. Derivation of the Kalman filter equations is given in numerous sources and will not be duplicated here. (Ref 50, 54) Only the equations mechanized to accomplish the prediction and correction elements of the Kalman filter function will be stated.

The form of the equations necessary for the Kalman filter computation is given below.

$$\dot{\bar{x}}(t) = A(t) \bar{x}(t) + B(t) \bar{u}(t) + G(t) \bar{w}(t) \quad (3-15)$$

$$\bar{z}(t_1) = C(t_1) \bar{x}(t_1) + \bar{v}(t_1) \quad (3-16)$$

where

$$E(\bar{v}(t_1)) = E(\bar{w}(t)) = 0 \quad \text{all } t, t_1 \in T \quad (3-17)$$

$$E(\bar{v}(t_1) \bar{v}^T(t_j)) = \begin{cases} R(t_1) & t_1 = t_j \\ 0 & t_1 \neq t_j \end{cases} \quad (3-18)$$

and

$$E[\bar{w}(t) \bar{w}^T(s)] = Q(t) \delta(t-s) \quad (3-19)$$

$$E[\bar{w}(t) \bar{v}^T(t_1)] = 0 \quad \text{for all } t, t_1 \quad (3-19a)$$

i.e.: $\bar{\delta x}(t_0)$ Gaussian, mean $\hat{\delta x}_0$, covariance P_0

v and w independent of $\delta x(t_0)$

The equations in Chapter II are of this form, and all noises are assumed white and Gaussian in this research. In the control portion of this chapter the noises are not considered because, as forced separation is assumed, no noise description is necessary.

For the measurement update (corrector) the necessary equations are

$$K(t_1) = P(t_1^-) C^T(t_1) \left[C(t_1) P(t_1^-) C^T(t_1) + R(t_1) \right]^{-1} \quad (3-20)$$

$$\hat{\delta x}(t_1^+) = \hat{\delta x}(t_1^-) + K(t_1) \left[\xi_1 - C(t_1) \hat{\delta x}(t_1^-) \right] \quad (3-21)$$

$$P(t_i^+) = P(t_i^-) - K(t_i) C(t_i) P(t_i^-) \quad (3-22)$$

For these equations the notation t_i^- refers to the appropriate matrix or vector at time t_i before measurement incorporation, and t_i^+ refers to the appropriate evaluation at time t_i after measurement incorporation.

The δx notation refers to the optimal estimate of the state vector δx , and $P(\cdot)$ refers to the covariance of the state $\delta x(\cdot)$, equal to the covariance of errors committed by the state estimate. The predictor equations are

$$\hat{\delta x}(t_i^-) = \Phi(t_i, t_{i-1}) \hat{\delta x}(t_{i-1}^+) + \int_{t_{i-1}}^{t_i} \Phi(t_i, \tau) B(\tau) \delta u(\tau) d\tau \quad (3-23)$$

$$P(t_i^-) = \Phi(t_i, t_{i-1}) P(t_{i-1}^+) \Phi^T(t_i, t_{i-1}) + \int_{t_{i-1}}^{t_i} \Phi(t_i, \tau) G(\tau) Q(\tau) G^T(\tau) \Phi^T(t_i, \tau) d\tau \quad (3-24)$$

At this point an explanation is in order. The assumption has been made that F° discrete and F° continuous are approximately equal. With this assumption the above equations depict a discrete-time estimator, while the controller equations, equations (3-1) to (3-10) depict a continuous controller. This assumption was made to keep the amount of computation required at a minimum. As the controller gains could be computed separately and integrated efficiently because of the simplifications explained in Appendix 1, they were computed with the continuous formu-

AD-A066 193

AIR FORCE INST OF TECH WRIGHT-PATTERSON AFB OHIO SCH--ETC F/G 1/3
AN ADAPTIVE CONTROLLER WHICH DISPLAYS HUMAN OPERATOR LIMITATION--ETC(U)
NOV 78 E K LINDBERG
AFIT/DS/EE/78-1

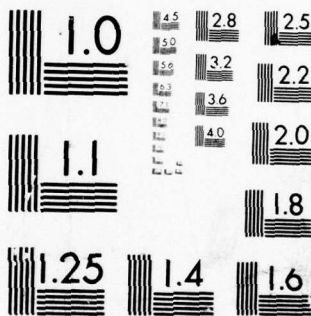
UNCLASSIFIED

NL

2 OF 4

AD
A066 193





MICROCOPY RESOLUTION TEST CHART
NATIONAL BUREAU OF STANDARDS-1963-A

lation. Though the formulation does not give the exact LQG control, it is felt that the reduced computation involved was worth the reduced precision. This computation reduction via the continuous formulation is due to the necessity to generate a state transition matrix, for the controller separate from the state transition matrix used in the Kalman filter. This is necessary because of the augmented state space used to generate control rate terms in the cost functional. It was found that to generate the state transition matrix, even though it was a one time operation, was much less efficient than to generate the control gains directly from the continuous Riccati equation. Because of the special estimator form imposed by the decision process, precomputed Kalman filter gains could not be used. It was necessary for the estimator therefore to be computed "on-line". By using the discrete formulation, "on-line" computation can be reduced since integration can be replaced by multiplication using the state transition matrix. Therefore the discrete Kalman filter formulation was used for the estimation task.

Initial conditions are

$$P(t_0) = P_0 \quad (3-25)$$

$$\hat{\bar{\delta}x}(t_0) = \bar{0} \quad (3-26)$$

From Equations (3-15) to (3-26) $B(\tau)$ and $G(\tau)$ are specified as in Chapter II and the state transition matrix $\Phi(t_1, t_{1-1})$ is determined from $A(t)$ which is also specified in Chapter II. An

elaboration of the actual state transition matrix determination is given in Appendix 1. The $\bar{u}(\tau)$ term is the control computed at the last computation time and is assumed constant between control computation times.

$\xi_j(t_1)$ is the actual measurement available at time t_1 .

At time point, three matrices are left to be determined, $Q(t)$, $R(t_1)$, and $C(x, t_1)$. It is necessary to note that the conditioning on the state, x , implies conditioning on the decision process. This aspect will be discussed later. The $Q(t)$ and $R(t_1)$ matrices are matrices consisting of parameters for this system; however, as in the case of the controller, some guidelines are available.

The $Q(t)$ matrix is assumed diagonal for this problem, an assumption generally made unless some specific problem insight is available that suggest non-diagonal terms. This matrix, once specified, will be assumed constant and therefore time-invariant for the problem. The diagonal terms for the Q matrix correspond to the expected value of the square of the respective error states, as given Equation (3-19). These values were determined by author experience and AFM 51-37.

A similar process was used for determining the values of $R(t_1)$. The matrix was assumed diagonal, and the individual values were determined by taking the expectation of the square of the measurement errors. Because the measurements involve a human operator as the measuring device, it is impossible to predict these errors with complete accuracy. The prediction was therefore done using personal experience and guidelines presented in human operator literature. (Ref 2,24) $R(t_1)$ will be time-varying due to the $C(x, t_1)$ variations described next.

At this point in time the measurements that the pilot samples in the aircraft as well as the method the pilot uses to process those measurements is not well defined. For the purposes of this research, these measurements will be divided into three groups: direct visual, peripheral visual, and secondary.

Extensive research is being accomplished in each of the three groups to define the pilot measurement process further. Curry and Young are developing sensor models for a number of the secondary sensors. Their work involves modeling the vestibular sensors, but presently does not include the processing of those sensors' outputs. (Ref 19) Peripheral visual experimentation has resulted in answers to some generally applicable questions, but little work on a peripheral visual sensor model has been accomplished.

(Ref 19) Some experimentation has been accomplished on the visual system which has resulted in definition of human thresholds of visual perception, as well as information on human scanning characteristics.

(Ref 2)

Using this research and the structure imposed by the human operator assumptions in the introduction as background, a method for arriving at an estimate of the error states was formulated. This formulation was based upon the assumption that an output from the decision process would specify the channel receiving the attention at a specific time. The channels for consideration are altitude, airspeed, pitch, roll, and heading. Most of these channels translate into distinct observations of flight instruments, the exception being roll

and pitch. These channels are displayed on the same instrument, but measurements are read from separate indices on that instrument, which preserves the individual measurement identity. Therefore, though the decision process is assumed to output attention and not eye position, a correlation is apparent. This fact is also used to aid in parameter determination in the decision process, an aspect discussed in the next chapter.

This correlation is also used in the definition of the observation matrices, $C_j(x_0, t_1)$ ($j = R, P, H, V, A$). The R, P, H, V and A correspond to the matrices where roll, pitch, heading, velocity, and altitude are available, and those matrices are defined below. As it is assumed that full attention cannot be given to all channels equally, and the decision process outputs the attention channel, that channel will also be the observed channel. The physical measurements that correspond to each attention or observation channel are

- altitude - altitude indication
- pitch - pitch angle, pitch angle rate indications
- roll - roll angle, roll angle rate indications
- heading - heading angle indication
- airspeed - airspeed indication

These measurements were used because of the trajectory chosen. In that trajectory it was felt that aircraft orientation was the crucial aspect to the pilot, therefore pitch and roll had not only angles, but also angle rates. It is expected that rate information could be necessary on altitude, heading, and/or airspeed depending upon the specific trajectory chosen. The next step is to define the $C_j(x_0, t_1)$

matrix functionally for the above physical measurements. There is a one-to-one correspondence between states and measurements on all the values except airspeed and rates, and the airspeed measurement is defined by Equation (3-12). Since for this trajectory, roll angle and pitch angle are small, pitch angle rate and roll angle rate correspond respectively to states Q and P.

Identifying these direct visual channels leaves measurements in the peripheral visual system and secondary systems to be considered. Two assumptions are made about these two systems. The first is that the measurement accuracy of those systems is not as good as the measurement accuracy of the direct visual system. The second assumption is that the information from these two systems is available at each discrete time. That is C contains these measurements at each measurement time unlike the visual measurements which are available only when the particular channel is receiving attention.

The last assumption, implied in preliminary work by Curry and Young, is physically appealing from personal experience. (Ref 19) That assumption is embodied in this research by a grouping of the secondary systems and the visual peripheral system to provide measurements of lateral and normal accelerations. From flight experience, a continuous measurement of these quantities appears realistic, as long as the measurements are not considered to be accurate.

An important aspect in defining the above measurements is that they are at the pilot position and not at the aircraft body axis origin. This involves a translation from body axis to the pilot position for

the acceleration terms. The perturbation equations for normal and lateral acceleration errors are given below:

$$\delta A_n = \frac{\partial A_n}{\partial Q} \delta Q + \frac{\partial A_n}{\partial \phi} \delta \phi + \frac{\partial A_n}{\partial \theta} \delta \theta + \frac{\partial A_n}{\partial u} \delta u \quad (3-27)$$

$$\delta A_L = \frac{\partial A_L}{\partial u} \delta u + \frac{\partial A_L}{\partial v} \delta v + \frac{\partial A_L}{\partial w} \delta w \quad (3-28)$$

Therefore, five observation matrices have been specified.

Those five are

1. normal and lateral acceleration, pitch, pitch rate; $C_p(x_0, t_1)$
2. normal and lateral acceleration, roll, roll rate; $C_R(x_0, t_1)$
3. normal and lateral acceleration, heading; $C_H(x_0, t_1)$
4. normal and lateral acceleration, airspeed; $C_V(x_0, t_1)$
5. normal and lateral acceleration, altitude; $C_A(x_0, t_1)$

The decision process specifies the particular matrix, and the realization of that matrix is the $C_j(x, t_1)$ matrix to be used in the update equations. The appropriate $R_j(t_1)$ must be used in conjunction with $C_j(x, t_1)$ to assure that the measurements are aligned with their associated noises. It is important to note that these matrices, $R_j(t_1)$ and $C_j(x, t_1)$ are considered fixed for each decision, that is they only vary because the decision outcome has changed them from one representation to another, or because the $C_j(. , .)$ matrix is a function of the nominal trajectory.

The pilot model has now been specified except for the decision process. For completeness it should be noted that other mechanizations of the C matrix are available. One mechanization which was considered was to specify the C matrices and corresponding R matrices as above but allow those matrices to cycle rather than be chosen by a decision process. This method was not chosen because it would not allow the human operator to dwell on an instrument which displays information which requires attention.

At this point by the mechanization chosen the only restriction on that process is that it produce a decision for emphasis on one of the five possible channels - pitch, roll, heading, airspeed, or altitude. Because of the implementation considered in this research, this one decision then specifies attention position, control position, and eye position. As mentioned earlier it would not be difficult to expand the mechanization to a separate decision process for each, but because of the added complexity, and the lack of empirical data to define this expansion, only the one-decision case was used.

CHAPTER IV

THE DECISION PROCESS

In the preceding chapter, the approach used for both the controller and the estimator assumed the existence of a decision process. The substance of the decision process was not specified, but the output of the process was required to be the channel of control and attention that required emphasis.

Figure 10 amplifies the decision process portion of Figure 2. This Figure displays each of the individual elements of the decision process addressed in this chapter, and the interrelationships. Some examination of that interrelationship is necessary for this diagram.

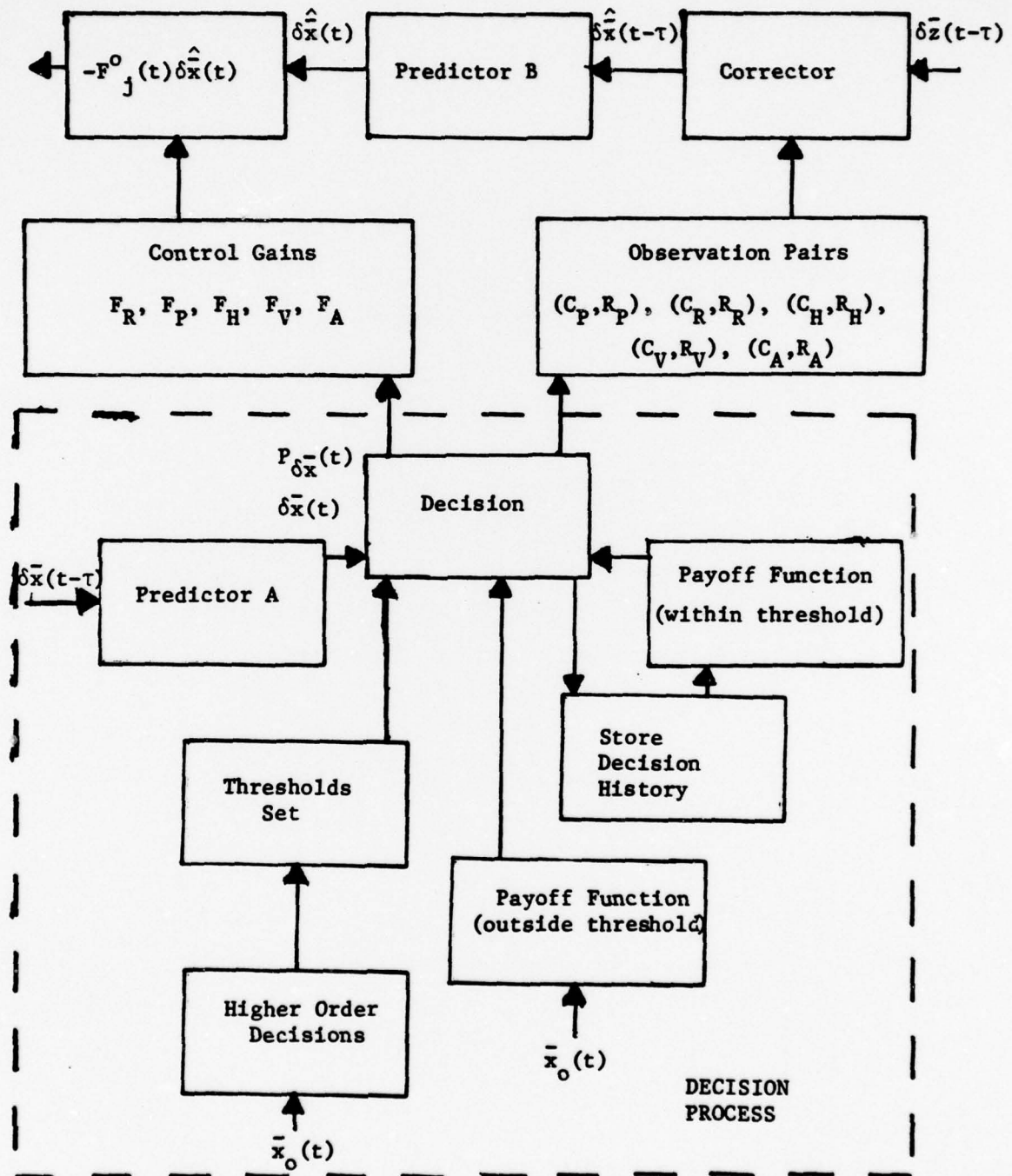
The decision process outputs a specific decision (j) from the set (P, R, A, H, V) . i.e., (Pitch, Roll, Altitude, Heading, Velocity). This decision sets the control gain matrix F_j and the observation matrix pair (C_j, R_j) . These realizations allow computation of the Kalman Filter/controller combination.

The inputs to the decision process are the nominal trajectory $\bar{x}^0(t)$ and the delayed aircraft states $\bar{x}(t - \tau)$, both defined in Figure 2. Each of the other elements will be defined later in the chapter, but a short discussion of these elements here should help understand that definition. The nominal trajectory defines the higher order decisions which in turn sets the thresholds. The nominal trajectory also specifies the payoff for being outside threshold.

The payoff for lying within threshold is dependent upon the history of the past decisions.

Figure 10

Decision Process Functional
Block Diagram



The last element of the decision process is the set of internal estimates of the states and their covariance. Input to the Predictor A which supplies these elements are the delayed state values of Figure 2.

Figure 10 and this discussion should add clarity and coherence to the succeeding analysis of the decision process.

4.1 DECISION THEORY

In the introduction it was mentioned that five modes of decision making were evaluated. Two of those modes, dynamic programming and the Jaffer and Gupta approach, were examined but not used. (Ref 65, 35) The third mode, Bayesian decision function theory, was selected as the basis for the decision necessary in this research. (Ref 56) As explained in the introduction, this was because of its computational feasibility and problem adaptability.

The two other approaches considered, a cueing approach used by both Pollard and Onstatt and a fuzzy set approach examined by Jain were to have limited use in formulating the decisions in this research. (Ref 58, 56, 36) The fuzzy set approach can be used when no definite measure of probability is available for decision determination. This approach requires general descriptors such as poor, fair, or good of the possibility of occurrence of states of nature in a decision process in lieu of a probability of occurrence. (Ref 36) This process lends itself to higher order decisions that will be discussed later in this chapter.

The cueing approach taken by Pollard considers the length of time since a channel was last attended and the deviation of each channel from the nominal. Though the cue method was not employed in this research, Pollard's work provided some of the concepts used in the Bayesian approach. Those concepts will be detailed later.

As mentioned earlier, one purpose for imposing a mathematical model structure that closely aligns with the physical system is to aid in parameter identification in the mathematical mode. For this purpose, informal research was conducted into the structure of the decision process employed by the pilot. This research included conversations with numerous pilots as well as a thorough examination of the manuals that govern the training for and the grading criteria applied to maneuver accomplishment. An important result of this research was that in almost every case a hierarchal structure was identified. The hierarchy can be traced backward to the decision to get into the aircraft, on one extreme, and forward to the channel to be controlled, on the other.

4.2 HIGHER ORDER DECISIONS

For the pilot modeling task considered, that research led to a two-step decision process. The first step of the process is to determine the function the aircraft is performing. Possible functions are:

- 1) Take-off and climbout
- 2) Enroute

- 3) Air-to-air encounter
- 4) Air-to-ground encounter
- 5) Air drop (munitions or cargo)
- 6) Descent
- 7) Approach
- 8) Landing

Once the function determination is made the next step is to determine the channel to which attention and control are directed. The possible decision channels are pitch, roll, heading, airspeed, and altitude.

The specification of this tiered decision approach, with the function decision necessary before the channel decision, allows the structure suggested by most pilots and specified by regulation. This structure demands more accuracy for particular channels in some phases of flight and less accuracy for those channels in other phases. An excellent example of this is the contrast between the crosstrack requirements in the enroute flight function and the crosstrack requirements in the approach function. Because high altitude airways are generally 10 miles wide in the enroute function, precision is not necessary. In the approach phase, assuming that the instrument landing system is used, the crosstrack precision must be considerably less than 100 feet when under 500 feet in altitude.

The above example demonstrates the necessity for identifying the flight function in order to specify tolerances. If this function decision were to be used in the mechanization, the fuzzy set approach

would be an excellent vehicle for instituting that decision. In this research all the higher order decisions are considered fixed by the selection of a trajectory which would be considered of an air-to-air type. If a generalization of this or a like problem was desired for higher order decisions, the fuzzy set approach would be the means chosen to implement those decisions.

The flight functions in the higher order case can be considered as sets such that the boundaries between the functions are not distinctly defined, a condition that readily leads to the fuzzy set approach. An example of this is that by separating the possible functions into sets such as air-to-air, air-to-ground, air refueling, enroute navigation, and terminal navigation sets, indistinct boundaries related to states can be identified for each set. A combination of fuzzy set theory and physical system understanding can then be employed to establish a measure that will identify the set most likely in use by the pilot. After this measure is applied at each time, t_i , the flight function most likely being used by the pilot is identified.

Once the function decision has been made, the channel decision becomes realizable. As mentioned, the Bayesian decision function was chosen as the means of generating the appropriate decision. In the following explanation, the structure of that decision process will be defined, and the individual elements of the structure will be specified.

4.3 BAYESIAN DECISION FUNCTION APPROACH

The structure of the decision process can best be defined by a decision tree, a mechanism used extensively in the decision theory literature. (Ref 70) This tree is given in Figure 11.

4.3.1 Decision Space

The set of possible occurrences, the state space of the decision process, is defined as

$$\theta = [\theta_R, \theta_P, \theta_H, \theta_V, \theta_A] \quad (4-1)$$

where

$$\theta_R = [\theta_{R0}, \theta_{R1}] \quad (4-2)$$

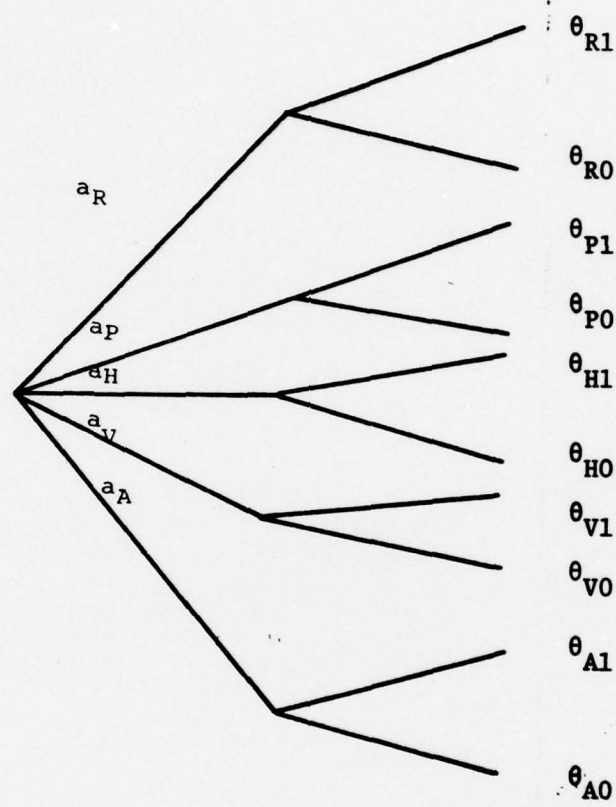
$$\theta_P = [\theta_{P0}, \theta_{P1}] \quad (4-3)$$

$$\theta_H = [\theta_{H0}, \theta_{H1}] \quad (4-4)$$

$$\theta_V = [\theta_{V0}, \theta_{V1}] \quad (4-5)$$

$$\theta_A = [\theta_{A0}, \theta_{A1}] \quad (4-6)$$

Figure 11
DECISION TREE



θ_R is the roll state space, θ_P is the pitch state space, θ_H is the heading state space, θ_V is the airspeed state space and θ_A is the altitude state space. The first state in each set refers to that portion of the state space below a specified threshold, the second state is that portion of the state space above the specified

threshold. For example, θ_{RO} refers to the roll state in which the roll channel error is below a specified roll threshold. θ_{R1} refers to the roll state where the roll channel error is above that specific roll threshold.

4.3.2 Possible Decisions

The set of possible decisions, the decision space of the decision process, is defined as

$$A = [a_R, a_P, a_H, a_V, a_A] \quad (4-7)$$

where a_R refers to the decision to control roll, a_P to the decision to control pitch, a_H to the decision to control heading, a_V to the decision to control airspeed, and a_A to the decision to control altitude. When the state space is coupled with a decision, a measure of benefit to the decision maker can be hypothesized. For instance, given that the decision was made to control pitch, the benefit or payoff of lying within the tolerance threshold for pitch would be substantial, whereas the benefit for not being within the tolerance threshold for pitch would be slight. An alternate representation would be to allow negative payoffs, however as specified in (4-8) negatives will not be allowed.

4.3.3 Payoff Function

The mathematical definition of this payoff function is

$$u_{ij} \quad (i = R, P, H, V, A; j = 0, 1)$$

This function specifies a positive real number to correspond with each action $a_i \in A$ and each state $\theta_{ij} \in \Theta$. This function is defined by

$$u: A \times \Theta \rightarrow R^+$$

(4-8)

The numerical evaluation of this function is generally subjective. (Ref 70) For the decision process employed in this work, the evaluations of the payoff function will be partially subjective, because the experimental research literature on human operator measurement choice between aircraft instruments yields no usable information. The objective feature of this decision process is based on results on average and minimum instrument dwell times. Using this information, the payoff functions at any time t_1 specify the exact instrument and control attended. When each attention position is noted over the total problem time, it is possible to calculate the average dwell times and the minimum dwell time and assure these values are consistent with previous research. No attempt will be made to match a specific attention pattern, because previous research implies that, unless an unusual event such as an engine failure occurs, attention patterns are unlikely to display repeatability.

4.3.4 Probability Function

The final requirement for the formal structure is a probability function $p(\cdot)$, where $p(\cdot)$ is the probability that the state θ_{1j} occurs. The requirements for $p(\cdot)$ are, for

$$\theta_1 = [\theta_{10}, \theta_{11}] \quad (4-9)$$

that

$$a) p(\theta_{j0}), p(\theta_{j1}) \geq 0 \quad (4-10)$$

$$b) p(\theta_{j0}) + p(\theta_{j1}) = 1 \quad (4-11)$$

The quadruplet (A, θ, p, u) is defined to be a single-stage decision process. The Bayesian decision function approach involves a mapping of the quadruplet into the positive reals.

This function uses probabilities to weight the state payoffs. The payoff for being within threshold is multiplied by the probability of being within threshold; the resultant reduced payoff accounts for the fact that it is not certain that that payoff is realized. The same multiplication (payoff times probability) is performed for not being within threshold. Adding the two products produces a revised cumulative payoff for the state. This process is the Bayesian decision function approach; it yields the following payoffs, L_1 , for each decision:

$$L_1 = u(a_R, \theta_{R0}) p(\theta_{R0}) + u(a_R, \theta_{R1}) p(\theta_{R1}) \quad (4-12)$$

$$L_2 = u(a_P, \theta_{P0}) p(\theta_{P0}) + u(a_P, \theta_{P1}) p(\theta_{P1}) \quad (4-13)$$

$$L_3 = u(a_H, \theta_{H0}) p(\theta_{H0}) + u(a_H, \theta_{H1}) p(\theta_{H1}) \quad (4-14)$$

$$L_4 = u(a_V, \theta_{V0}) p(\theta_{V0}) + u(a_V, \theta_{V1}) p(\theta_{V1}) \quad (4-15)$$

$$L_5 = u(a_A, \theta_{A0}) p(\theta_{A0}) + u(a_A, \theta_{A1}) p(\theta_{A1}) \quad (4-16)$$

4.3.5 Payoff Functions

As the final step, a comparison of L_1 's is necessary to determine which has the largest value or payoff. The decision that corres-

ponds to the largest value is then chosen as the decision to be conveyed to the estimator and the controller for the required structure specification of each.

The above approach satisfies the mathematical requirements for the Bayesian decision function method. The appropriate structure is therefore set; the individual parameters must now be identified. Because the structure was chosen to correspond closely to the actual decisions made by the human operator, physical interpretations will be used to identify some model parameters. Some of these physical interpretations are very similar to those employed by Pollard and Onstatt, and to a degree account for a cueing process employed by each. (Ref 56, 58)

4.4 DECISION REALIZATION

The parameters yet to be specified are $p(\cdot)$ and $u(\cdot, \cdot)$, and the thresholds described later which determine $p(\cdot)$. The appropriate probabilities are the probability that a channel is within threshold $p(\theta_{i0})$ or that it is out of threshold $p(\theta_{i1})$. The threshold required is a parameter for the problem and will be varied in two ways. The first way that the threshold can be varied is by the type of instrument that displays that threshold to the pilot. The reason for this variation is evident: if the pilot can visually detect a one-degree variation in pitch on one type of instrument but can see only a two-degree variation in pitch on another similar instrument, his error threshold will be greater for the second. The second determinant of threshold is the flight function effect noted earlier. Because

the air-to-air flight function is the only function to be considered for this discussion, it is assumed that the trajectory errors the pilot will accept before he responds are constant for this problem.

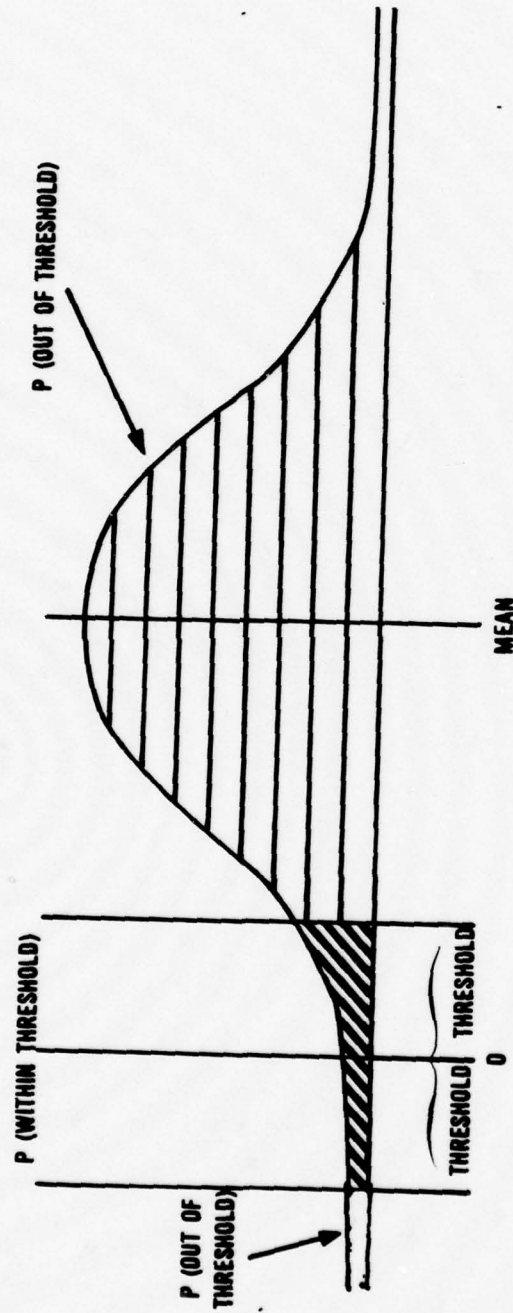
It is important to note at this point that though the thresholds are considered parameters of this system, some information is available to aid in their determination. With no indifference on the part of the pilot considered these thresholds correspond to visual perception thresholds, a quantity well defined once given a specific instrument and a specific distance for that instrument from the viewer. In this problem no added error is assumed for indifference because the urgency of the air-to-air function suggests that once an error is identified, it will be acted upon. (Ref 34) One factor not considered but deemed necessary for further model usage is peripheral vision thresholds. As pertinent literature was not found dealing with thresholds for subjects who were not viewing the instrument in direct vision, only the direct vision thresholds were used. Experimentation in this area would enhance model applicability.

Once the thresholds are determined, considering instrument distance and instrument size for each channel, the probability of each state can be determined. This is done using both the predetermined threshold and the Kalman filter statistics for the states corresponding to each channel. It is important to note that the channels that have corresponding error states are roll angle, pitch angle, heading angle and altitude. Airspeed, however,

is not one state, but a combination of three states. To simplify this variable, it is assumed that the major contribution of airspeed is from the body x-axis velocity. The statistics of this velocity will therefore define the airspeed channel error state. Therefore, error-state means and error-state standard deviations are available for each of the above channels from the Kalman filter conditional density functions. Figure 12 illustrates the appropriate probability determination.

It is necessary at this point to explain one aspect of the Predictor A - decision process link. That aspect is that Predictor A outputs a conditional probability density function, that is a probability density function conditioned on measurements history, control history, and in this forced separation case, past decisions. Therefore in the decision process, $p(\cdot)$ are conditional probabilities that the state is either not in or in threshold. This conditional nature is consistent with the mathematical probability definition necessary for the decision process, and adds physical significance to the process. This is due to the fact that the payoffs used are also conditioned on the past problem history and therefore the definition of the probability applied to those payoffs is consistent with the payoff definition.

FIGURE 12
PROBABILITY DETERMINATION



is not one state, but a combination of three states. To simplify this variable, it is assumed that the major contribution of airspeed is from the body x-axis velocity. The statistics of this velocity will therefore define the airspeed channel error state. Therefore, error-state means and error-state standard deviations are available for each of the above channels from the Kalman filter conditional density functions. Figure 11 illustrates the appropriate probability determination.

It is necessary at this point to explain one aspect of the Kalman filter estimate - decision process link. That aspect is that the Kalman filter outputs a conditional probability density function, that is a probability density function conditioned on measurements history, control history, and in this forced separation case, past decisions. Therefore in the decision process, $p(\cdot)$ are conditional probabilities that the state is either in or not in threshold. This conditional nature is consistent with the mathematical probability definition necessary for the decision process, and adds physical significance to the process. This is due to the fact that the payoffs used are also conditioned on the past problem history and therefore the definition of the probability applied to those payoffs is consistent with the payoff definition.

By bracketing the nominal trajectory, or the zero error state, for each channel with both a plus and a minus threshold for that channel, the area under the probability density function between the two thresholds can be determined. This area corresponds to the probability that a specific channel's error state lies within the threshold. By subtracting that probability from 1, the probability that that channel's error state lies outside the threshold is also determined. In the above case in which the Kalman filter supplies the density function, the evaluation can be simplified, because the stochastic processes are Gaussian. This allows one to look up the values in a precomputed table rather than determining them from on-line integrations to yield area under the density function.

With the method for probability determination specified, only the payoff functions which aid in defining the specific decision are yet to be determined. To define these payoff functions, physical aspects of the actual pilot decision were investigated. Some gross aspects such as average dwell time and minimum dwell time will be determined as noted earlier, with a final "tune" once model parameters are set. The specific decision to be made is now considered. From Pollard's work, it was determined that the length of time since attention was given to a specific channel was one consideration in the decision process. Another consideration identified was a preference on the pilot's part for specific attentions during specific maneuvers. This preference is also apparent from the Air Force Manual 51-37, which defines each maneuver. The third aspect accounted for

in the decision process is the time between successive decisions. This aspect was identified by Machuca and Lind, and data from their report were used as the basis for making the decision process output coincide with an average 0.2 seconds between decision changes. This average dwell time was indicated in their work as an appropriate attention span for the type of trajectories considered in this research. (Ref 48)

Once the above three aspects are identified as important entities in the decision process, a method of accounting for those aspects within the mathematical framework is necessary. Two parameters for each channel are left open for this accounting: the payoff associated with the probability that the channel is within threshold, $u(.,.,_0)$, and the payoff associated with the probability that the channel is outside threshold, $u(.,.,_1)$.

The payoff for the channel being within threshold will be addressed first. The payoff function used takes into account two aspects, a specified mean time between attention changes, and a cue for the channels based upon the time elapsed since attention was last given to the channel. To display how these aspects are considered, a demonstration of the determination of $u(.,.,_0)$ is given.

Consider being at time t_1 and that a decision was made one discrete time period ago at time $t_1 - \Delta t$ to change attention to channel 1 from channel 5. Δt is the time between decision options, which is assumed to be .05 seconds for this example. The rationale for choosing this time for this research problem will be given in Chapter V.

Assume channel 2 was last attended 10 seconds ago, channel 3 last attended 8 seconds ago, and channel 4 last attended 3 seconds ago. At this point assume that, at the first time interval after decision change, the payoff value for each channel is

TABLE I
Payoff Function for Lying Within Threshold

<u>Channel</u>	<u>$u(\cdot, \cdot 0)$</u>
Channel 1	6
Channel 2	4
Channel 3	3
Channel 4	2
Channel 5	1

There is considerable subjectivity in the choice of these values, however some considerations identified below, aid in their choice. Integers were chosen for these values for ease in manipulation. The value 1 was chosen as the base integer to keep the integers as small as possible. Considerations such as these could pay benefits by allowing integer arithmetic in the decision process determination. Integer computation is one of the fastest available on present computers.

There are two basic aspects inherent in this set of numbers, the sequencing and the relative magnitudes. The first aspect, the sequencing for all except the present decision, is dependent on time

since last attended, with the longest time taking the 4 value and the shortest time taking the 1 value. These values are realized at .05 seconds after the decision is made, and the values of the channels not receiving attention, the last four values, 1, 2, 3, and 4, are incremented by .5 each succeeding .05 seconds until a decision change occurs. Therefore, for the first .25 seconds, the present decision would have the largest payoff value. This also coincides with the dwell time previously considered. By having the last four numbers initially 4,3,2,1, it is still possible to have the channel corresponding to 1 display the highest output value of L by having its associated probability be four times as great as the channel associated with the four. This aspect allows decision states that have a high probability of realization to be chosen, even though the payoff for those decision states is low. This provides quick attention to error states that are rapidly increasing, an aspect considered essential for the human operator model. By having the sequence as above, when the out-of-threshold probabilities are low the relative magnitudes are far enough apart to keep the filter from sequencing at each decision time, yet close enough that if one channel is far above threshold, it will draw the focus of attention.

The 0.5 value added at each 0.05 seconds can be altered to change the average dwell time on a decision. By decreasing that value, the average dwell time becomes longer and by increasing that value, the average dwell time becomes shorter. This aspect was found during tuning runs of the simulation where average dwell times

were changed from .1 seconds to .3 seconds. To demonstrate the sequencing, after one half second (ten sample-times separated by .05 sec), assuming no change in attention position, the $u(a_j, \theta_{j0})$ value for each channel would be as follows:

TABLE II
Payoff Function for Lying Within
Threshold After .5 Seconds

<u>Channel</u>	<u>$u(.,.,0)$</u>
Channel 1	6
Channel 2	9
Channel 3	8
Channel 4	7
Channel 5	6

Thus, if the attention has just shifted from that described in the example of Table I, the scheme assigns the highest payoff for being within threshold to the channel that receives the attention. If the attention has been on one channel for some time, the method gives the highest payoff to the channel which has not received attention for the longest time (as shown by the 9 on Channel 2 in Table II). Each time the attention shifts, the numbers initialize to the first set 6,4,3,2,1, with only the channel ordering changing.

The payoff for being outside threshold, $u(.,.,1)$ is the next parameter to be considered. As referenced earlier, there is a

distinct preference by pilots for specific attention patterns for particular maneuvers. (Ref 48) To convey this preference in the air-to-air function, the following table was formulated. It is considered necessary to have an individual table for each flight function.

TABLE III

Payoff Function for Lying Outside Threshold

		$u(a, \theta_1)$				
θ	a	Straight and Level	Change in Airspeed	Change in Pitch	Change in Roll	Change in Pitch and Roll
PITCH		5	5	3	1	2
ROLL		1	1	2	2	1
HEADING		4	4	1	0	0
AIRSPEED		2	2	0	0	0
ALTITUDE		3	3	0	0	3

The table lists the channels from 5, most likely to hold attention, to 1, least likely to hold attention. The zeros indicate that there is no desire to attend to those channels during the maneuver specified. The maneuvers specified are considered comprehensive for the air-to-air task. Important aspects of the air-to-air task deal with orientation information since it is felt the pilot will fly a predetermined trajectory to achieve the desired orientation. This corresponds to the control philosophy that requires the pilot to have an idea of both trajectory and final time.

When Table III is entered with the maneuver desired, the payoffs for being outside threshold in each channel are determined. These payoffs are considered constant for the maneuver. They can change with time, since choice of maneuvers can vary, but they will be invariant between two samples of the same maneuver.

As the nominal trajectory is necessary for the approach in this research, no decision is required to specify the maneuver with which to enter Table III. That maneuver is apparent when the nominal trajectory, available apriori, is investigated. Therefore Table I can be entered before each decision is made, and the required set of weightings determined.

At this point the parameters of the decision process are defined. Those parameters are divided into two categories: those apparent when the appropriate channels are within measurement thresholds, and those apparent when the appropriate channels are not within the thresholds. The parameter apparent when the channels are within the thresholds is a parameter representing a cue for attention currency. The parameter taken into account when the measurements are out of threshold accounts for pilot preference for that particular channel during a specific maneuver. The effects of the magnitudes of each of these parameters when their time histories are considered, combine to duplicate the empirical average and empirical minimum dwell times. When the scenario is restricted to air-to-air, the above set of considerations and the proposed framework allows the parameter freedom and physical correlation to define the pilot decision task.

The next chapter addresses the simulation construction and discusses the parameter freedom inherent in the human operator model. Each set of parameters will be considered, and a specific method for numerical definition of that set will be outlined.

CHAPTER V

SIMULATION

5.1 GENERAL

With the structure of the estimator, the controller, and the decision process specified, it next becomes necessary to evaluate the performance of the total system. Because of the size and the nonlinear properties of the system, a Monte Carlo simulation is the most practicable mode of analysis available, hence the mode chosen. Because this choice entails extensive computer resources, other options were investigated before this commitment was made. These options involved using a covariance analysis with or in lieu of the Monte Carlo analysis. In each case examined, it would have been necessary to linearize either the decision process or the aircraft model or both to make use of the easier covariance analysis, and this type problem alteration was counter to the goals of this research. This chapter defines those research goals in terms of the simulation. Once this definition has been established, Appendix I outlines an algorithm for implementing the Monte Carlo analysis.

5.2 LONGITUDINAL AXIS SIMULATION

Because of the decision to implement a Monte Carlo analysis and the resources necessary for this analysis, a careful investigation was made of the purpose of the example problem. This analysis

led to four desired objectives:

1. The example problem would utilize the entire aircraft control system and equations of motion as represented in Chapter II.

2. Using this entire system a realistic problem would be investigated to display the useful and general nature of the model.

3. A demonstration of the decision process and the controller derived using this process is necessary.

4. A demonstration of the stability of this structure is necessary. This demonstration is in lieu of a mathematical proof of stability which, because of the size and stochastic nonlinear structure of the system, is not considered plausible at this time. Some work is being done in robustness and stability of nonlinear stochastic controllers, however, extension of this work has not yet been made to a controller of the structure proposed in this research (Ref 62, 63) The first two objectives and a portion of the third can be accomplished using the constructed controller operating on the mathematical representation of the entire aircraft, and a careful explanation of this simulation is given later in this section.

However, because of the size of the entire aircraft problem, and the computer resources necessary for a lengthy run of the problem, it was determined that a reasonable demonstration of the stability would not be feasible. Therefore to present a demonstration of the stability and to further display the decision process, a reduced order problem was investigated. The succeeding discussion will only provide the detail to allow the reader to reconstruct this simulation. The next section will define the methodology for deriving the full order simulation, the area where this work is considered to have the most useful application.

The reduced order problem investigates only the longitudinal axis of Figure 3 as shown in Figure 55. The noises used to display errors in the longitudinal axis of the aircraft control system were used with the same strengths in the reduced order problem as in the total aircraft model specified in Appendix 6.

To isolate the longitudinal axis the following assumptions were made:

1. Aircraft body y-axis velocity $V=0$.
2. Roll angle, ϕ , and yaw angle, ψ , both zero.
3. Moments about body x axis, P , and z axis, R , are zero.

This reduces the aircraft equations of motion to six including equations for \dot{U} , \dot{W} , \dot{S}_x , \dot{S}_z , \dot{Q} , and $\dot{\theta}$.

Combining these with the seven equations available from Figure 13 gives the aircraft equations used for the reduced order investigation. The next equations necessary for the subproblem are equations necessary for the controller. The linearized equations used for the controller are those of Appendix 3 with the control equations and assumptions cited above.

Two controls were assumed available to the pilot, the throttle for airspeed, and longitudinal stick for pitch. Two observation sets were available to the pilot; the first associated with the throttle or airspeed control was

1. Thrust.
2. Normal acceleration
3. x and z body axis velocities U , W

and the second associated with pitch control was

1. Longitudinal stick
2. Pitch angle
3. Pitch angle rate
4. Normal acceleration

These sets were used as specified in Chapter V.

This specifies the A, B, and C matrix of (3-1) and (3-2). The G matrix is given by Figure 51 and the assumption that light turbulence is present as specified earlier. With this definition, the aircraft nonlinear model, and the linearization necessary for the estimator and predictor can be readily accomplished. To define the controller the controlled variables defined by the D matrix of Equation (3-3) are necessary. For this subproblem those variables are: thrust, longitudinal stick position, elevator position, x and z body axis velocities, U and W; and pitch angle and pitch angle rate. The last definition necessary is that of the decision process. For that process since only two controls are assumed in this subproblem, only two Bayesian decision functions are necessary:

$$L_{1S} = u(a_P, \theta_{P0}) P(\theta_{P0}) + u(a_P, \theta_{P1}) P(\theta_{P1}) \quad (5-1)$$

$$L_{2S} = u(a_V, \theta_{V0}) P(\theta_{V0}) + u(a_V, \theta_{V1}) P(\theta_{V1}) \quad (5-2)$$

where the $p, v, 0, 1$ are subscripts as defined in Chapter IV. The payoff functions are defined as follows:

a) The $u(a, \theta_0)$ of the channel being controlled is given the value 8. The $u(a, \theta_0)$ of the channel not being controlled is, on the change from being controlled to not being controlled, assigned 1. This is incremented by 1 each .05 seconds so that at .4 seconds the two payoff functions are equal.

b) The $u(a, \theta_1)$ of the pitch channel is assigned the value 2 and the airspeed channel is assigned the value 1. This corresponds with the pilot emphasis on pitch during a maneuver such as that chosen for this demonstration. That maneuver is basically a perfect loop with the uncoupling assumptions discussed earlier. These values correspond to Table I values when no roll is present.

With the decision process outlined, only the parameters of the model; the controller, the Kalman filter, the predictor, and the decision process are required to define the simulation. This information is contained in Appendix 6 along with the parameters used in the entire aircraft problem.

5.3 FULL AIRCRAFT SIMULATION

The next aspect considered is the entire aircraft simulation. This discussion emphasizes the entire methodology for constructing this entire aircraft simulation. This approach was taken because it is felt that one of the strengths of the method lies in its ability to address full scale problems. Therefore a comprehensive discussion of the full scale problem and what is demonstrated by the full scale problem is both necessary and desirable.

5.3.1 Trajectory

The first step in constructing this simulation is determining an appropriate trajectory. That determination must be made in order to specify $A(t)$ needed for the perturbation methods employed and in order to specify the outerloop needed for the decision process. To select the most appropriate trajectory, the specific problem must be considered. As one research goal was to investigate regions of the flight regime in which nonlinearities are very significant, a trajectory in this region is necessary. To enhance problem validity a second requisite, that the trajectory lie in a realistic segment of the flight regime, must also be met.

With these general guidelines for trajectory determination in mind, available sources were examined to specify the trajectory to be used in this research more completely. Examining previous experiments in the field of attention led to Allen and Clement's research. In their work a primary and a secondary task were used, with the subjects aware of the difference in task importance. The difficulty was varied in each of the individual tasks, and each subject's response, was recorded. The minimum recorded dwell time of the subject on the primary task was .2 seconds. (Ref 2)

With this as a basis, in this research where two tasks of equal importance are used, and a trajectory is constructed so that the human operator is concentrating his full attention on the task, a minimum dwell time of somewhat less than .2 seconds, and the average of about .2 seconds appears resonable. This decrease in dwell time is attributed to the importance of the tasks that the

human operator is performing. In the experiment conducted by Allen and Clement, the two tasks given each subject to measure his dwell time were artificial, and the test subjects were instructed that one task was of primary importance, and the other of secondary importance. (Ref 2) The secondary task was only to be given time not needed for the primary task. In the trajectory considered in this research, the human operator has definite tasks, with the importance of each equal and linked to maneuver accomplishment. It is felt that having a definite motivation and goal, as is the case in this research, would account for a reduced average dwell time and a reduced minimum dwell time. A similar reduction is apparent from flight experience when contrasting landing approach flying to cruise flying. Much more attention is devoted to the landing approach, than is devoted to normal cruise. This increased attention is also apparent in the pilot's instrument crosscheck, which is much more intense during landing approach.

By using this information, it is now possible to define the trajectory further. For this definition, the use of .2 seconds as an average dwell time, and the desire that a minimum of two attention shifts be expected per run, indicate that the minimum run time should be .5 seconds. Because of the computer costs, mostly attributed to the integration encountered in exercising this problem simulation, this minimum value of .5 seconds for the trajectory run was chosen.

The duration of the trajectory is not the only essential element in computer time costs; the number of intervals into which

the duration is segmented is also a factor. In their analysis to determine digital flight control update rates for the F-4 (an aircraft comparable to the one used in this research), Honeywell determined that 80 updates per second were necessary to describe the aircraft adequately during maneuvering flight. (Ref 43) According to this data, if the most highly varying dynamics were used, about 40 intervals would be necessary for a half-second flight. This Honeywell analysis was based on a simple integration scheme that had no corrector capability. Because this integration scheme used herein was a fourth-order predictor-corrector, it is felt that part of the high update rate effect can be absorbed in the better integration routine, and therefore 20 cycles per second was chosen as the problem update rate.

The last factor that entered into the trajectory decision is displayed by Table 1 in Chapter 4. That table shows that in some flight phases, some control elements are considered not essential because of pilot experience or prior training. This aspect of the decision process can be used to control the computer time needed; as is evident in the table, only three controls need be emphasized in some flight phases.

To satisfy all the enumerated specifications and to take advantage of the above specific problem aspects, a climbing right turn much like that used in the initiation of a cloverleaf was chosen as the trajectory for consideration. This turn was made at 15,000 feet and Mach 0.9. The pitch rate for the maneuver was approximately

.02 radians per second, and the roll rate was approximately .2 radians per second. These rates are fast enough that the cross-coupling terms in the equations of motion are a factor. This was demonstrated by the fact that the variations in the $A(t)$ matrix in some cases were a factor of 1000 over the .5 second trajectory.

With the trajectory specified above, and the simulation methodology specified in Appendix 1, the final simulation step is to outline the procedures used to set the parameters to values that would produce a logical problem flow and would assure that previous empirical data relative to the problem was not violated. For this purpose a parameter variation analysis was accomplished.

5.3.2 Analysis of Parameter Variations

During the parameter variation analysis, the model variables were identified and partitioned into three categories: the decision process variables, the estimation process variables, and the control process variables. After this categorization it becomes important to examine each set of variables or parameters for its impact on problem results. A substantial number of parameters are inherent in the model. If it were not possible to prespecify some parameters and present a methodology for determining the remaining ones, the model complexity would undoubtedly frustrate possible users. To avoid this frustration and to provide this parameter specification, consider first the estimation parameters.

5.3.2.1 Estimation Parameters

In the estimation problem, three sets of parameters are available, the measurement noise matrix time history $R_j(t_1)$, the state noise matrix time history, $Q(t)$, and the initial condition on the covariance matrix, P_0 . Two aspects of the problem aid in the specification of these parameters. The first is that the full set of states and measurements is considered, not just a reduced-order model. This allows the noise covariance associated with the full state model to be utilized directly without requiring noise covariance values to be increased artificially to account for state reduction. Therefore, as the state noise covariances are representative of only the states considered, and as the trajectories of the states are known, good estimates of the state noise covariances are possible.

Two state error driving noises considered to demonstrate this aspect are sensor errors and gusts. For the determination of these gust values, AF MIL SPEC 8785B was considered. (Ref 16) Light turbulence was used at 15000 feet, the run altitude of the trajectory. Light turbulence was used because if a higher level of turbulence is encountered, little maneuvering is done. The sensor error values of the Q matrix associated with gyroscopic errors were obtained through cross referencing the models in Britting and in Chapter III with company brochures on gyro performance. (Ref 13, 56)

The other sensor considered is the angle of attack indicator. By referencing Figure 8, the appropriate standard deviation for a particular angle of attack was noted. From this observation of

the angle of attack from the prespecified trajectory information, the time-varying nature of the Q value associated with the angle of attack state is established.

The second problem aspect that aids in parameter specification involves the initial value for the covariance matrix. Because of the implementation envisioned, for this time-varying analysis, this matrix would already be available. This implementation involves partitioning a general problem into two phases, a phase in which the problem nonlinearities can be neglected, which can be considered using a steady state analysis model, and a phase in which the problem nonlinearities must be considered, using the more extensive model above. Therefore the initial value of the covariance matrix for the above analysis would be the final value of the covariance matrix for the previous segment of the steady state analysis. This method also assumes that any problem starts with the steady state analysis, an assumption that matches the pilot practice of getting "set up" or stabilized before maneuver start. For the trajectory considered, P_0 was assumed diagonal since no information was available on the cross terms, and the diagonal values were set at values considered reasonable initial variance values for each state.

The final problem aspect that aids in parameter specification affects the measurement noise covariances. These direct visual noises were defined earlier as a combination of human perception error and instrument error. For this research, the human perception error is considered purely dynamic, except for thresholds which are

specified directly, and will be represented in the simulation by the time delay and predictor. The instrument error will supply the value for the measurement noise matrix. The instrument error values were taken from company specifications on the various visual instruments, by modeling the errors with white Gaussian or shaped Gaussian noise.

The non-visual sensor errors are accounted for using previously established guidelines. The lateral and normal acceleration measurements were considered to have a .1 g standard deviation error. This coincides with experimental data on g perception.

(Ref 51)

With the above aspects considered, the estimation process measurement parameters are specified, and no variation in these parameters is allowed.

5.3.2.2 Controller Parameters

5.3.2.2.1 General Results

Two things are observed concerning the controller parameters. The first is that less physical significance can be attached to these parameters than to the other parameter sets, and the second is that extensive work has been accomplished regarding these parameters in optimal pilot modeling literature. From the discussion in Chapter III, the methodology for parameter specification is detailed.

To simplify this methodology, the control process is divided into three sets of parameters, the control weightings R_2 , the state weightings R_3 , and the terminal state weightings P_1 . The interaction

of these parameters was discussed in Chapter III and in various references. (Ref 5, 44) This interaction basically requires that, if an individual diagonal element of the R_2 or R_3 matrix is increased, the increase displays a tendency to maintain the state or control associated with that diagonal element at a low value. In the same vein, a high value for an individual diagonal element in P_1 displays a strong desire to make the associated state or control zero at the final time.

The first determination is made on the control weighting matrix, R_2 . This matrix is predetermined by the control lag. The control problem Riccati solution must be solved iteratively, varying the respective R_2 matrix value, to arrive at the appropriate values for the control lags. The R_3 matrix is then set so that control magnitudes for the initial stages of the problem coincide with control magnitudes expected for that phase of the trajectory. These magnitudes have been determined by examining comparable data runs from a like aircraft simulation on the AFFDL LAMARS (Large Amplitude Multimode Aerospace Research Simulator) simulator. The Riccati equation is then taken to steady state, and the values of the steady state solution are examined for irregularities. Some possible irregularities would be order of magnitude differences in values which should be comparable, or values either approaching zero or infinity, when similar state values are remaining constant.

For the simulation, this process was altered to simplify computation. As in the methodology above, the R_2 matrix was first

set to satisfy the desired control lags. Because of the short trajectory time interval, it was felt that the Riccati control equation would be in the steady state condition, in an intermediate condition, or in the transient condition, so either R_3 or P_1 would be superfluous. Individual values in R_3 or P_1 were varied, therefore, to determine sensitivities. Because this analysis showed that, for this problem, the Riccati solution was insensitive to a wide variation in the individual diagonal elements of the P_1 and R_3 matrices, no further attempt was made to effect solution changes with those elements. This insensitivity is felt to be due to the short duration of the trajectory. With such a short duration, and starting with only diagonal values of P_1 , there is not enough time to affect the elements of the P matrix, significant for control, with the changes made to the R_3 or P_1 matrices.

This alternate method was used because the computation required for determining the steady state Riccati solution for an alteration of each value would be extensive, and if unneeded as above, too costly. As detailed above, using this method proved efficient because the results from the runs were insensitive to both R_3 and P_1 . One possible reason for this insensitivity was that the Riccati solution lay in the slowly varying range of values, that is between the steady state value and the final large transient region. Another reason was that the error states for the altered parameters were small, and therefore their effect on control was small. Since the last control was applied .05 seconds from the final problem time, this appears realistic; there is still time for

the final transient to occur. Therefore, in this region the sensitive parameters are only the R_2 matrix values. The preceding discussion has detailed general parameter specifications. The specific realizations used and rational for those realizations are discussed next.

When considering the specific realizations, two other aspects also affect the problem of selecting values for the P_1 , R_2 , and R_3 matrices. The first is that, for this research, all are assumed to be diagonal matrices. This assumption is consistent with Kleinman's work on multiple controls (Ref 46), and is made with the further assumption that enough parameter freedom is available with only the diagonal terms. If enough parameter freedom is not available, off-diagonal terms would be considered.

The second aspect is that the R_2 , R_3 , and P_1 matrix elements cannot in general be chosen independently. Therefore a strategy for setting the relative values is necessary. (Ref 44) This will assure that when emphasis is necessary on a particular state, such emphasis can be given by changing the relative weight on that state.

5.3.2.2.2 R_2 Matrix Determination

With the above guidelines and using the procedures described, the specification of the initial weightings was made by dividing each of the squared values of the maximums of the estimated states and estimated controls by the maximum value anticipated from that set. The next step was to implement Kleinman's method for considering the neuromuscular lag. By adding four states to the system, two in conjunction with the stick, one in conjunction with the rudder, and

one in conjunction with the throttle, and substituting those states for the normal stick, throttle, and rudder inputs in the aircraft control equations, the control rates are also weighted. (Ref 10) By setting each of the derivatives of these states equal to the negative of the reciprocal of the neuromuscular lag time, multiplied by each state plus each old control, and by requiring a value in the gain matrix corresponding with the additional state to take on a value corresponding to the neuromuscular lag, the control solution will display the desired neuromuscular lag. (Ref 10) This process specifies the values in the R_2 matrix corresponding to the control rates. As noted above, the neuromuscular time lag can range from below .1 seconds to above .4 seconds. When these values are used in the context of a demanding task it is assumed that the .1 second value would be applicable. Therefore .1 seconds was chosen as the appropriate neuromuscular lag when attention was given to that particular control. Because this investigation is focused on a highly maneuvering trajectory it is assumed attention will be substantial on all flight channels. Therefore, .2 seconds was chosen as the neuromuscular lag when attention is not given to that particular channel. By altering the diagonal terms of the R_2 matrix in an iterative fashion it was possible to set these lags to .2 for the controls not emphasized and to .1 for the emphasized controls, as desired.

Because the trajectory determination had limited the necessary controls to pitch, roll, and airspeed, only three matrices

were produced by this process, rather than the five necessary in the general case. It is felt that this is adequate exercise for the concept feasibility demonstration. It is interesting to observe that the R_2 roll value obtained by Kleinman in his paper, "A Control Theoretic Approach to Manned Vehicle Systems Analysis" (Ref 38), was .00017, with a resulting lag of .08 seconds, and the R_2 value for the roll control in this work was .0005 with a .1 second lag resulting. It is emphasized that a fourth control, the rudder control, was considered in this problem and was assumed initially to have the larger neuromuscular lag time of .2 seconds. This assumption proved unusable for this problem, in that when this value was achieved, and the control matrix $F^0(t)$ used in the actual simulation, Step 8 of Appendix I, the resulting control was too large for the system. It required forces on the rudder in the order of ten times that which would be expected for a realistic maneuver. Therefore the neuromuscular lag used for the rudder was iteratively set to two seconds.

This presents an interesting result since it radically departs from previously established values. These previously established values, however, have been eye-hand values, with no values experimentally determined that required the foot as the input device. As the rudder requires foot movement, it is felt that this divergence is acceptable, and probably realistic. The other aspect that can account for this divergence is that the

mechanism for sensing the rudder input was the vestibular sensors. This information is assumed to be noisier than the direct eye measurements and therefore could account for part of the added lag time.

As a result of the above analysis and computer work, the three R_2 matrices derived, each for a specific control emphasis, resulted in neuromuscular lag time constants of .1, .2, .2, and 2.0 seconds. The .1 was associated with the control requiring emphasis, the two .2 values were associated with the controls not requiring emphasis, and the 2.0 was associated with the rudders.

5.3.2.2.3 R_3 Matrix Determination

Once the above values were set, a variation in the R_3 matrix was investigated. The five states corresponding to the 5 diagonal values of the matrix are pitch, pitch rate, roll, roll rate, and airspeed. Each of the R_3 matrix diagonal values was varied as follows: with all other values constant, the normalized individual value was first multiplied by 1,000,000 and run, and then divided by 1,000,000 and run. Smaller intermediate values were first investigated, however 1,000,000 was chosen because it proved to be the first value to give a reasonable variation in results. The baseline values used are given in Appendix 6. Each resulting $F^0(t)$ was then used in determining the time history of controls as specified in Step 8 of Appendix 1, and the control magnitudes and the error states were recorded. In each case only minor changes occurred. In the most severe case, an alteration of a factor of ten occurred. As was expressed previously, it is felt that the

Riccati equation was not in the steady state mode, so that the R_3 effect was reduced. During this time the transient condition of the equation is still evident but as steady state is approached the values start to level off. If the equation were allowed to run to steady state, then the contributions by the R_3 terms would have time to enter into the cross terms in the $P(t)$ matrix of Equation (3-7) and an effect would be shown. For this reason, the high values necessary for R_3 terms to effect control change were not used. If the high values were used, and the problem were allowed to run for a longer time, the control commanded by the system could be impractical.

5.3.2.2.4 P_1 Matrix Determination

The next parameters considered were the parameters in the P_1 matrix diagonal. As there were 63 possible choices, one for each of the 63 state initial conditions, the problem had to be limited. Also it was concluded using the test runs on the control-weighting matrix R_3 as a basis, that by "tuning" values from only the R_2 matrix a control considered appropriate by any measure could be attained. For these reasons, two of these parameters were chosen for a sensitivity analysis. Those parameters are pitch, and pitch rate terms. These terms were varied both by multiplying the assumed normalized value by 1000 and by dividing that value by 1000. In both cases, the control and the state errors were unchanged. This insensitivity is assumed to be due to the Riccati equation solution for the problem time lying between steady state and the final large

transient. If the equation has only started to respond to the final transient, little effect from P_1 should be realized.

With the above analysis complete the parameters of the control problem are set.

5.3.2.3 Decision Process

The next group of parameters to consider is the set of decision process parameters. These parameters fall into two groups, those associated with thresholds and those associated with payoff functions.

The threshold parameters are specified by perception thresholds, specific instrument size, and pilot-to-instrument distance. The last two are necessary because the perception thresholds are given in degrees of travel at the human's eye which corresponds to inches of travel on the applicable instrument. As previously stated, the thresholds are assumed the same for direct visual measurements and the measurements in the peripheral vision. With experimentation on peripheral cues, that assumption could be modified.

The payoff-function parameters are considered next. For this analysis, requirements for the decision are examined. The first requirement is that if one measured value is grossly out of alignment, it will be attended to; the second is that dwell times, both average and minimum, must be consistent with previous experimentation. As the exact instrument sampled at any nominal condition is not constant between two pilots or even for one pilot on two separate runs of the same trajectory, an attempt to duplicate a

specific pattern is not considered meaningful. Therefore, the ad hoc method described in Chapter IV is used to determine specific decisions. This method will also produce proper decisions if one measurement is grossly out of line. The average dwell time and minimum dwell time information is used after the rest of the problem parameters are determined to "tune" the payoff function parameters to proper relative magnitudes. This procedure then specifies the values for the decision function parameters.

At this point, all parameters either are specified by the problem or can be determined by the methodology prescribed above. It has been the intent of this section to provide the information necessary for a user to adapt the model through parameter variation to a desired problem. To this end the parameters were segmented into three categories: estimation process parameters, control process parameters, and decision process parameters. This breakdown facilitated identification of the parameter set to vary if a specific facet of the problem required alteration. The specific variation in each parameter set was then addressed by detailing the expected effect of variation and interrelationships excited by a variation. This methodology allows the user to take advantage of problem understanding to identify and alter the proper parameters.

5.4 SUMMARY

This chapter has been devoted to outlining the method for determining the aspects of the reduced order simulation, and specifying in detail the salient aspects of the full order. Appendix 1 provides a roadmap of computation necessary for both problems,

and Appendix 6 provides the parameters necessary for the simulation.

With this understanding, the next chapter details the approach employed to demonstrate the model.

CHAPTER VI

DEMONSTRATION

This chapter on demonstration is divided into five sections. The first section covers the simulation implementation, and the second covers the longitudinal axis simulation. The third section addresses the validation of the full order simulation with previously collected data, and the fourth section displays the results and analysis of the angle of attack example, which is considered to be one highly lucrative area opened by this research. Finally, the fifth section comments on model flexibility.

6.1 IMPLEMENTATION

The implementation of the simulation is included in the results because the form of the implementation is considered essential to the validity of the results. Consider the implementation suggested by Figure 2 in Chapter II. The first essential aspect of the implementation is the aircraft equation block. By using the complete nonlinear equations in this block, an accurate account of the error states δx_i 's can be computed. An alternate form of the equations, and one that is much easier to implement, is attained by replacing the nonlinear equations with the linearized equations.

In that implementation, the question of "small perturbations" arises. As long as the perturbations remain "small", this realization is valid. However, because "small" is not defined in a quantitative

sense, a continuing question exists regarding the validity of the simulation. The trajectory followed by the linearized equations could diverge from the trajectory followed by the nonlinear equations; no indication of this divergence is possible if the nonlinear equations are not computed. If this research is used as a design tool, as proposed, an accurate assessment of errors is essential. By using the nonlinear equations, this assessment is obtained. A parallel result is obtained on the validity of the controller. As the derived controller is a function of the "small perturbation" assumption, large error state inputs make the controller performance suspect. By using the nonlinear equations in the simulation, a true analysis of controller performance is available.

This closely parallels an implementation of this research which is proposed for a possible autopilot device. Consider the possibility that a trajectory were derived for a fighter-type aircraft that maximized the probability that a surface-to-air missile, SAM, once fired, would miss that aircraft. An automatic system on the aircraft could be activated to follow that trajectory once a SAM firing was detected. It is unlikely that the traditional lateral and longitudinal uncoupled autopilots would display desired characteristics for this type of situation, as not only pitch, roll, and yaw control would be necessary, but also control of inertial position in time. Therefore, a controller as in Chapter III could be derived to zero out the errors from this known attitude and position trajectory. This type of utilization suggests that a course

0

somewhat different from this research be used in controller design. Because of the precision desired in such a trajectory it is suggested that it is most efficient to use an automatic pilot rather than allowing a pilot to respond to a specific display. This automatic pilot would be constrained only by the aircraft equations of motion, because it would be most efficient to have the automatic pilot controlling the control surfaces directly, rather than controlling the surfaces through the control stick. Also, the automatic pilot would have the benefit of a complete measurement set within the capabilities of the onboard sensors. A decision process might still be used to identify the channel or channels most in need of control since conflicting control situations can happen in specific instances, and a designated control could then be selected that would concentrate on these channels. It is felt, however, that one time-varying set of controller gains could be attained that would be satisfactory for the maneuver, thus eliminating the decision process. This discussion of alternate autopilot implementations is provided because it appears to be an area where immediate applications are possible. An understanding of possible realizations can therefore pay immediate dividends.

A second aspect of the implementation lies in the decision process. This decision process is the diversion point from current human-response modeling work, which uses a "steady state" decision process realized in the estimator. This decision process specifies a value for the measurement noise covariance in the estimator by

assuming that value should be chosen to minimize a quadratic cost function. The solution then determines the steady state values of the measurement noise covariances, constituting a form of decision implementation. The outcome of this method gives a relative frequency determination of decisions, with no indication of the decision time history.

In this work the decision process is translated to real problem time and it admits the cases in which some measurements are not available to the pilot. This research also extends the decision process to the controller, a factor not previously examined in real problem time. These two diversions are considered essential to further human controller work in multiple-input/multiple-output applications. These implementation features are then factors that affect the scope of usage of this model. This expanded scope is considered one of the essential contributions of this work.

6.2 LONGITUDINAL AXIS SIMULATION

In this section an analysis will be made of the longitudinal axis simulation concentrating on three factors, the total problem stability, the effects of the alternating gain matrices induced by the decision process, and the decision process.

For this, two sets of graphs are given in Appendix 5. The first is a ten run, ten second Monte Carlo analysis of the longitudinal axis simulation. The graphs depict the ten run mean of the quantity, bracketed by the one standard deviation envelope for those ten runs. The quantities displayed are considered those of most

interest and are:

1. Body x axis velocity
2. Body z axis velocity
3. Pitch angle
4. Pitch angle rate
5. Thrust
6. Longitudinal stick force

The major factor examined in the Monte Carlo analysis is the stability of the derived controller, and special attention is paid to any decision process effects on that stability.

This approach to stability was taken, because the first choide, mathematical proof, was not possible. This is the case because the decision process makes the system nonlinear and the large scale system makes present nonlinear stability theory methods intractable.

Though it is not a proof and is not presented as one, one observation may be appropriate to this class of problems. That observation is, if each LQG control set $(F_j(t_1), C_j(t_1), R_j(t_1))$ stabilizes the system, then at the switch point between channels, if the state trajectories lie within the controllable region of the new LQG control set, the system will be stable. The ability to define this region accurately is where the present methods are inadequate.

Since proof cannot be furnished, the next alternative was taken, that of demonstrating stability for a particular problem.

To make this stability investigation credible, a Monte Carlo method using multiple runs was selected as the mode of demonstration. By using multiple noise realizations, each without any resultant system instability, confidence in the stability demonstration can be generated.

It is important to note that the pitch angle, pitch angle rate, and body x and z axis velocities identified in the Figures 58 and 59 of Appendix 5 are actual deviations, that is, deviations between the respective aircraft noise model state and the nominal state. This aspect is important because, though these are the most meaningful quantities in evaluating controller performance, they are not the values that are applied to the controller gain matrix, F , to attain the controls; longitudinal stick and throttle. Therefore considering cause-effect relationships, the longitudinal stick and throttle inputs should have almost immediate impact on the graphed states, but those states furnish only noise corrupted measurements to the Kalman filter and, depending upon the measurement noise matrix, $R(t_1)$, values, take a finite time to effect the filter estimates which are applied to the optimal gain matrix, F . To analyze the figures, consider first the body x and z axis velocities. Each quantity has a mean which stays very close to zero, and standard deviation envelopes which stabilize by seven seconds.

Though the angle of attack parameter was not measured, that quantity is a function of the x and z axis velocity, each of

which is well behaved, so the inference is made that angle of attack should also be well behaved. The controls, longitudinal stick and thrust, are of mean close to zero and both have a decreasing one standard deviation envelope. An examination of the $F(t)$ control gain matrix values shows that though these values are time varying, they reach a pseudo steady state by approximately three seconds. Since the only other ingredient in the determination of the control is the predictor estimated state, it is apparent that the predictor is outputting state estimates which are becoming very small by the end of the ten seconds. This aspect is more pronounced in the thrust control than in the longitudinal stick control, which indicates that the states predominant in computing the longitudinal stick control are the states whose variances in the Kalman filter remain large in a relative sense.

This is an aspect of the estimation process which this analysis suggests must be carefully considered in formulating any lengthy problem. That aspect is that care must be taken to assure the estimation process remains responsive to measurements, or that the estimator doesn't get to "know" the error states too well. This can be assured by increasing the $Q(t)$ values. This could be done in one of three ways; first begin the problem with large Q values, second institute a $Q(t)$ matrix that changes with time, or third use an adaptive technique such that when the covariance of a state becomes low and continues at that level, then that covariance is artificially increased to allow measurement effectiveness.

Definitive values of the above generic terms must be obtained through simulation.

Therefore, though the values of the longitudinal stick control and the thrust control are demonstrated stable, and the system being controlled remains stable, care must be taken by any user to assure that for a lengthy problem the controls remain effective.

The last states to consider are the pitch angle and pitch angle rate states. As with the previous considerations, the pitch angle rate is well behaved, that is its mean is maintained close to zero, and the one standard deviation envelope is not expanding after about one second. The pitch angle state is, however, not quite so well behaved. The mean increases to approximately .0025 radians in 9 seconds, and from that point on, levels.

This aspect is undoubtedly due to the selection of controlled variable weights, or the elements of the R_1 matrix. These values were chosen so that more emphasis was placed on keeping the pitch angle rate low than was placed upon keeping the pitch angle itself low. This choice was due to the chosen trajectory where it is felt pilot emphasis would be placed on smoothness of the maneuver rather than on precise pitch angle control. In this case then, the pitch rate has been constrained from completely compensating for the pitch angle "creep". This situation, however, when examining the "micro" problem would terminate when the pitch angle error state became large enough to dominate the longitudinal stick control.

It is necessary to note that one computer simulation was conducted with no control. In all four cases; pitch angle, pitch angle rate, and x and z axis velocities, the values sampled were above the one standard deviation envelop for the times examined. This would indicate that control effectiveness is present, and is acting in the proper manner. Considering Figures 56 through 61, then, the desired stability has been demonstrated by the ten second Monte Carlo analysis, and no adverse effect due to the decision process has been noted.

The second part of this investigation is a three-second run displaying the same graphed quantities, however, only considering a single run so that the decision process effects can be examined. For this process the state where the decision process resides is shown in Figure 62. In examining this process three aspects must be discussed. The first is that the process only has three .05 second periods of emphasized throttle control until the last .5 seconds of the problem. This is mainly due to the fact that the threshold chosen for airspeed was nominally somewhat higher than the threshold chosen for pitch angle. Therefore it required a longer time interval for the airspeed state to move out of the threshold portrayed on the Gaussian distribution of Figure 12 than it does for the pitch angle state. It should be noted, however, that due to the cue aspect of the decision process, the airspeed was observed and controlled at least once each second.

The second aspect is the cause-effect relationship between decision and control. The decision history is given in Figure 62. Three decision changes, at 1.45 seconds, 2.15 seconds, and 2.80 seconds correspond with the changes in the thrust, Figure 68, and in the longitudinal stick, Figure 67. Since changes are made in the control gains during this time, this result is expected.

The third aspect is the control-state relationship. Logically this relationship would not be as strong or as immediate as the decision-control relationship, because the control must be interpreted by the entire system. With this in mind, the impact on the x-axis velocity, Figure 65, by the thrust changes, Figure 68, is examined. Two significant thrust changes are made, the first at approximately 1.6 seconds, and the second at approximately 2.3 seconds. Also two significant x-axis velocity changes are made, the first at approximately 2 seconds, with a marked increase in velocity and the second at approximately 2.7 seconds with an apparent decrease in velocity. Each x-axis velocity change is approximately .4 seconds after the thrust input. Since the control-state interaction is correct; increased thrust leads to increased x-axis velocity, decreased thrust leads to decreased x-axis velocity, and the delay is consistent, .4 seconds in both cases, it appears the delay is due to the system response to that magnitude of control. Therefore this control-state interaction is functioning properly.

For further analysis it is important to note that in Chapter IV, airspeed was to be controlled by thrust, and pitch by longitudinal stick. This is more of an observation than a choice, since the strongest coupling lies in these relationships. Unfortunately these

are not independent relationships, and since the major changes in the controls occur at the same time, it is difficult to attribute state changes to control changes. It is apparent by inspecting the state responses, the pitch angle, Figure 63, and the pitch angle rate, Figure 64, that soon after the control changes at 1.45, 2.15, and 2.85 seconds, corresponding changes occur in these states. It is also noticeable in the x-axis velocity, Figure 65, and in the z-axis velocity, Figure 66, but not to the extent exhibited in pitch angle and pitch angle rate. This is probably due to the fact that the thrust controls applied and the longitudinal stick controls applied have varying impact on the system response. Since this impact is run dependent, it is impossible to assure equal effectiveness of the two controls for each run. Therefore this contrast in effectiveness of the two controls is both logical and expected.

This analysis of Figures 56 to 68 has demonstrated the stability of the aggregate model and displayed the decision process and its effects. With this insight it is now possible to address the full aircraft simulation problem. To address this problem adequately, first a validation of the simulation results will be discussed.

6.3 VALIDATION

In this section, previous works containing experimental results consistent with the aircraft control problem in this research are considered, particularly works from which error state and control magnitude correspondence can be drawn. This is not considered the best of the possible validation procedures: that would have been an error state and control input correlation with a direct simulation or an actual flight of the aircraft described in Chapter II, flying the trajectory considered

in the analysis. Unfortunately simulation time is difficult to procure and costly, and it was not available to the author.

Part of the cost involved in the procurement of such a simulation would be the device necessary to display the desired trajectory to the pilot. An observation is necessary at this point. It is not obvious how an experiment could be performed to maintain a highly dynamic trajectory with perturbations about that trajectory displayed as required for the proposed analysis. Two possible devices were examined for relevance to this task. The first was a flight director that would follow the desired trajectory with the zero position of the bank-steering and the pitch-steering bars. It would be used much as is the present aircraft instrument landing system mode, except that the trajectory required for the flight director is the maneuvering trajectory described previously. The second choice for trajectory display was a second aircraft on which the maneuvering aircraft would fly trail formation. The second aircraft could be programmed to fly the desired trajectory, and trail formation would require the maneuvering aircraft to match the second aircraft's programmed trajectory.

If the opportunity would avail itself, the first method suggested would be the method selected for analysis because of the better experiment control available in that implementation. As neither version of this validation method was available, it was necessary to obtain salient data from experiments already conducted. To correlate available data with the simulation results of this research, it was necessary to choose a simulation procedure and a method for displaying simulation results. For the simulation

procedure a Monte Carlo analysis was implemented. This implementation was primarily due to two factors. The first is that using a nonlinear aircraft model and a decision process limit the available modes of analysis to primarily a Monte Carlo type. The second is that the type results attainable from the Monte Carlo procedure correlate well with the available physical data, in that one trajectory run of the simulation corresponds to one trajectory run of a manned simulation or aircraft. Twenty runs of each simulation were accomplished for the Monte Carlo analysis, each run with a different realization of the white Gaussian noise driving the system. The error states corresponding to P , Q , R , ϕ , θ , ψ , U , V , W , and S_z were recorded each .05 seconds throughout the .5 second simulation. This data rate was chosen due to the implementation. The discrete formulation used for the estimation task allowed estimates to be available only every .05 seconds. A discussion of the twenty samples per second rate is given in Chapter V. The computed controls from .25 seconds to .5 seconds along the trajectory were also recorded. As the control is based upon a Kalman filter estimate through a .2 second time delay, the first control that can be applied is at .2 seconds. Because the error states were assumed to be zero at initial time zero, the first nonzero control enters then at .25 seconds.

The method used to portray the information described above was a plot of the mean plus or minus one standard deviation method. That is, the value of each variable was averaged over the twenty runs at each .05 seconds, and that mean is recorded along the center line

of the presentation. The standard deviation of each of these time interval sets was next computed, and the plotted mean was bracketed by plus and minus the standard deviation. These charts are presented in Appendix 2. They form the basis for the model validation, and are used below in a comparative value investigation and a comparative trend analysis.

Three steps were taken in the validation process. The first step was to examine the decision process, the second step was to examine the error states, and the third step was to examine the controls. Each step was assumed to be independent because no usable cross-correlation data were available.

6.3.1 Decision Process Validation

The validation of the decision was based upon data obtained from experiments conducted by Machuca and Lind and by Allen and Clement (Ref 2,48). This information addressed the problem of defining the dwell time of the visual system. The decision model parameters defined in Chapter IV were tuned to account for this information. Those parameters were set so that the average dwell time for the twenty-run Monte Carlo analysis was .17 seconds. This was .03 seconds short of the desired .2 second dwell time deemed appropriate from analysis of the previous experiments, but within a reasonable tolerance. It is possible to adjust this average dwell time to the .2 seconds desired by altering the increment added to the payoff values. The increment used in the decision process example of Chapter IV was 0.5. This is part of the decision process tuning

procedure referred to in that Chapter, and was used in preliminary runs to adjust the dwell time to .17 seconds. Because of computer time costs, further tuning past the .17 second time achieved was not accomplished.

It is necessary to note at this point that other problem parameters could be varied to achieve the desired dwell times. For instance, though the thresholds were considered fixed by apriori knowledge of human thresholds, allowing those thresholds to vary could alter dwell times. Also the payoff for being outside threshold could be varied to alter dwell times. Neither of these parameter sets were considered acceptable for dwell time specification, because complex multiple changes would have been necessary in each group to effect the same outcome as the one increment change noted above.

Two aspects must be addressed at this time in the interest of validation completeness. The first aspect is the contrast between scanning and attention, and the second is the correlation of the decision process output to the actual human decision. The first aspect, the distinction between scanning and attention, is presently drawing experimental attention. (Ref 25) Unfortunately the experimentation process used is a control task coupled with a mathematical problem, which is not of a form admissible for use in validation of the present model. Further and more realistic experiments which involve the human making decisions for an aircraft control task should provide better statistics usable for decision process parameter determination.

The second aspect, that of detailed correlation of the proposed decision process with the human decision process, is theoretically interesting, but was not considered to be within the scope of this research. A proper correlation would involve extensive experimentation showing relationship between the decision process hypothesized above and an actual human operator decision process, in like tasks. This experimentation in itself is an extensive research project. Unless one pilot/aircraft variable progresses to a critical state, it is very unlikely that attention patterns will be the same between two individuals, or even between two runs of the same task for one individual. Because of these two aspects, properties which the decision process must possess were chosen, and the decision process was mathematically implemented so that it displayed those properties. Those properties were:

1. Empirical attention dwell time information could be duplicated.
 2. Attention during a critical state, such as engine loss could be duplicated.
 3. Logical pattern is followed when not in critical state.
- By choosing the decision process in this manner it is felt that the process structure is flexible enough that further research will not change structure only parameters within the structure.

By allowing this flexibility, many diverse uses of the decision process can be considered. One of these uses could be in the field of human operator training. If a decision pattern is shown to

produce a divergent trajectory or a less precise trajectory than another realization, this pattern information could be used to teach a pilot good scanning techniques, or keep the pilot from bad techniques.

6.3.2 Error State Validation

The second aspect necessary for validation is the set of error state responses. For this purpose the figures referred to earlier in this chapter and displayed in Appendix 2, coupled with data from previous experiments, will be examined. It is important to note at this point that usable pilot/aircraft experimental data taken from an aircraft and/or simulation similar to the one modelled in this experiment was not available. With that realization, a decision was necessary; what available data would be the most useful in validating the concept? The available data grouped into two categories: first, similar aircraft (fighter type, but not force stick and not fly-by-wire) flying an uncoupled longitudinal or lateral task, and second, dissimilar aircraft, or experimental plant model dynamics, but flying a coupled dynamic trajectory. Because the available fighter type aircraft were not similar to the aircraft used in this research it was felt that no usable information could be attained by this comparison. Therefore, since the dynamic trajectory is a major element of this research and the raw information on trajectory errors is partially aircraft-independent, the decision was made to use the data available from dissimilar aircraft flying a dynamic trajectory. Because of this decision, the criteria for

comparison of the chosen experimental data detailed in the following discussion, and the data generated by this research must be qualitative rather than quantitative. Since data from similar aircraft was not available, a detailed comparison is neither useful nor valid, necessitating the comparisons to be of a general nature.

The previous experiments that will be investigated are those recorded by Harrington (Ref 30), Hess (Ref 32,33), Moriarty (Ref 55), and Elkind and Miller (Ref 24). Harrington's data present the most relevant data, in that time histories of ten runs were accomplished, and the data were displayed by the mean \pm standard deviation format described above for altitude error, crosstrack error, pitch angle error, roll angle error, elevator deflection and aileron deflection. This is the same portrayal of actual man-in-the-loop simulation data that was chosen in the all-digital simulation in this research. Unfortunately two aspects degrade this data's relevance to the present problem. The first aspect is that a C-135 was simulated, which has flight dynamics and control inputs much different from the fighter-type aircraft used in this research. Because of this difference, the elevator and aileron information was not used. The second aspect is that the aircraft was following a localizer/glide path on an ILS approach. This is much less dynamic than the situation simulated in the present research. Despite these two drawbacks, the experimental procedure and the data available from that procedure present the most realistic comparison available to the author.

The model used in this work was not adapted to the C-135, because of the very limited maneuvering done by that aircraft and the relatively unknown control system model. These two aspects make

application of this type model impractical.

The second and third sources are attributed to Hess. (Ref 32,33) His research provides data on a task with time varying dynamics. As this is a single channel task, no decision process is necessary. Stick input information and display error information are available in this research.

The third source is Moriarty's dissertation. This source provides information in the form of stick deflection and state error. This information is presented with the plant dynamics displaying slowly time-varying characteristics.

The last source, Elkind and Miller, also considers time-varying systems. Their systems change gain and system description instantaneously. This is a rather artificial situation, but as it is at the opposite extreme from Moriarty's slowly time-varying systems, it is felt that it can therefore be considered along with Moriarty's work to make observations on systems such as the one considered, which has dynamics which lie somewhere in the middle of the time-varying dynamic system spectrum.

The basis for comparison was next considered and for this consideration two aspects of the simulation were investigated. First, the aircraft was assumed on the trajectory at the initial time. This assumption was made since no better information was available. This shortcoming is not considered to be a problem in further usage of this model, because as mentioned earlier, it is proposed that this model be coupled with a steady state model, to cover operator control over the aircraft flight regime. The steady state model would then

provide the initial condition information the error states need for start-up. This aspect was discussed further in Chapter V.

The second aspect affecting the basis for comparison is the short duration, half a second, of the trajectory. In comparison, Harrington's data were recorded over an ILS run that lasted approximately one and a half minutes.

Because of these two properties, the rates of change of the mean and of the standard deviation for the error states will be considered as the comparison metrics. These parameters are less sensitive than the error states themselves to the difference in error state initial conditions and should be a more comparable parameter between the short time trajectory of this research and the long trajectory of Harrington's research. The difference in aircraft, fighter versus transport, and in trajectory, dynamic versus steady state, would tend to drive these rates higher for this research simulation. The gust values considered, light in both cases, should have some effect since the light gusts during landing are higher by Mil Spec 8785B than during operation at 15,000 feet. Also those gusts will have more effect on a 125 knot approach, the C-135 path, than in a .9 Mach trajectory.

For the rate comparison, first consider roll angle. The error state mean change in this simulation was approximately .12 degrees per minute, and the standard deviation change was .18 degrees per minute. Examining Harrington's experimental data, maximum mean change for roll angle error state was 5 degrees per minute with a

maximum error state standard deviation change of 1 degree per minute. These maximums experienced in Harrington's experiment, accounted for less than 10 percent of the ILS trajectory considered in his data, with the remaining 90% of the trajectory lying very close to the .12 degree/min mean and .18 degree/min standard deviation range found in this research simulation. It is felt therefore that the short duration higher rates could be accounted for by realization of the increased gust level effects used by Harrington.

The altitude error is next considered. The altitude error state mean rate was 420 ft/minute, and the standard deviation change on altitude error state was 120 ft/minute for this research. In Harrington's data, the maximum recorded altitude error state mean was 140 ft/minute, and the maximum recorded standard deviation change in the altitude error state was 100 ft/min. These numbers are reasonably comparable when considering the trajectory differences and the response differences between a fighter aircraft and a transport aircraft.

The crosstrack deviation for this research displays an error state mean rate of 240 ft/min and an error state standard deviation rate of 120 ft/min. These values correspond well with Harrington's data, in which the maximum crosstrack deviation mean rate was 200 ft/min and the maximum crosstrack standard deviation rate was 90 ft/min. This error state match is very reasonable, as the rudder inputs were apparent in this research simulation in what would be considered small to moderate amounts. This input realization should correspond well with maximum rates from the less maneuverable transport aircraft that corrects for crosstrack mainly with roll.

The last correspondence is drawn between the pitch angle error state mean rate of .1 deg/min and the pitch angle error state standard deviation rate of .3 deg/min for this simulation, and the maximum pitch angle error state mean rate of 10 degree/min and a standard deviation rate of 10 degrees/min for Harrington's experiment. Specifically, in a pitch approximately 95% of Harrington's data was very close to the rates experienced in this research, and 5% was at the higher rates above. These diversions as in pitch are thought to be attributed to the increased effect of gusts. The rates are within the range of Harrington's data and therefore felt to be realistic.

In review the values derived for the mean rates and standard deviation rates of the two experiments are comparable, with the differences caused by the factors noted earlier. In examining the data taken by Hess (Ref 32,33), Moriarty (Ref 55), and Elkind and Miller (Ref 34), long periods of minimum excursion from zero error with small standard deviations were experienced. Also when errors that could be attributed to startup were translated into mean and standard deviation rates, those errors would have had values below the maximums experienced in Harrington's data. In Moriarty's work some periods with large standard deviation rates occurred during the time-varying dynamics runs. These values correlate with the time-varying dynamics runs assumed in this research.

One factor was apparent in comparing the above references to this research. That is that, though some short data periods in

each paper were markedly different, all four of the references displayed long data periods wherein the tracking accuracy was the same order of magnitude as in this research.

6.3.3 Control Validation

In this research, a force stick was chosen as one of the input devices. This type device was considered more precise, and therefore more amenable to analysis, than the older displacement stick. This choice unfortunately made numerical correlation with the research sources above almost impossible, as each of those considered a displacement-type stick. Therefore to establish force stick input trends, and relative force magnitudes, simulation results previously run on the Air Force Flight Dynamics Laboratory Large Amplitude Multimode Aerospace Research Simulator, LAMARS, were used. In this simulation an F-16 was used with a force stick. Numerous runs were monitored, with the pilot trying to maintain straight and level non-accelerating flight. This accomplishes part of the "correcting to a trajectory" task. It is only a partial task, however, as information on position relative to a trajectory is not part of the straight and level trajectory.

In the trajectories monitored, only gross information - maximum force exerted during the run and average force exerted during the run - were observed. The rudder was not used during any of the trajectories. Possibly because of the task, the maximum forces exerted were 16 pounds in the roll channel and 5 pounds in the pitch channel. The average forces were approximately 8 pounds in the pitch channel and 5 pounds in the roll channel. As the trajectory

flown while recording this information was simpler to fly than the trajectory in the research, these values were considered less in magnitude than those that could be considered representative for the research. Comparing the research simulation with these values, it is found that the simulation exerts, at maximum, a force correction of 1/2 pound in either pitch or roll, well within the boundaries. This aspect is representative, since in the LAMARS simulation the maximum forces were usually experienced after a 3 or 4 second period of increasing force. Therefore, half a pound of force in half a second represents the observed data reasonably.

The purpose of this comparison was to ensure that control magnitudes were realistic. Because of control system and aircraft differences, direct comparisons are impossible. This is emphasized by the contrast between the hydraulically assisted control system on the C-135 activated by a yoke and designed for two hand operation, and a "Fly-by-Wire" control system activated by a side stick controller designed for wrist operation. However, the trends realized by the comparison, the desired result, are considered valuable.

6.4 ANGLE OF ATTACK INFORMATION DEGRADATION

In the above analysis, the three-standard-deviation value for the angle of attack information was considered to be one degree. The 1 degree value was taken from Figure 8 considering an angle of attack of two degrees. This value was considered representative for the run desired. It is very likely that the measurement is less accurate than this in certain flight regimes. It is also very likely that each angle-of-attack sensing unit has different expected accuracies,

with the more accurate systems being more costly. Therefore, a sensitivity analysis on the angle of attack measurement could prove desirable in determining necessary instrument accuracy. The present angle-of-attack instrument accuracy is a function of the flight state, since a typical instrument computes angle-of-attack at numerous aircraft positions and then votes to determine which measurement to use. Because the nominal trajectory of the aircraft is known in advance, angle of attack accuracy can be determined, and a Gaussian noise with time-varying statistics can be used to represent the resulting inaccuracy. This provides a sensitivity analysis of the angle of attack measurement by varying the expected three-standard-deviation error for the angle-of-attack measurement to determine if measurement degradation adversely affects flight control.

With this in mind, the three-standard-deviation measurement accuracy for the angle of attack was varied from one degree for Figures 13 and 26, to 3 degrees for Figure 27 through 40 to 9 degrees for Figures 41 through 54. This analysis was made to determine the effect of the angle-of-attack inaccuracy on the aircraft control inputs and error states. The angle of attack measurement is essential, as it is one of the feedback elements in the inner loop control of the aircraft in question.

In general, when varying the angle of attack statistics from a three-standard-deviation value of 1 degree to one of 9 degrees, the largest effect was observed in the applied control. The statistics of each of the error states remained consistent throughout the angle-of-attack variations. The control required for the one degree, three-standard-deviation value for angle-of-attack and the three degree,

three-standard-deviation value for angle-of-attack are of about the same magnitudes. However, using the model of this research, when the three-standard deviation value increases to 9 degrees, about twice as much force is required in the roll control channel and in the pitch control channel. Though the control magnitudes required for this task are not large, the increased activity in each of these channels could signal an increased pilot workload and therefore degraded handling qualities.

6.5 MODEL FLEXIBILITY

The preceding sections in Chapter VI have outlined the model implementation and have detailed a general correspondence with previously recorded data. These sections, along with the estimator, controller, and decision process sections, group to display the basic result of this research, model flexibility and applicability.

The model flexibility allows the user to adapt the output characteristics of the decision process, the controller, and the estimator to his problem characteristics by altering the appropriate parameters. To provide guidelines for this alteration, the available parameters and a variance-effect relationship of those parameters are detailed in the corresponding chapters.

Some other general elements which contribute to the flexibility are the ability to analyze a general aircraft trajectory, and an analysis technique which, since the entire nonlinear model is used as the basis, allows an accurate state error performance depiction. At this point, uses for the model derived in this work have been motivated. In that motivation care has been taken to point out present problems this model can address where no other mode of analysis other than flight test, a very costly option, is available. Once

these reasons for considering this model, or method of analysis were presented, a demonstration of its usage was suggested. The purpose of this demonstration was to display to the engineer that the model presents usable results; usable considering both previous data and physical realizability.

Now given the reasons for using the model and given the confidence that the model will provide the needed information, a methodology for employing the model will be provided. This methodology is meant to complement the other sections by supplying practicalities and considerations necessary in using each stage of the model. This methodology considered with Figure 2, the model flow chart which specifies these stages; Appendix 1, the computer program flow chart which implements Figure 2; Appendix VI, the parameter list which identifies the parameters in the programs of Appendix I; and Chapters III and IV which detail the adjustments available so that Appendix VI parameters can be altered for an individual problem, should allow a potential user an excellent roadmap for this model's use.

It is necessary to note that this methodology is applicable whether the human operator is assumed to have a full order system description or a reduced order system description as his inherent Kalman filter-predictor-controller model. This aspect is important, because the complexity of the full order model makes a reduced order model desirable, and in some cases, a reduced order model is a reasonable alternative. One such case is when human operator data

is available for the trajectory which you are attempting to control, a reasonably frequent occurrence. In this case the standard is the data, and the desirable outcome is to match the model's performance to that data.

In other cases, as was the case with this research, no reasonable data was available, so the full order model must become the standard, and the performance of the reduced order models, if they are appropriate must be considered against this full order model. With this distinction in mind and understanding that the processes to obtain the model will be essentially the same, consider the aircraft motion and control equations. In this set the equations of motion are given by 2-55, 2-56, 2-57 for position, 2-13, 2-14, 2-15 for velocity, 2-48, 2-49, and 2-50 for angular position, and 2-31, 2-32, and 2-33 for angular velocity. This set of equations will be used regardless of aircraft type, with only the components: X_S , Y_S , Z_S , 2-37, 2-38, and 2-39, and L_S , M_S , and N_S , 2-45, 2-46, and 2-47 reflecting the individual aircraft. These quantities can usually be found in documents published by aircraft manufacturers, and for this problem was taken from Ref 62. An analysis of the conditions required for simulation can significantly reduce computation of these quantities since these quantities are usually given in tabular form for flight condition, so specifying a flight condition reduces the tables needed.

At this point it is necessary to emphasize model validation. A necessary step before construction of a model is to analyze the

proposed construction for modules that can be individually validated so that when the entire model is constructed, the only validation left is the module interfaces.

The set of twelve equations referenced above is the first convenient validation module. It is a logical module for two reasons. First, it is the first building block that can test the individual aircraft information; X, Y, Z, L, M, and N; and second it is also the first information usually available in terms of transfer functions that can be used for validation.

After this module has been considered, the second module is the control system equations.

For this portion of the Model a block diagram description such as Figure 3 is usually available. In modelling this function digitally, two special considerations are necessary. First, if the control system is not digital, as in Figure 3, digital models of the nonlinear gains will have to be constructed. Second, an analysis of the error sources will be required so that models of those sources which will be significant can be incorporated.

Once the control system is constructed, the model excluding the error sources should be combined with the equations of motion, to form the second module. Because of the coupling between the equations of motion and the control system, it is not practical to check only the control system other than with simple cases which can be done without the computer. Time plots or transfer functions for this module are usually available, however not necessarily for

the conditions that are chosen for the simulation. It will be necessary therefore to analyze the expected differences between the data available and the simulation condition to accomplish validation of this module. It is important to exercise all controls because sign conventions on the control surface/equations of motion interfaces are not well specified. Physical examination of the results of each input will easily identify any irregularities.

After this is accomplished, the error states should be added, and each control should be exercised to assure the magnitudes of the error states are consistent with their military specifications or published accuracies.

At this point the aircraft model is set and the next step is to start construction of the controller model. For this purpose, the observations that the controller is to make should first be identified. For those observations two subdivisions need be considered. The first is the observations that will be intermittent as a result of the decision process, and the second is the observations that will be continuous. In this research, the continuous observations were lateral and normal accelerations while the decision dependent observations, the intermittent observations, were those displayed on aircraft instruments. It is anticipated that the decision dependent measurements will continue to be based upon the visual interpretation of instruments, however the set of continuous measurements should be expanded as better models evolve for human perceptions. (Ref 19)

Once these observations are identified, the mathematical representation of the observations must be formulated, and error models for the observations should be derived. Numerous error models are available (Ref 19) and problem insight should suggest which models are applicable.

The validation of these measurements can be accomplished by augmenting the second module of aircraft equations with the error models for the observations. By running these equations and obtaining the true observations and the noisy observations, it is possible to assure that the proper error models were used, and the magnitude of the noise assumed in the observations is appropriate.

Now that the observations are included, the next step is to include the states for the neuromuscular lags assumed for the human controller. These states are added to each input device in the aircraft control equations. In this research, there were four assumed, fore and aft stick, left and right stick, rudders, and throttle.

At this point, the entire set of aircraft equations including the observation equations are specified. It is next necessary to linearize this set. This linearization is not done earlier because changes in signs and magnitudes made while validating the equations above would present a large bookkeeping problem. Also, the entire set of equations was not available until this time.

Once the linearization has been accomplished, the estimator can be constructed. This construction is detailed in Chapter III. For this construction, the observation error matrix associated with each observation has already been discussed, as has the initial covariance matrix. If a reduced order model is to be used, once the errors are determined on the full order model, insights into the reduced order model errors can be achieved with a covariance analysis.

At this point, the next validation step is necessary. Using the linearized equations in the Kalman filter, a check can be run on the linearization process and the Kalman filter implementation. By considering a simple trajectory and setting all the error sources to zero, the Kalman filter estimates of the error states should remain small. The trajectories chosen should be simple but exercise pitch, roll, yaw, and throttle control. Though this is not a comprehensive check, sign errors and erroneous equations can be identified through this procedure.

The next step is to determine the control gains. As with the observations, the first step is to determine which controls will be accentuated for the problem in question. Table 3, when applied to an individual problem, should provide an indication of the control gain matrices necessary. It may be necessary at this point to identify the need for separate decision processes for observations and controls. Should this be the case, or should different types of

controls be necessary, as in helicopters, an analysis as was accomplished in Chapter IV to identify the controls pertinent to each maneuver is necessary. Once these controls have been identified, parameters for the control gain matrices should be set as detailed in Chapter III to assure that the control desired is available, and the control specified is physically appropriate.

With each of these control gain matrices specified, the next validation step is appropriate. Each of the control gain matrices should be run with the Kalman filter and aircraft equations complete with noises to assure that the resulting controls are appropriate and the resulting error states are controlled with the computed control gains. Running each of the controls individually should assure that minimum interface problems are encountered by incorporation of the decision process.

The outcome of this process also provides an indication of controller stability. That is, if each of the controllers are stable, then it would appear that a control structure that constantly chooses one of the stable controllers should be stable. This hypothesis is however not proved in this work. After the control gains have been validated with the Kalman filter estimates, the next step is to apply the gains to the predictor estimates. This application can best be made on the trajectory which will be examined, because the validation can only be examined in general terms such as magnitudes of control inputs and error states. It is appropriate to contrast the previous analysis accomplished with Kalman filter

estimates with this analysis accomplished with the predictor estimates. If both analyses produce very similar results for the particular trajectory considered, it may be desirable to assume the time delay is not a factor in the problem, and therefore streamline the analysis by omitting the time delay.

The last aspect, the decision process, can be considered a module in itself for preliminary analysis. After this module has been constructed and validated, application to the total problem should be straightforward. The first step in constructing this model is to identify the decision states. The states used in this research, pitch, roll, yaw, airspeed, and altitude, are an excellent indication of possibilities, but individual problems may require either additions or deletions from this set.

For the decision process, the parameters were identified and discussed in Chapter IV. The visual thresholds used were standard; .5 degrees change at the eye for visual angle detection, and .5 degrees/second change at the eye for visual angle rate detection. (Ref 32)

The initial validation of this process is accomplished independent of the previously discussed procedures. By assuming a constant mean and standard deviation for each of the decision states, it is possible to assure that for the steady state case the desired minimum dwell time and average dwell time is achieved. By perturbing the mean and standard deviation of the decision states both in a constantly increasing path, and in a cycling path,

further checks are made to assure appropriate dwell times. These checks should also assure that decision states that are badly out of threshold are being attended, and when decision states are comparably within threshold, the process cycles through the states. Information available in specific problems can give further insights into the functioning of the applied decision process which can be incorporated into the decision process validation.

At this point all that is left is to couple the decision process with the previously constructed controller and perform the necessary analysis.

By applying the construction techniques detailed above, and by using the validation procedures as each module is constructed, confidence is achieved at each step so that minimum uncertainty exists when the total system is interfaced. This method is especially necessary in cases such as this research where no data will be available to compare with this model.

CHAPTER 7

RECOMMENDATIONS AND CONCLUSIONS

7.1 CONCLUSIONS

The intent of this research has been to construct a controller with human operator limitations capable of general aircraft control. General aircraft control refers to the condition under which no constraints are placed on maneuver. To this end, human operator research, control theory, estimation theory, decision theory, and the author's flying experience (2750 hours in 7 aircraft) were closely examined. Each of the above considerations was an integral part of the final pilot/aircraft model, and the synthesis of those considerations is the basic contribution of this research.

This synthesis begins with the small perturbation approach to nonlinear equations and applies optimal estimation-optimal control theory to those small perturbations to derive a set of possible estimations, and a set of possible controls. The decision process then enters by specifying which of the set of possible estimations and which set of possible controls will be applied. Human operator research provides the basic control structure and the basic estimator structure, and insights into the decision process.

Decision theory provides several alternative methods for the decision process, and personal experience, human operator research, and estimator and controller structure detail the impact upon the

definition of the decision process, as well as insights into how the process should be implemented. Each of these couplings is detailed in the appropriate chapters.

Because of financial pressure due to escalating flying hour costs, both actual airplane and simulator, increased use of mathematical models of the pilot/aircraft system is inevitable. It is felt that this research provides two needed ingredients to the present pilot/aircraft system model. The first is using rules and learning manuals common to military pilots to aid in specifying the model. The second is a very general structure that can be used for general pilot/aircraft control problems, or can be reduced for specific problems.

With these considerations in mind, four conclusions are drawn from this research.

1. The goal to construct a controller with human operator limitations for a general aircraft control task was realized.
2. The goal to mechanize the assumed human operator limitations logically into an estimator-controller structure was realized.
3. A decision process was incorporated into an estimator-controller structure. This composite structure extends the scope of nonlinear mathematical modeling, to systems which internally display a decision process.
4. Subsets of the approach taken by this dissertation can be applied to address a diverse set of current aircraft control problems.

These conclusions will now be expanded.

The first two conclusions are that the initial goal, to construct an estimator-controller with human limitations for a fighter-type aircraft flying a general aircraft maneuver, has been accomplished. This was evaluated and tested against presently available data and was found to correspond well to the aspects of that data pertinent to the research problem. The controller was stable over the time interval considered, and each control was well within a practical range of values. No theoretical proof of stability was presented; however a demonstration of stability was provided by the longitudinal axis subproblem.

It must be noted that because the available data for the full order problem was not of a form that could be compared directly with this research, the comparison with previous data is basically a trend analysis. This validation procedure was used because gathering data for a direct comparison would have involved a specially instrumented, dedicated simulation, and that was beyond the available resources. Though the trend analysis is not the best mode of validation, it provides a desired result: justification that the model acts in a manner comparable to the previous analyses. This result is necessary if this research is to be used as desired, a basis for further investigations into pilots' functioning in a dynamic environment.

The third conclusion is that this work has mechanized a decision process with the optimal estimator and optimal controller, to effect control of a plant. Although some of the benefits of this mechanization will be delineated in the discussion of the last conclusion, the mechanization is itself a basic contribution.

The fourth conclusion is that the derived structure of the controller is particularly usable over a spectrum of current problems. With this structure incorporating the decision process, an added dimension of the total pilot/aircraft system is introduced to the current pilot modeling framework. Subsets of an implemented decision process were discussed in previous literature, but always for very restricted problems. The model formulation allows the application of the model to an entire aircraft operating in a general trajectory, an aspect which is considered essential to future tasks required of human operator modeling.

This aspect also suggests investigation of the decision process in that by utilizing the structure provided in Chapter IV, experimentation must be conducted to provide better definition of the decision process parameters. Also the implementation of the decision process in such fields as simulator motion analysis, human vertigo analysis, and training methods must be investigated. The particular implementation chosen for the decision process also allows nonstationary statistics in the system dynamics. This makes the model well suited for sensor error analysis in nonlinear systems implemented through the perturbation approach. This aspect of analysis has not been previously available.

Another use of this work is that the method employed for a controller with human limitations can be readily extended to deriving an autopilot by the previously suggested simplification. The outcome of this methodology provides the basis of an autopilot that will

control through any given trajectory. The complete system as implemented in this research, provides a means needed for system complexity reduction, an aspect necessary in any realizable trajectory-following design.

7.2 RECOMMENDATIONS AND EXTENSIONS

This section can be decomposed logically into two categories, man-in-the-loop control and autopilot control. The autopilot control problem, though not addressed directly in this research, is a natural extension of this work. If the decision process and the time delay are removed from the problem, the result is an autopilot for a dynamic aircraft trajectory. An autopilot of this type could find use in problems in which specific trajectories requiring time-varying vehicle dynamics are desired. Some possibilities for this concept lie in air-to-ground attack and surface-to-air missile avoidance. A usable application of this research to either of these problems would require state variable reduction of the time-varying dynamics system. This simplification is necessary because any implementation on board an aircraft requires efficiency in both computer storage and computation. A construction such as this could use the full-order model as a performance reference, a step considered necessary in any state reduction procedure. The method is suggested because it reduces the full order equations as does the lateral, longitudinal reduction used in typical autopilot construction, but the reduction is very different. In the typical autopilot formulation, all terms coupling the lateral and longitudinal modes are

neglected, so that two separate systems, a lateral system and a longitudinal system, result. In this formulation, the coupling terms could remain, and terms found to be small during any particular trajectory could be neglected. By examining the problem in this state reduction manner, a more precise realization of control for a time-varying trajectory is expected than is presently available. This methodology could extend aircraft control into position and time considerations from the almost purely attitude consideration that is presently being stressed.

The full order equations or a small order reduction is an extreme case in which the trajectory is very dynamic and the control in time, of position, and attitude is necessary. In some simpler cases it is possible to identify the few specific cross-coupling terms in the nonlinear equations that will contribute the time-varying terms in the error state equations. For many of these situations, the order reduction can parallel typical autopilot analysis, with the addition of corrections for the coupled terms. A case in which this type of reduction is useful is in the lateral roll coupling terms that become necessary in direct side-force mechanisms. The cross-coupling terms in this usage are apparent and can be accounted for mathematically by adding specific term compensation. This mechanism however does not require the combination of both time and position control, a combination that severely increases problem complexity.

The second path of extension lies in pilot/aircraft simulation. The coupling of decision theory to the human operator simulation has benefits in many current problems. One possibility is a modeling definition of vertigo. The decision theory framework provides a basis for vertigo investigation by allowing multiple observation matrices, with elements of each matrix supplied by both visual and nonvisual cues. By allowing the visual and nonvisual cues to conflict and recording the effects of this conflict, it is hypothesized that vertigo effects can be duplicated.

A second usage is in the simulation field, where the question of whether motion is necessary in a flight simulator has stimulated extensive research by simulator users. By coupling the decision process with the observation matrix and allowing the observation matrix to contain measurements from either or both visual and nonvisual sources, the Kalman filter estimates can be traced in time using different combinations of measurements. These measurements could allow or exclude motion so that the mathematical effect of motion on the estimator can be recorded. This method could lead to some basic assumptions on motion effects that could be tested through physical experimentation.

This extension is contingent upon a well-developed model of the nonvisual and peripheral visual perceptions. A model such as this is being developed by Curry and Young. (Ref 19) Without an extensive sensor model such as this only the gross effects of the nonvisual senses can be represented, and, as in this research, an

extensive analysis of conflicting cues or of nonvisual cue effect cannot be made.

Behind each of the extensions suggested above is experimentation needed for specific data to define the decision process. Some possible areas of experimentation for decision process validation lie in correlating control input with eye position, in testing for individual thresholds when observations such as those listed above are available, in validating models of visual and nonvisual cues, and in testing for attention patterns which can be attributed to specific maneuvers or to imprecise information.

The initial data from this experimentation must be related to the decision modes suggested in Chapter IV, as that definition of mode is essential to the decision process development. Also, that definition of mode is felt to create the basis for allowing the model to be insensitive to aircraft. If this insensitivity could be established, the model usage would be considerably broadened.

Two other areas for experimentation have been identified while hypothesizing possible usages of a controller for a highly dynamic system. The first is a game theory problem: given that a surface-to-air or air-to-air missile was fired, identify the set of possible trajectories that will cause the aircraft to avoid the missile. Unfortunately these are nonlinear game theory problems of a high order, requiring costly computer time. The other area of suggested research lies in pilot/autopilot coupling suggested by current integrated fire control and flight control research. (Ref 20)

AD-A066 193

AIR FORCE INST OF TECH WRIGHT-PATTERSON AFB OHIO SCH--ETC F/G 1/3
AN ADAPTIVE CONTROLLER WHICH DISPLAYS HUMAN OPERATOR LIMITATION--ETC(U)
NOV 78 E K LINDBERG
AFIT/DS/EE/78-1

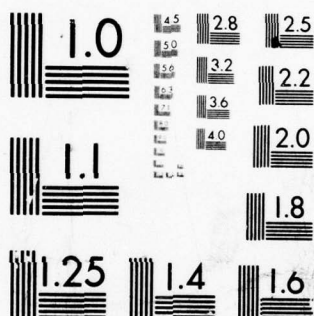
NL

UNCLASSIFIED

3 OF 4

AD
A066 193





MICROCOPY RESOLUTION TEST CHART
NATIONAL BUREAU OF STANDARDS-1963-A

One suggested usage of this coupling is to allow the pilot to have a decreasing ability to effect control as the target aircraft gets closer to the firing position. The proportion of manual control to automatic control is presently open for analysis, and a human operator as depicted above could be readily applied to this analysis.

There are four areas of suggested research, then, outlined above. The first area was in further validation of the suggested concepts by experimentation in highly dynamic systems with multiple controls and observation sets. The second area was in experimentation designed to define the decision process. The third area was applying the concepts of control for highly dynamic systems to an aircraft autopilot, and the fourth area was defining usages for the highly dynamic trajectory autopilots.

With the evolution of analog and digital computers, control theory has been called upon to play an increasing role in aircraft control. This role to date has been based almost solely on linear time-invariant system control theory. This research has defined a structure and a means for analyzing a general aircraft control problem. It is felt therefore that perturbations of the structure presented in this research will be invaluable in extending the role of control theory further into the general aircraft control problem.

Bibliography

1. Ackerson, G.A. and Fu, K.S., "On State Estimation in Switching Environments", IEEE Transactions on Automatic Control, pp. 10-18, Vol AC 15, Feb 70.
2. Allen, R. W., Clement, W. F., and Jix, H. P., "Research on Display Scanning and Reconstruction Using Separate Main and Secondary Tracking Tasks." Hawthorne, California, Systems Technology, Inc., NASA CR-1569, July 70.
3. Anderson, K., A New Approach to the Design of Optimal Compensators for Manual Control Systems Using the Dual Sub-Optimal Controller, University of Queensland, May 73.
4. Aoki, M., "On Decentralized Linear Stochastic Control Problem with Quadratic Cost." IEEE Transactions on Automatic Control, VOL AC-18, pp. 243-250, Jun 73.
5. Athans, M., and Tse, E., "Adaptive Stochastic Control for a Class of Linear Systems", IEEE Transactions on Automatic Control, pg. 38, 1972.
6. Athans, M., "The Discrete Time Linear-Quadratic Gaussian Stochastic Control Problem", Annals of Economic and Social Measurements, pg. 449, 1972.
7. Athans, M., and Tse, E., "On the Adaptive Control of Linear Systems Using the OLFO Approach", IEEE Transactions on Automatic Control, pg. 489, 1973.
8. Athans, M., "The Role and Use of the Stochastic Linear Quadratic-Gaussian Problem in Control System Design." IEEE transactions on Automatic Control, VOL AC-16, pp. 529-552, Dec 71.
9. Baron, S., et al, Application of Optimal Control Theory to the Prediction of Human Performance in a Complex Task, AFFDL TR 69-81, March 1970.
10. Baron, S., and Kleinman, D., The Human as the Optimal Controller and Information Processor, NASA CR-1151, Bolt, Beranek, and Newman, September 1968.
11. Beckett, R., Hurt, J., Numerical Calculations and Algorithms, McGraw Hill, 1967, New York.
12. Blakelock, J. H., Automatic Control of Aircraft and Missiles, John Wiley and Sons, Inc., New York, 1965.

13. Britting, K. R., Inertial Navigation Systems Analysis, Wiley-Interscience, New York, 1971.
14. Buckingham, R. A., Numerical Methods, Sir Isaac Pitman & Sons, Ltd., London, 1957.
15. Carnahan, B., Luther, H. A., Wilkes, J. O., Applied Numerical Methods, Wiley, New York, 1969.
16. Chalk, C. R., et al, Background Information and Users Guide for MIL-F-8785B(ASG), "Military Specification - Flying Qualities of Piloted Airplanes," Air Force Flight Dynamics Laboratory, AFFDL-TR-69-72, Wright-Patterson AFB, Ohio, August 1969.
17. Chong, C. Y., Athans, M., "On the Stochastic Control of Linear Systems with Different Information Sets." IEEE Transactions on Automatic Control, VOL AC-16, pp. 423-431, Oct 71.
18. Chu, K.C., "Team Decision Theory and Information Structures in Optimal Control Problems - Part II," IEEE Transactions on Automatic Control, VOL AC-17, pp. 22-28, Feb 72.
19. Curry, R.E., and Young, L.R., Pilot Modeling for Manned Simulation, AFFDL Contract No. F33615-75-C-3069, Aerospace Systems, Inc., 1975.
20. _____. "Definition and Preliminary Evaluation of Integrated Automatic Flight and Fire Control Systems," General Electric, Binghamton, New York, March 1975.
21. Degroot, M. H., Optimal Statistical Decisions. McGraw Hill, New York, NY, 1970.
22. Deshmursh, S. D., and Chikti, S.D., "Optimal Delays in Decision and Control," IEEE Transactions on Automatic Control, VOL AC-19, pp. 412-416, Aug 74.
23. Durrett, J., "A Linear Stochastic Model of the Human Operator," Proceedings of the Ninth Annual Conference on Manual Control, May 1973.
24. Elkind, J. I., and Miller, D. C., "The Process of Adaption by the Human Controller," Second Annual NASA University Conference on Manual Control, NASA-SP-128, 1966, pp. 47-63.
25. Enstrom, K. D., Rouse, W. B., "Real-Time Determination of How a Human has Allocated his Attention between Control and Monitoring Tasks." IEEE Transactions on Systems, Man, and Cybernetics, VOL SMC-7, Mar 77, pp. 153-161.

26. Farison, J., Graham, R., Sheldon, R., Identification and Control of Linear Discrete Systems," IEEE Transactions on Automatic Control, VOL AC-12, pp. 438-442, Aug 67.
27. Gilstad, D.W., and Fu, K.S., "A Two Dimensional Pattern Recognizing Adaptive Model of a Human Controller," Sixth Annual Conference on Manual Control, April 1970.
28. Hamilton, E., Chitwood, G., Reeves, R., General Covariance Program. "GCAP" An Efficient Implementation of the Covariance Analysis Equations Draft Technical Report, Air Force Avionics Laboratory, Wright-Patterson AFB, Ohio.
29. Hamming, R.W., Numerical Methods for Scientists and Engineers. McGraw Hill, New York, 1962.
30. Harrington, W., Unpublished Graphs on Results of the Flight Control Division's C-135 Simulation, Air Force Flight Dynamics Laboratory, Wright-Patterson AFB, Ohio.
31. Heath, R., State Variable Model of Wind Gusts, AFFDL FGC TM-72-12, July 1972.
32. Hess, R.A., "An Investigation of the Human Operator as an Element in Both Time Invariant and Equivalent Time Invariant Systems." Air Force Flight Dynamics Laboratory, Wright-Patterson AFB, Ohio.
33. Hess, R.A., "The Human Operator as an Element in a Control System with Time Varying Dynamics." Air Force Flight Dynamics Laboratory, Wright-Patterson AFB, Ohio, TM-65-34, June 1965.
34. Hsia, T.C., "Comparisons of Adaptive Sampling Control Laws," IEEE Transactions on Automatic Control, VOL AC-17, pp. 830-831, Dec 72.
35. Jaffer, A.G., Gupta, S.C., "Optimal Sequential Estimation of Discrete Processes with Markov Interrupted Observations," IEEE Transactions on Automatic Control, VOL AC-16 pp. 471-475, Oct 71.
36. Jain, R., "Decision Making in the Presence of Fuzzy Variables." IEEE Systems, Man, and Cybernetics, VOL SMC-6, pp. 698-703.
37. Jazwinski, A.H., Stochastic Processes and Filtering Theory. Academic Press, New York, 1970.
38. Kleinman, D., et al, "A Control Theoretical Approach to Manned-Vehicle Systems Analysis", IEEE Transaction on Automatic Control, Vol AC-16, pg. 824, December 1971.

39. Kleinman, D., and Baron, S., Manned Vehicle Systems Analysis by Means of Modern Control Theory, NASA CR-1753, June 1971.
40. Kleinman, D.L., Perkins, T.R., "Modeling Human Performance in a Time-Varying Anti-Aircraft Tracking Loop," IEEE Transaction on Automatic Control, VOL AC-19, pp. 297-306, Aug 74.
41. Kleinmantz, B., Formal Representation of Human Judgement, Wiley, 1968.
42. Kokotovic, P.V., and Yackel, R.A., "Singular Perturbation of Linear Regulators: Basic Theorems," IEEE Transactions on Automatic Control, pg. 29, February 1972.
43. Konar, A.F., et al, Digital Flight Control Systems for Tactical Fighters, Honeywell, Inc., Air Force Flight Dynamics Laboratory, AFFDL-TR-74-69, Wright-Patterson AFB, Ohio, July 74.
44. Kwakernaak, H., Sivan, R., Linear Optimal Control Systems, Wiley-Interscience, 1972.
45. Ku, R., Athans, M., "On the Adaptive Control of Linear Systems Using the Open-Loop-Feedback-Optimal Approach." IEEE Transactions on Automatic Control, VOL AC-18, pp. 489-493, Oct 73.
46. Levison, W.H., Applications of Optimal Control Theory to the Prediction of Human Performance in a Complex Task, Wright-Patterson AFB, Ohio. Air Force Flight Dynamics Laboratory TR-69-81, AFSC, Mar 70.
47. Levison, W. and Turner, R., A Control Theory Model for Human Decision Making, NASA CR-1953, Bolt, Beranek, and Newman, Dec 1971.
48. Machuca, L.A., Lind, J.M., "Verification and Extension of Display Scanning and Remnant Models Using Aircraft Lateral and Longitudinal Dynamics as Controlled Elements." Masters Thesis Air Force Institute of Technology, Wright-Patterson AFB, Ohio, 1971.
49. Magdaleno, R., and McRuer, D., Experimental Validation and Analytical Evaluation of Models of the Pilot's Neuromuscular Subsystem in Tracking Tasks, NASA CR-1757, STI, April 1971.
50. Maybeck, P.S., Notes from AFIT Class on Optimal Estimation, 1975.

51. McCormick, E. J., Human Factors Engineering, McGraw Hill, 1964.
52. McRuer, D. T. and Krendel, E. S., "Dynamic Response of Human Operators," Wright Air Development Center, WADC-TR-56-524, October 1957.
53. McRuer, D. T., Mathematical Models of Human Pilot Behavior, AGARD AG-181, January 1974.
54. Meditch, J. S. Stochastic Optimal Linear Estimation and Control, McGraw Hill, New York, 1969.
55. Moriarty, T. E., The Manual Control of Vehicles Undergoing Slow Transition in Dynamic Characteristics, NASA-CR-132442, 1974.
56. Onstott, E., Multi Axis Pilot Vehicle Dynamics During VTOL Flight, Northrop Corp., Proceedings of the 10th Annual Conference on Manual Control, 9-11 April 1974.
57. Paskins, H., A Discrete Stochastic Optimal Control Model of Human Operator in a Closed Loop Tracking Task, AFIT PhD Thesis, DS-33-70-1, June 1970.
58. Pollard, J. J., All Digital Simulation for Manned Flight in Turbulence, AFIT PhD Thesis, DS-EE-75-1, 1975.
59. Potter, R. M., Tanner, T. A., Application of Research on Human Decision Making. Symposium at Ames Research Center, Moffett Field, California, Jan 31 - Feb 2, 1968.
60. Raiffa, H., and Schlaifer, R., Applied Statistical Decision Theory, Cambridge, Massachusetts: MIT Press, 1968.
61. Rauch, H. E., "Order Reduction in Estimation with Singular Perturbation", Fourth Symposium on Nonlinear Estimation and its Applications, 10 September 1973.
62. Sanctuary, G. E., Stability & Flight Control, 12 Jan 73, General Dynamics Corp., FZM-401-048, Fort Worth.
63. Safanov, M. G., Athans, M., "Robustness and Computational Aspects of Nonlinear Stochastic Estimators and Regulators." IEEE Transactions on Automatic Control, Vol AC-30, pp. 717-725. Aug 78.
64. Safanov, M. G., Unpublished PhD Dissertation, MIT, 1978.
65. Sandell, N. R., Athans, M., "Solutions of Some Nonclassical LQG Stochastic Decision Problems." IEEE Transactions on Automatic Control, VOL AC-19, pp. 108-116.

66. Senders, J., et al, Human Visual Sampling Processes: A Simulation Validation Study, NASA CR-1258, Bolt, Beranek, and Newman, January 1969.
67. Sheilly, N. W., and Bryan, G. L., Human Judgements and Optimality, Wiley, 1964.
68. Speyher, D., Et al , Development of Techniques for Measuring Pilot Workload, NASA CR-1888, Honeywell, November 1971.
69. Tse, E., and Bar-Shalom, Y., "An Actively Adaptive Control for Linear Systems with Random Parameters Via the Dual Control Approach," IEEE Transactions on Automatic Control, pg. 109, 1973.
70. Tummala, V.M.R., Decision Analysis with Business Applications. Intext Educational Publishers, New York, 1973.
71. Wargo, M., et al, Human Operator Response Speed, Frequency, and Flexibility, NASA CR-874, Dunlop and Associates, September 1967.
72. Weir, D., and McRuer, D., Pilot Dynamics for Instrument Approach Tasks, NASA CR-2019, STI, May 1972.
73. Weir, D., and Klein, R., Measurement and Analysis of Pilot Scanning and Control Behavior During Simulated Instrument Approaches, NASA CR-1535, STI, June 1970.
74. Witsenhausen, H. S., "Separation of Estimation and Control for Discrete Systems," IEEE Proceedings VOL 59, pp. 1557-1566, Sep 71.
75. Witsenhausen, H. S., "A Counterexample in Stochastic Optimal Control," Siam Journal on Control, VOL 6, No. 1, pp. 131-147, 1968.
76. Wrigley, W., Hollister, W. M., Denhard, W. G., Gyroscopic Theory, Design, and Instrumentation, M.I.T. Press, 1969.

APPENDIX 1

Computation Methodology Outline

One of the most fruitful practical aspects of this research lies in the methodology employed to simulate the system of Figure 2. This methodology is strongly a function of the present computational algorithms used to solve optimal estimation and optimal control problems. The challenge to construct the methodology is twofold, first to find routines to determine a 63×63 state transition matrix and to propagate the 63×63 Riccati equation, and second to modularize the programs to the maximum amount possible in order to run the programs efficiently on the machines in minimum turn-around time.

The minimization of turn-around time is essential, as debugging one program with a one-day turn-around time would be much less desirable than debugging two subprograms with a half-day turn-around time for each, that together accomplish the same as the big program. With these objectives in mind, the subprograms used are listed below by function.

- 1) Trajectory generator
 - a) Generate and record states and parameters of a trajectory each .05 seconds
- 2) $A(t)$ matrix generator
 - a) Use the states and parameters developed by the trajectory generator to determine the $A(t)$ matrix

to be used every .05 seconds.

- 3) State transition matrix generator for one time interval of .05 seconds

- a) Generate the state transition matrix for each time propagation from

i) $\Phi(t_0, t_0) = I$

ii) $\Phi(t, t_0) = A(t) \Phi(t, t_0)$

- 4) State transition matrix generator for .2 second propagation

- a) Generate the state transition matrix for the period inherent in the human operator's information processing. This is done from

i) $\Phi(t_4, t_0) = \Phi(t_4, t_3) \Phi(t_3, t_2) \Phi(t_2, t_1) \Phi(t_1, t_0)$

- 5) Reverse the $A(t_i)$ sequence

- a) Given $A(t_1), A(t_2), \dots, A(t_{10})$, output $A(t_{10}), A(t_9), \dots, A(t_1)$

- 6) Generate the control matrix $F^O(t)$ using the backward sequence of $A(t_i)$'s from Step 5.

- a) Generate by propagating the Riccati equation for $P(t)$ backward in time from t_f . Then store

i) $F^O(t_i) = R_2^{-1}(t_i) B^T(t_i) P(t_i)$ at each

t_i or each .05 seconds for the problem

formulated.

- 7) Reverse the sequence of control matrices so that they are sequenced properly in time.
 - a) Change $F(t_{10}), F(t_9), \dots, F(t_1)$, to $F(t_1), F(t_2), \dots, F(t_{10})$
- 8) Determine the time history of error states and controls, given (1), (3), (4), and (7).
 - a) Includes predicted error states with their covariance as well as actual error states.

From the above description, (2), (4), (5), and (7) are self-explanatory and warrant no further explanation.

The first point to be addressed is (1), and for that explanation, all that is necessary is the fact that a fourth-order predictor-corrector routine was used for the differential equation propagation. This routine, mentioned earlier, is explained in Pollard's dissertation. (Ref 34)

A1.1 State Transition Matrix Generator

From the equations given in (3) it is apparent that a differential equation solving routine is necessary for this task. This in itself is of no difficulty because there are numerous routines in the literature. The difficulty arises in the consideration of the number of integrated variables. As the $A(t)$ matrix is a 63×63 matrix, the state transition matrix involves 63×63 or 3969 separate integrations.

To attack the size of this particular problem, one aspect proves significant. That aspect is the sparseness of the $A(t)$

matrix. For this problem the matrix contains only about 310 non-zero terms out of the 3969 terms possible. The sparseness has been exploited by Hamilton, Chitwood, and Reeves, in their multiplication routine. (Ref 28) This reduces the multiplication tremendously by not using the terms from the $A(t)$ matrix that are multiplied by zero.

Each of the integration routines considered required determination of $\Phi(t, t_0)$ by evaluating the product $A(t) \Phi(t, t_0)$. As this multiplication was done numerous times in any routine that was found stable, reducing the multiplications in this equation significantly reduces computation time.

Three different routines were tested for three propagations each. Each routine was a fixed interval integration routine because of the nature of the problem. The first of these routines was the second order Runge Kutta routine. The second routine was the fourth-order predictor-corrector routine mentioned above, and the third was Hamming's method with a Runge Kutta starter. (Ref 29)

The fourth-order predictor corrector was considered the benchmark routine, and the other two routines were evaluated against it. This was due to an evaluation of the published accuracy of each of the routines. The first to be evaluated was the Runge Kutta routine. It of course had the advantage of speed due to a minimum of computation. Unfortunately the errors experienced between it and the predictor-corrector were excessive.

The second method evaluated was the Hamming method. It was considered in lieu of the predictor-corrector because, though more storage is required - eighteen 63×63 matrices needed for storage instead of the fifteen 63×63 matrices needed for the predictor-corrector, the routine ran about two times faster. The accuracy of the Hamming and predictor corrector routines appeared to be about the same. Because of the speed the Hamming method was chosen to determine the state transition matrix between sample times.

A1.2 Propagation of the Riccati Equation

Because the dimension of the Riccati equation for a system of 63 states is 63×63 , a problem of the same size is encountered with the propagation of that equation as is encountered with the propagation of the state transition matrix. However, because of some of the unique properties of the Riccati equation, that size can be cut substantially. The ability to reduce the equations to be propagated by approximately one half made it feasible to use the predictor-corrector integration routine, which was considered the most precise of the above methods discussed.

The first special aspect of the propagation was discussed in the state transition matrix section. That is the sparseness of the $A(t)$ matrix. By exploiting this, the $P(t) A(t)$ term can be multiplied much more efficiently than by a usual multiplication routine. Also recognizing that

$$A^T(t) P(t) = (P(t) A(t))^T$$

because of the symmetry of the $P(t)$ matrix and the properties of a transpose, suggests that the $A^T(t) P(t)$ term does not need to be multiplied. The $P(t) A(t)$ term need only be transposed and added to itself.

Another aid in computation comes from the $B(t) R_2^{-1}(t) B^T(t)$ term not being a function of time. This matrix therefore can be precomputed and used as an entity. Using the sparseness of this matrix also reduces computation time.

The last trait exploited is the symmetry of the $P(t)$ matrix, because of which only the upper triangular portion of the matrix needs to be considered by the integration routine. This cuts the storage for the integration routine from fifteen 63×63 matrices of 3969 elements to fifteen arrays of 2016 elements each. This is a saving in storage of about half, and a parallel saving of about two thirds occurs in computation time.

A1.3 The System Computation

By using the above routines in steps (1) - (7), the storage and the computation required in the complete system routine has been significantly reduced.

The controller gains were precomputed, so that no on-line computation is required for them. The gains are obtained on-line rapidly by reading a storage device.

The Kalman filter is more involved. The update portion of the filter is merely a matrix multiplication, addition, and inversion. As the matrix inversion required is only for a 4×4 matrix, it does not present a significant problem.

The predictor equations of the filter are of the discrete form; if the state transition matrices are precomputed, most equations involve only multiplication. This is true for the mean equations when the delta control is computed for the human operator and applied. At this point, an integral is also present in the mean equations. The covariance equations used in the propagation also always contain an integral.

In both of the above equations, the mean and the covariance propagations, the characteristics of the Kalman filter predictor-corrector were examined. The predictor portion is merely an estimate of the state at a future time. The quality of this estimate is displayed to the mathematics via the $R(t)$ term. If that term is large, the mathematics will pay more attention to the propagation and less to the measurements. If the $R(t)$ term is small, more attention will be paid to the measurements.

Using this understanding, the integral in both the mean and the covariance cases was determined by a Runge Kutta method, and the terms of the $R(t)$ matrix were decreased in value from what was initially considered the covariance of the measurements. This decrease was used to display to the mathematics that the measurements were of more value than the propagation.

The nonlinear system of Figure 2 with the appropriate noises was propagated using the fourth-order predictor-corrector routine, and the noise models used to add noise to this model were models constructed by Maybeck. (Ref 50)

APPENDIX II

Error State Plots

Appendix II contains the plots of the mean and standard deviation time history for the states P , Q , R , ϕ , θ , ψ , U , V , W , and S_z , and the control stick forces necessary to control aileron, rudder, elevator, and engine thrust. The center line on the plot is the mean value of the state or control referred to in that plot, and the top and bottom lines are that value plus and minus one standard deviation value respectively. Table A-1 identifies the figure number corresponding to each error state or control and angle-of-attack realization pair.

TABLE A-1

Angle of Attack Instrument Standard Deviation .09 Degree

Figure 13	Label X35	P
Figure 14	Label X36	Q
Figure 15	Label X37	R
Figure 16	Label X38	ϕ
Figure 17	Label X39	θ
Figure 18	Label X40	ψ
Figure 19	Label X41	U
Figure 20	Label X42	V
Figure 21	Label X43	W
Figure 22	Label X46	S_z
Figure 23	Label U1	left or right or stick force
Figure 24	Label U2	rudder force
Figure 25	Label U3	foreward or aft stick force
Figure 26	Label U4	thrust increase or decrease

Angle of Attack Instrument Standard Deviation 1 Degree

Figure 27	Label X35	P
Figure 28	Label X36	Q
Figure 29	Label X37	R
Figure 30	Label X38	ϕ
Figure 31	Label X39	θ
Figure 32	Label X40	ψ
Figure 33	Label X41	U
Figure 34	Label X42	V
Figure 35	Label X43	W
Figure 36	Label X46	S_z
Figure 37	Label U1	left or right stick force
Figure 38	Label U2	rudder force
Figure 39	Label U3	fore or aft stick force
Figure 40	Label U4	thrust force

Angle of Attack Instrument Standard Deviation 3 Degrees

Figure 41	Label X35	P
Figure 42	Label X36	Q
Figure 43	Label X37	R
Figure 44	Label X38	ϕ
Figure 45	Label X39	θ
Figure 46	Label X40	ψ
Figure 47	Label X41	U
Figure 48	Label X42	V
Figure 49	Label X43	W
Figure 50	Label X46	S_z
Figure 51	Label U1	left or right stick force
Figure 52	Label U2	rudder force
Figure 53	Label U3	fore or aft stick force
Figure 54	Label U4	thrust force

FIGURE 13

35 ALPHA SO .09

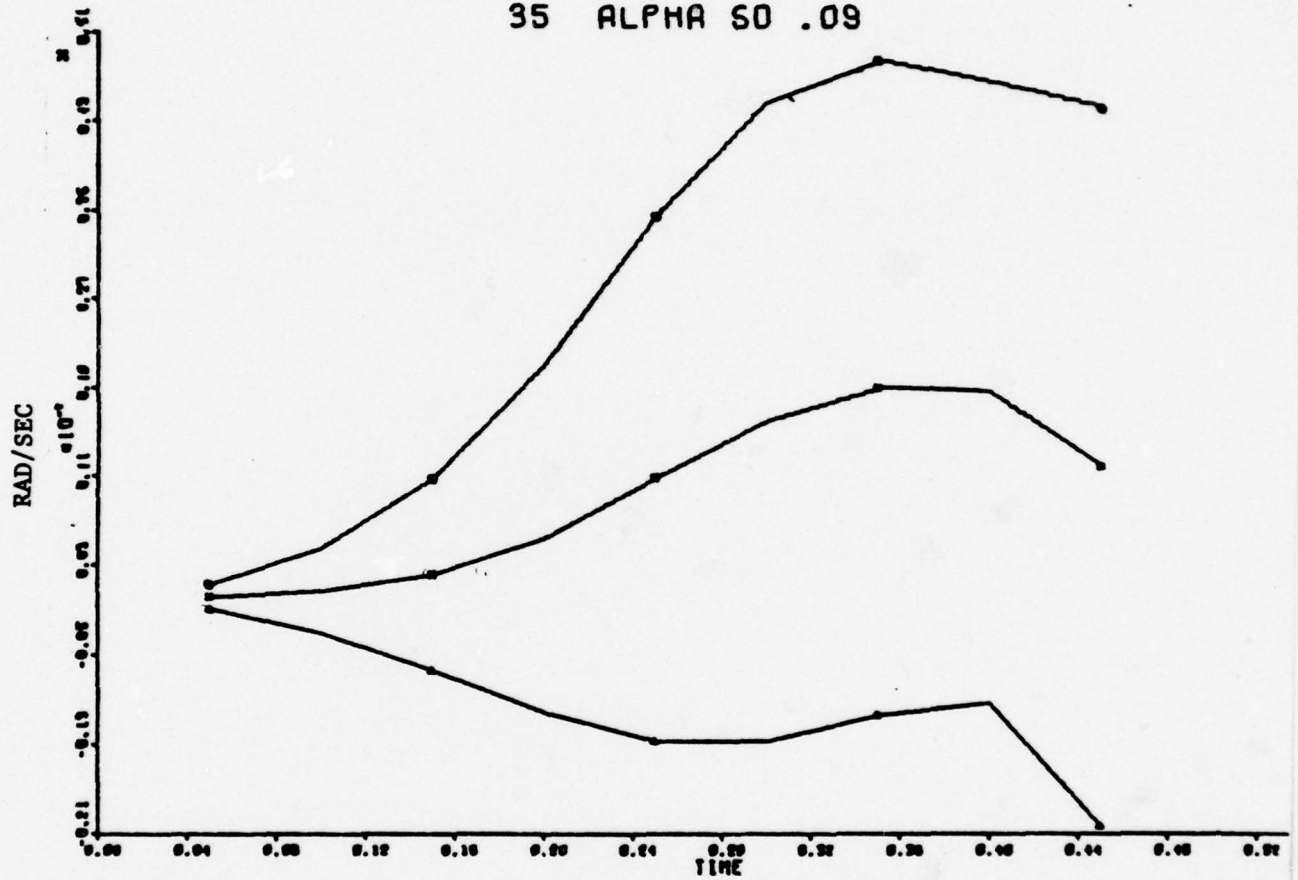


FIGURE 14

36 ALPHA SD .09

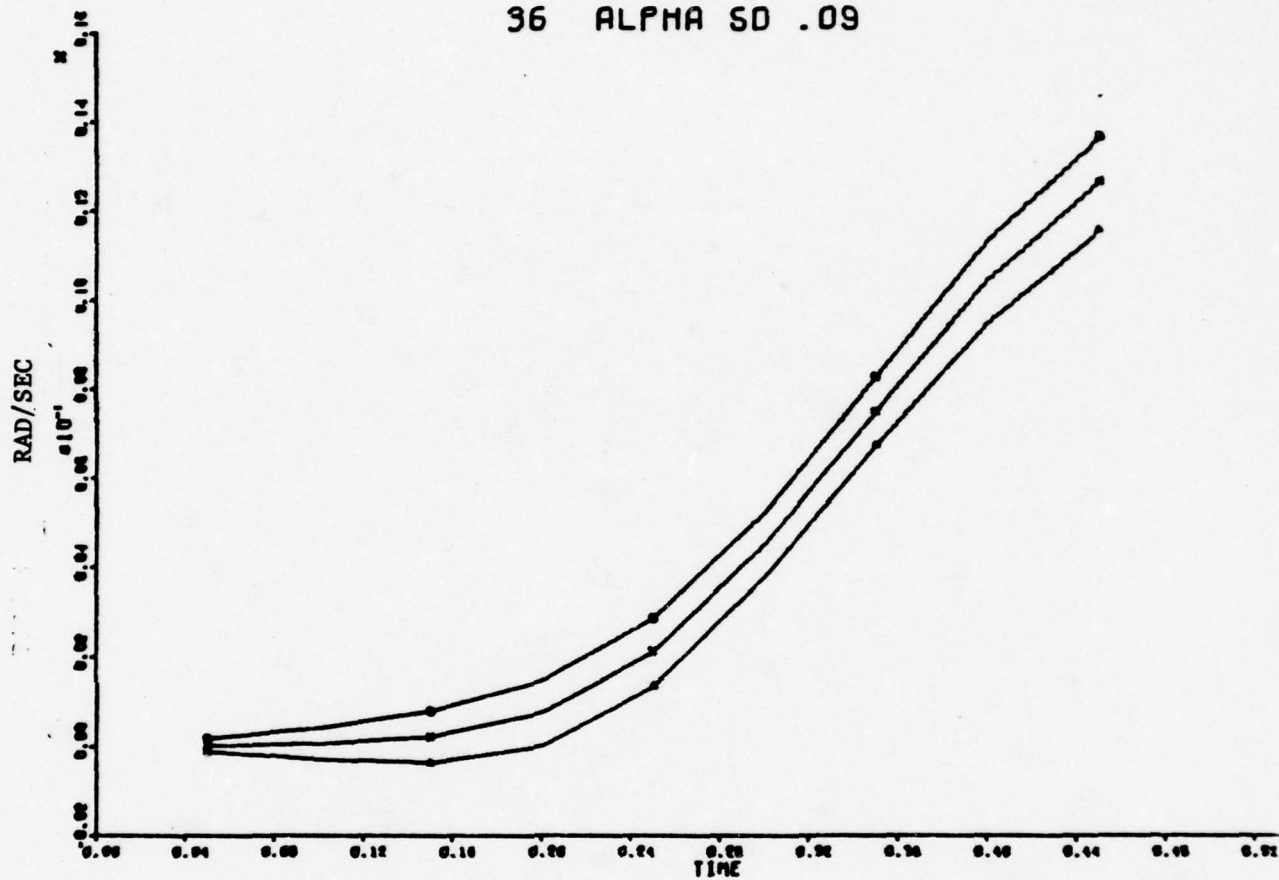


FIGURE 15

37 ALPHA SD .09

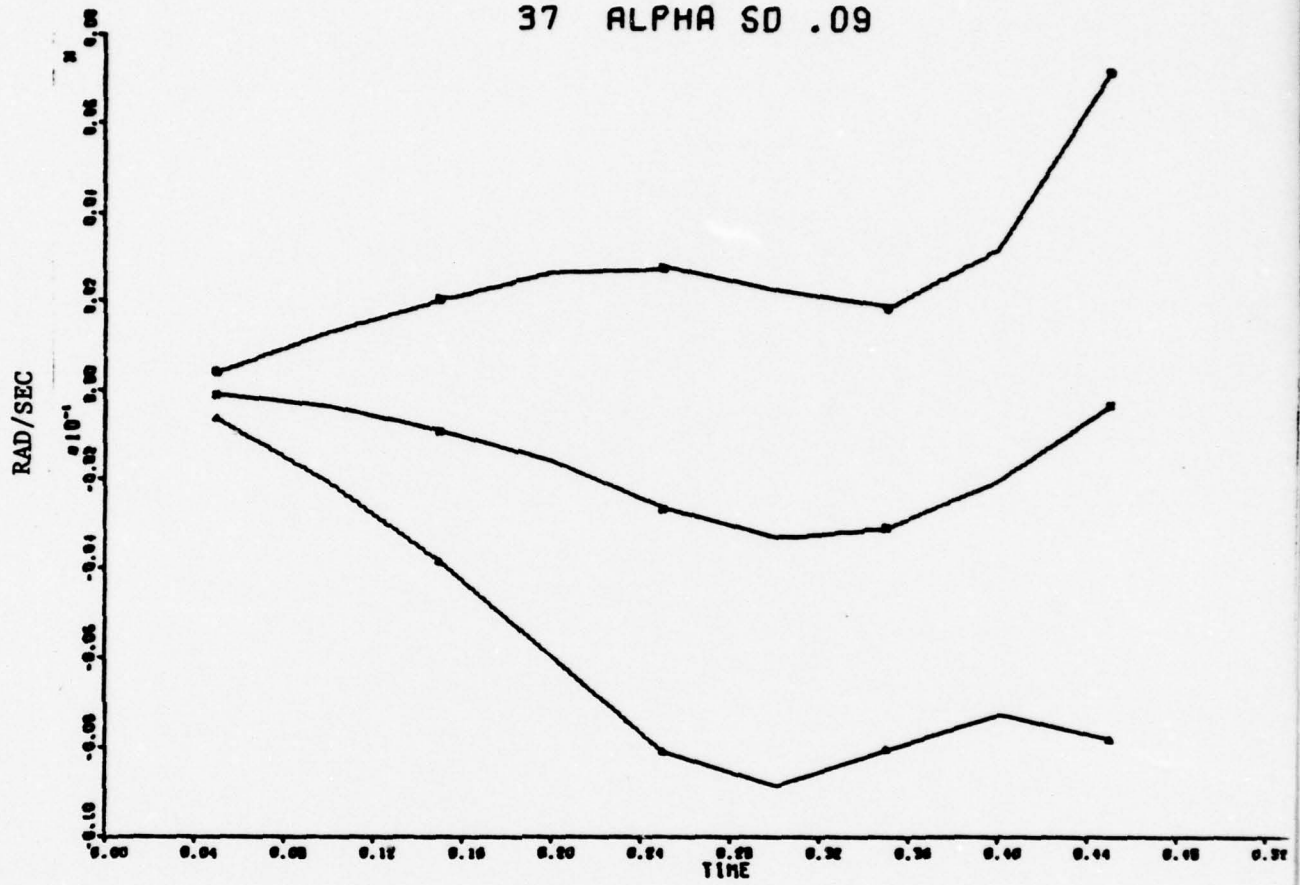


FIGURE 16

98 ALPHA SD .09

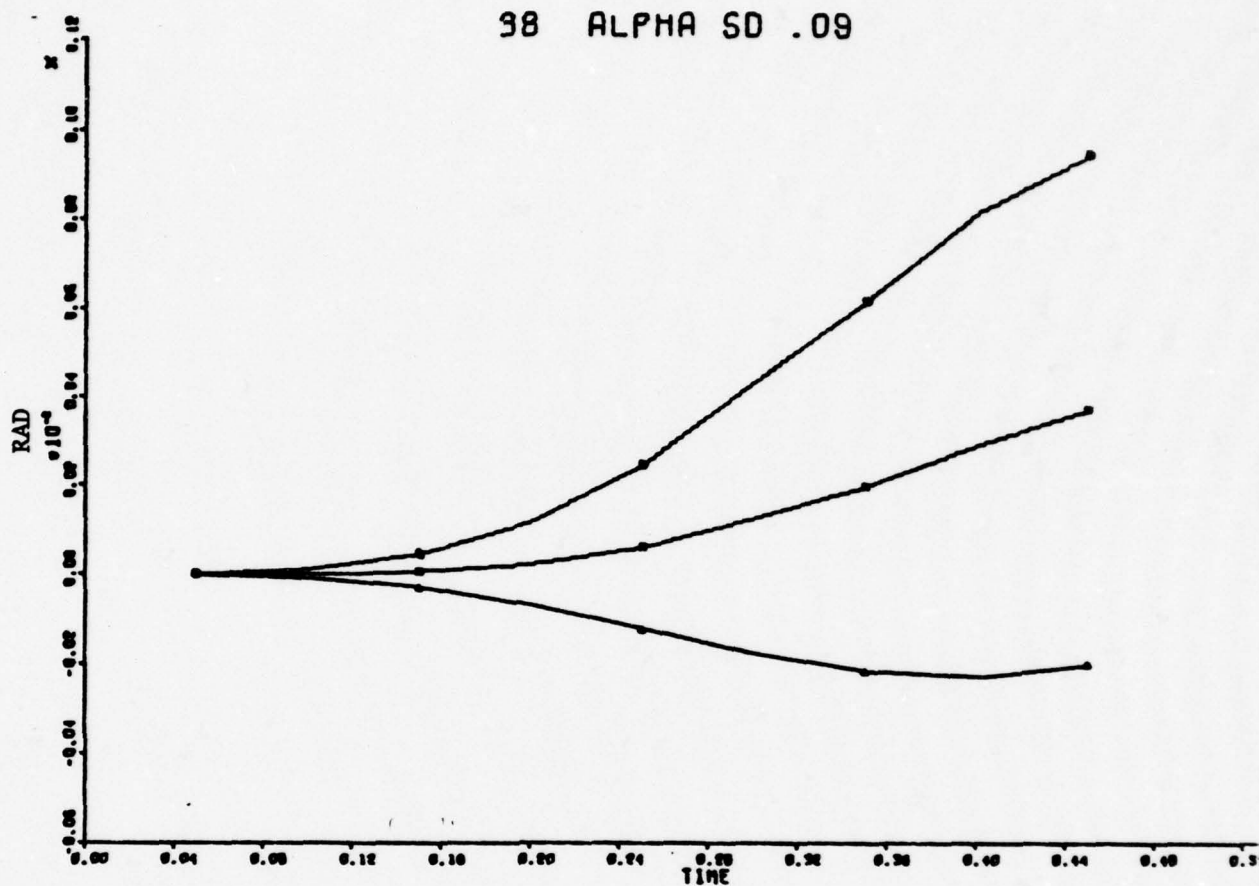


FIGURE 17

39 ALPHA SO .09

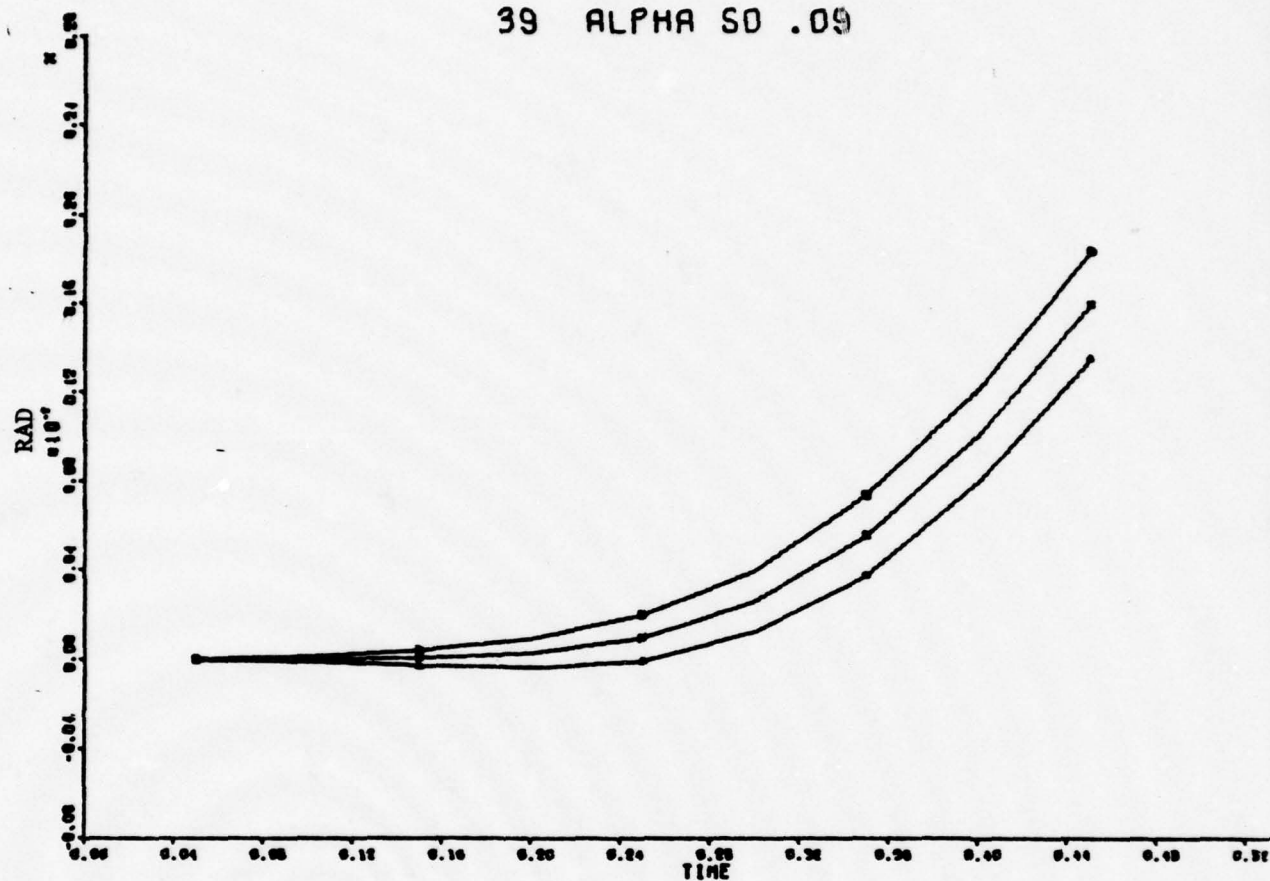


FIGURE 18

40 ALPHA SD .09

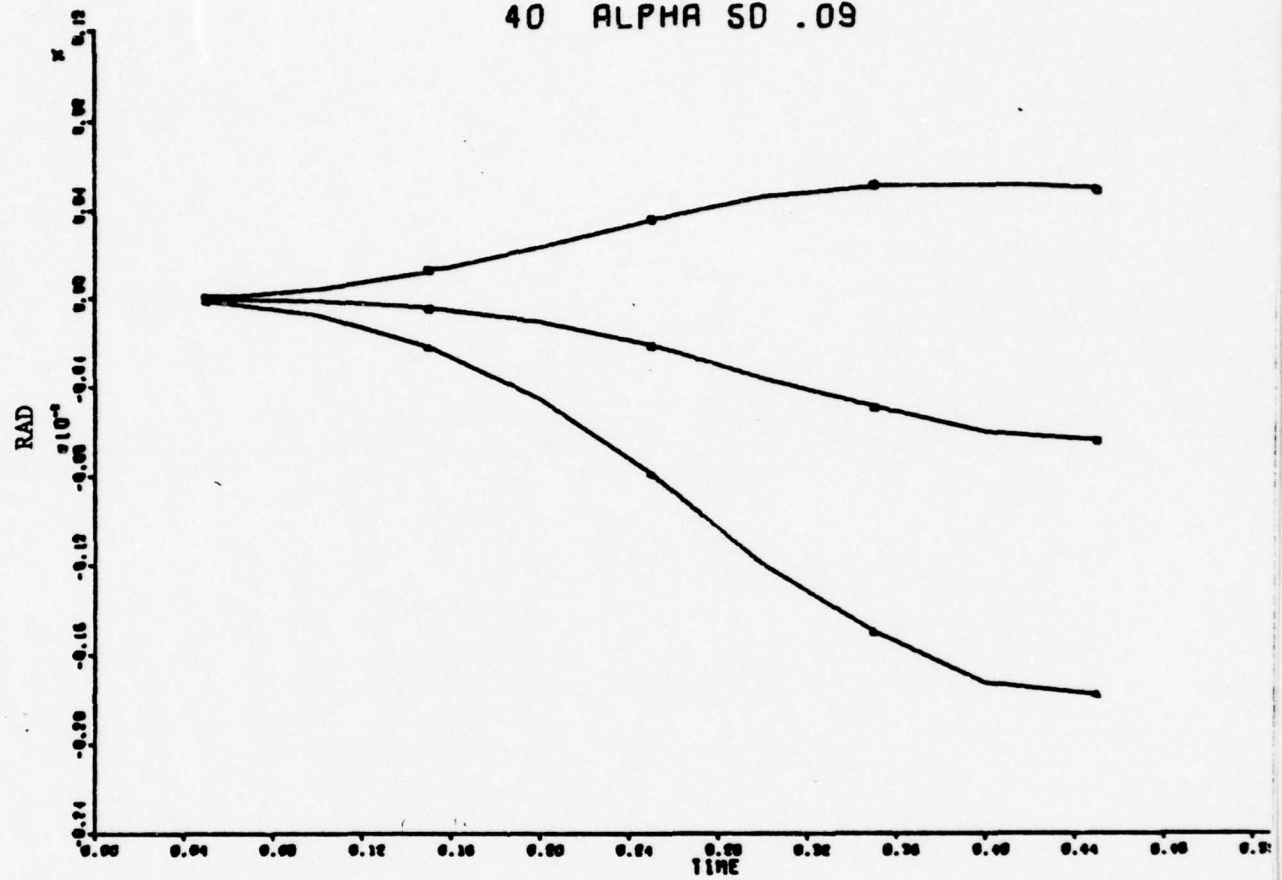


FIGURE 19

41 ALPHA SD .09

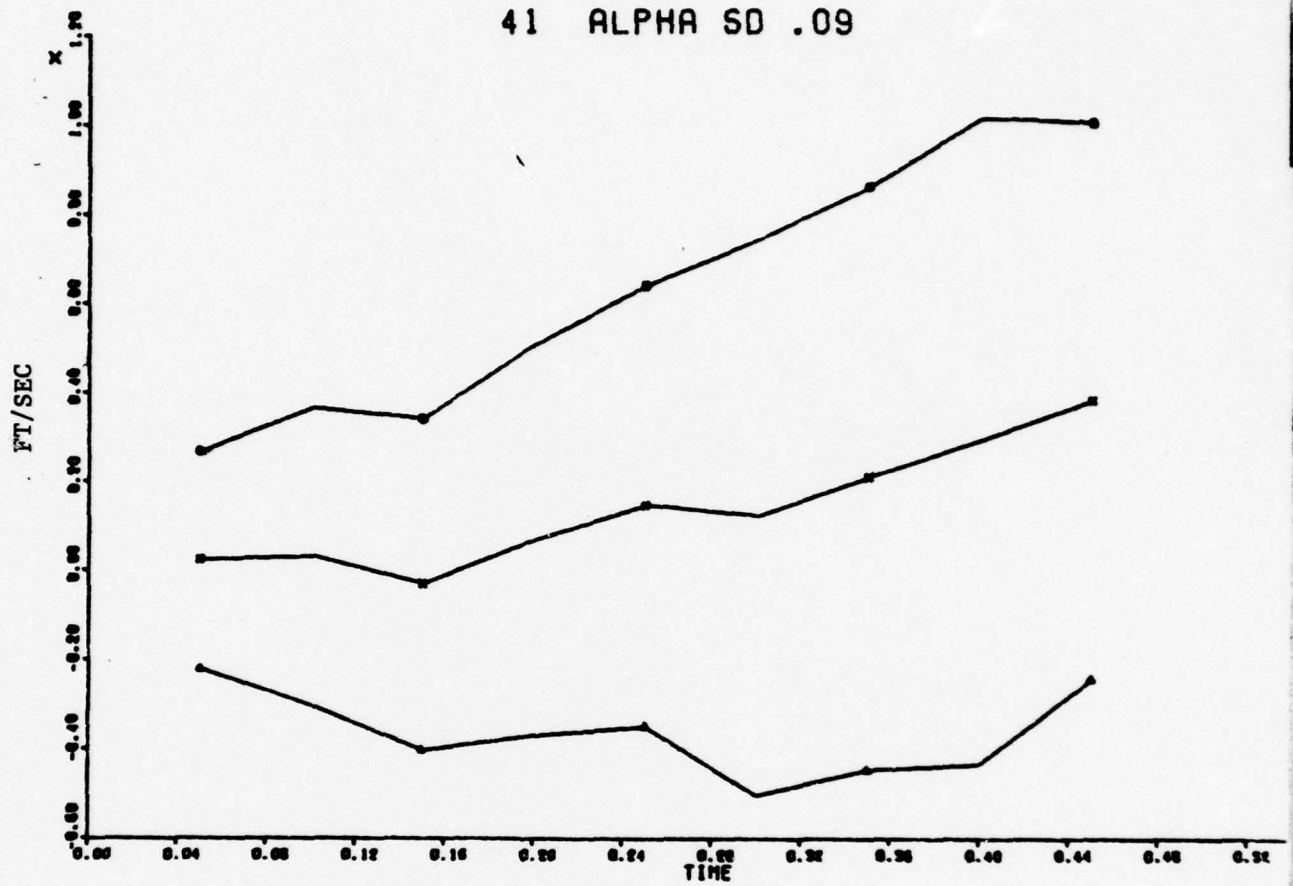


FIGURE 20

42 ALPHA SD .09

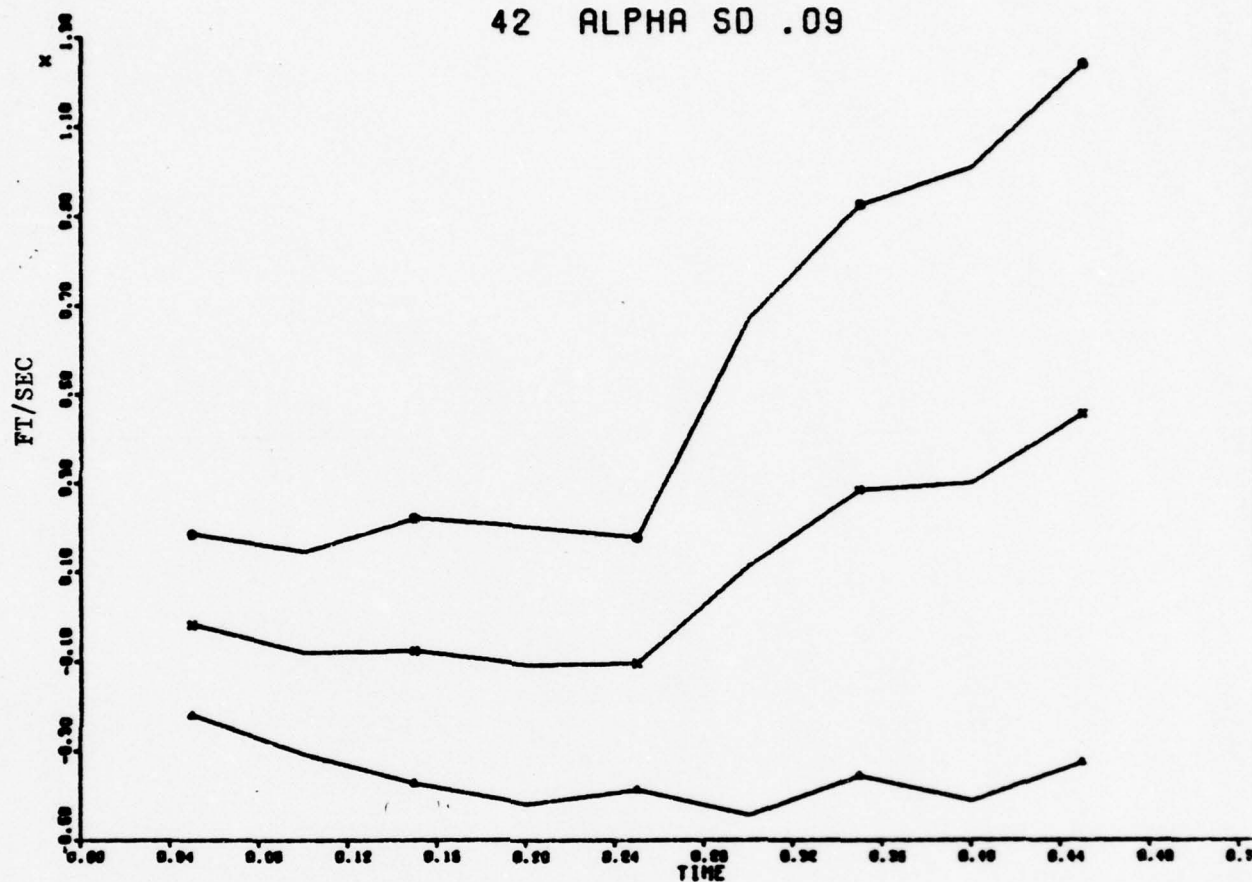


FIGURE 21

43 ALPHA SD .09

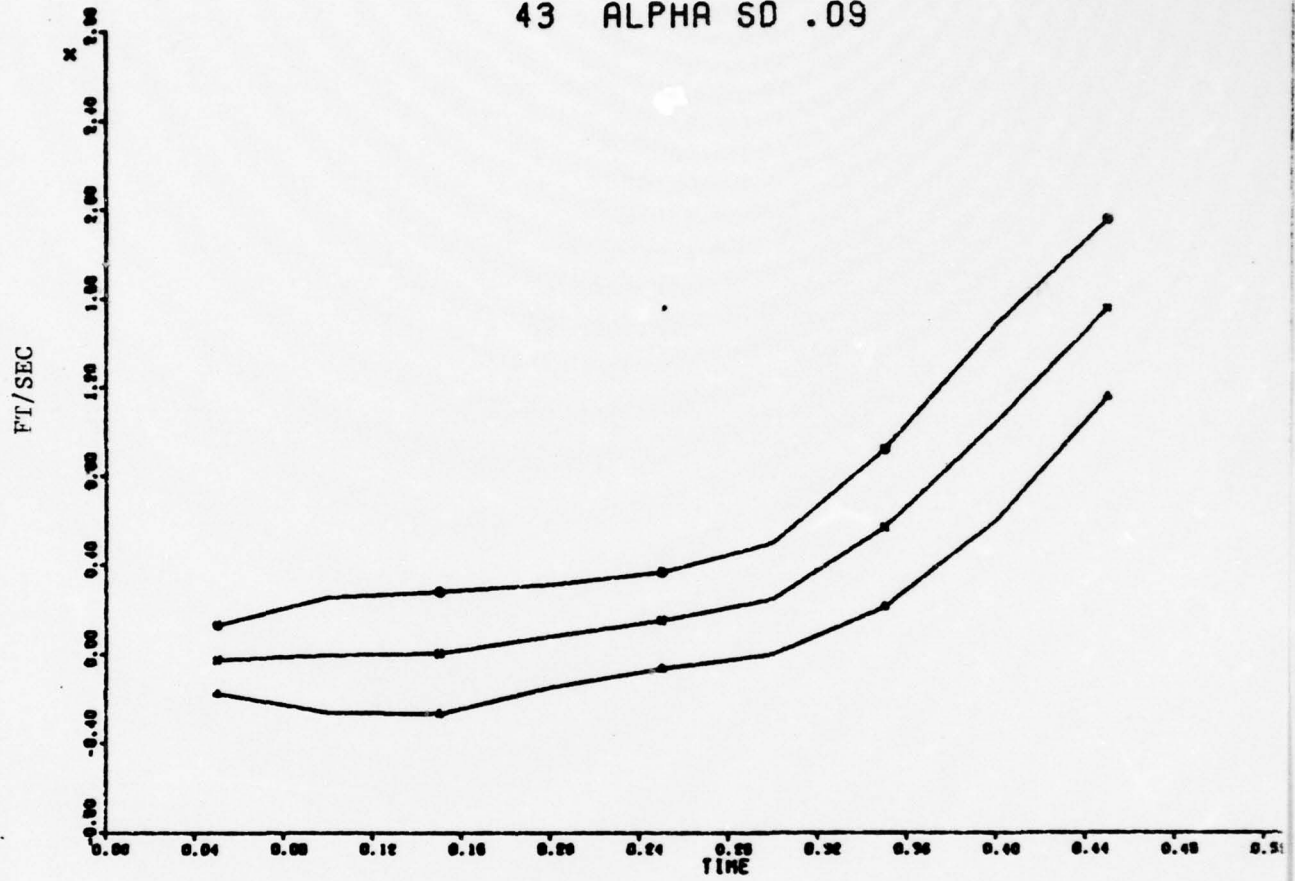


FIGURE 22

46 ALPHA SD .09

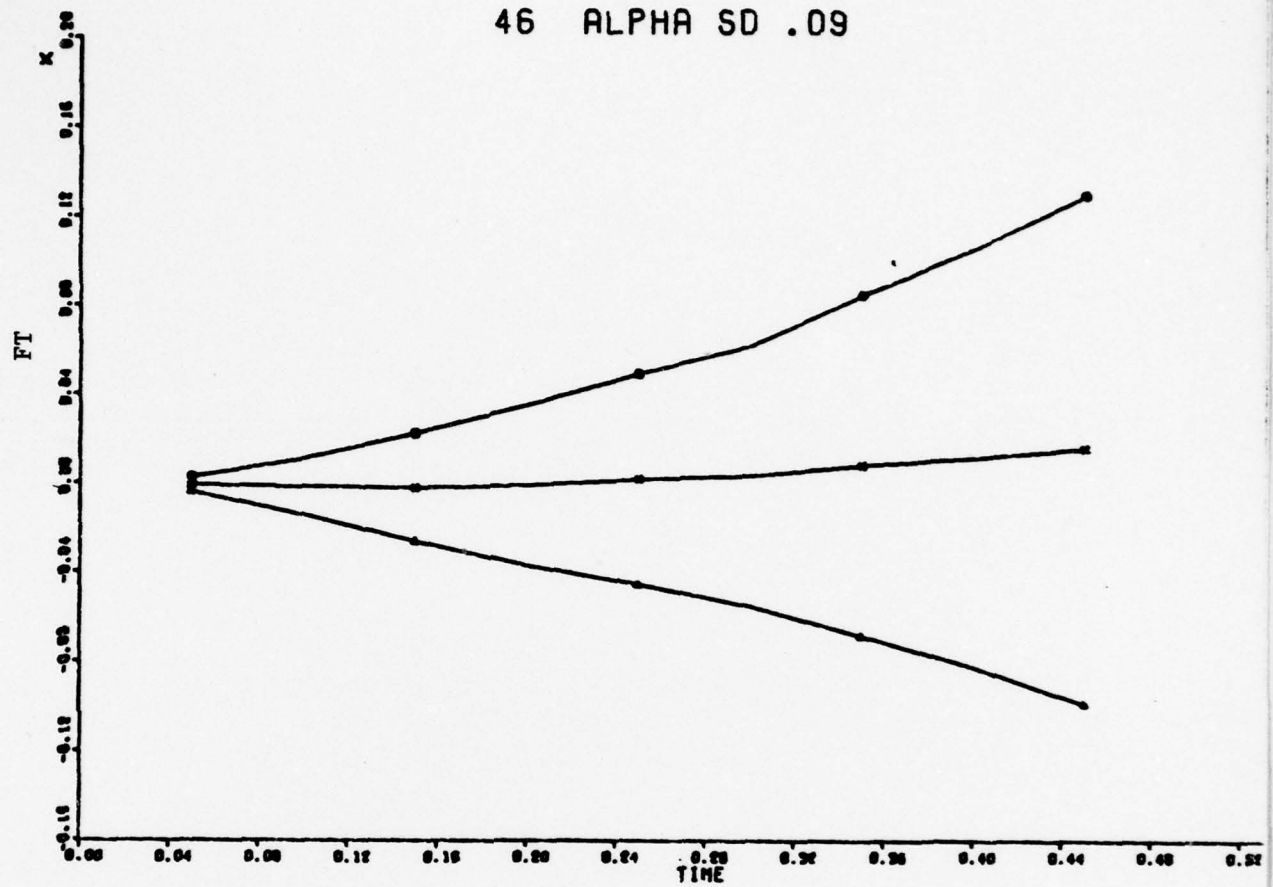


FIGURE 23

U1 ALPHA SD .09

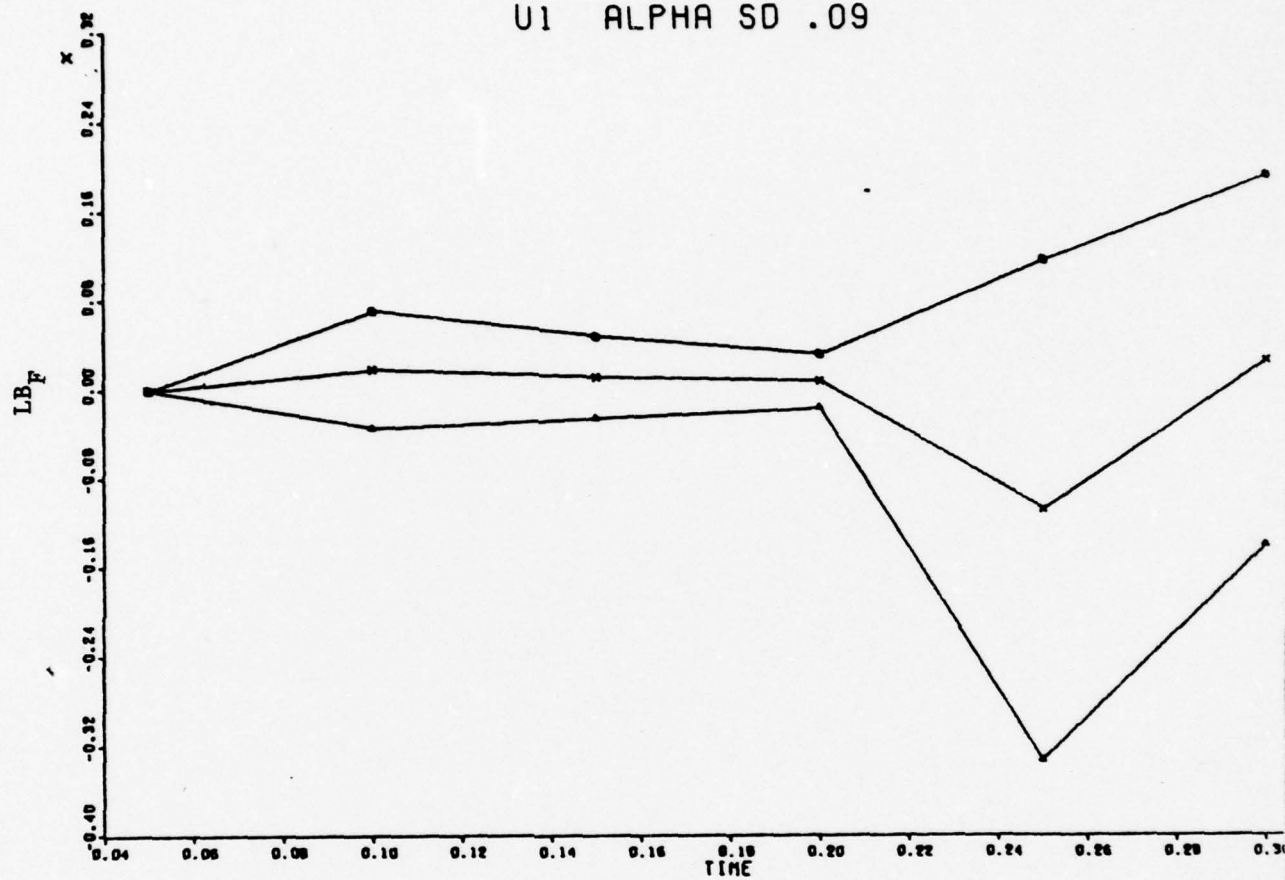


FIGURE 24

U2 ALPHA SD .09

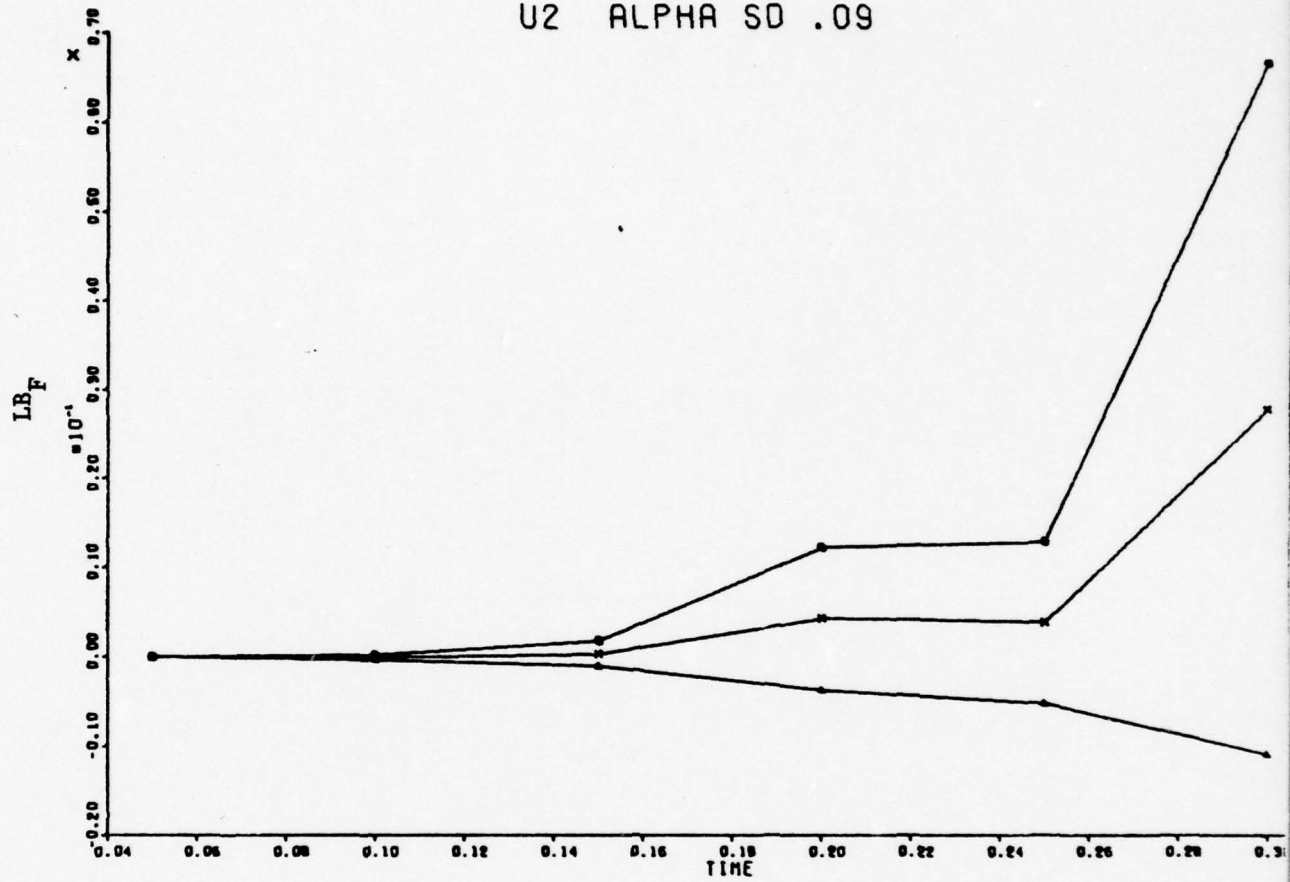


FIGURE 25

U3 ALPHA SD .09

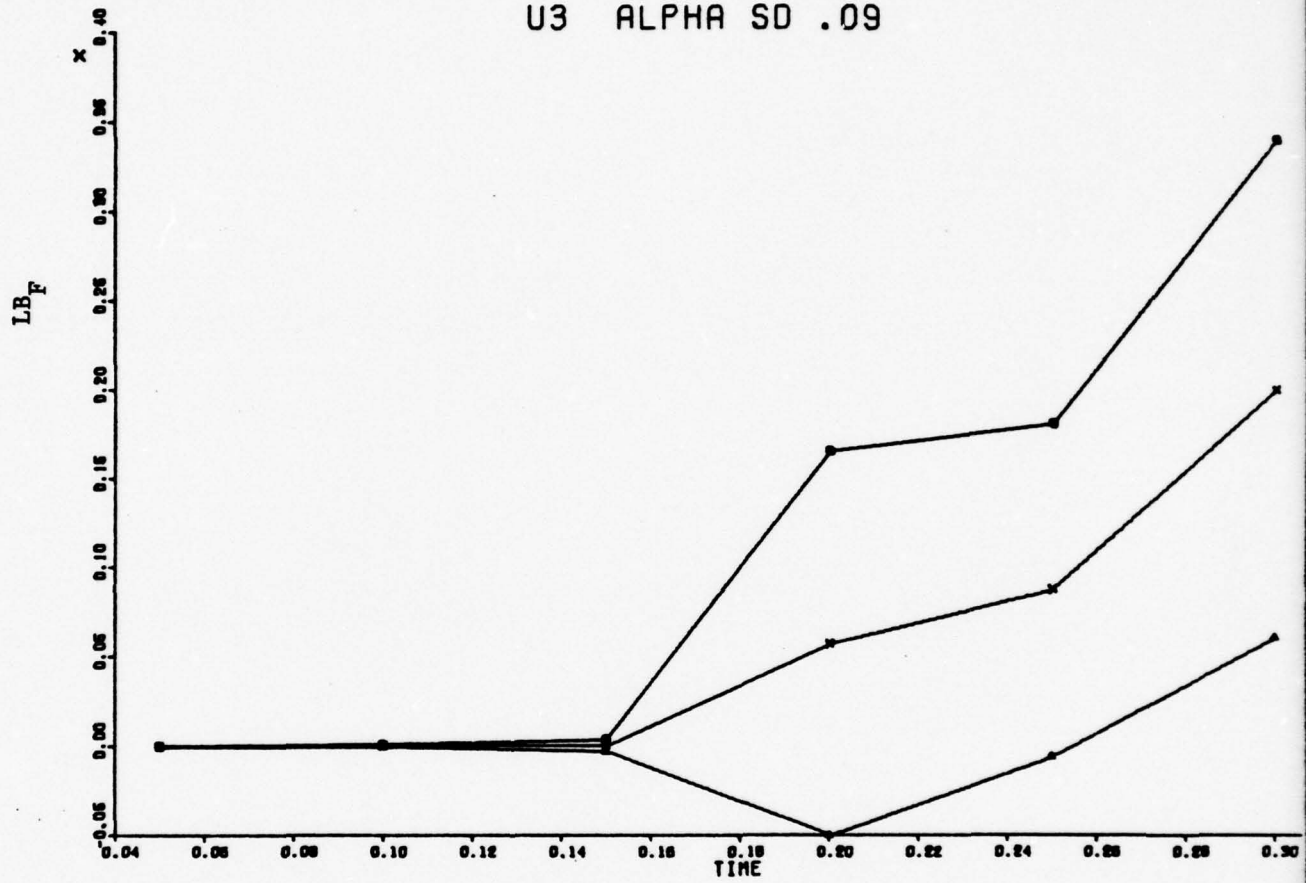


FIGURE 26

U4 ALPHA SD .09

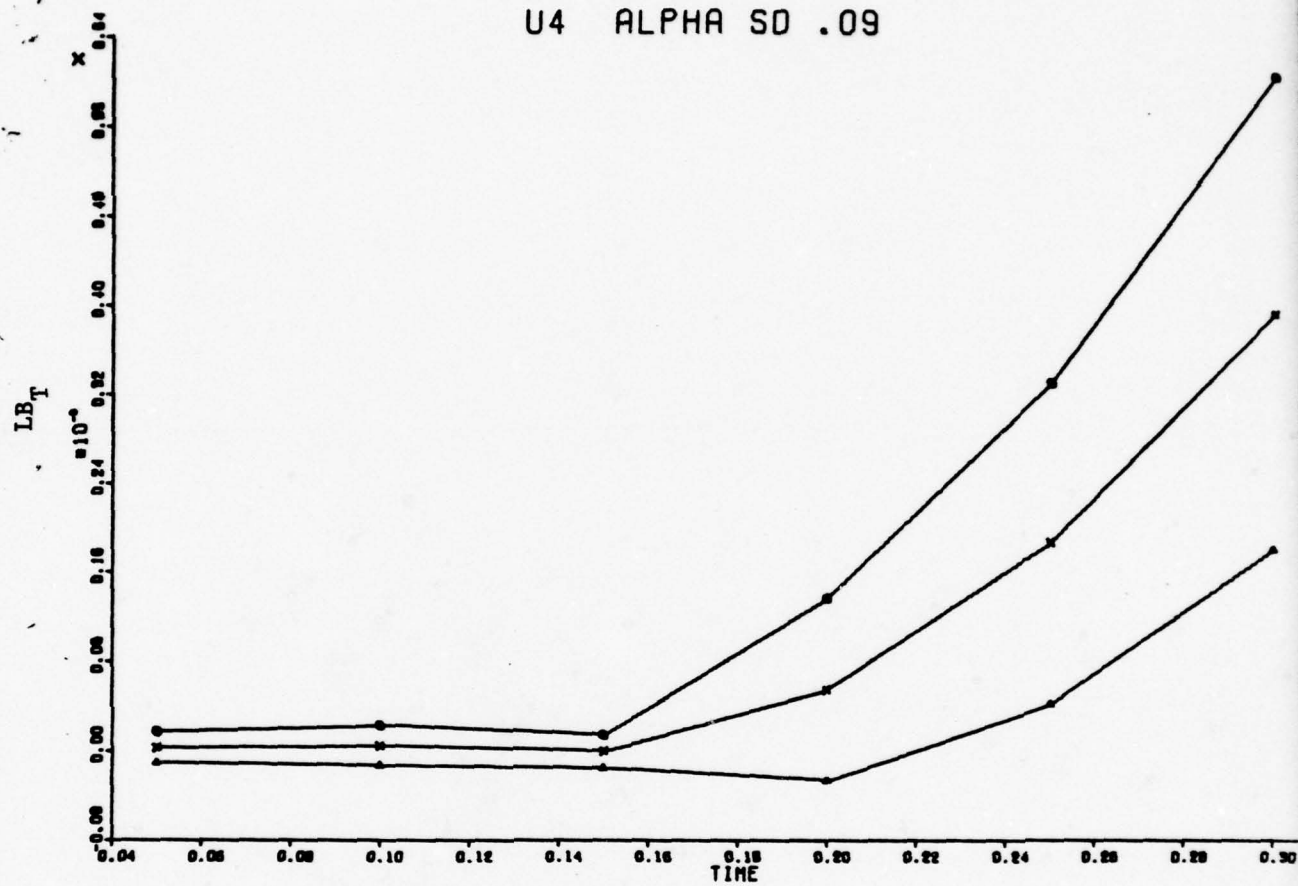


FIGURE 27

35 ALPHA SD 1.

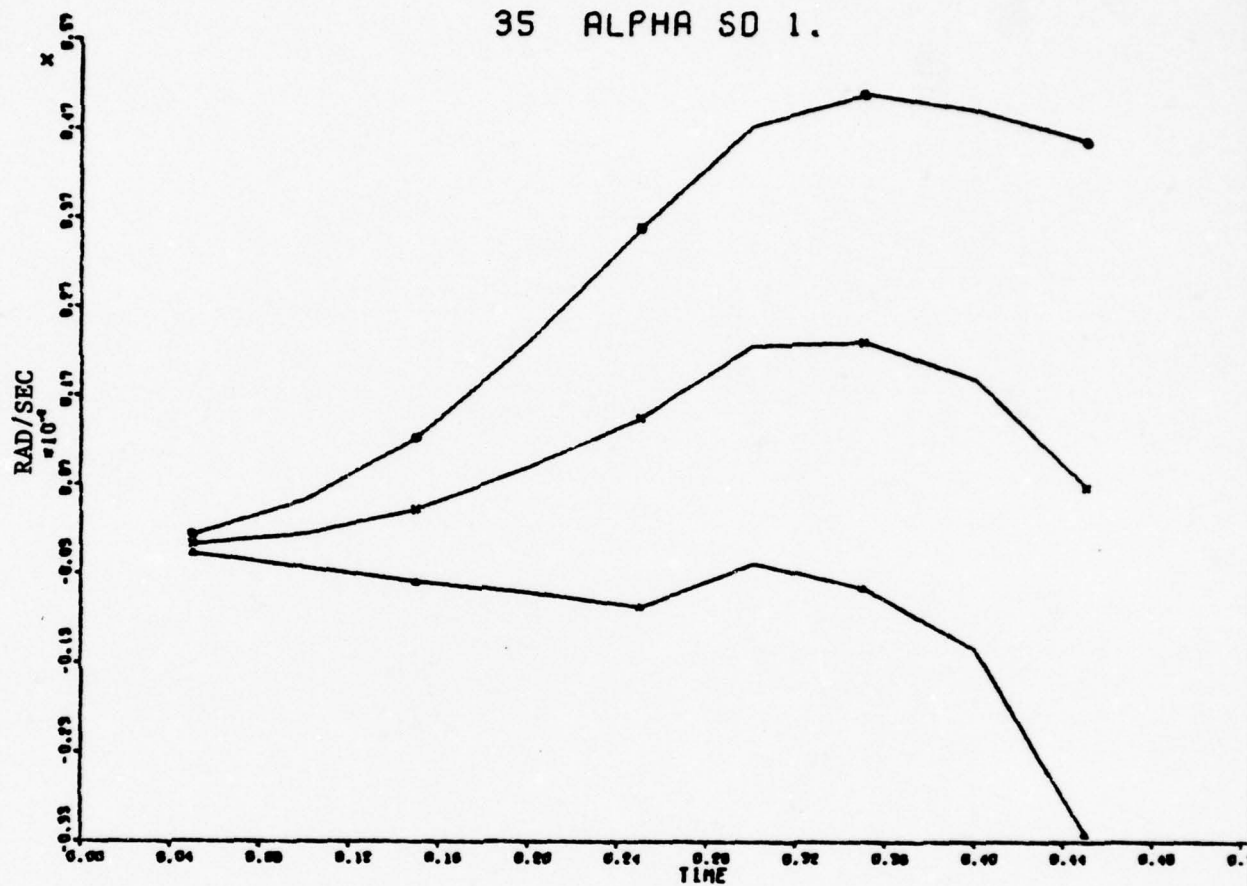


FIGURE 28

36 ALPHA SD 1.

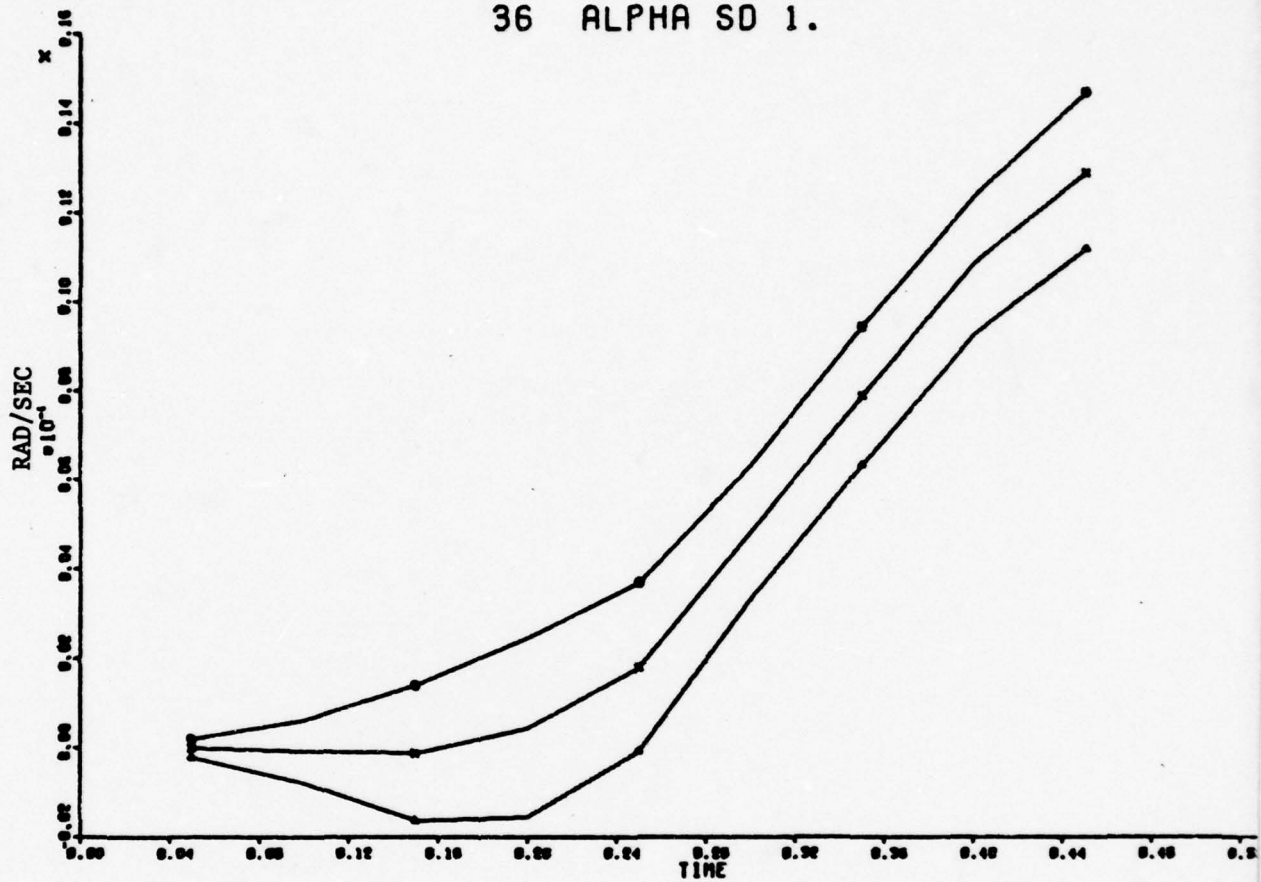


FIGURE 29

37 ALPHA SD 1.

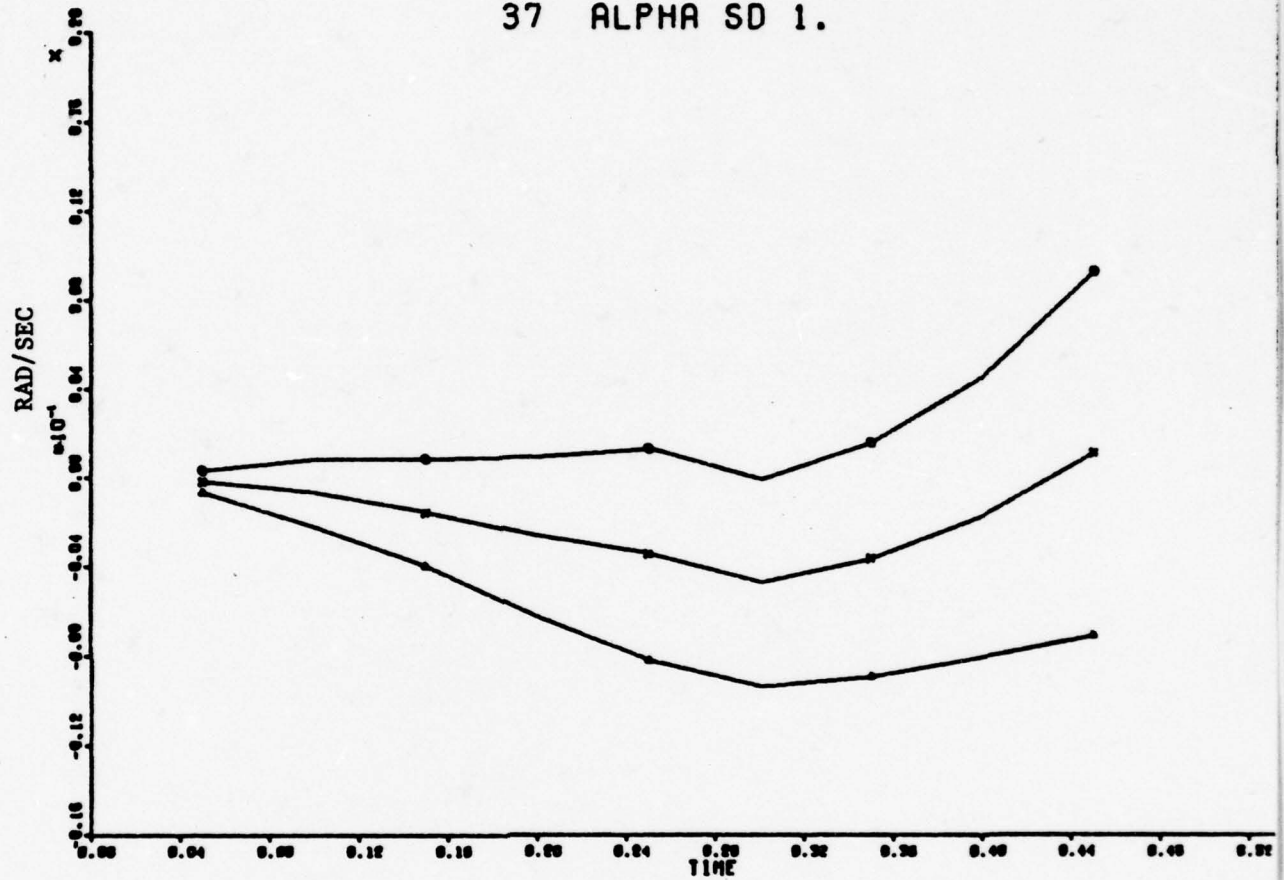


FIGURE 30

38 ALPHA SD 1.

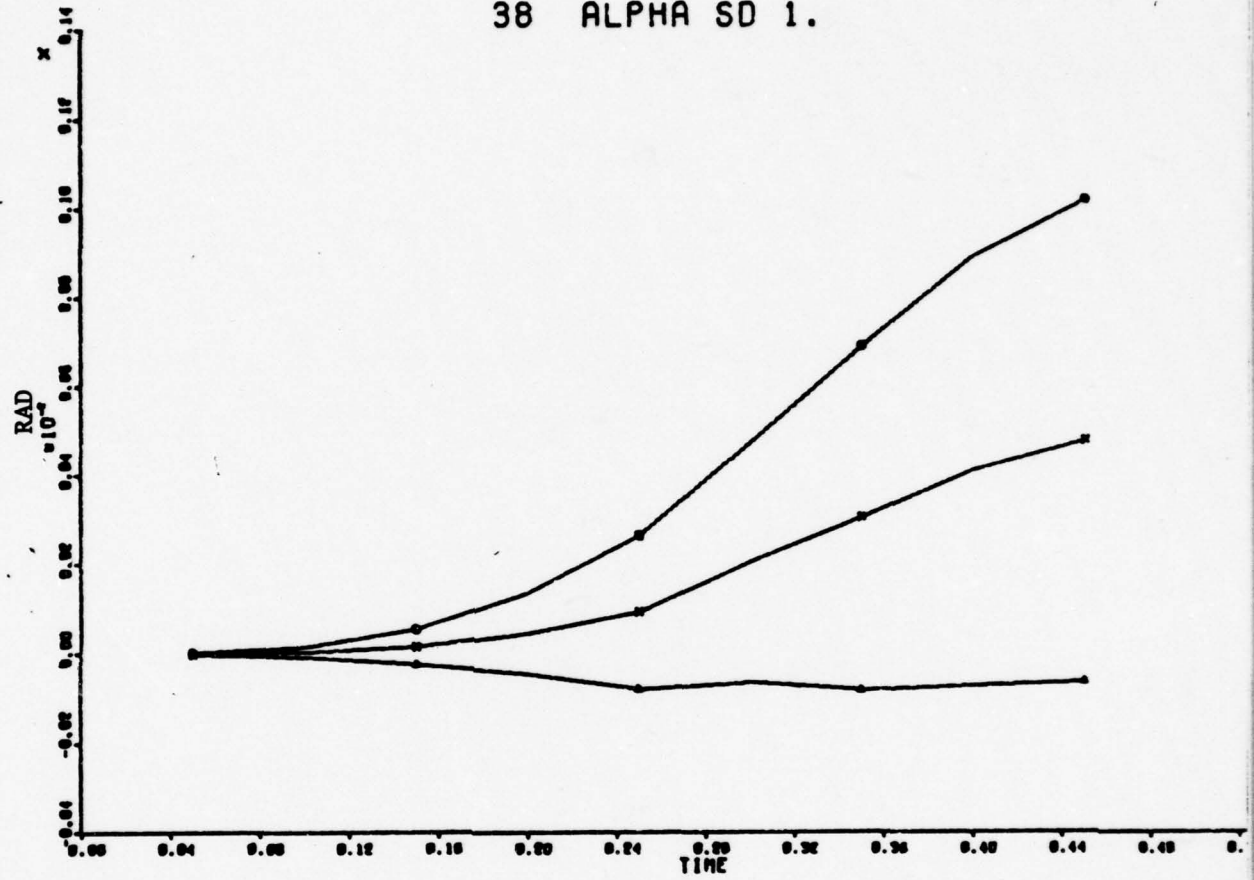


FIGURE 31

39 ALPHA SD 1.

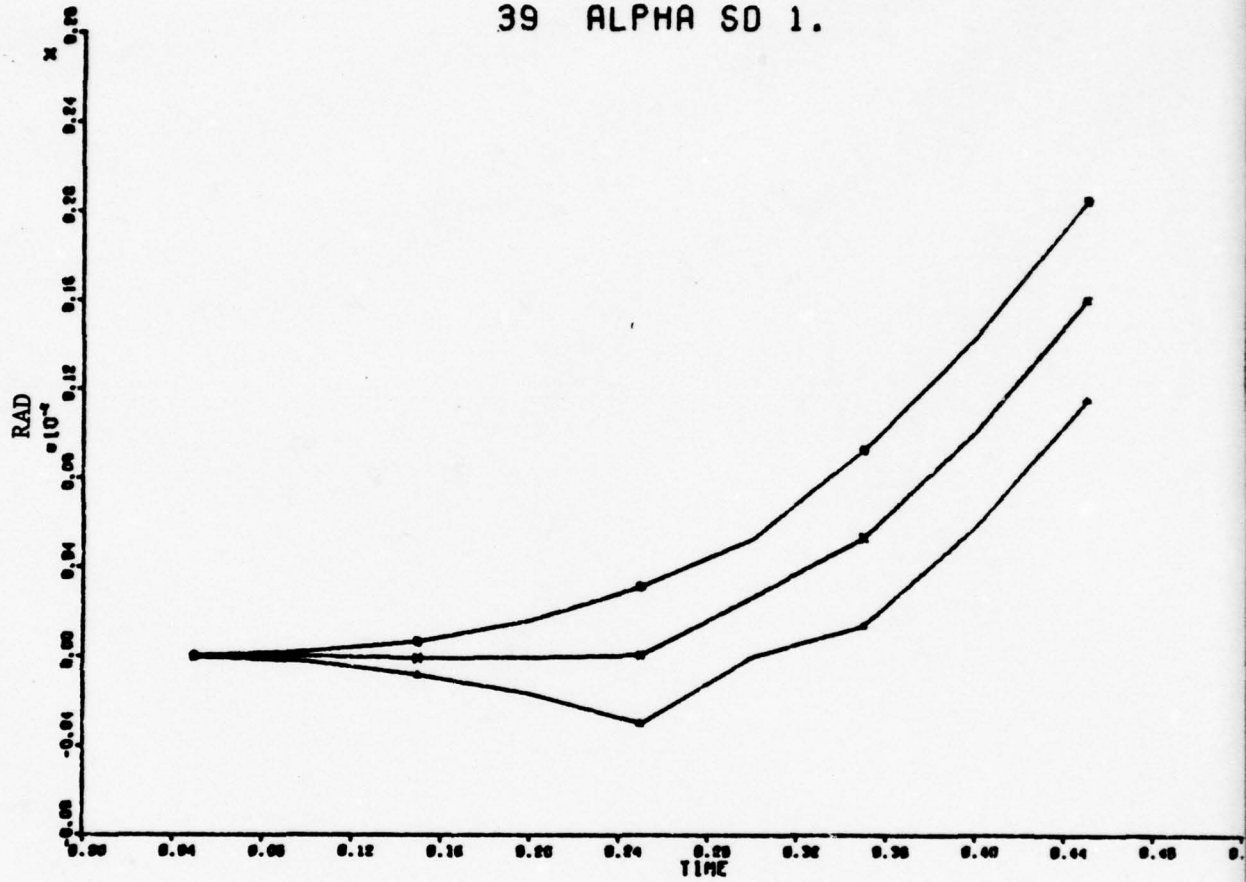


FIGURE 32

40 ALPHA SD 1.

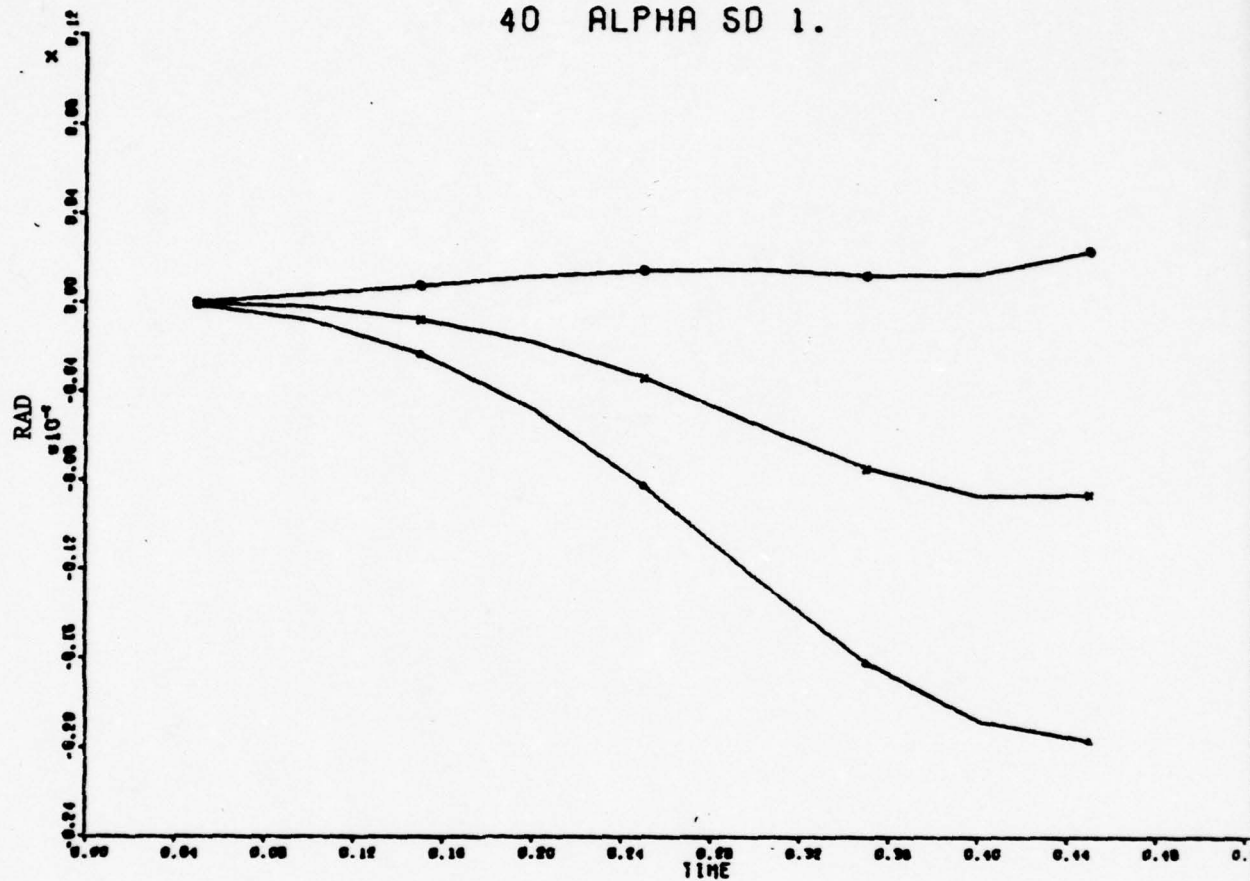


FIGURE 33

41 ALPHA SD 1.

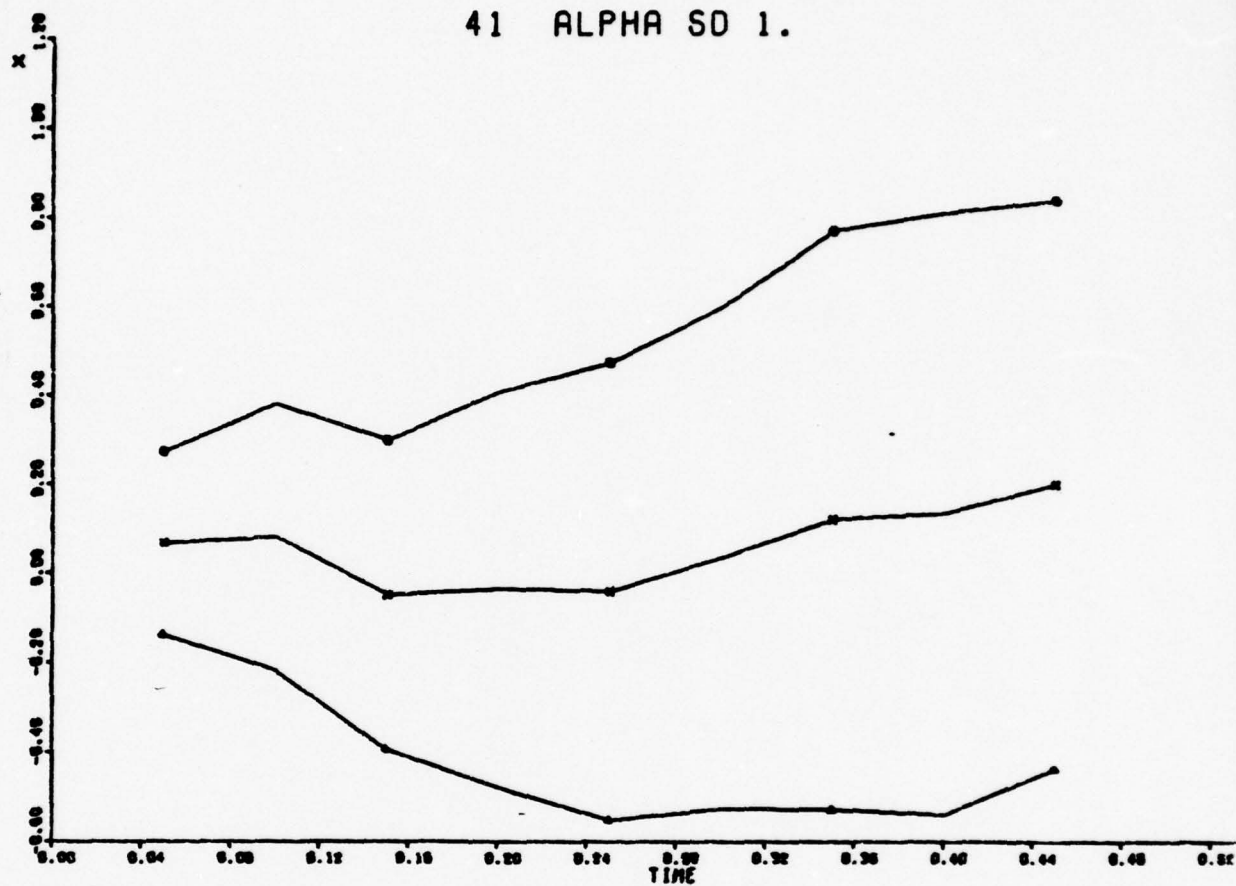


FIGURE 34

42 ALPHA SD 1.

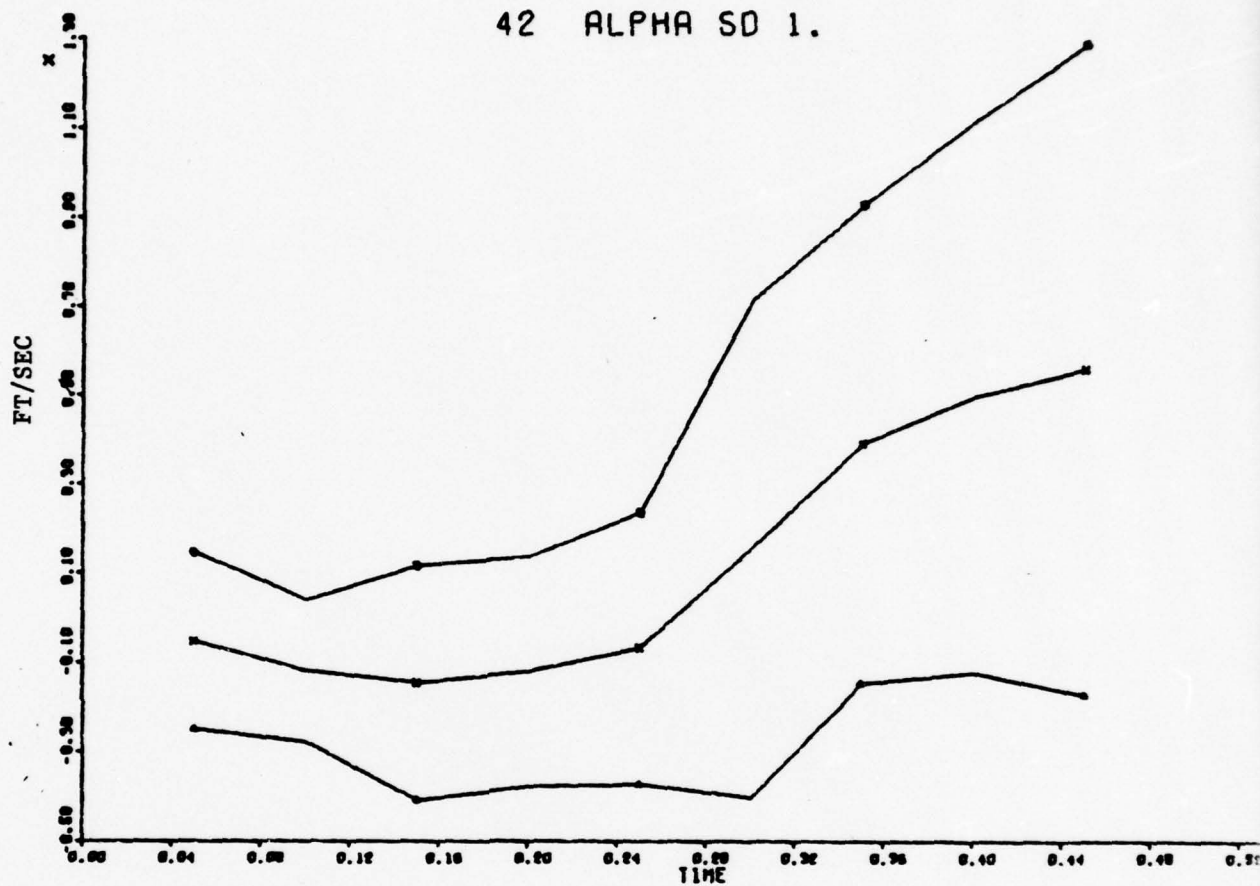


FIGURE 35

43 ALPHA SD 1.

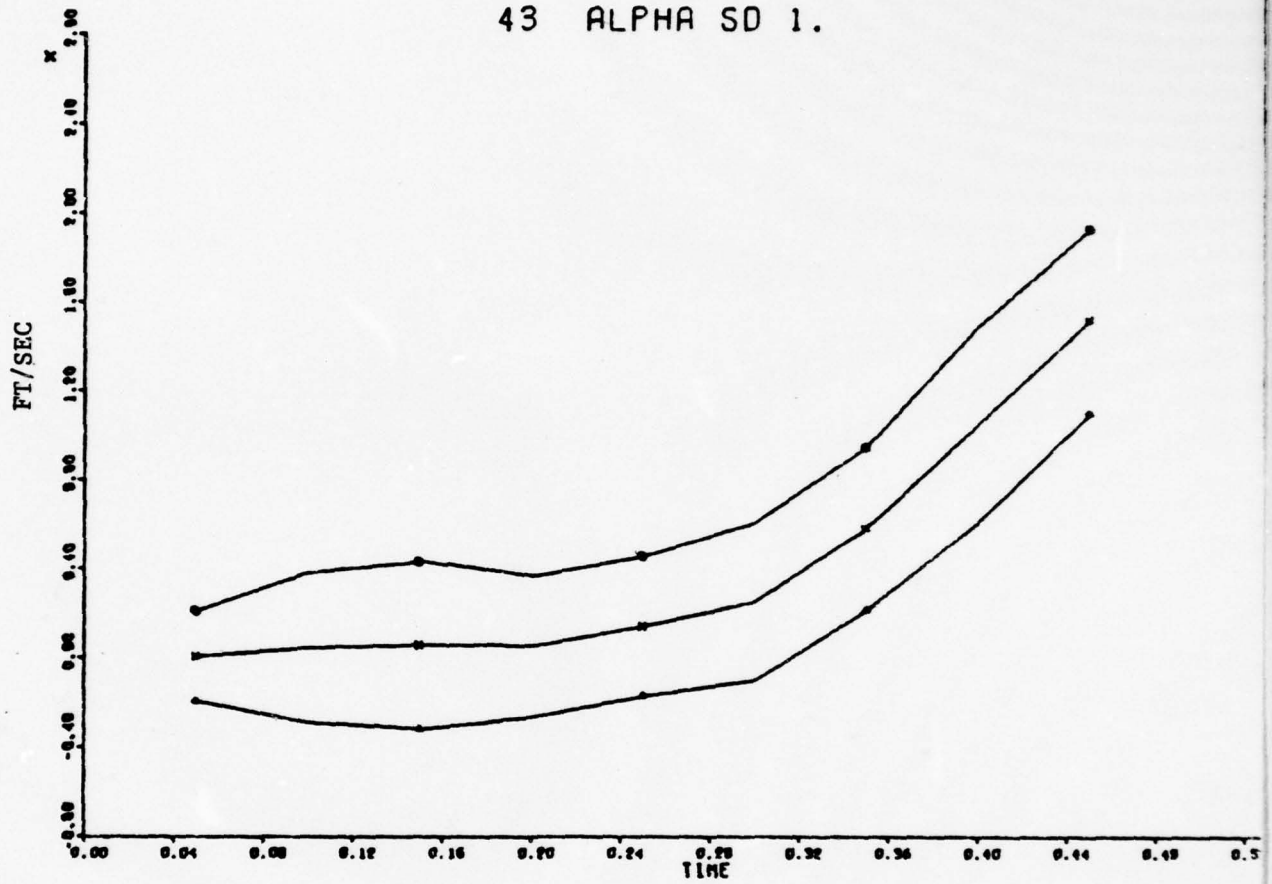


FIGURE 36

46 ALPHA SD 1.

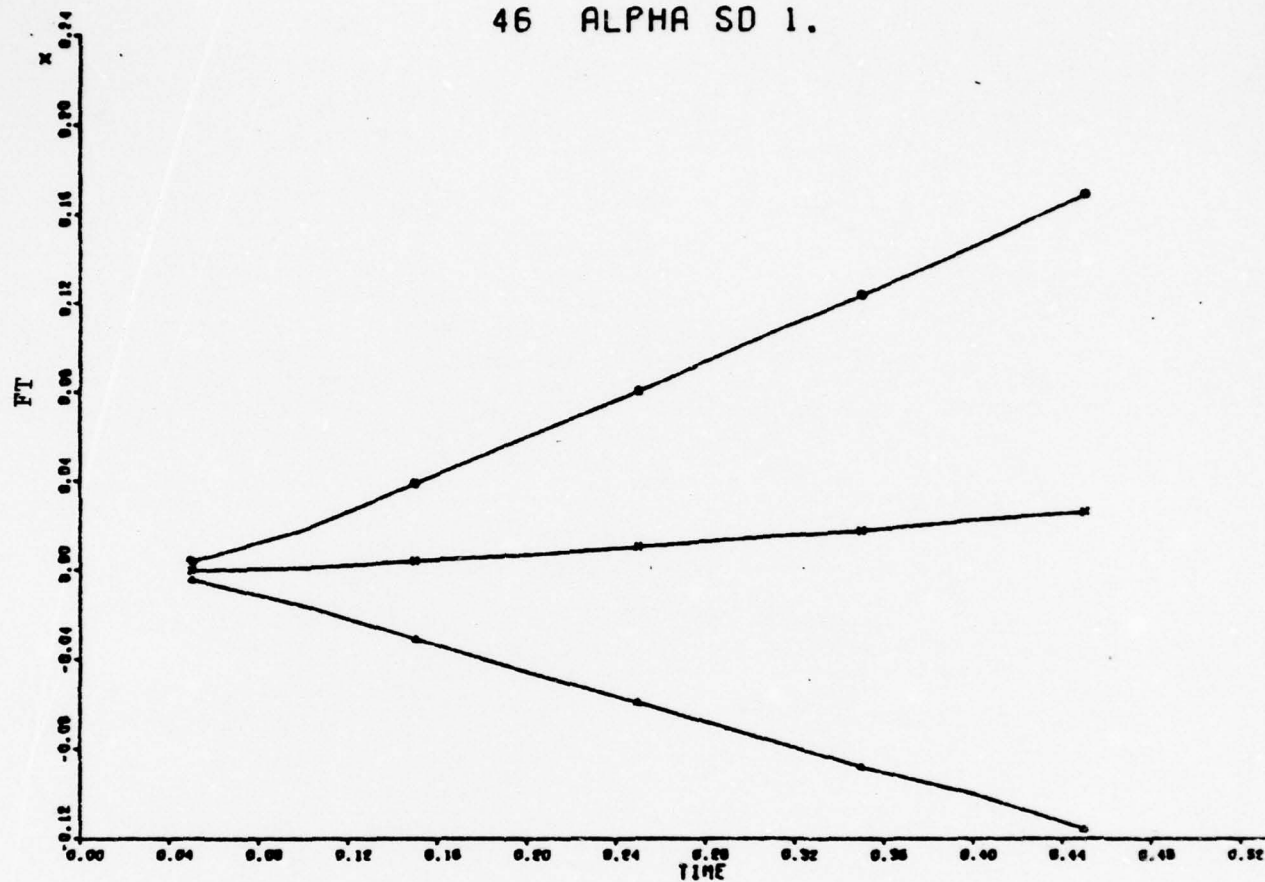


FIGURE 37

U1 ALPHA SD 1.

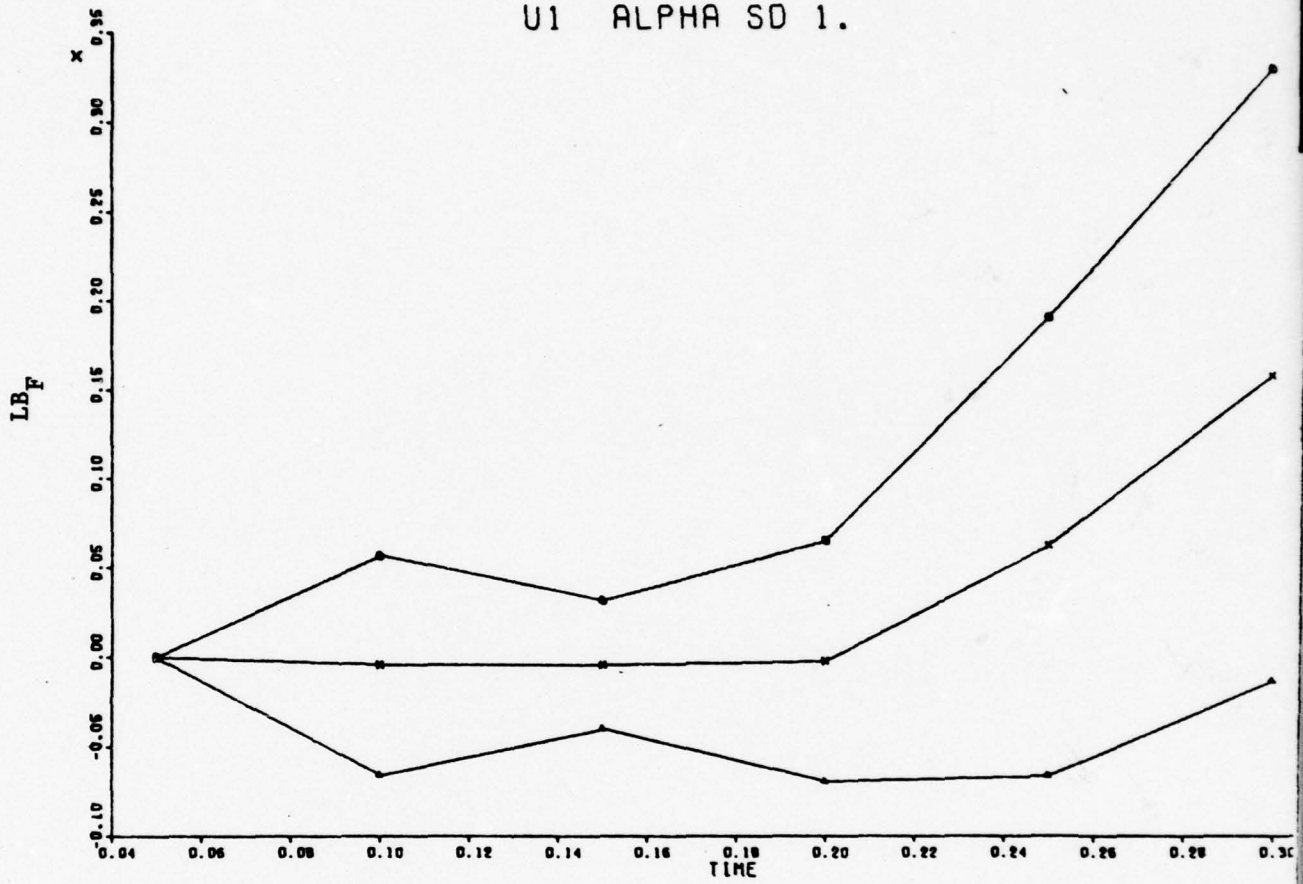


FIGURE 38

U2 ALPHA SD 1.

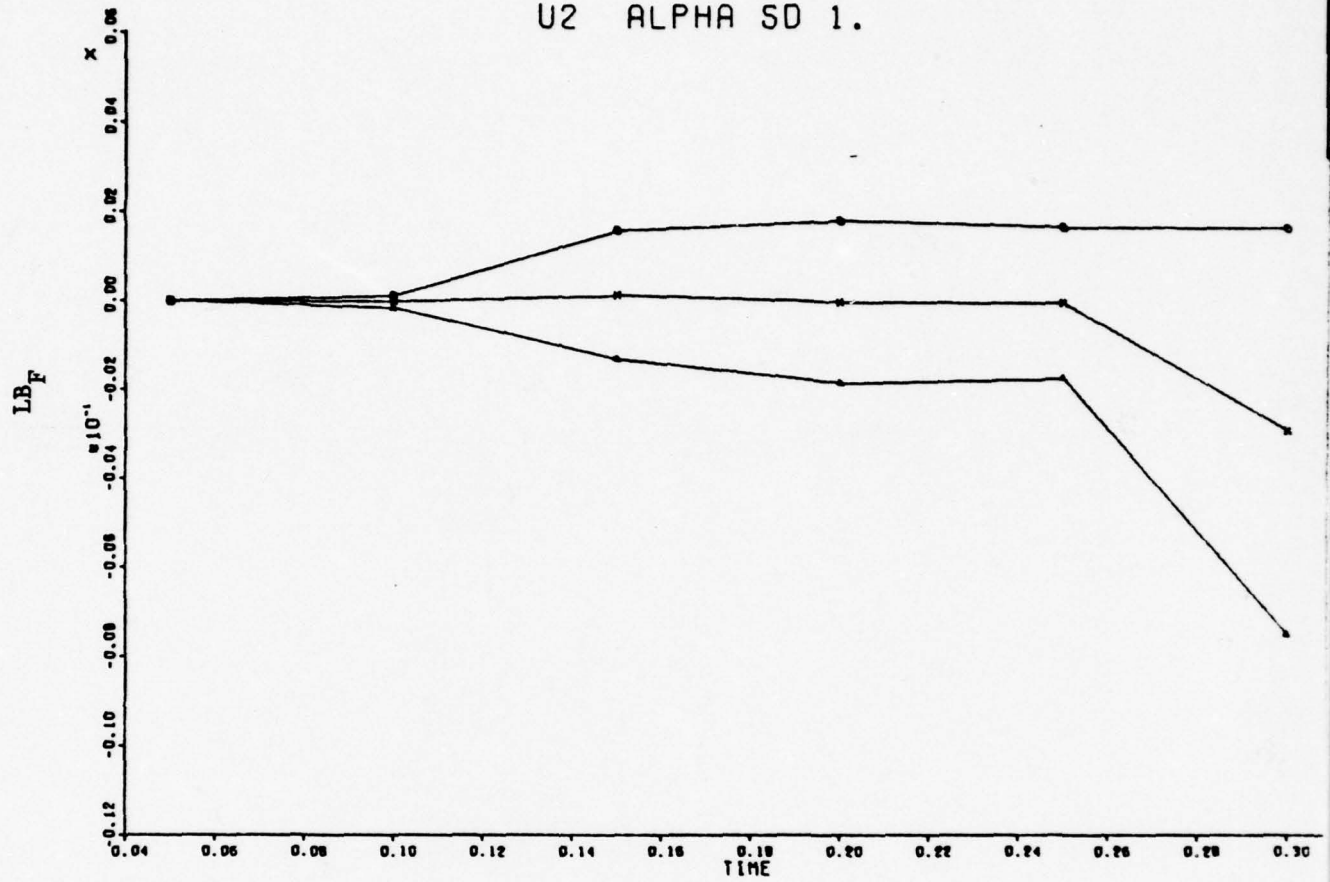


FIGURE 39

U3 ALPHA SD 1.

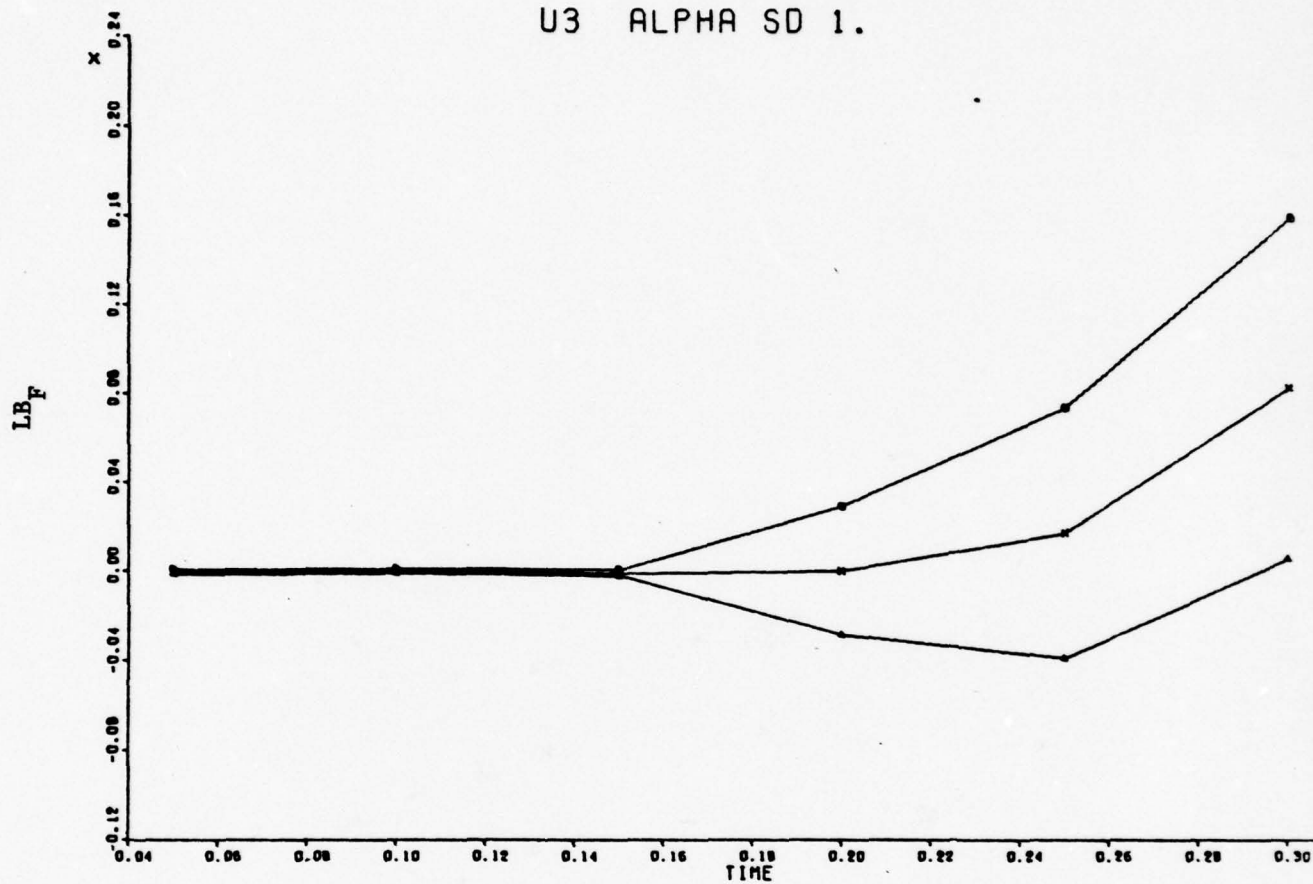


FIGURE 40

U4 ALPHA SD 1.

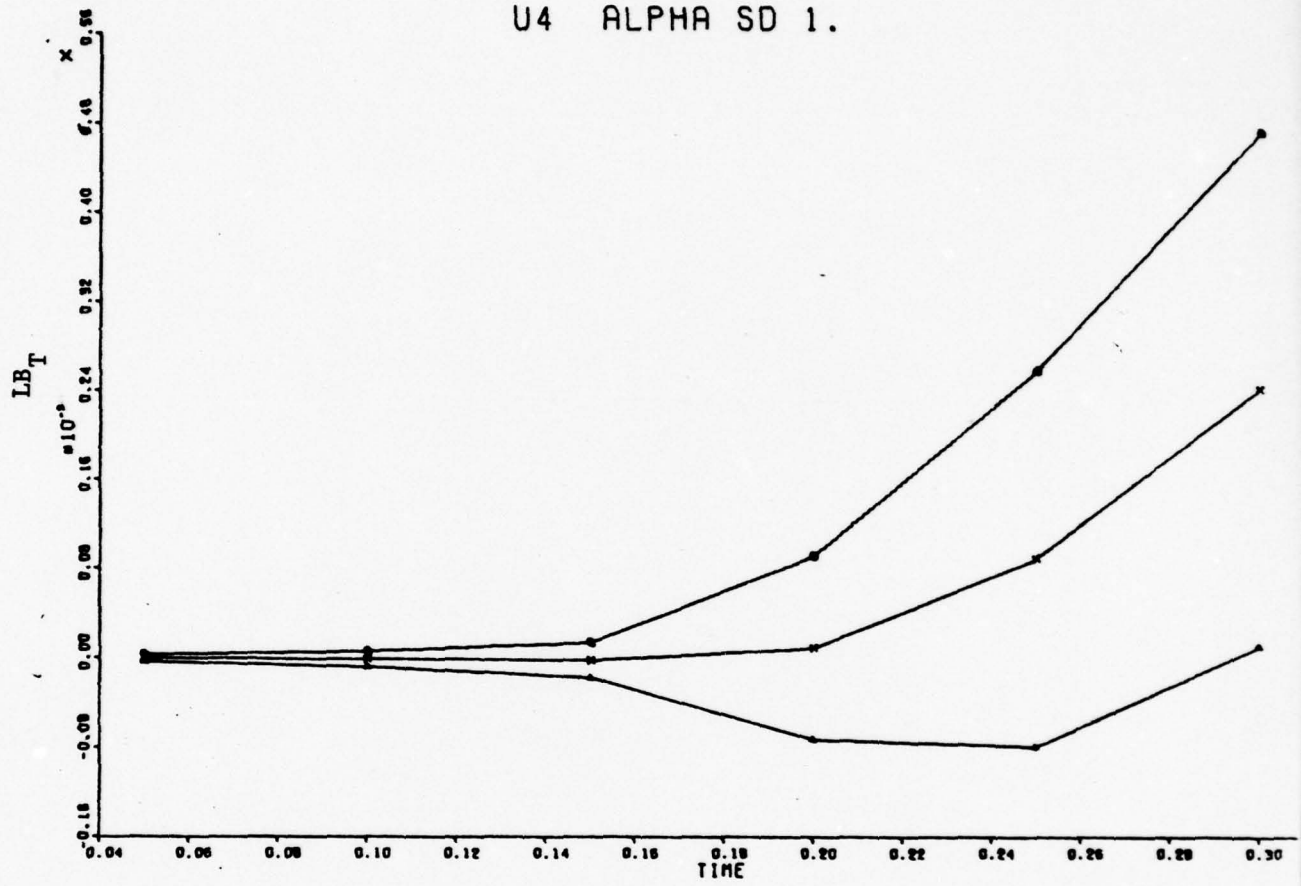


FIGURE 41

35 ALPHA SD 3.

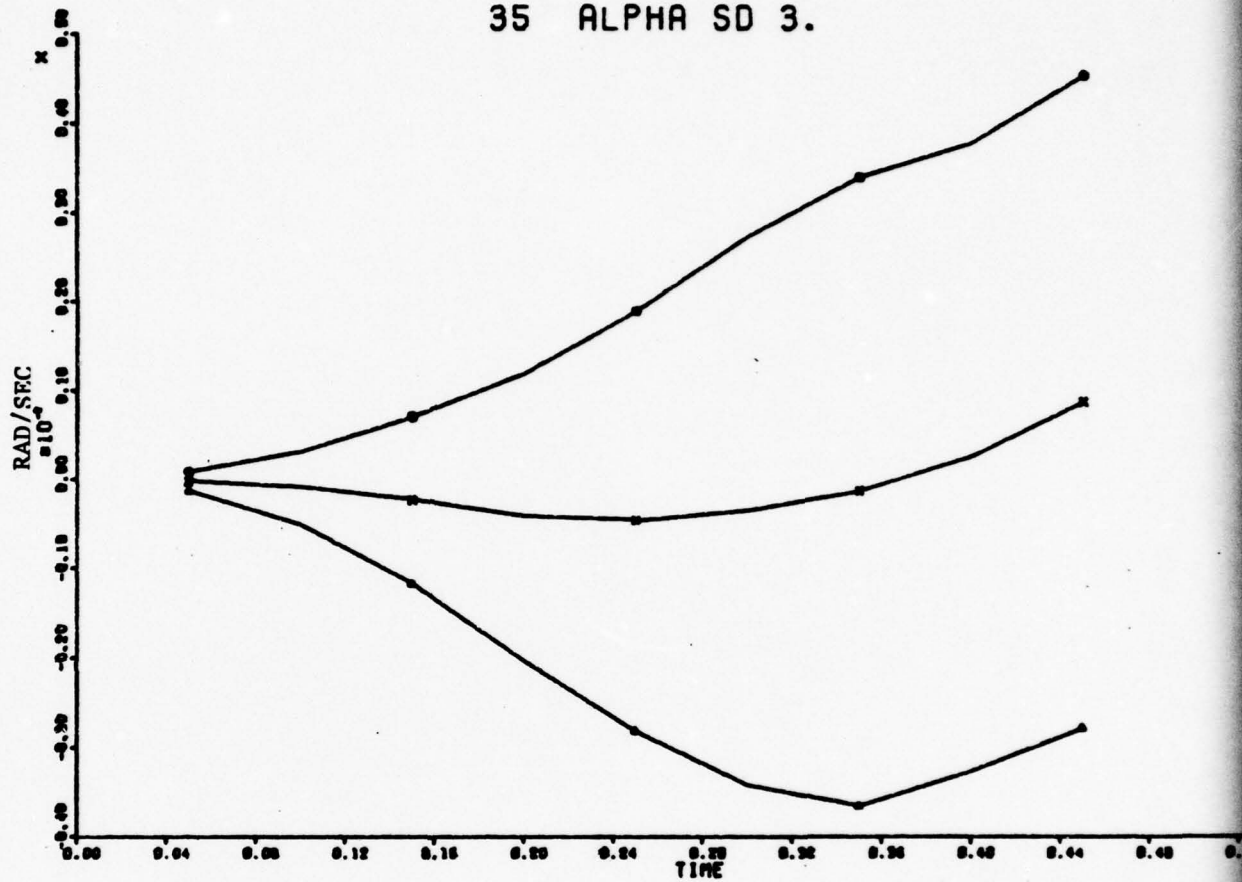


FIGURE 42

36 ALPHA SD 3.

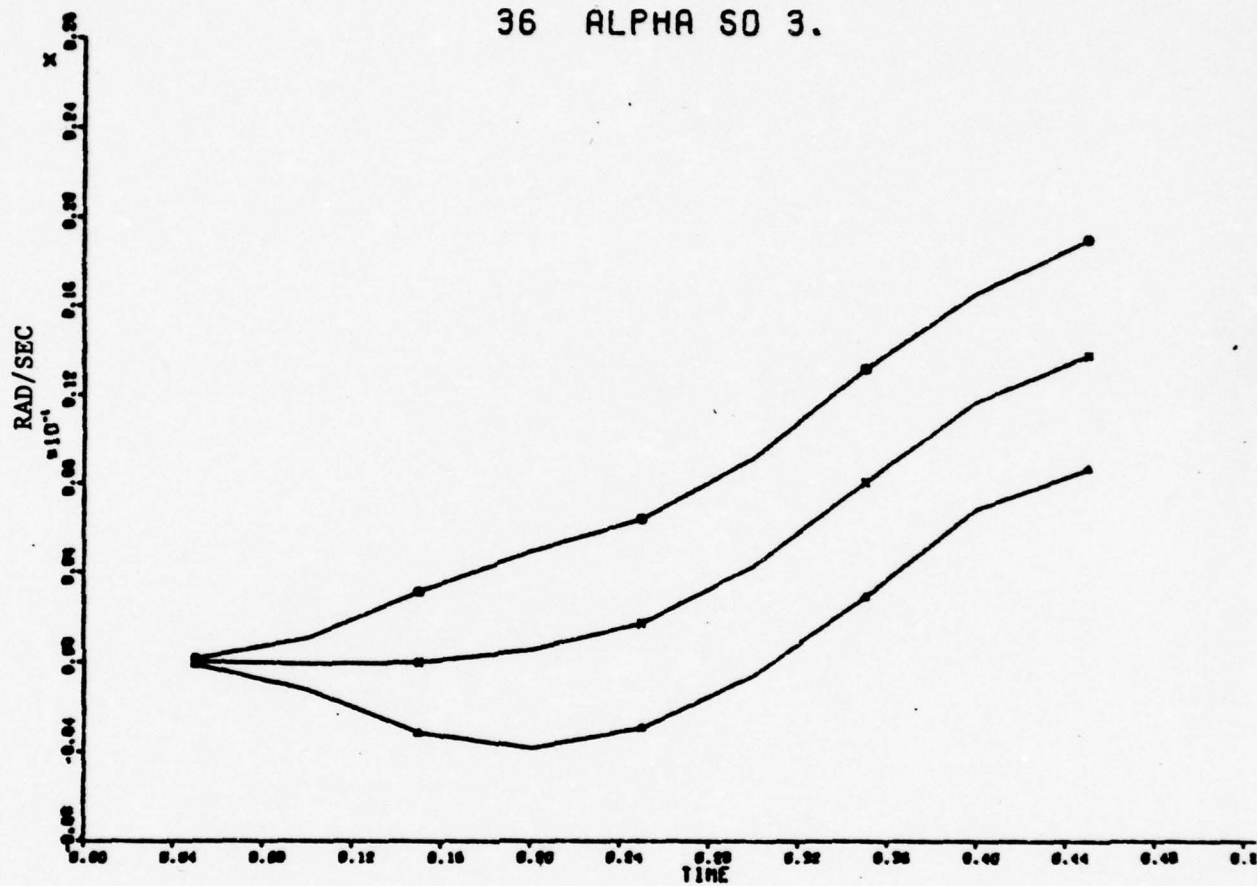


FIGURE 43

37 ALPHA SD 3.

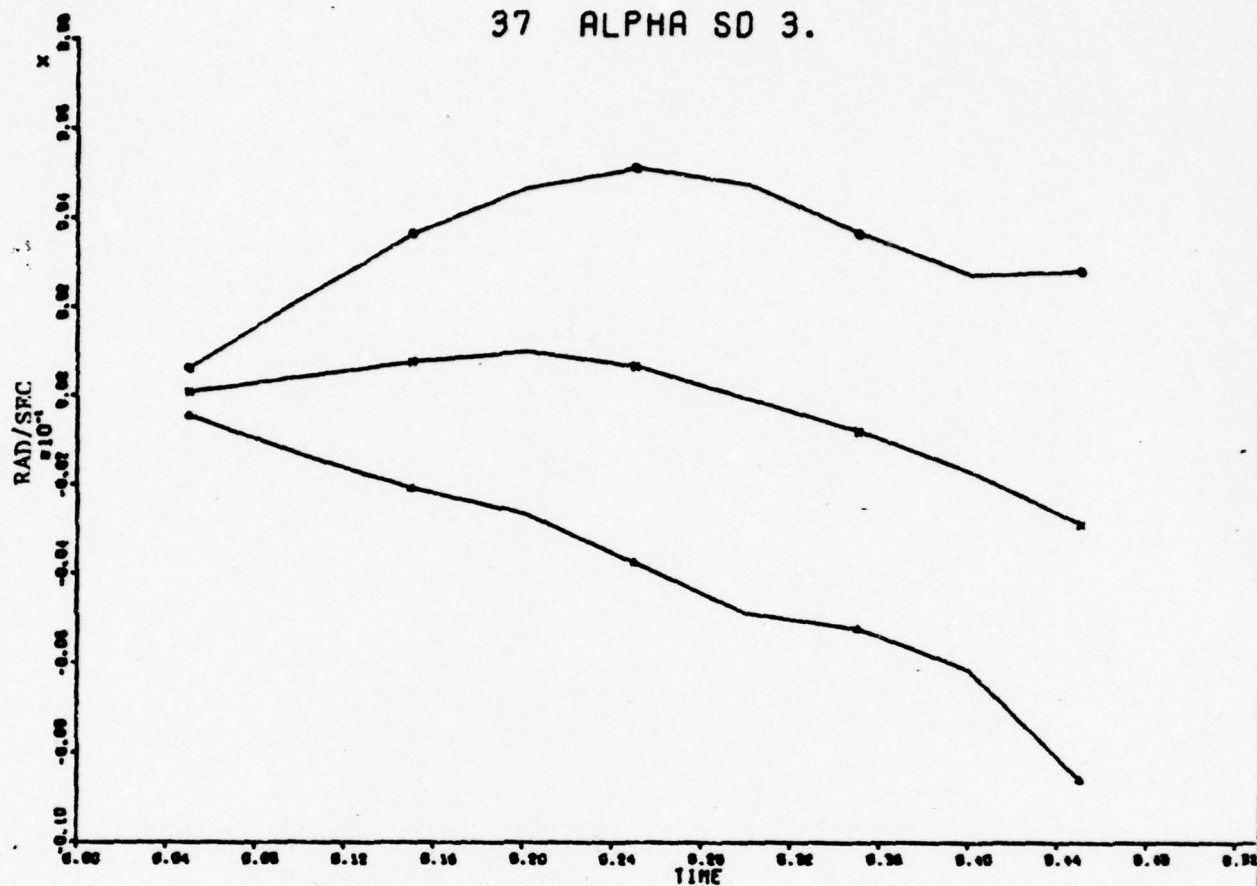


FIGURE 44

38 ALPHA SD 3.

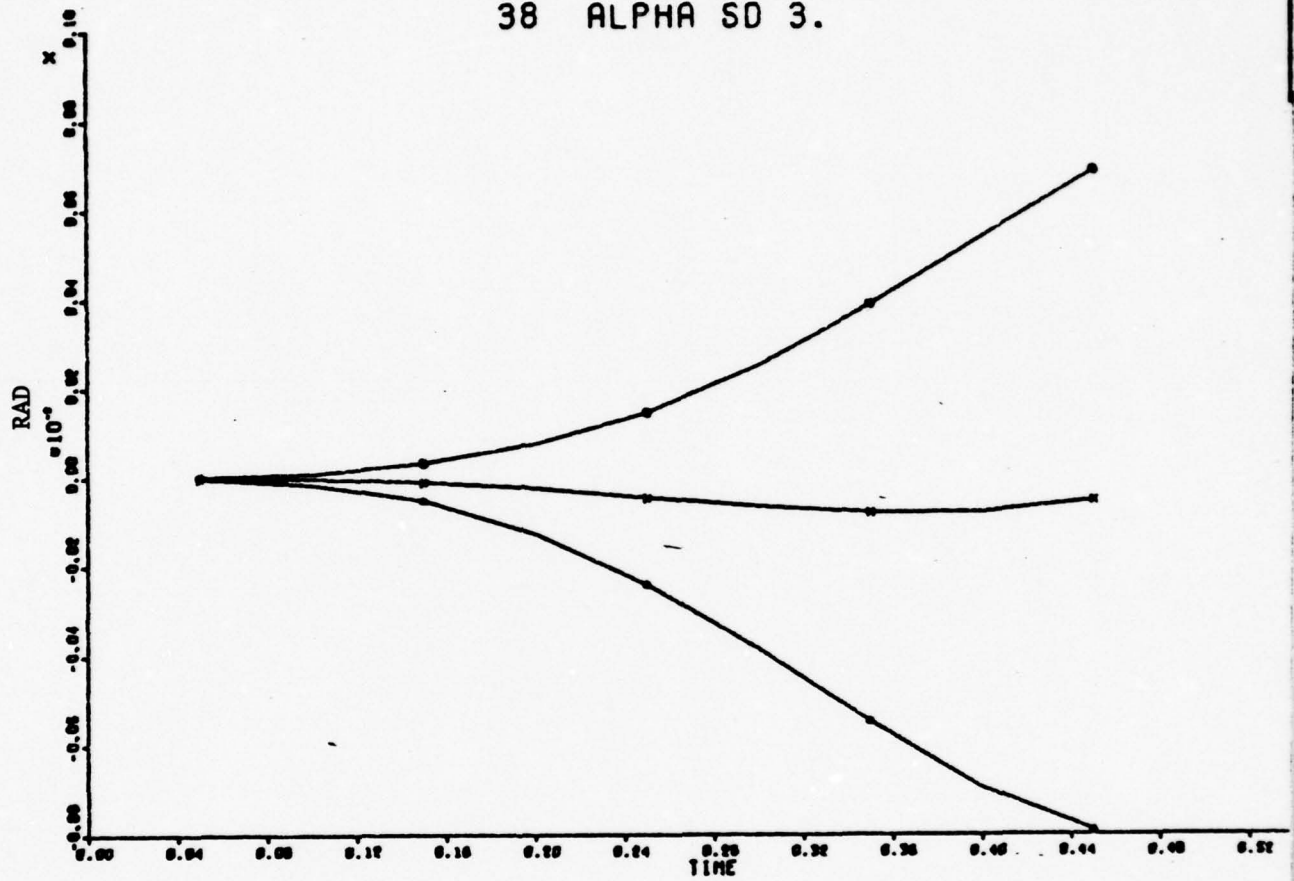


FIGURE 45

39 ALPHA SD 3.

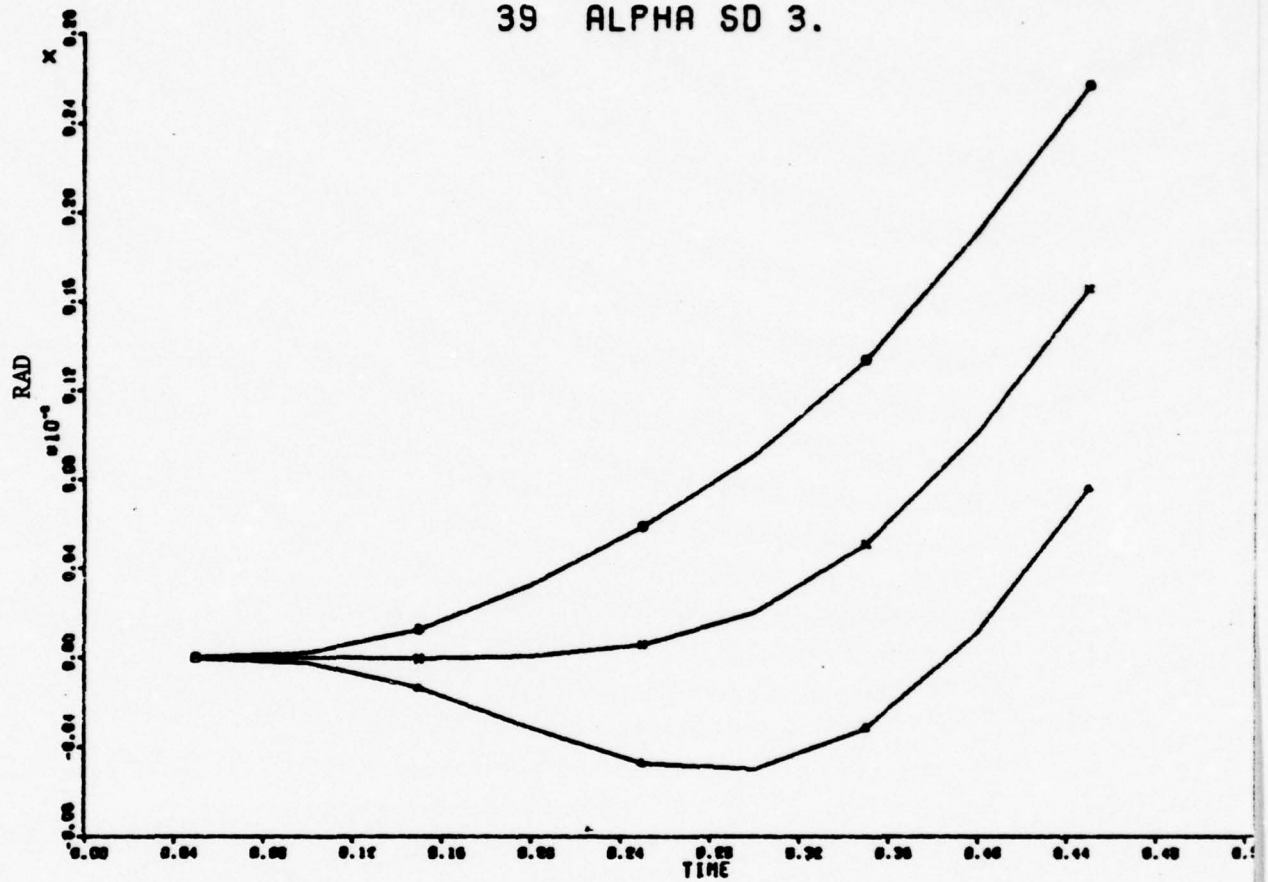


FIGURE 46

40 ALPHA SD 3.

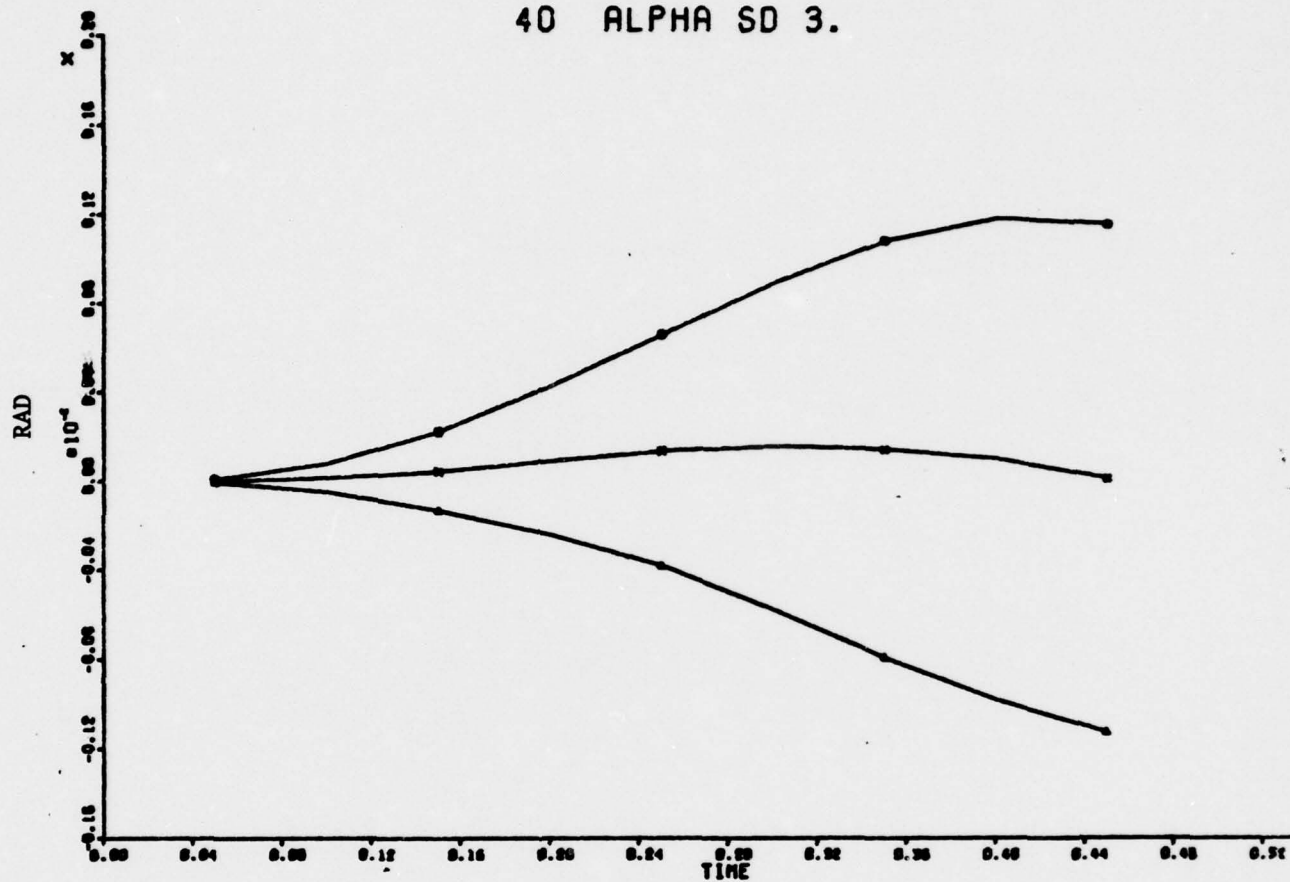


FIGURE 47

41 ALPHA SD 3.

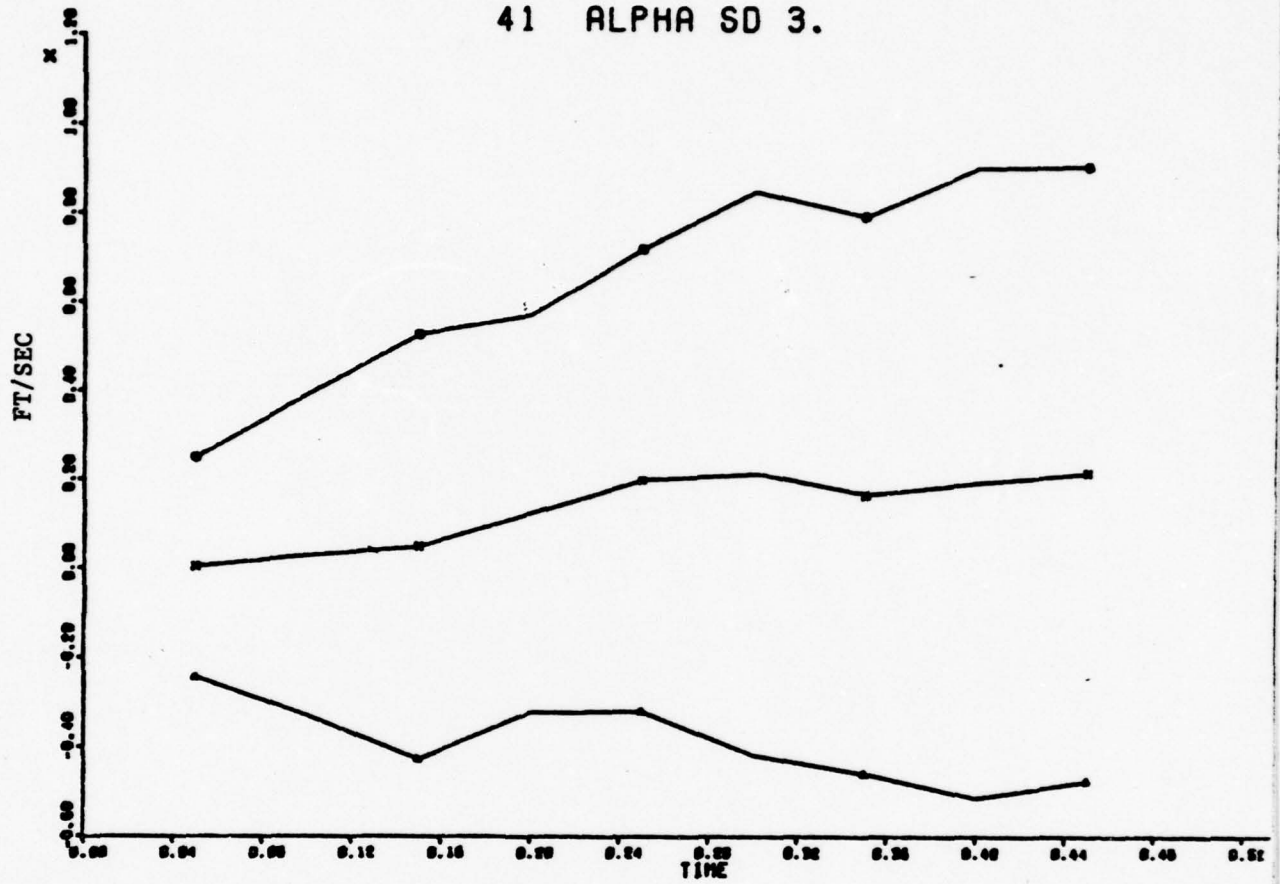


FIGURE 48

42 ALPHA SD 3.

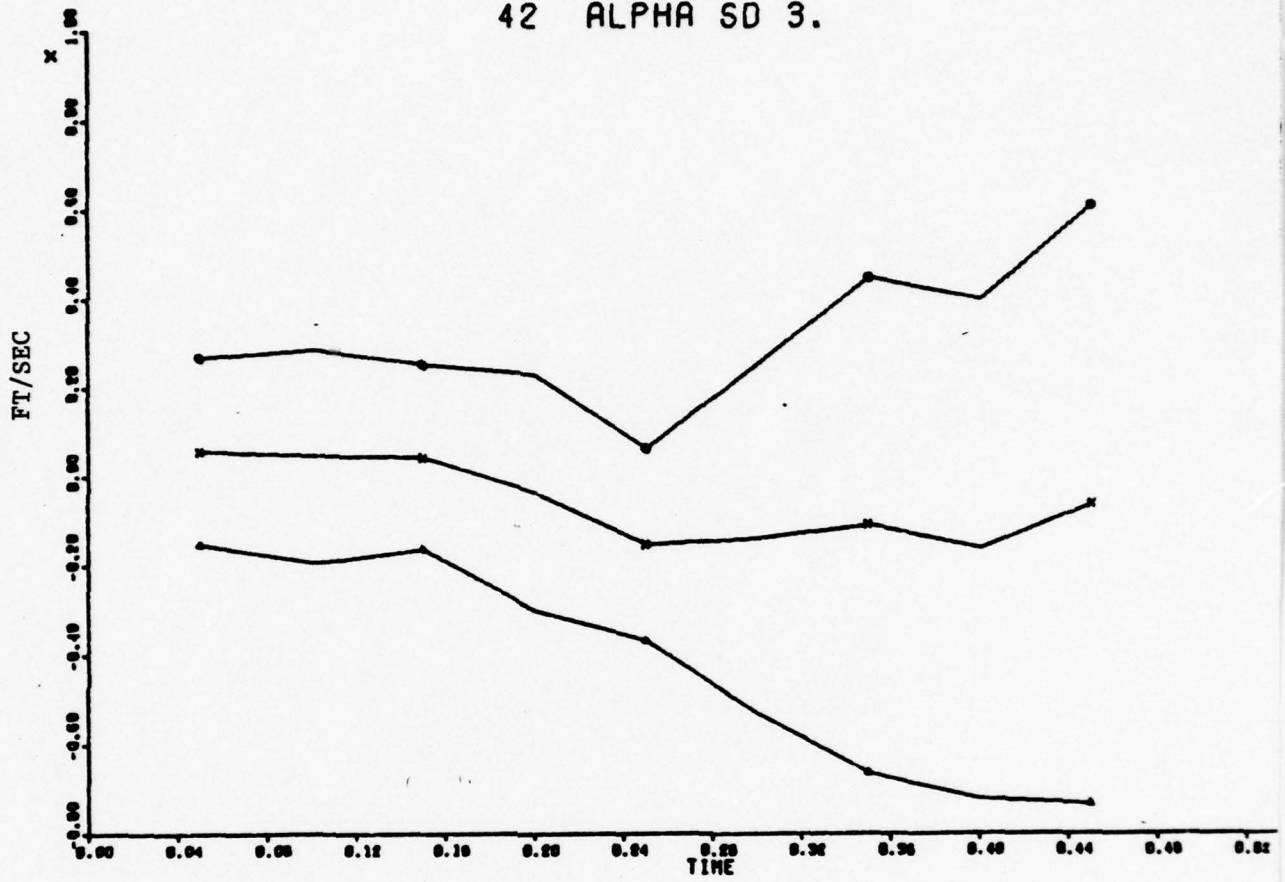


FIGURE 49

43 ALPHA SD 3.

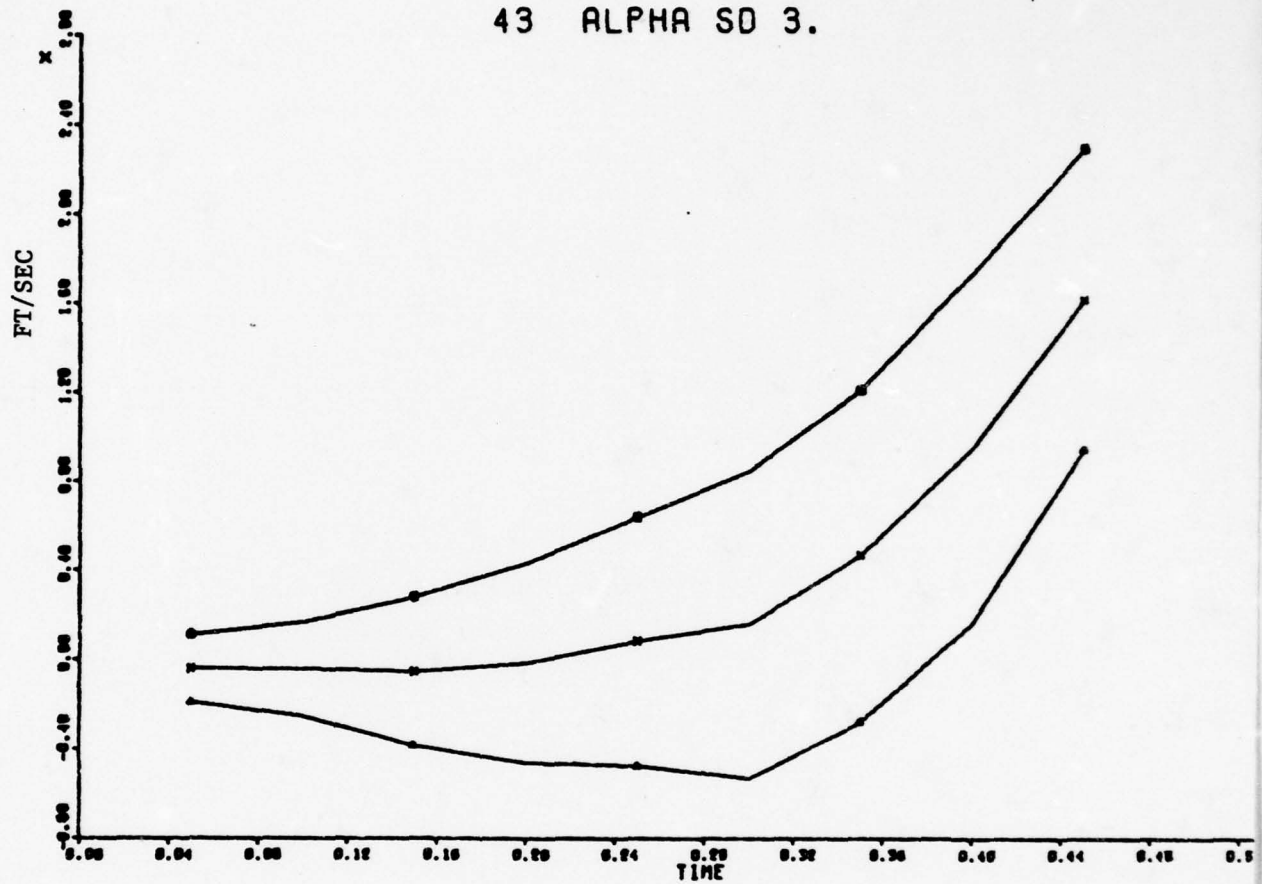


Figure 50

46 ALPHA SD 3.

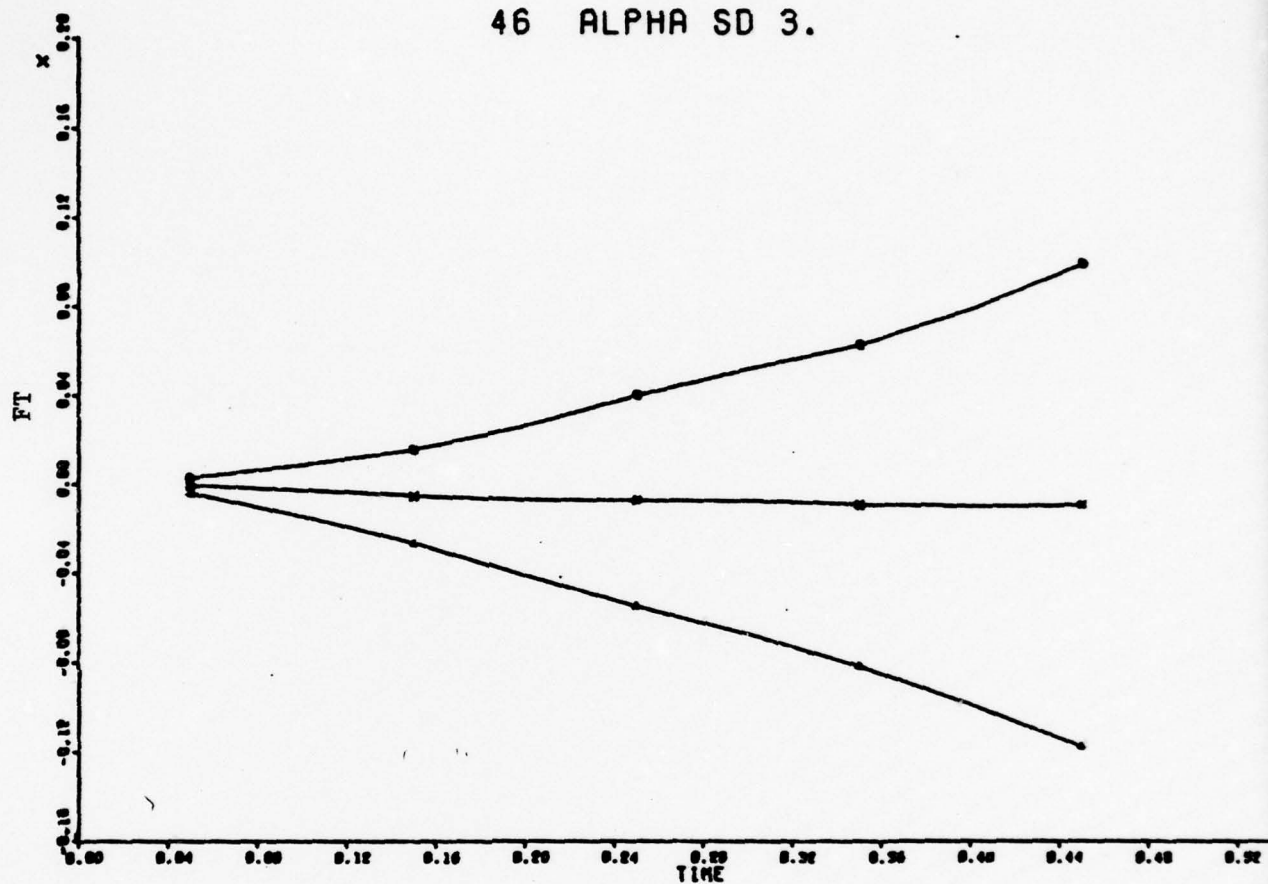


Figure 51

U1 ALPHA SD 3.

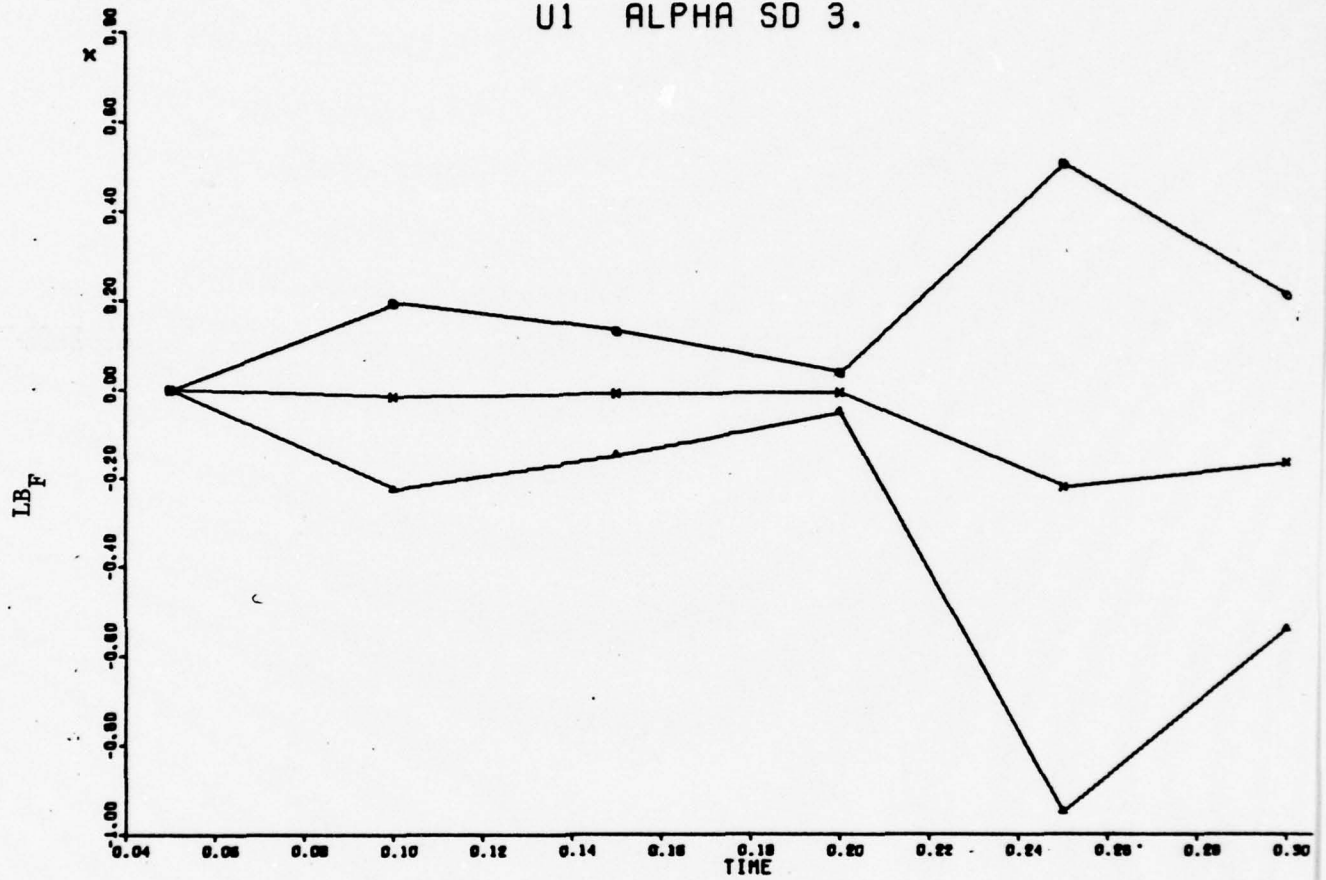


Figure 52

U2 ALPHA SD 3.

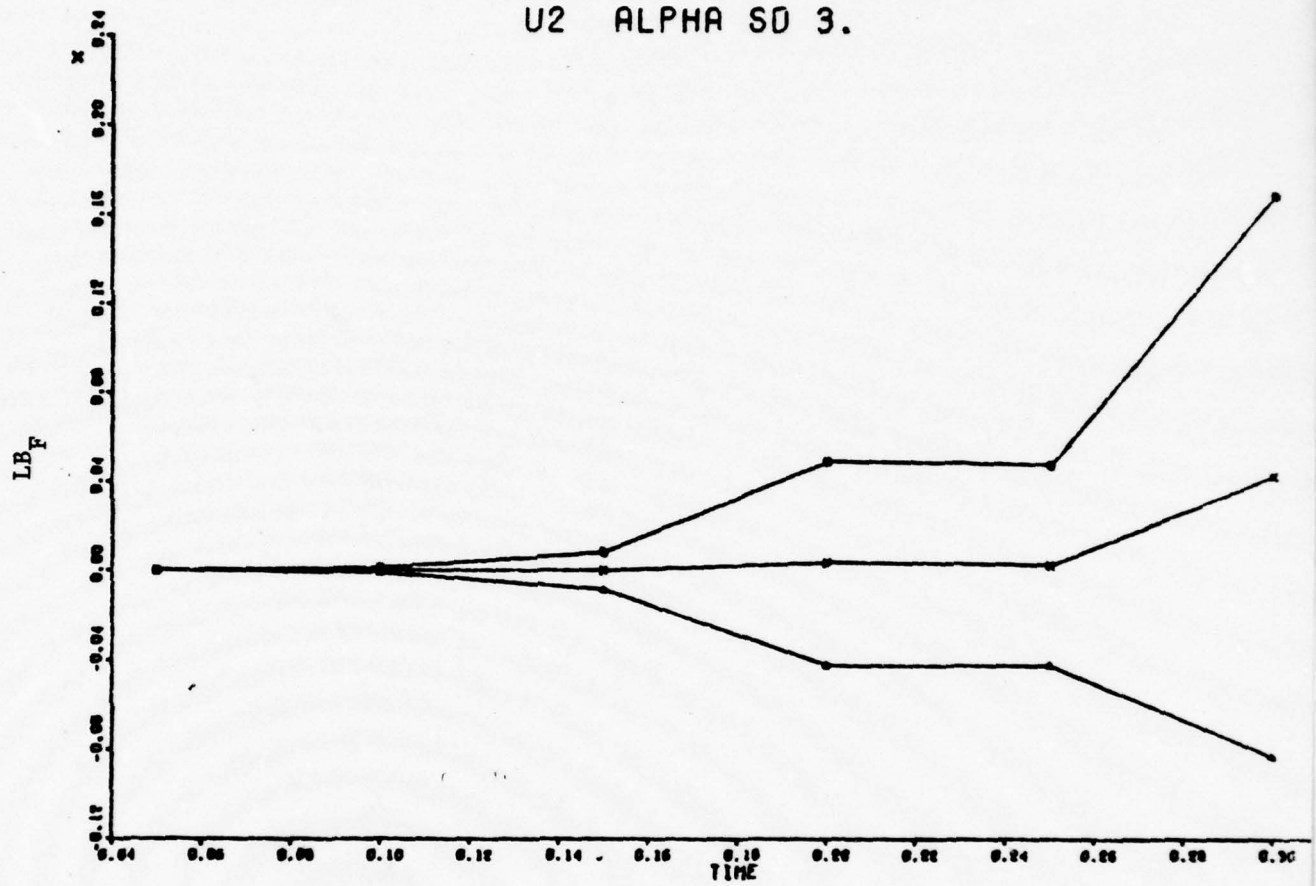


Figure 53

U3 ALPHA SD 3.

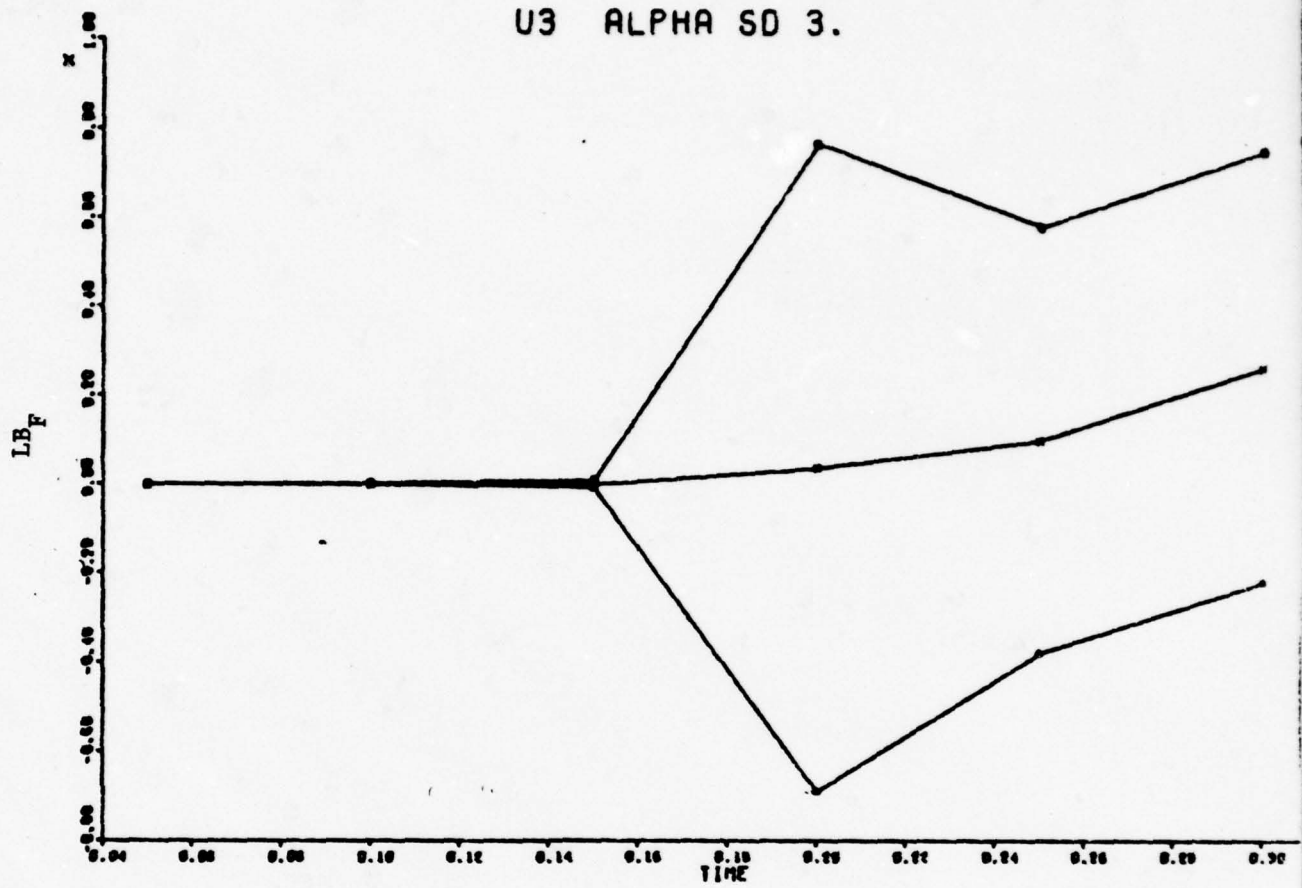
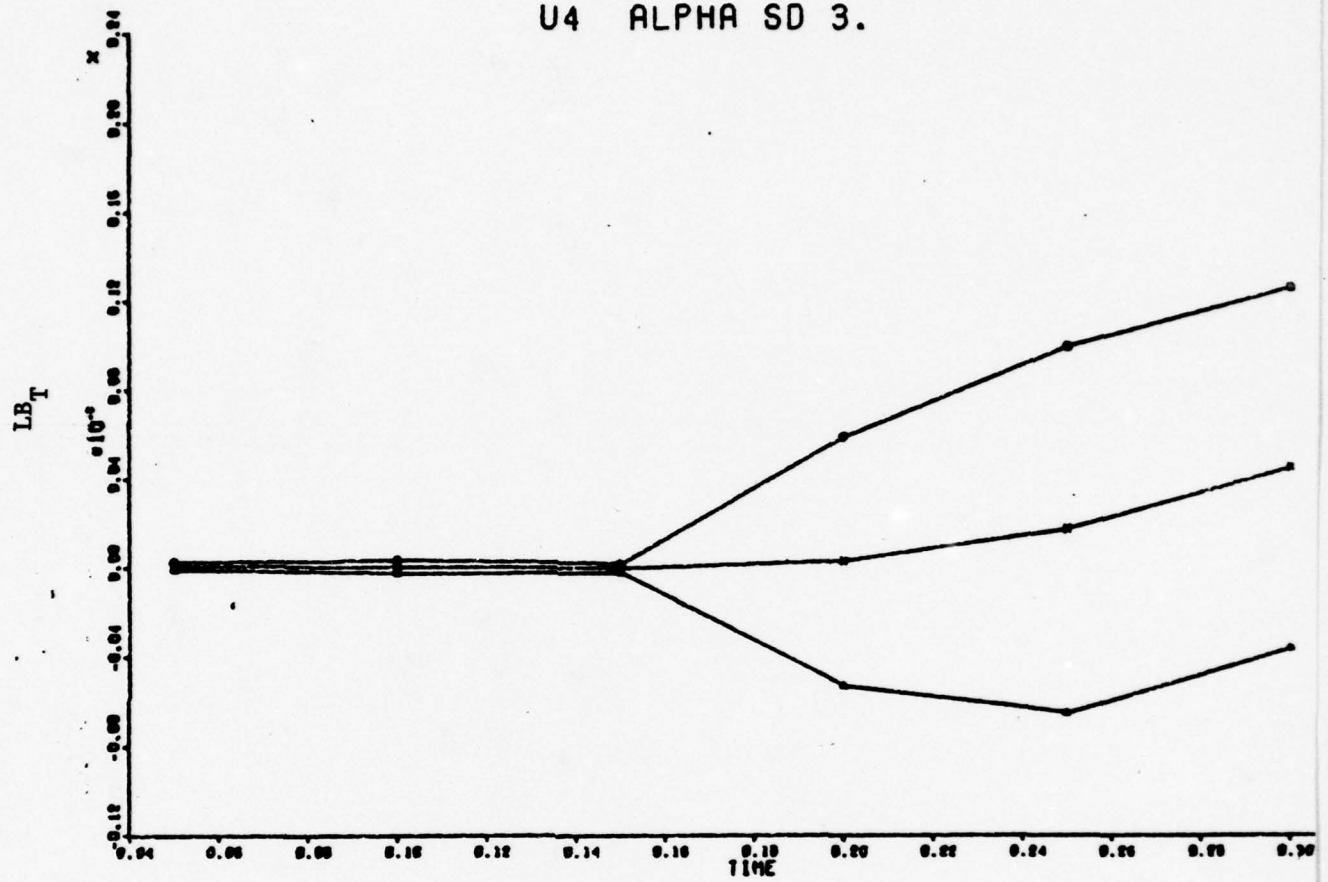


Figure 54

U4 ALPHA SD 3.



APPENDIX 3

Linearization Process

A3-1 General

In Chapter II the mathematical model of the control system and of the aircraft equations of motion was specified in the form of Equations (3-1) and (3-2).

$$\dot{\bar{x}}(t) = \bar{f}(\bar{x}(t), \bar{u}(t), t, \bar{w}(t)) \quad (A3-1)$$

$$\bar{y}(t) = \bar{g}(\bar{x}(t), t, \bar{v}(t)) \quad (A3-2)$$

Unfortunately, the evolution of control theory has not progressed to the point that desirable feedback controls can be computed for this set of equations. An alternative for a usable control design is the method of linearized perturbations. (Ref 6) Though this method cannot address the general control of Equations (3-1) and (3-2), it can address a valid subproblem of control. This subproblem requires that a nominal trajectory be generated from Equations (3-1) and (3-2). As the physical system is only approximated by the mathematical description of these equations, some results of the approximations can be readily identified. The most significant of these results are identified as noises in Chapter II, some of which are state dependent. By applying these noises as perturbations, the system will deviate from the nominal trajectory. As it is essential to keep the system around the nominal trajectory as closely as possible to assure controller

validity, some means of control for these perturbations is desired. Therefore the control subproblem addressed by linear perturbations is to design a control law that will regulate a perturbed system about a precomputed nominal trajectory. These equations are used in the estimator and controller portion of Figure 2.

The first step in control law design using linear perturbations is to linearize Equations (3-1) and (3-2). The derivation of this linearization is given in control literature. (Ref 6,50) The logic inherent in the linearization process is that, if the actual trajectory remains close to the nominal trajectory, the departures from the nominal trajectory are well approximated by first-order differential equations. These first-order differential equations are given in the forms of Equations (3-3) and (3-4).

$$\dot{\bar{x}}(t) = A(t) \bar{x}(t) + B(t) \bar{u}(t) + G(t) \bar{w}(t) \quad (A3-3)$$

$$\dot{\bar{y}}(t) = C(t) \bar{x}(t) + \bar{\gamma}(t) \quad (A3-4)$$

In this form each component of $\bar{x}(t)$, $\bar{u}(t)$, or $\bar{y}(t)$ is the difference between the actual nominal trajectory value and trajectory value, and the matrices are defined below in terms of Equations (A3-1) and (A3-2).

$$A(t) = \left. \frac{\partial \bar{f}}{\partial \bar{x}_1} \right|_0 \quad (A3-5)$$

or the specific terms of the $A(t)$ matrix are

$$A_{1j}(t) = \left. \frac{\partial f_1}{\partial x_j} \right|_0 \quad (A3-6)$$

where $|_0$ refers to the evaluation of $\partial f_1 / \partial x_j$ along the nominal trajectory.

The $B(t)$ and $C(t)$ matrix are defined comparably by

$$B(t) = \left. \frac{\partial \bar{f}}{\partial u} \right|_0 \quad (A3-7)$$

$$C(t) = \left. \frac{\partial \bar{y}}{\partial \bar{x}} \right|_0 \quad (A3-8)$$

The rest of this appendix is devoted to a precise mathematical description of equations (A3-3) and (A3-4) for the specific fighter-type aircraft described in Chapter II.

A3-2 Aerodynamics Equations

The first equations to be addressed are the force equations.

Those equations are

$$\dot{U} = \frac{1}{m} (-WQ + VR - g \sin \theta + P_x + X_s \cos \alpha - z_s \sin \alpha) \quad (A3-9)$$

$$\dot{V} = \frac{1}{m} (-UR + WP + g \cos \theta \sin \phi + Y_s) \quad (A3-10)$$

$$\dot{W} = \frac{1}{m} (UQ - VP + g \cos \theta \cos \phi + X_s \sin \alpha + Z_s \cos \alpha) \quad (A3-11)$$

where

$$X_s = -\frac{1}{2} \rho V_T^2 S C_D \quad (2-37)$$

$$Y_s = \frac{1}{2} \rho V_T^2 S C_Y \quad (2-38)$$

$$Z_s = -\frac{1}{2} \rho V_T^2 S C_L \quad (2-39)$$

Wind-tunnel data is used to determine values which, when combined with appropriate current flight states, result in numerical values for C_D , C_Y , and C_L . The equations that specify this appropriate combination for the fighter-type aircraft considered are given below:

$$C_D = C_{D_{BASIC}} + \frac{\partial C_D}{\partial \delta_H} \delta_H + \frac{\partial C_D}{\partial \delta_{LEF}} \delta_{LEF} \quad (A3-12)$$

$$C_Y = \frac{\partial C_Y}{\partial \beta} \beta + \frac{\partial C_Y}{\partial \delta_{FA}} \delta_{FA} + \frac{\partial C_Y}{\partial \delta_{HA}} \delta_{HA} + \frac{\partial C_Y}{\partial \delta_R} \delta_R \quad (A3-13)$$

$$+ \frac{\partial C_Y}{\partial P_s} P_s + \frac{\partial C_Y}{\partial R_s} R_s$$

$$C_L = C_{L_{BASIC}} + \frac{\partial C_L}{\partial \delta_H} \delta_H + \frac{\partial C_L}{\partial Q_s} Q_s + \frac{\partial C_L}{\partial \dot{\alpha}} \dot{\alpha} + \frac{\partial C_L}{\partial \delta_{LEF}} \delta_{LEF} \quad (A3-14)$$

Now combining the above with the linearized equations of forces gives

$$m d\dot{U} = \frac{\partial \dot{U}}{\partial \dot{W}} d\dot{W} + \frac{\partial \dot{U}}{\partial \dot{Q}_B} d\dot{Q}_B + \frac{\partial \dot{U}}{\partial \dot{V}} d\dot{V} + \frac{\partial \dot{U}}{\partial \dot{R}} d\dot{R} + \frac{\partial \dot{U}}{\partial \dot{\theta}} d\dot{\theta} + \frac{\partial \dot{U}}{\partial \dot{P}_x} d\dot{P}_x +$$

$$\frac{\partial \dot{U}}{\partial \dot{\alpha}} d\dot{\alpha} + \frac{\partial \dot{U}}{\partial \dot{V}_1} d\dot{V}_1 + \frac{\partial \dot{U}}{\partial \dot{\delta}_H} d\dot{\delta}_H + \frac{\partial \dot{U}}{\partial \dot{\delta}_{LEF}} d\dot{\delta}_{LEF} +$$

$$\frac{\partial \dot{U}}{\partial \dot{Q}_s} d\dot{Q}_s + \frac{\partial \dot{U}}{\partial \dot{\alpha}} d\dot{\alpha} \quad (A3-15)$$

$$m d\dot{V} = \frac{\partial \dot{V}}{\partial \dot{U}} d\dot{U} + \frac{\partial \dot{V}}{\partial \dot{R}} d\dot{R} + \frac{\partial \dot{V}}{\partial \dot{W}} d\dot{W} + \frac{\partial \dot{V}}{\partial \dot{P}} d\dot{P} + \frac{\partial \dot{V}}{\partial \dot{\theta}} d\dot{\theta} + \frac{\partial \dot{V}}{\partial \dot{\psi}} d\dot{\psi} +$$

$$\frac{\partial \dot{V}}{\partial \dot{\phi}} d\dot{\phi} + \frac{\partial \dot{V}}{\partial \dot{V}_1} d\dot{V}_1 + \frac{\partial \dot{V}}{\partial \dot{\beta}} d\dot{\beta} + \frac{\partial \dot{V}}{\partial \dot{\delta}_{FA}} d\dot{\delta}_{FA} + \frac{\partial \dot{V}}{\partial \dot{\delta}_{HA}} d\dot{\delta}_{HA} +$$

$$\frac{\partial \dot{V}}{\partial \dot{\delta}_R} d\dot{\delta}_R + \frac{\partial \dot{V}}{\partial \dot{P}_s} d\dot{P}_s + \frac{\partial \dot{V}}{\partial \dot{R}_s} d\dot{R}_s \quad (A3-16)$$

$$m d\dot{W} = \frac{\partial \dot{W}}{\partial \dot{U}} d\dot{U} + \frac{\partial \dot{W}}{\partial \dot{Q}} d\dot{Q} + \frac{\partial \dot{W}}{\partial \dot{V}} d\dot{V} + \frac{\partial \dot{W}}{\partial \dot{P}} d\dot{P} + \frac{\partial \dot{W}}{\partial \dot{\theta}} d\dot{\theta} + \frac{\partial \dot{W}}{\partial \dot{\phi}} d\dot{\phi} +$$

$$\begin{aligned} & \frac{\dot{\partial W}}{\partial \psi} d\psi + \frac{\dot{\partial W}}{\partial V_1} dV_1 + \frac{\dot{\partial W}}{\partial \beta} d\beta + \frac{\dot{\partial W}}{\partial Q_s} dQ_s + \frac{\dot{\partial W}}{\partial \dot{\alpha}} d\dot{\alpha} + \frac{\dot{\partial W}}{\partial \delta_{LEF}} d\delta_{LEF} + \\ & \frac{\dot{\partial W}}{\partial \delta_H} d\delta_H + \frac{\dot{\partial W}}{\partial \delta_{LEF}} d\delta_{LEF} + \frac{\dot{\partial W}}{\partial \alpha} d\alpha \end{aligned} \quad (A3-17)$$

Assumptions inherent in the above linearization are rigid body, constant gravity, and constant aircraft mass. A further simplification is made in the actual usage of the equations: The partial derivatives taken with respect to α and $\dot{\alpha}$ are zero. Since α and $\dot{\alpha}$ change very little in a sample period of .05 seconds, as explained in Chapter V, these terms involving $\frac{\partial \alpha}{\partial \cdot}$ and $\frac{\partial \dot{\alpha}}{\partial \cdot}$ are small compared to the other terms in the equations which they enter, and so assumed to be negligible. If trajectories are to be considered with α rapidly changing over the sample period, it would become necessary to include those terms, but it would be very difficult to generate a trajectory displaying a profile for angle of attack that would change that rapidly.

The moment equations are the next to be linearized. The equations in combined form are

$$\dot{P} = \frac{I_{zz}}{(I_{xx}I_{zz} - J_{xz}^2)} (I_{yy} - I_{zz} - \frac{J_{xz}^2}{I_{zz}}) QR + \frac{J_{xz}}{I_{zz}} (I_{xx} - I_{yy}) PQ +$$

$$\frac{J_{xz}}{I_{zz}} N + J_{xz} PQ + L \quad (A3-18)$$

$$\dot{Q} = \frac{1}{I_{yy}} -PR(I_{xx} - I_{zz}) + (R^2 - P^2) J_{xz} + M \quad (A3-19)$$

$$\dot{R} = \left(\frac{I_{xx}}{I_{xx}I_{zz} - J_{xz}^2} \right) (I_{xx} - I_{yy} + \frac{J_{xz}^2}{I_{zz}}) PQ +$$

$$\left(\frac{J_{xz}}{I_{xx}} (I_{yy} - I_{zz}) - J_{xz} \right) QR + \frac{J_{xz}}{I_{xx}} L + N \quad (A3-20)$$

In the above moment equations the L, M and N values are determined by wind tunnel data. The equations which relate the wind tunnel data to L, M and N values are given in stability axis so that

$$L_B = L_s \cos \alpha - N_s \sin \alpha \quad (A3-21)$$

$$M_B = M_s \quad (A3-22)$$

$$N_B = L_s \sin \alpha + N_s \cos \alpha \quad (A3-23)$$

where

$$L_s = \frac{1}{2} \rho V_T^2 b C_l S \quad (2-45)$$

$$M_s = \frac{1}{2} \rho V_T^2 \bar{c} C_m S \quad (2-46)$$

$$N_s = \frac{1}{2} \rho V_T^2 b C_n S \quad (2-47)$$

Now, the definition of C_l , C_m , and C_n from wind-tunnel data is

$$C_l = \frac{\partial C_l}{\partial \beta} \beta + \frac{\partial C_l}{\partial \delta_{FA}} \delta_{FA} + \frac{\partial C_l}{\partial \delta_{HA}} \delta_{HA} + \frac{\partial C_l}{\partial \delta_r} \delta_r + \frac{\partial C_l}{\partial P_s} P_s + \frac{\partial C_l}{\partial R_s} R_s \quad (A3-24)$$

$$C_m = C_{m_{BASIC}} + \frac{\partial C_m}{\partial \delta_H} \delta_H + \frac{\partial C_m}{\partial Q_s} Q_s + \frac{\partial C_m}{\partial \dot{\alpha}} \dot{\alpha} + \frac{\partial C_m}{\partial \delta_{LEF}} \delta_{LEF} \quad (A3-25)$$

$$C_n = \frac{\partial C_n}{\partial \beta} \beta + \frac{\partial C_n}{\partial \delta_{FA}} \delta_{FA} + \frac{\partial C_n}{\partial \delta_{HA}} \delta_{HA} + \frac{\partial C_n}{\partial \delta_r} \delta_r + \frac{\partial C_n}{\partial P_s} P_s + \frac{\partial C_n}{\partial R_s} R_s \quad (A3-26)$$

These equations relate system states or parameters of the partial derivatives given by the wind tunnel to output expressions for the moments. By using the assumptions below the linearized

equations for the moments become

$$\begin{aligned} \dot{dP} = & \frac{\partial \dot{P}}{\partial Q} dQ + \frac{\partial \dot{P}}{\partial R} dR + \frac{\partial \dot{P}}{\partial P} dP + \frac{\partial \dot{P}}{\partial V_1} dV_1 + \frac{\partial \dot{P}}{\partial \beta} d\beta + \frac{\partial \dot{P}}{\partial \delta_{FA}} d\delta_{FA} + \\ & \frac{\partial \dot{P}}{\partial \delta_{HA}} d\delta_{HA} + \frac{\partial \dot{P}}{\partial \delta_r} d\delta_r + \frac{\partial \dot{P}}{\partial P_s} dP_s + \frac{\partial \dot{P}}{\partial R_s} dR_s \end{aligned} \quad (A3-27)$$

$$\begin{aligned} \dot{dQ} = & \frac{\partial \dot{Q}}{\partial P} dP + \frac{\partial \dot{Q}}{\partial R} dR + \frac{\partial \dot{Q}}{\partial V_1} dV_1 + \frac{\partial \dot{Q}}{\partial H} d\delta_H + \frac{\partial \dot{Q}}{\partial Q_s} dQ_s + \\ & \frac{\partial \dot{Q}}{\partial \alpha} d\alpha + \frac{\partial \dot{Q}}{\partial \delta_{LEF}} d\delta_{LEF} \end{aligned} \quad (A3-28)$$

$$\begin{aligned} \dot{dR} = & \frac{\partial \dot{R}}{\partial P} dP + \frac{\partial \dot{R}}{\partial Q_s} dQ_s + \frac{\partial \dot{R}}{\partial R} dR + \frac{\partial \dot{R}}{\partial V_1} dV_1 + \frac{\partial \dot{R}}{\partial \beta} d\beta + \frac{\partial \dot{R}}{\partial \delta_{FA}} d\delta_{FA} + \\ & \frac{\partial \dot{R}}{\partial \delta_{HA}} d\delta_{HA} + \frac{\partial \dot{R}}{\partial \delta_r} d\delta_r + \frac{\partial \dot{R}}{\partial P_s} dP_s + \frac{\partial \dot{R}}{\partial R_s} dR_s \end{aligned} \quad (A3-29)$$

Other assumptions inherent in the above equations are:

- 1) The moments and products of inertia are constant.
- 2) Air density is constant for the time interval under consideration.
- 3) The coefficients from wind-tunnel data are considered constant over the .05 sample period.
- 4) α and $\dot{\alpha}$ are considered constant for the interval in question.

A3-3 Euler Angle Equations

The next step in the linearization process involves the angle and position equations, Equations (2-54), (2-55), (2-56), (2-61), (2-62) and (2-63). Linearization of these equations is accomplished in Pollard's dissertation and will not be duplicated here.

The resulting linearized angle equations are

$$\dot{\theta} = \frac{\partial \theta}{\partial Q} \dot{dQ} + \frac{\partial \theta}{\partial R} \dot{dR} + \frac{\partial \theta}{\partial \theta} \dot{d\theta} + \frac{\partial \theta}{\partial \psi} \dot{d\psi} + \frac{\partial \theta}{\partial \phi} \dot{d\phi} \quad (\text{A3-30})$$

$$\dot{\phi} = \frac{\partial \phi}{\partial R} \dot{dR} + \frac{\partial \phi}{\partial Q} \dot{dQ} + \frac{\partial \phi}{\partial P} \dot{dP} + \frac{\partial \phi}{\partial \phi} \dot{d\phi} + \frac{\partial \phi}{\partial \theta} \dot{d\theta} + \frac{\partial \phi}{\partial \psi} \dot{d\psi} \quad (\text{A3-31})$$

$$\dot{\psi} = \frac{\partial \psi}{\partial R} \dot{dR} + \frac{\partial \psi}{\partial Q} \dot{dQ} + \frac{\partial \psi}{\partial \phi} \dot{d\phi} + \frac{\partial \psi}{\partial \psi} \dot{d\psi} + \frac{\partial \psi}{\partial \theta} \dot{d\theta} \quad (\text{A3-32})$$

and the resulting position equations are

$$\dot{dS}_x = \frac{\partial S_x}{\partial U} \dot{dU} + \frac{\partial S_x}{\partial V} \dot{dV} + \frac{\partial S_x}{\partial W} \dot{dW} + \frac{\partial S_x}{\partial \phi} \dot{d\phi} + \frac{\partial S_x}{\partial \psi} \dot{d\psi} + \frac{\partial S_x}{\partial \theta} \dot{d\theta} \quad (\text{A3-33})$$

$$\dot{dS}_y = \frac{\partial S_y}{\partial U} \dot{dU} + \frac{\partial S_y}{\partial V} \dot{dV} + \frac{\partial S_y}{\partial W} \dot{dW} + \frac{\partial S_y}{\partial \theta} \dot{d\theta} + \frac{\partial S_y}{\partial \psi} \dot{d\psi} + \frac{\partial S_y}{\partial \phi} \dot{d\phi} \quad (\text{A3-34})$$

$$\dot{dS}_z = \frac{\partial \dot{S}_z}{\partial U} dU + \frac{\partial \dot{S}_z}{\partial V} dV + \frac{\partial \dot{S}_z}{\partial W} dW + \frac{\partial \dot{S}_z}{\partial \theta} d\theta + \frac{\partial \dot{S}_z}{\partial \phi} d\phi + \frac{\partial \dot{S}_z}{\partial \psi} d\psi \quad (A3-35)$$

These last six equations display the new perturbation states in the state variable form. Functional descriptions for the $\frac{\partial \dot{S}_z}{\partial \cdot}$ terms are derived from Equations (2-54), (2-55), and (2-56), and (2-61), (2-62), and (2-63). Above are the general linearized equations of motion. These equations, when coupled with the control system equations, give the desired mathematical description of the aircraft.

The next step involves linearization of the control system equations. These linearizations are derived from the control system block diagram, Figure 4.

A3-4 Total System Equations

$$d\dot{x}_1 = \frac{\partial \dot{x}_1}{\partial x_1} dx_1 + \frac{\partial \dot{x}_1}{\partial \text{PITCA}} d \text{PITCA} + W_{11} \quad (A3-36)$$

$$d\dot{x}_2 = \frac{\partial \dot{x}_2}{\partial x_1} dx_1 + \frac{\partial \dot{x}_2}{\partial x_2} dx_2 + \frac{\partial \dot{x}_2}{\partial x_3} dx_3 + \frac{\partial \dot{x}_2}{\partial x_4} dx_4 + \frac{\partial \dot{x}_2}{\partial x_5} dx_5 + \\ \frac{\partial \dot{x}_2}{\partial \theta} d\theta + \frac{\partial \dot{x}_2}{\partial x_6} dx_6 + \frac{\partial \dot{x}_2}{\partial x_7} dx_7 + \frac{\partial \dot{x}_2}{\partial x_{53}} dx_{53} + \frac{\partial \dot{x}_2}{\partial x_{64}} dx_{64} \quad (A3-37)$$

$$d\dot{x}_3 = \frac{\partial \dot{x}_3}{\partial x_3} dx_3 + \frac{\partial \dot{x}_3}{\partial \alpha} d\alpha + W_{12} \quad (A3-38)$$

$$d\dot{x}_4 = \frac{\partial \dot{x}_4}{\partial x_4} dx_4 + \frac{\partial \dot{x}_4}{\partial \theta} d\theta + \frac{\partial \dot{x}_4}{\partial x_5} dx_5 + \frac{\partial \dot{x}_4}{\partial x_6} dx_6 + \frac{\partial \dot{x}_4}{\partial x_7} dx_7 + \frac{\partial \dot{x}_4}{\partial x_3} dx_3 +$$

$$\frac{\partial \dot{x}_4}{\partial x_{53}} dx_{53} + \frac{\partial \dot{x}_4}{\partial x_{64}} dx_{64} \quad (A3-39)$$

$$d\dot{x}_5 = \frac{\partial \dot{x}_5}{\partial x_5} dx_5 \quad (A3-40)$$

$$d\dot{x}_6 = \frac{\partial \dot{x}_6}{\partial x_6} dx_6 + \frac{\partial \dot{x}_6}{\partial \theta} d\theta + \frac{\partial \dot{x}_6}{\partial x_{53}} dx_{53} + \frac{\partial \dot{x}_6}{\partial x_{64}} dx_{64} \quad (A3-41)$$

$$d\dot{x}_7 = \frac{\partial \dot{x}_7}{\partial x_7} dx_7 + \frac{\partial \dot{x}_7}{\partial W} dW + \frac{\partial \dot{x}_7}{\partial x_{59}} dx_{59} + \frac{\partial \dot{x}_7}{\partial x_{61}} dx_{61} + W_8 \quad (A3-42)$$

$$d\dot{x}_8 = \frac{\partial \dot{x}_8}{\partial x_8} dx_8 + \frac{\partial \dot{x}_8}{\partial x_9} dx_9 + \frac{\partial \dot{x}_8}{\partial x_{10}} dx_{10} + \frac{\partial \dot{x}_8}{\partial RC} dRC + W_{13} \quad (A3-43)$$

$$d\dot{x}_9 = \frac{\partial \dot{x}_9}{\partial x_8} dx_8 + \frac{\partial \dot{x}_9}{\partial x_9} dx_9 \quad (A3-44)$$

$$d\dot{x}_{10} = \frac{\partial \dot{x}_{10}}{\partial x_8} dx_8 + \frac{\partial \dot{x}_{10}}{\partial x_{10}} dx_{10} \quad (A3-45)$$

$$d\dot{x}_{11} = \frac{\partial \dot{x}_{11}}{\partial x_{12}} dx_{12} \quad (A3-46)$$

$$d\dot{x}_{12} = \frac{\partial \dot{x}_{12}}{\partial x_{11}} dx_{11} + \frac{\partial \dot{x}_{12}}{\partial x_{12}} dx_{12} + \frac{\partial \dot{x}_{12}}{\partial \phi} d\dot{\phi} + \frac{\partial \dot{x}_{12}}{\partial x_{54}} dx_{54} + \frac{\partial \dot{x}_{12}}{\partial x_{63}} dx_{63} \quad (A3-47)$$

$$d\dot{x}_{13} = \frac{\partial \dot{x}_{13}}{\partial x_{13}} dx_{13} + \frac{\partial \dot{x}_{13}}{\partial x_{14}} dx_{14} + \frac{\partial \dot{x}_{13}}{\partial x_{54}} dx_{54} + \frac{\partial \dot{x}_{13}}{\partial x_{63}} dx_{63} + \frac{\partial \dot{x}_{13}}{\partial \phi} d\dot{\phi} \quad (A3-48)$$

$$d\dot{x}_{14} = \frac{\partial \dot{x}_{14}}{\partial x_{13}} dx_{13} \quad (A3-49)$$

$$d\dot{x}_{15} = \frac{\partial \dot{x}_{15}}{\partial x_{15}} dx_{15} \quad (A3-50)$$

$$d\dot{x}_{16} = \frac{\partial \dot{x}_{16}}{\partial x_{17}} dx_{17} \quad (A3-51)$$

$$d\dot{x}_{17} = \frac{\partial \dot{x}_{17}}{\partial x_{16}} dx_{16} + \frac{\partial \dot{x}_{17}}{\partial x_{17}} dx_{17} + \frac{\partial \dot{x}_{17}}{\partial x_3} dx_3 + \frac{\partial \dot{x}_{17}}{\partial x_{55}} dx_{55} + \frac{\partial \dot{x}_{17}}{\partial x_{62}} dx_{62} +$$

$$\frac{\partial \dot{x}_{17}}{\partial x_{54}} dx_{54} + \frac{\partial \dot{x}_{17}}{\partial x_{63}} dx_{63} + \frac{\partial \dot{x}_{17}}{\partial x_{12}} dx_{12} + \frac{\partial \dot{x}_{17}}{\partial \psi} d\dot{\psi} + \frac{\partial \dot{x}_{17}}{\partial \phi} d\dot{\phi} \quad (A3-52)$$

$$d\dot{x}_{18} = \frac{\partial \dot{x}_{18}}{\partial x_{19}} dx_{19} \quad (A3-53)$$

$$\begin{aligned}
d\dot{x}_{19} = & \frac{\partial \dot{x}_{19}}{\partial x_3} dx_3 + \frac{\partial \dot{x}_{19}}{\partial x_8} dx_8 + \frac{\partial \dot{x}_{19}}{\partial \phi} d\phi + \frac{\partial \dot{x}_{19}}{\partial x_{13}} dx_{13} + \frac{\partial \dot{x}_{19}}{\partial x_{14}} dx_{14} + \\
& \frac{\partial \dot{x}_{19}}{\partial x_{15}} dx_{15} + \frac{\partial \dot{x}_{19}}{\partial \dot{V}} d\dot{V} + \frac{\partial \dot{x}_{19}}{\partial x_{16}} dx_{16} + \frac{\partial \dot{x}_{19}}{\partial x_{17}} dx_{17} + \frac{\partial \dot{x}_{19}}{\partial \psi} d\psi + \\
& \frac{\partial \dot{x}_{19}}{\partial x_{12}} dx_{12} + \frac{\partial \dot{x}_{19}}{\partial x_{19}} dx_{19} + \frac{\partial \dot{x}_{19}}{\partial x_{18}} dx_{18} + \frac{\partial \dot{x}_{19}}{\partial RPF} d RPF + W_6 + \\
& W_7 + \frac{\partial \dot{x}_{19}}{\partial x_{58}} dx_{58} + \frac{\partial \dot{x}_{19}}{\partial x_{54}} dx_{54} + \frac{\partial \dot{x}_{19}}{\partial x_{63}} dx_{63} + \frac{\partial \dot{x}_{19}}{\partial x_{60}} dx_{60} + \\
& \frac{\partial \dot{x}_{19}}{\partial x_{62}} dx_{62} + \frac{\partial \dot{x}_{19}}{\partial x_{55}} dx_{55}
\end{aligned} \tag{A3-54}$$

$$d\dot{x}_{20} = \frac{\partial \dot{x}_{20}}{\partial x_{21}} dx_{21} \tag{A3-55}$$

$$d\dot{x}_{21} = \frac{\partial \dot{x}_{21}}{\partial x_{22}} dx_{22} \tag{A3-56}$$

$$\begin{aligned}
d\dot{x}_{22} = & \frac{\partial \dot{x}_{22}}{\partial x_2} dx_2 + \frac{\partial \dot{x}_{22}}{\partial x_3} dx_3 + \frac{\partial \dot{x}_{22}}{\partial x_1} dx_1 + \frac{\partial \dot{x}_{22}}{\partial x_4} dx_4 + \frac{\partial \dot{x}_{22}}{\partial x_5} dx_5 + \\
& \frac{\partial \dot{x}_{22}}{\partial x_7} dx_7 + \frac{\partial \dot{x}_{22}}{\partial \phi} d\phi + \frac{\partial \dot{x}_{22}}{\partial x_6} dx_6 + \frac{\partial \dot{x}_{22}}{\partial \theta} d\theta + \frac{\partial \dot{x}_{22}}{\partial x_8} dx_8 +
\end{aligned}$$

$$\begin{aligned} & \frac{\partial \dot{x}_{22}}{\partial x_{13}} dx_{13} + \frac{\partial \dot{x}_{22}}{\partial x_{14}} dx_{14} + \frac{\partial \dot{x}_{22}}{\partial x_{15}} dx_{15} + \frac{\partial \dot{x}_{22}}{\partial x_{22}} dx_{22} + \frac{\partial \dot{x}_{22}}{\partial x_{21}} dx_{21} + \\ & \frac{\partial \dot{x}_{22}}{\partial x_{20}} dx_{20} + \frac{\partial \dot{x}_{22}}{\partial x_{53}} dx_{53} + \frac{\partial \dot{x}_{22}}{\partial x_{64}} dx_{64} + \frac{\partial \dot{x}_{22}}{\partial x_{54}} dx_{54} + \frac{\partial \dot{x}_{22}}{\partial x_{63}} dx_{63} \end{aligned} \quad (A3-57)$$

$$d\dot{x}_{23} = \frac{\partial \dot{x}_{23}}{\partial x_{24}} dx_{24} \quad (A3-58)$$

$$d\dot{x}_{24} = \frac{\partial \dot{x}_{24}}{\partial x_{25}} dx_{25} \quad (A3-59)$$

$$\begin{aligned} d\dot{x}_{25} = & \frac{\partial \dot{x}_{25}}{\partial x_2} dx_2 + \frac{\partial \dot{x}_{25}}{\partial x_3} dx_3 + \frac{\partial \dot{x}_{25}}{\partial x_4} dx_4 + \frac{\partial \dot{x}_{25}}{\partial x_1} dx_1 + \frac{\partial \dot{x}_{25}}{\partial \theta} d\theta + \\ & \frac{\partial \dot{x}_{25}}{\partial x_6} dx_6 + \frac{\partial \dot{x}_{25}}{\partial x_3} dx_3 + \frac{\partial \dot{x}_{25}}{\partial x_5} dx_5 + \frac{\partial \dot{x}_{25}}{\partial x_7} dx_7 + \frac{\partial \dot{x}_{25}}{\partial x_{13}} dx_{13} + \\ & \frac{\partial \dot{x}_{25}}{\partial x_{14}} dx_{14} + \frac{\partial \dot{x}_{25}}{\partial x_8} dx_8 + \frac{\partial \dot{x}_{25}}{\partial x_{15}} dx_{15} + \frac{\partial \dot{x}_{25}}{\partial \phi} d\phi + \frac{\partial \dot{x}_{25}}{\partial x_{23}} dx_{23} + \\ & \frac{\partial \dot{x}_{25}}{\partial x_{24}} dx_{24} + \frac{\partial \dot{x}_{25}}{\partial x_{25}} dx_{25} + \frac{\partial \dot{x}_{25}}{\partial x_{53}} dx_{53} + \frac{\partial \dot{x}_{25}}{\partial x_{64}} dx_{64} + \frac{\partial \dot{x}_{25}}{\partial x_{63}} dx_{63} + \\ & \frac{\partial \dot{x}_{25}}{\partial x_{54}} dx_{54} \end{aligned} \quad (A3-60)$$

$$d\dot{x}_{26} = \frac{\partial \dot{x}_{26}}{\partial x_{27}} dx_{27} \quad (A3-61)$$

$$d\dot{x}_{27} = \frac{\partial \dot{x}_{27}}{\partial x_{28}} dx_{28} \quad (A3-62)$$

$$d\dot{x}_{28} = \frac{\partial \dot{x}_{28}}{\partial x_{28}} dx_{28} + \frac{\partial \dot{x}_{28}}{\partial x_{27}} dx_{27} + \frac{\partial \dot{x}_{28}}{\partial x_{26}} dx_{26} + \frac{\partial \dot{x}_{28}}{\partial x_8} dx_8 + \frac{\partial \dot{x}_{28}}{\partial x_{13}} dx_{13} + \\ \frac{\partial \dot{x}_{28}}{\partial x_{14}} dx_{14} + \frac{\partial \dot{x}_{28}}{\partial x_{15}} dx_{15} + \frac{\partial \dot{x}_{28}}{\partial \phi} d\phi + \frac{\partial \dot{x}_{28}}{\partial x_{54}} dx_{54} + \frac{\partial \dot{x}_{28}}{\partial x_{63}} dx_{63} \quad (A3-63)$$

$$d\dot{x}_{29} = \frac{\partial \dot{x}_{29}}{\partial x_{30}} dx_{30} \quad (A3-64)$$

$$d\dot{x}_{30} = \frac{\partial \dot{x}_{30}}{\partial x_{31}} dx_{31} \quad (A3-65)$$

$$d\dot{x}_{31} = \frac{\partial \dot{x}_{31}}{\partial x_{31}} dx_{31} + \frac{\partial \dot{x}_{31}}{\partial x_{30}} dx_{30} + \frac{\partial \dot{x}_{31}}{\partial x_{29}} dx_{29} + \frac{\partial \dot{x}_{31}}{\partial x_8} dx_8 + \frac{\partial \dot{x}_{31}}{\partial \phi} d\phi + \\ \frac{\partial \dot{x}_{31}}{\partial x_{13}} dx_{13} + \frac{\partial \dot{x}_{31}}{\partial x_{14}} dx_{14} + \frac{\partial \dot{x}_{31}}{\partial x_{15}} dx_{15} \quad (A3-66)$$

$$d\dot{x}_{32} = \frac{\partial \dot{x}_{32}}{\partial x_{33}} dx_{33} \quad (A3-67)$$

$$d\dot{x}_{33} = \frac{\partial \dot{x}_{33}}{\partial x_{34}} dx_{34} \quad (A3-68)$$

$$\begin{aligned} d\dot{x}_{34} = & \frac{\partial \dot{x}_{34}}{\partial x_{34}} dx_{34} + \frac{\partial \dot{x}_{34}}{\partial x_{33}} dx_{33} + \frac{\partial \dot{x}_{34}}{\partial x_{32}} dx_{32} + \frac{\partial \dot{x}_{34}}{\partial x_{19}} dx_{19} + \frac{\partial \dot{x}_{34}}{\partial x_8} dx_8 + \\ & \frac{\partial \dot{x}_{34}}{\partial x_8} dx_8 + \frac{\partial \dot{x}_{34}}{\partial \phi} d\phi + \frac{\partial \dot{x}_{34}}{\partial x_{13}} dx_{13} + \frac{\partial \dot{x}_{34}}{\partial x_{14}} dx_{14} + \frac{\partial \dot{x}_{34}}{\partial x_{15}} dx_{15} + \\ & \frac{\partial \dot{x}_{34}}{\partial x_3} dx_3 + \frac{\partial \dot{x}_{34}}{\partial RPF} dRPF + \frac{\partial \dot{x}_{34}}{\partial \dot{V}} d\dot{V} + \frac{\partial \dot{x}_{34}}{\partial \dot{\psi}} d\dot{\psi} + \frac{\partial \dot{x}_{34}}{\partial x_{12}} dx_{12} + \\ & \frac{\partial \dot{x}_{34}}{\partial x_{16}} dx_{16} + \frac{\partial \dot{x}_{34}}{\partial x_{17}} dx_{17} + W_6 + W_7 + \frac{\partial \dot{x}_{34}}{\partial x_{58}} dx_{58} + \\ & \frac{\partial \dot{x}_{34}}{\partial x_{54}} dx_{54} + \frac{\partial \dot{x}_{34}}{\partial x_{63}} dx_{63} + \frac{\partial \dot{x}_{34}}{\partial x_{62}} dx_{62} + \frac{\partial \dot{x}_{34}}{\partial x_{55}} dx_{55} + \frac{\partial \dot{x}_{34}}{\partial x_{60}} dx_{60} \end{aligned} \quad (A3-69)$$

$$d\dot{x}_{47} = \frac{\partial \dot{x}_{47}}{\partial x_{47}} dx_{47} + \frac{\partial \dot{x}_{47}}{\partial \theta} d\theta \quad (A3-70)$$

$$d\dot{x}_{48} = \frac{\partial \dot{x}_{48}}{\partial x_{48}} dx_{48} + \frac{\partial \dot{x}_{48}}{\partial \alpha} d\alpha \quad (A3-71)$$

$$d\dot{x}_{49} = \frac{\partial \dot{x}_{49}}{\partial x_{49}} dx_{49} + \frac{\partial \dot{x}_{49}}{\partial x_{50}} dx_{50} + \frac{\partial \dot{x}_{49}}{\partial x_{47}} dx_{47} + \frac{\partial \dot{x}_{49}}{\partial x_{48}} dx_{48} + \frac{\partial \dot{x}_{49}}{\partial \theta} d\theta \quad (A3-72)$$

$$d\dot{x}_{50} = \frac{\partial \dot{x}_{50}}{\partial x_{49}} dx_{49} \quad (A3-73)$$

$$d\dot{x}_{51} = \frac{\partial \dot{x}_{51}}{\partial x_{50}} dx_{50} + \frac{\partial \dot{x}_{51}}{\partial x_{51}} dx_{51} \quad (A3-74)$$

$$d\dot{x}_{52} = \frac{\partial \dot{x}_{52}}{\partial x_{52}} dx_{52} + \frac{\partial \dot{x}_{52}}{\partial TP} dTP \quad (A3-75)$$

$$d\dot{x}_{53} = \frac{\partial \dot{x}_{53}}{\partial RC} dRC \quad (A3-76)$$

$$d\dot{x}_{54} = \frac{\partial \dot{x}_{54}}{\partial RPC} dRPC \quad (A3-77)$$

$$d\dot{x}_{55} = \frac{\partial \dot{x}_{55}}{\partial x_{55}} dx_{55} + W_1 \quad (A3-78)$$

$$d\dot{x}_{56} = \frac{\partial \dot{x}_{56}}{\partial x_{56}} dx_{56} + W_2 \quad (A3-79)$$

$$d\dot{x}_{57} = \frac{\partial \dot{x}_{57}}{\partial x_{57}} dx_{57} + W_3 \quad (A3-80)$$

$$d\dot{x}_{58} = \frac{\partial \dot{x}_{58}}{\partial x_{58}} dx_{58} + W_4 \quad (A3-81)$$

$$d\dot{x}_{59} = \frac{\partial \dot{x}_{59}}{\partial x_{59}} dx_{59} + W_5 \quad (A3-82)$$

$$\dot{\bar{x}}_{60} = 0 \quad (A3-83)$$

$$\dot{\bar{x}}_{61} = 0 \quad (A3-84)$$

$$\dot{\bar{x}}_{62} = 0 \quad (A3-85)$$

$$\dot{\bar{x}}_{63} = 0 \quad (A3-86)$$

$$\dot{\bar{x}}_{64} = 0 \quad (A3-87)$$

The above equations describe the linearized aircraft equations. The system is now in the state variable form

$$\dot{\bar{x}} = A(t) \bar{x} + B(t) \bar{u}(t) + G(t) \bar{w}(t).$$

The problem is now adequately detailed to attack the quadratic cost-deterministic optimal control portion of the stochastic control problem. This controller design is addressed in Chapter II, as is the observation equation and the estimation equation development required in the overall LQG controller structure.

APPENDIX IV

Example: P_1 Matrix Not Diagonal

$$\dot{\bar{x}} = \begin{bmatrix} 1 & 0 & 1 & 0 \\ 0 & 1 & 0 & 1 \\ 0 & 0 & 0 & 0 \\ 0 & 0 & 0 & 0 \end{bmatrix} \bar{x} + \begin{bmatrix} 0 \\ 0 \\ 1 \\ 0 \end{bmatrix} \bar{u} + \begin{bmatrix} 0 \\ 0 \\ 0 \\ 1 \end{bmatrix} \bar{w}$$

This system representation can easily arise in the type of problem considered because of the practice of assuming the control weighting on rate of control. The other zero state can be considered a representation of error on state two.

Now consider

$$\dot{P} = PB R_2^{-1} B^T P - PA - A^T P - R_1$$

with initial conditions

$$R_2^{-1} = 1$$

$$R_1 = \begin{bmatrix} 0 & 0 & 0 & 0 \\ 0 & 0 & 0 & 0 \\ 0 & 0 & 0 & 0 \\ 0 & 0 & 0 & \frac{1}{2} \end{bmatrix}$$

$$P = \begin{bmatrix} 0 & 0 & 0 & 0 \\ 0 & 0 & 0 & 0 \\ 0 & 0 & 0 & 1 \\ 0 & 0 & 1 & 1 \end{bmatrix}$$

Again, this is a possible representation of initial conditions. It is different from the research problem in that the initial

condition matrices are not diagonal. The matrices do display the requirements necessary to apply the Riccati equation (Ref 35).

Now

$$\dot{P} = \begin{bmatrix} 0 & 0 & 0 & 0 \\ 0 & 0 & 0 & 0 \\ 0 & 0 & 0 & 0 \\ 0 & 0 & 0 & 1 \end{bmatrix} - \begin{bmatrix} 0 & 0 & 0 & 0 \\ 0 & 0 & 0 & 0 \\ 0 & 0 & 0 & 0 \\ 0 & 0 & 0 & 0 \end{bmatrix} - \begin{bmatrix} 0 & 0 & 0 & 0 \\ 0 & 0 & 0 & 0 \\ 0 & 0 & 0 & 0 \\ 0 & 0 & 0 & 0 \end{bmatrix} -$$

$$\begin{bmatrix} 0 & 0 & 0 & 0 \\ 0 & 0 & 0 & 0 \\ 0 & 0 & 0 & 0 \\ 0 & 0 & 0 & \frac{1}{2} \end{bmatrix} = \begin{bmatrix} 0 & 0 & 0 & 0 \\ 0 & 0 & 0 & 0 \\ 0 & 0 & 0 & 0 \\ 0 & 0 & 0 & \frac{1}{2} \end{bmatrix}$$

Consider now the computation for the control gains.

$$F = R_2^{-1} B^T P$$

$$= \begin{bmatrix} 0 & 0 & 1 & 0 \end{bmatrix} \begin{bmatrix} 0 & 0 & 0 & 0 \\ 0 & 0 & 0 & 0 \\ 0 & 0 & 0 & 1 \\ 0 & 0 & 1 & x \end{bmatrix}$$

Since the derivative of the \dot{P} (3,4) term is zero, there will be no change in it and the term displayed in that position will be in this case the complete determinate of control for the problem. Therefore the control is completely dependent on the initial condition of the P_0 matrix. Care must be taken in the selection of the P matrix when zero rows and columns of the $A(t)$ matrix occur. Ensuring that the diagonal elements of P_0 are filled determines that there will be values for \dot{P} in the positions of the \dot{P} matrix where P_0 is filled. This would ensure that the problem mentioned above is not encountered.

APPENDIX 5

LONGITUDINAL AXIS SIMULATION RESULTS

5.1 The listed figures reflect the simulation results obtained for the reduced order simulation. Also included is the system block diagram for the longitudinal axis simulation. Those results are organized into two groups. Figures 55-60 reflect the results of the 10 run Monte Carlo analysis described in Chapter VI; 61 reflects the channel which draws the control emphasis for the 3 second run explained in Chapter VI and Figures 62-67 display the results of those emphases on the respective states. A more comprehensive list is given below:

Figure 55	Longitudinal Axis System Block Diagram	
Figure 56	Pitch Angle	(Radians)
Figure 57	Pitch Angle Rate	(Radians/sec)
Figure 58	X Axis Velocity	(Ft/sec)
Figure 59	Axis Velocity	(Ft/sec)
Figure 60	Longitudinal Stick	LB_F
Figure 61	Thrust	LB_F
Figure 62	Channel Emphasized for Observation and Control	
Figure 63	Pitch Angle	Radians
Figure 64	Pitch Angle Rate	Radians/sec
Figure 65	X Axis Velocity	Ft/sec
Figure 66	Axis Velocity	Ft/sec
Figure 67	Longitudinal Stick	LB_F
Figure 68	Thrust	LB_F

Figure 55

LONGITUDINAL AXIS SYSTEM BLOCK DIAGRAM

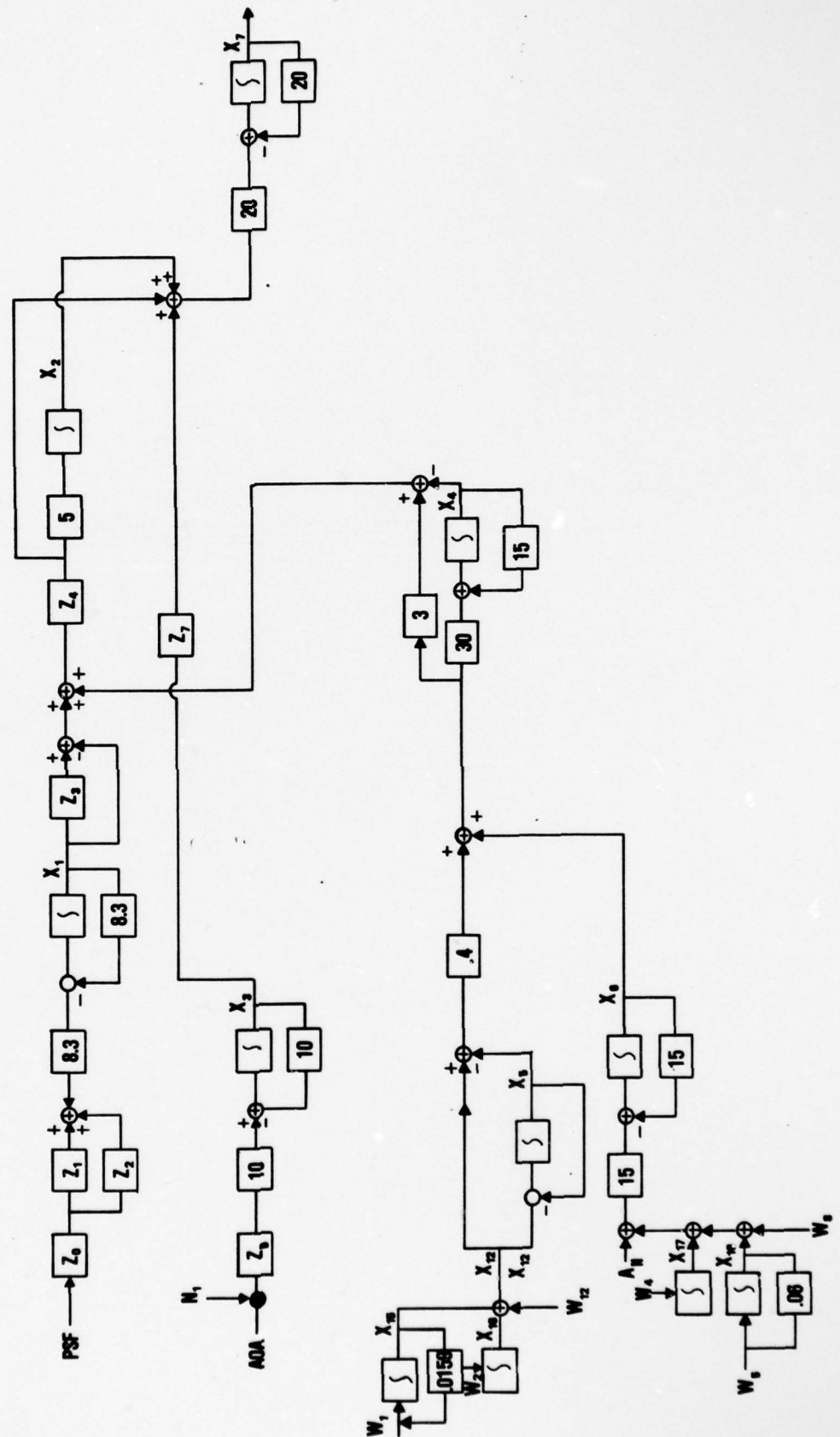


Figure 56

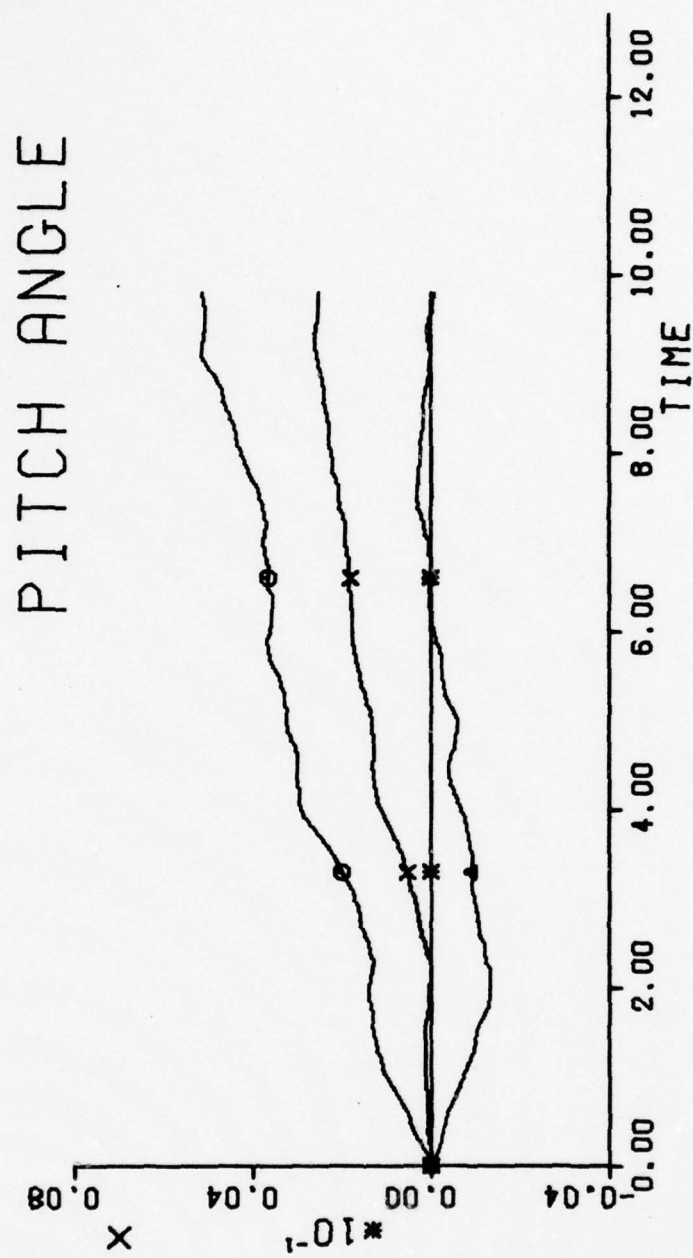


Figure 57

PITCH ANGLE RATE

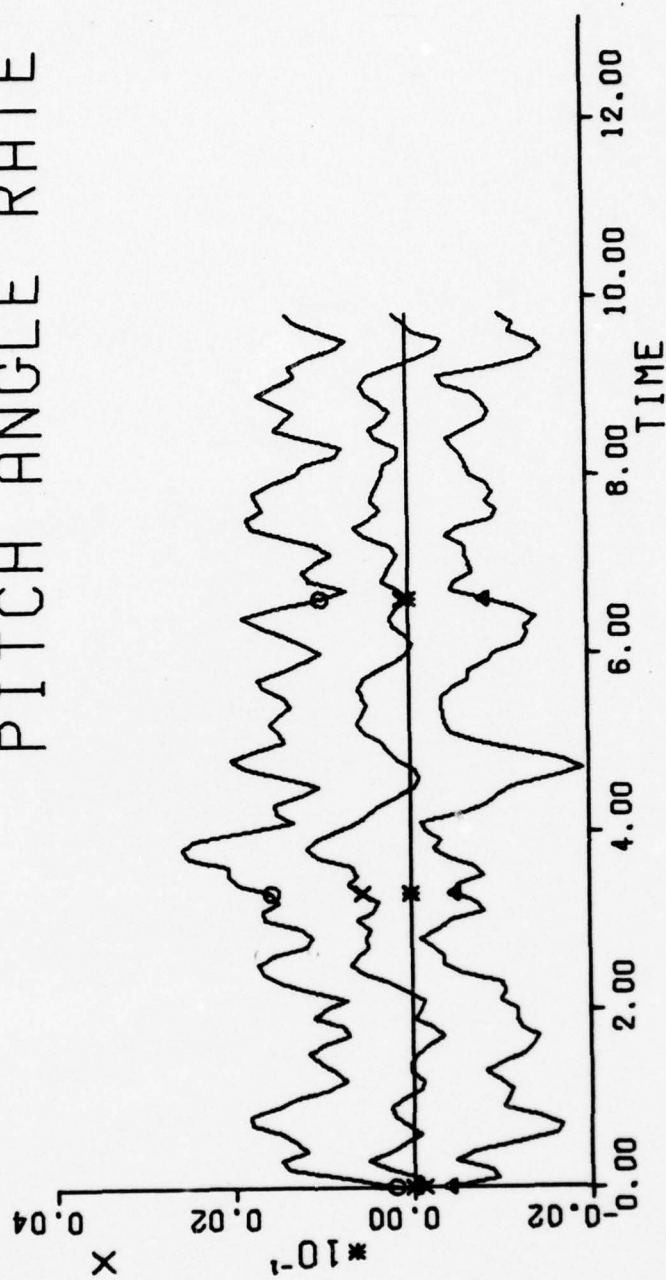


Figure 58

X AXIS VELOCITY

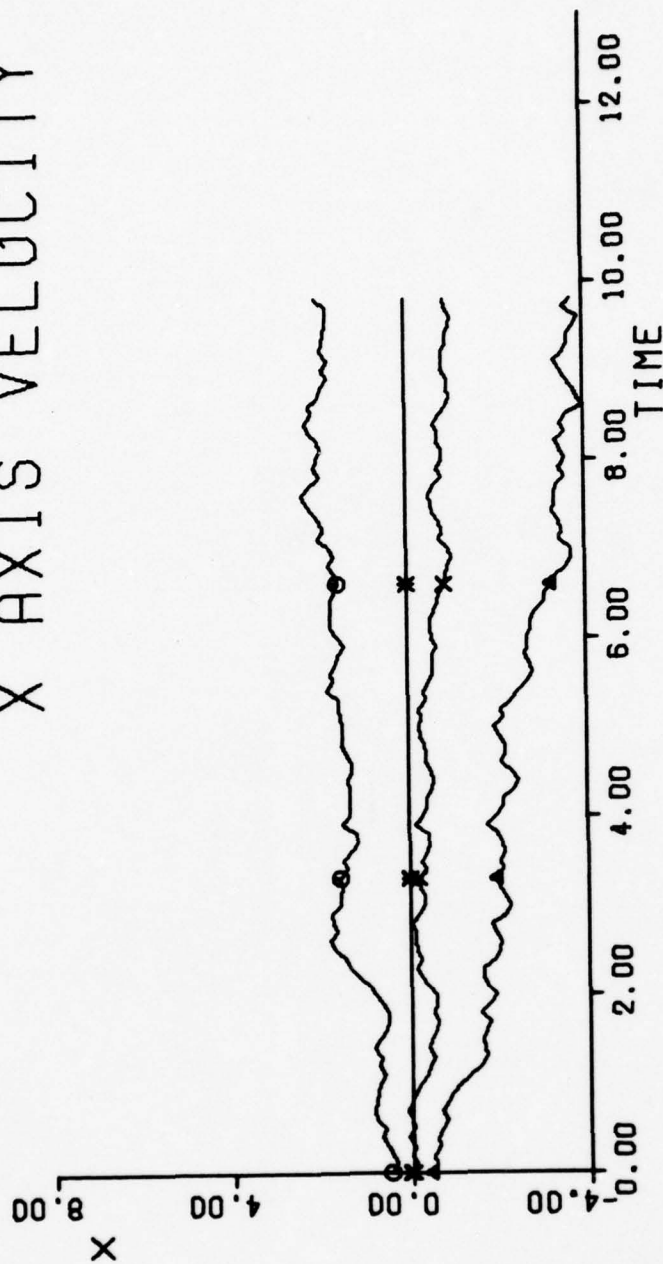


Figure 59

Y AXIS VELOCITY

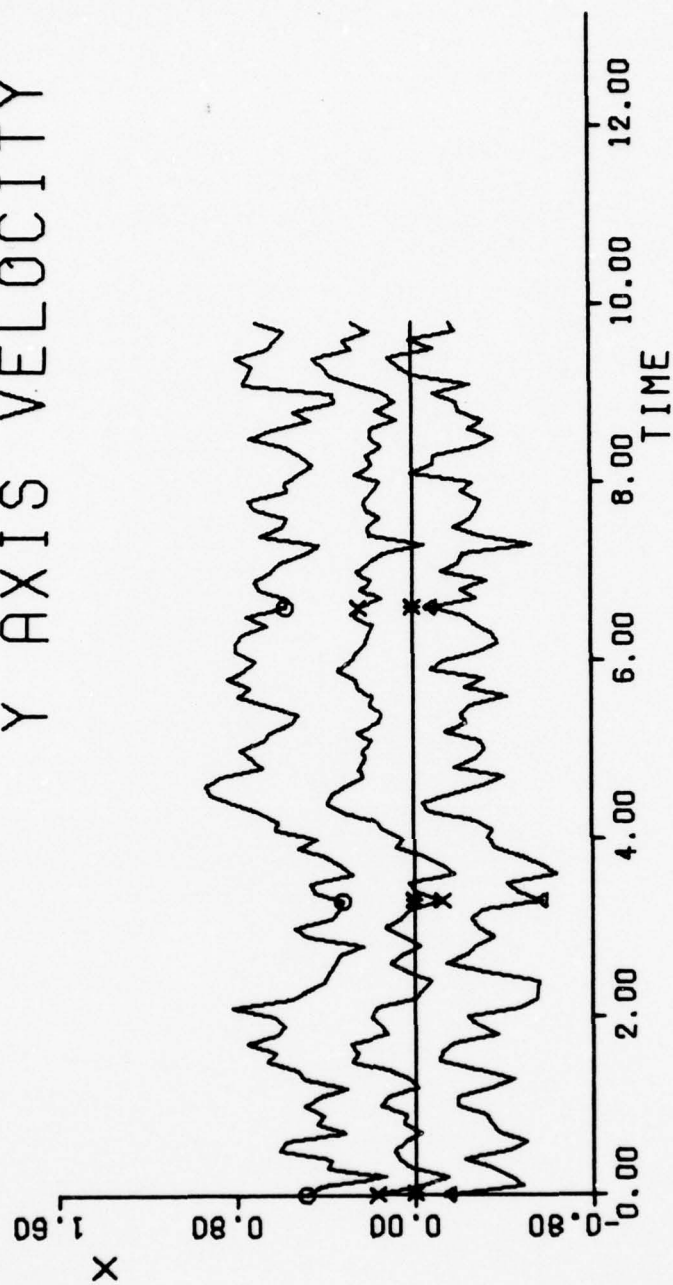


Figure 60

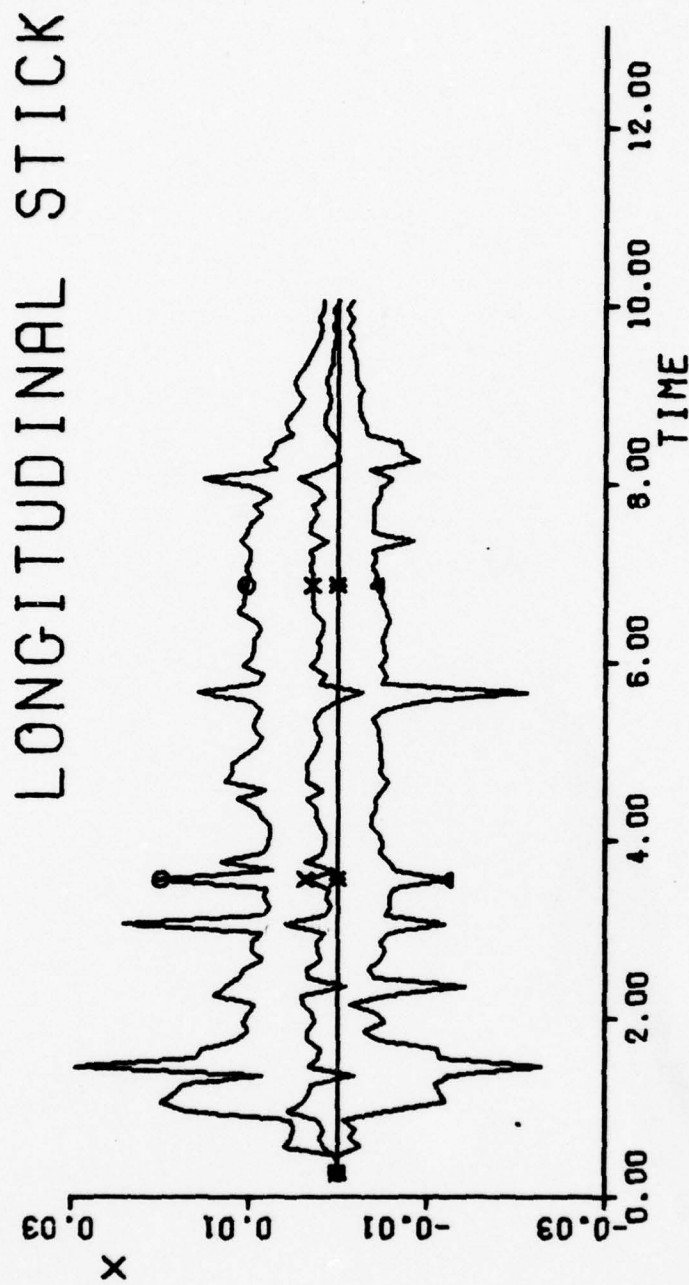


Figure 61

THRUST

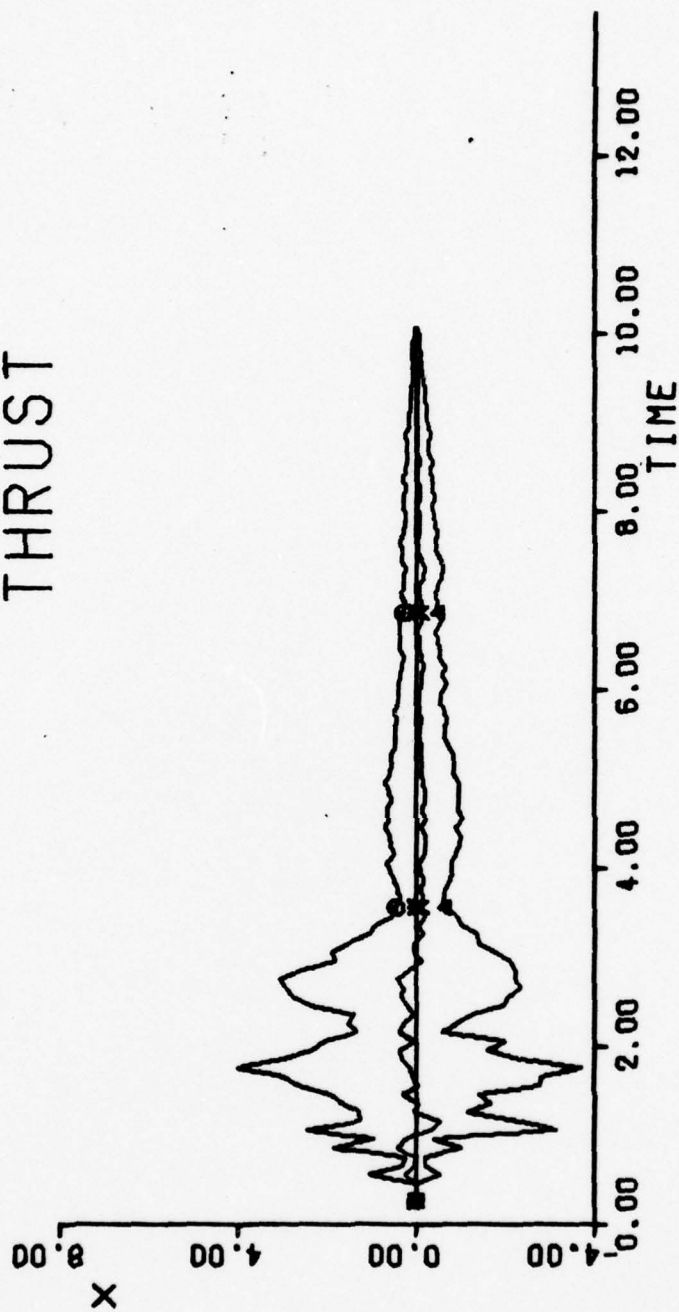


Figure 62
Applied Decision Channel

PITCH

AIRSPEED

1 SEC 2 SEC 3 SEC

Figure 63

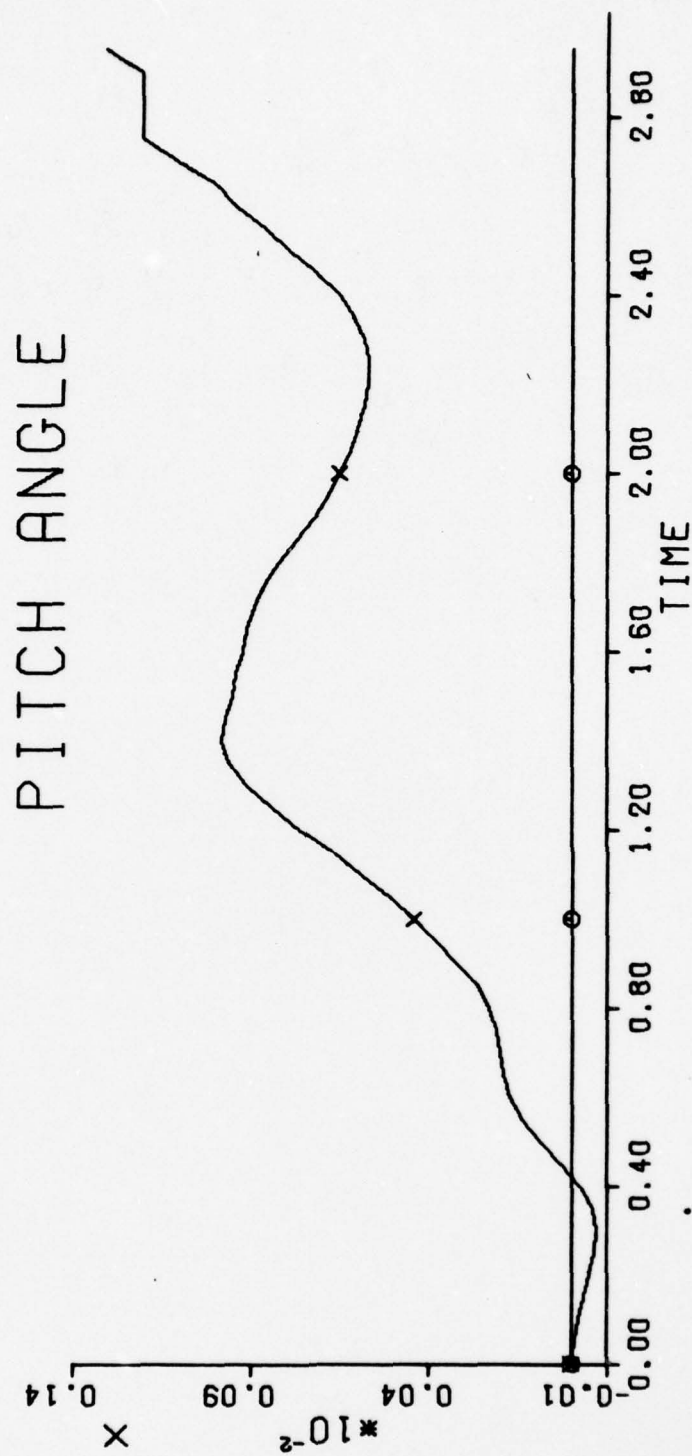


Figure 64

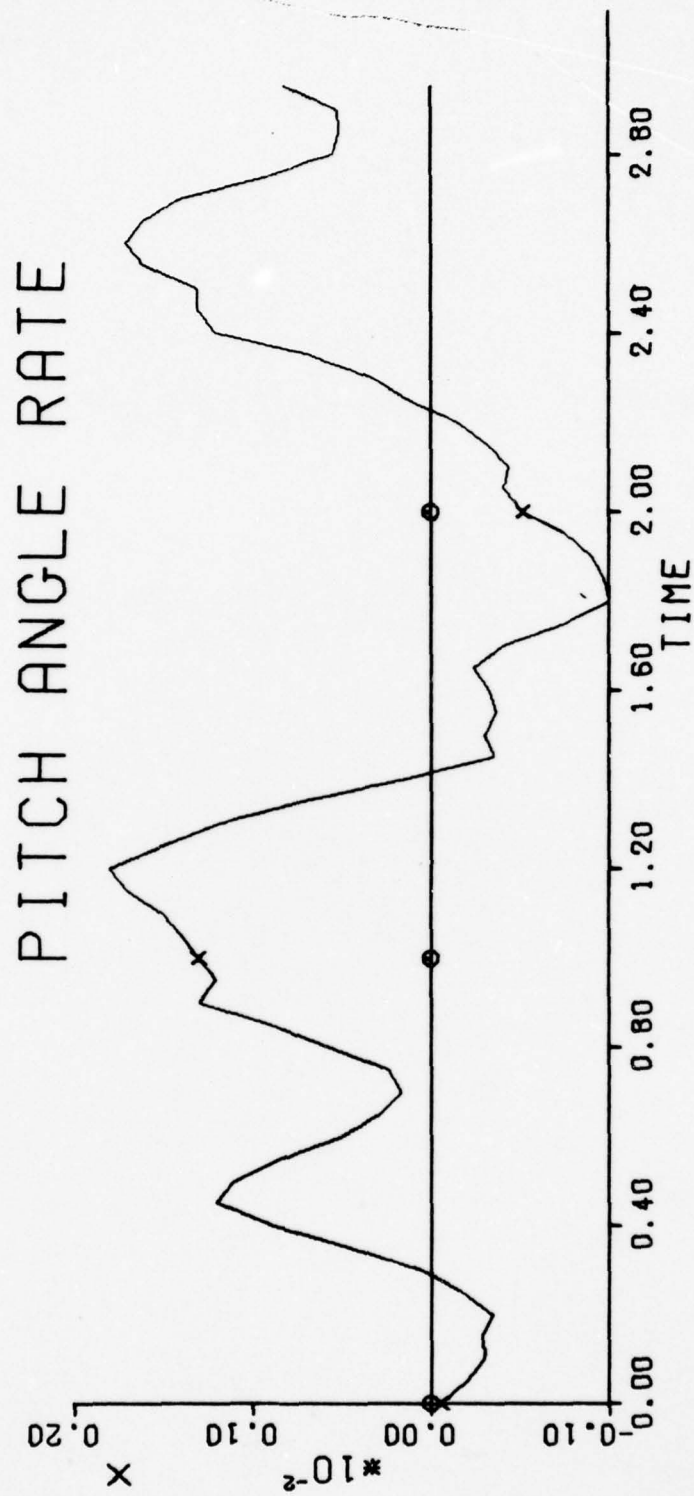


Figure 65

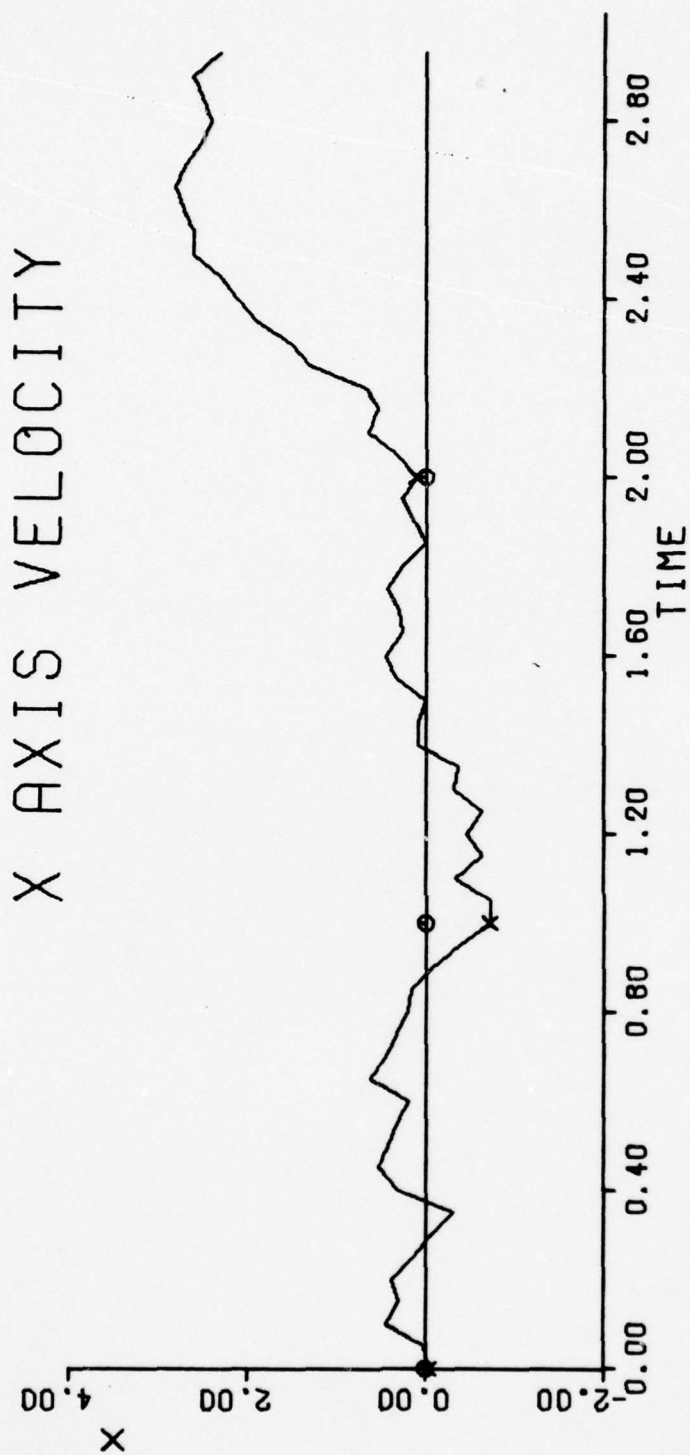


Figure 66

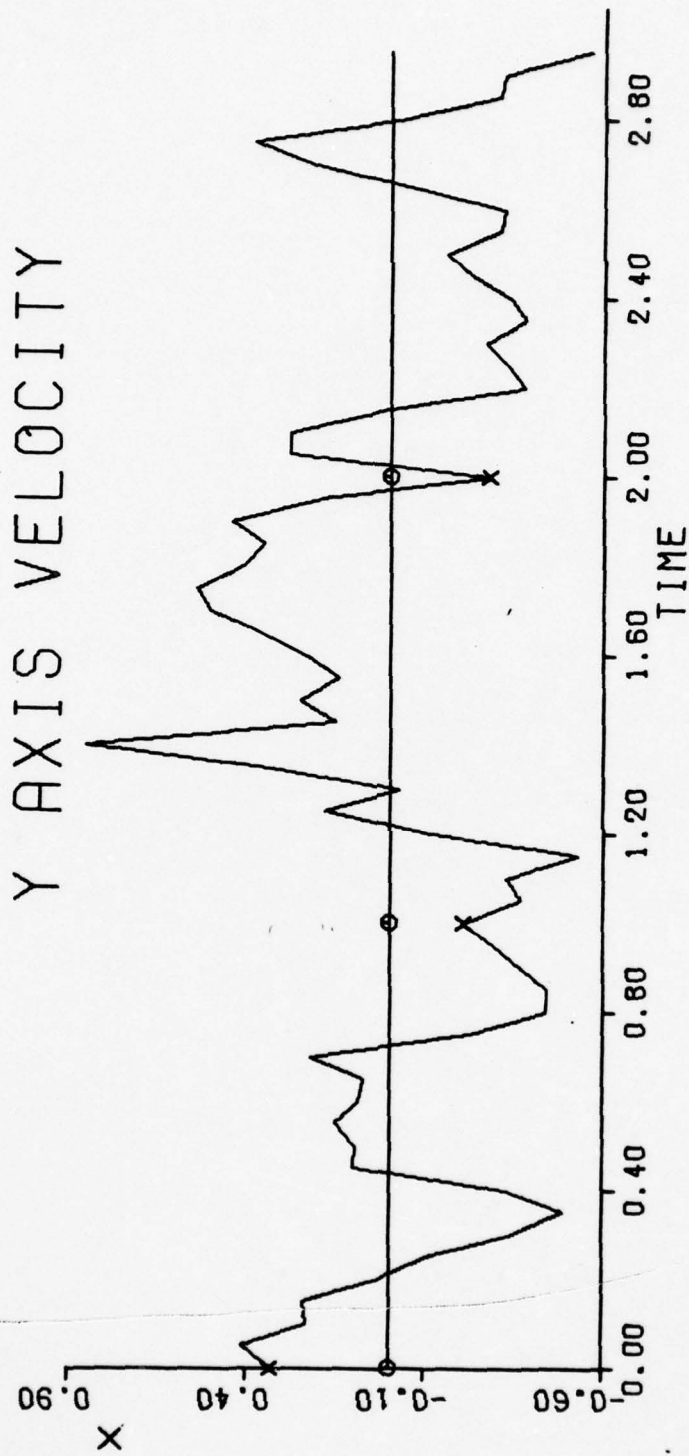


Figure 67

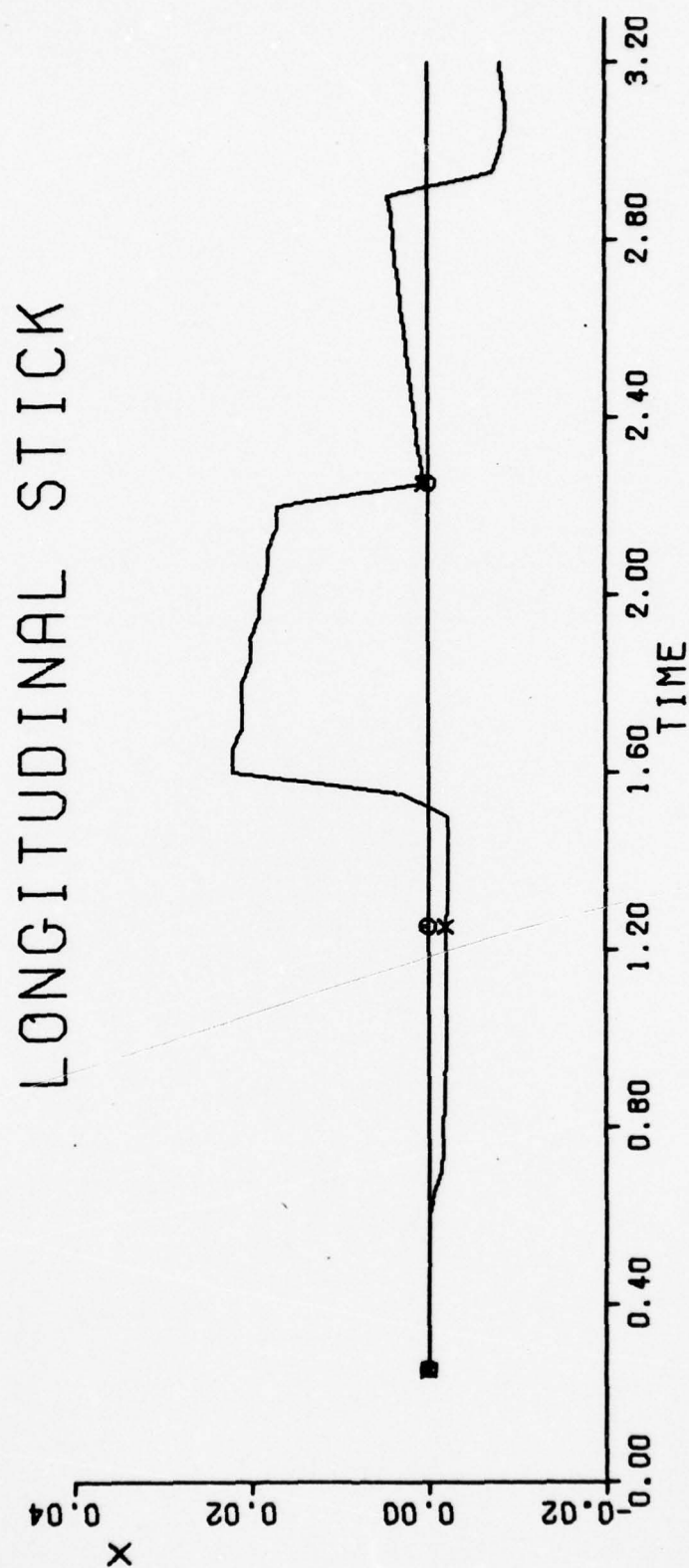
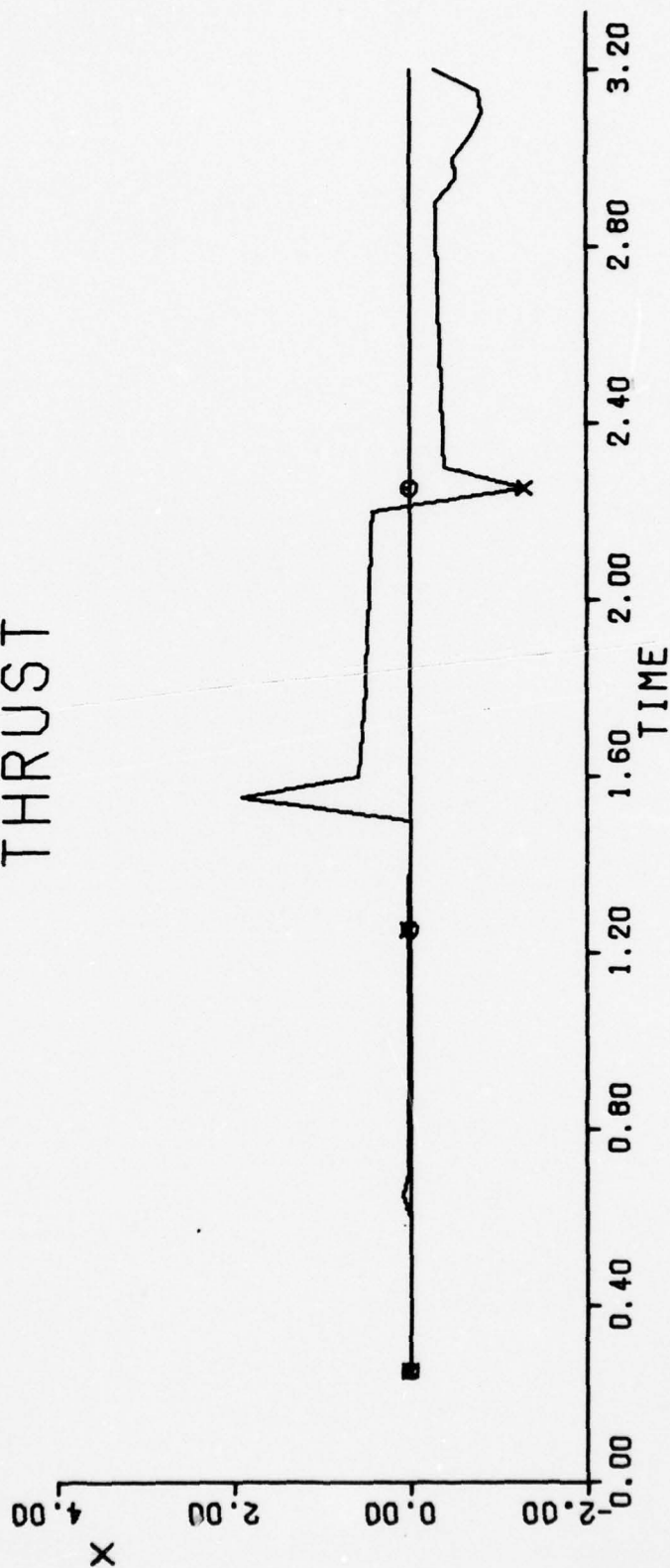


Figure 68

THRUST



APPENDIX 6

PARAMETER SPECIFICATION

This appendix is devoted to the delineation of the values used in the different phases of the simulation. It is broken into two subsections, each addressing one of the simulations. Each subsection is further broken into the major aspects of the simulation: aircraft model, controller, Kalman filter-predictor, and decision process. The values contained in this section are included to provide insights to and starting points for using this method on this and other problems.

A6.1 TOTAL AIRCRAFT SIMULATION

To provide a basis for the parameters, first the state vector used in the simulation is defined. For that definition, states number 1 - 34 and 48 through 51 are defined on Figure 5. States 35 - 47 are defined by previously cited equations and represent the following quantities:

- 35 - P
- 36 - Q
- 37 - R
- 38 - ϕ
- 39 - θ
- 40 - ψ
- 41 - U
- 42 - V

AD-A066 193

AIR FORCE INST OF TECH WRIGHT-PATTERSON AFB OHIO SCH--ETC F/G 1/3
AN ADAPTIVE CONTROLLER WHICH DISPLAYS HUMAN OPERATOR LIMITATION--ETC(U)
NOV 78 E K LINDBERG
AFIT/DS/EE/78-1

UNCLASSIFIED

NL

4 OF 4

AD
A066 193



END
DATE
FILMED

5-79

DDC



NATIONAL BUREAU OF STANDARDS-1963-2

43 - W

44 - S_x

45 - S_y

46 - S_z

State 52 is thrust and is modeled as a first order lag with a time constant of one second. States 53 through 61 are noise states. The first of these states 53 - 55 are defined as the X2 state in Figure 6. Because the rate gyros for each axis of this aircraft were the same, these three states have the same model. However, because three separate instruments are used, each state has its separate model which gives different realizations of the noise. The parameters used for these models as per Figure 6 are $\alpha_N = .0159$ and the noise N_2 is white Gaussian with

$$E(N_2) = 0$$

$$E(N_2(t)N_2(t+\tau)) = .0006 \delta(\tau)$$

The next states 58, 60, and 61 are defined as state X1 of Figure 6 and as before three separate states are necessary because of the three individual instruments involved in the model. The statistics of the white Gaussian input noise N_1 which completes definition of Figure 6 are

$$E(N_1(t)) = 0$$

$$E(N_1(t)N_1(t+\tau)) = .001 \delta(\tau)$$

The next to consider, the accelerometer noise states, states 56

and 57, are defined as per Figure 7 with $\beta_N = .06$. N_4 is white Gaussian with

$$E(N_4(t)) = 0$$

$$E(N_4(t)N_4(t+\tau)) = .01 \delta(\tau)$$

The N_5 of Figure 7 is white and Gaussian with

$$E(N_5(t)) = 0$$

$$E(N_5(t)N_5(t+\tau)) = .001 \delta(\tau)$$

State 59 and 62 are state X_4 of Figure 7 with N_3 white and Gaussian, with statistics

$$E(N_3(t)) = 0$$

$$E(N_3(t)N_3(t+\tau)) = .01 \delta(\tau)$$

Because these states are tied to the instrument, and not to the orientation of the instrument, the states have thus far been defined independent of the control model of Figure 5. For completeness, however, the state orientations are now defined

Pitch Rate Gyro	53 - 58
Roll Rate Gyro	54 - 60
Yaw Rate Gyro	55 - 61
Normal Acceleration	57 - 59
Lateral Acceleration	56 - 62

The last items necessary are the magnitudes of the noises assumed as remnant or operator noise on each control. These are all white Gaussian noises with the respective assumed statistics:

Pitch (fore-aft stick)

$$E(W_{11}(t)) = 0$$

$$E(W_{11}(t)W_{11}(t+\tau)) = .005 \delta(\tau)$$

Roll (left-right stick)

$$E(W_{13}) = 0$$

$$E(W_{13}(t)W_{13}(t+\tau)) = .005 \delta(\tau)$$

Yaw (rudders)

$$E(W_6(t)) = 0$$

$$E(W_6(t)W_6(t+\tau)) = .0000005 \delta(\tau)$$

or the rudder remnant was basically considered zero.

With these specifications, the model is complete and only the initial conditions and controls are necessary to specify the particular trajectory used in this problem. For that specification, all initial conditions were assumed zero except the following which are noted below.

2	=	-2.455
3	=	1.2
20	=	-2.74
23	=	-2.74
39	=	.02095
41	=	945
43	=	19.79775
52	=	5699

These states were found to provide straight, level, and unaccelerated flight when the simulation was initiated. The controls which provided the climbing turn used for the simulation of Chapter 5 were:

Pitch Control - 9.0 lbs

Roll Control - 3.0 lbs

The next aspect to consider is the controller.

For this specification three matrices are necessary:

P_1 , R_2 , and R_1 . Since all matrices are assumed diagonal as discussed in Chapter III, only the diagonal elements will be specified.

Those matrices are

P_1 Matrix

$P_1(1) = .2$	$P_1(13) = .01$	$P_1(25) = .002$	$P_1(37) = .01$
$P_1(2) = .2$	$P_1(14) = .01$	$P_1(26) = .2$	$P_1(38) = .01$
$P_1(3) = .2$	$P_1(15) = .01$	$P_1(27) = .02$	$P_1(39) = .01$
$P_1(4) = .2$	$P_1(16) = .01$	$P_1(28) = .002$	$P_1(40) = .01$
$P_1(5) = .2$	$P_1(17) = .10$	$P_1(29) = .2$	$P_1(41) = 10$
$P_1(6) = .2$	$P_1(18) = .0000001$	$P_1(30) = .02$	$P_1(42) = 10$
$P_1(7) = .2$	$P_1(19) = .0001$	$P_1(31) = .002$	$P_1(43) = 10$
$P_1(8) = .5$	$P_1(20) = .2$	$P_1(32) = .2$	$P_1(44) = 100$
$P_1(9) = .5$	$P_1(21) = .02$	$P_1(33) = .02$	$P_1(45) = 100$
$P_1(10) = .5$	$P_1(22) = .002$	$P_1(34) = .002$	$P_1(46) = 100$
$P_1(11) = .01$	$P_1(23) = .2$	$P_1(35) = .01$	$P_1(47) = .1$
$P_1(12) = .01$	$P_1(24) = .02$	$P_1(36) = .01$	$P_1(48) = 1.$

$$P_1(49) = 1.$$

$$P_1(50) = 1.$$

$$P_1(51) = 1.$$

$$P_1(52) = 10$$

$$P_1(53) = .01$$

$$P_1(54) = .01$$

$$P_1(55) = .01$$

$$P_1(56) = .01$$

$$P_1(57) = .01$$

$$P_1(58) = .001$$

$$P_1(59) = .001$$

$$P_1(60) = .001$$

$$P_1(61) = .001$$

$$P_1(62) = .001$$

$$P_1(63) = .001$$

$$P_1(64) = .001$$

R_2 Matrix

Pitch Emphasis

$$R_1(1) = .001$$

$$R_1(2) = 1$$

$$R_1(3) = 1$$

$$R_1(4) = 4$$

Roll Emphasis

$$.0005$$

$$1$$

$$2$$

$$4$$

Thrust Emphasis

$$.001$$

$$1$$

$$2$$

$$.01$$

R_3 Matrix

$$R_3(1) = 1$$

$$R_3(2) = 1$$

$$R_3(3) = 1$$

$$R_3(4) = .001$$

$$R_3(5) = .001$$

$$R_3(6) = .001$$

$$R_3(7) = .001$$

$$R_3(8) = .001$$

$$R_3(9) = .001$$

$$R_3(10) = .001$$

This completes specification of the controller, next consider the estimator. For this task, matrices are required. These matrices are P_0 , $\bar{x}_0(t)$, $R(t)$, and $Q(t)$.

Since it was assumed that the aircraft was on the nominal trajectory at time 0, then $\bar{x}_0(t) = \bar{0}$. Again all matrices are assumed diagonal and those elements are specified below.

P_0 Matrix

$P_0(1) = .2$	$P_0(18) = .0000001$	$P_0(35) = .01$
$P_0(2) = .2$	$P_0(19) = .0001$	$P_0(36) = .01$
$P_0(3) = .2$	$P_0(20) = .001$	$P_0(37) = .01$
$P_0(4) = .2$	$P_0(21) = .001$	$P_0(38) = .01$
$P_0(5) = .2$	$P_0(22) = .01$	$P_0(39) = .01$
$P_0(6) = .2$	$P_0(23) = .001$	$P_0(40) = .01$
$P_0(7) = .2$	$P_0(24) = .001$	$P_0(41) = 10.$
$P_0(8) = .5$	$P_0(25) = .01$	$P_0(42) = 10.$
$P_0(9) = .5$	$P_0(26) = .001$	$P_0(43) = 10.$
$P_0(10) = 5.$	$P_0(27) = .001$	$P_0(44) = 100.$
$P_0(11) = .01$	$P_0(28) = .01$	$P_0(45) = 100.$
$P_0(12) = .01$	$P_0(29) = .001$	$P_0(46) = 100.$
$P_0(13) = .01$	$P_0(30) = .001$	$P_0(47) = .1$
$P_0(14) = .01$	$P_0(31) = .01$	$P_0(48) = 1.$
$P_0(15) = .01$	$P_0(32) = .001$	$P_0(49) = 1.$
$P_0(16) = .01$	$P_0(33) = .001$	$P_0(50) = 1.$
$P_0(17) = .1$	$P_0(34) = .001$	$P_0(51) = 1.$

$P_0(52) = 10.$	$P_0(57) = .01$	$P_0(61) = .001$
$P_0(53) = .01$	$P_0(58) = .001$	$P_0(62) = .001$
$P_0(54) = .01$	$P_0(59) = .001$	$P_0(63) = .001$
$P_0(55) = .01$	$P_0(60) = .001$	$P_0(64) = .001$
$P_0(56) = .01$		

The R matrix was changed with the varying observations as specified in Chapter IV. The values used when each of the channels, pitch, roll and thrust, was accentuated are given below:

	<u>Pitch</u>	<u>Roll</u>	<u>Airspeed</u>
R (1)	20.	20.	20.
R (2)	.01	.01	.01
R (3)	.05	.05	5
R (4)	.01	.01	0

The last matrix required is the Q matrix defined as below:

Q (1) = .0001	Q (9) = .25
Q (2) = .0001	Q (10) = .0001
Q (3) = .0001	Q (11) = .01
Q (4) = .0001	Q (12) = 1.
Q (5) = .0001	Q (13) = 1.
Q (6) = 2.5	Q (14) = 1.
Q (7) = .0001	Q (15) = .0025
Q (8) = .0001	Q (16) = .04

To attach meaning to these values it is necessary to reference them to the model. This will be done using Figures 5, 6 and 7.

- Q (1) \rightarrow N_2 of Figure 6 (pitch)
- Q (2) \rightarrow N_2 of Figure 6 (roll)
- Q (3) \rightarrow N_2 of Figure 6 (yaw)
- Q (4) \rightarrow N_4 of Figure 7 (lateral)
- Q (5) \rightarrow N_4 of Figure 7 (normal)
- Q (6) \rightarrow W_6 of Figure 5
- Q (7) \rightarrow N_3 of Figure 7 (lat)
- Q (8) \rightarrow N_3 of Figure 7 (norm)
- Q (9) \rightarrow W_{11} of Figure 5
- Q (10) \rightarrow N_5 of Figure 7 (norm)
- Q (11) \rightarrow W_{13} of Figure 5
- Q (12) \rightarrow Wind Gust Effect on State 41
- Q (13) \rightarrow Wind Gust Effect on State 42
- Q (14) \rightarrow Wind Gust Effect on State 43
- Q (15) \rightarrow N_5 of Figure 7 (lat)
- Q (16) \rightarrow W_{12} of Figure 5

This completes the specification of the Kalman filter-predictor. The last aspect to be considered is the decision process. To specify this process, the thresholds of Figure 11 must be identified for each channel of interest, as well as the payoff functions. Table 3 specifies the payoff function for lying outside threshold so the only payoff function needed is that for lying within threshold.

The thresholds are first considered and are identified for the three channels of concern for this problem. They are

pitch angle	.01 radians
roll angle	.01 radians
airspeed	1 ft/sec

The final specification is for the payoff for being within threshold. This process is time dependent and explained thoroughly in Chapter V. Only the sequencing to establish the values will be pursued here.

At each shift of attention, the channel shifted to receive a value of 8, the remaining channel which has not been attended for the longest period receives the value 4, the second longest period 3, the third longest period 2, and the channel just shifted from 1. At each .05 second increment 1 is added to all channels other than the one currently being attended. This specifies the decision process used, and hence the simulation for the entire aircraft portion of the problem considered. The remaining section defines the reduced order, longitudinal axis simulation used to demonstrate problem stability.

A6.2 LONGITUDINAL AXIS SIMULATION

As in the above explanation, the first aspect considered is the aircraft model. The controller, Kalman filter-predictor, and decision process will then be addressed. Also as in the above specifications, to anchor the matrices to meaningful data, the first aspect considered is the definition of the states.

For this process, Figure 54 defines States 1 through 7. Figure 6 defines states 15 and 18, 15 corresponding to X_2 and 18 corresponding to X_1 . These states specify the inaccuracy of the pitch rate gyro.

The inaccuracy of the normal accelerometer is given using states 16 and 17 where 16 corresponds to X_3 of Figure 7 and 17 corresponds to X_4 of Figure 7.

The states 8 through 13 are defined from the quantities of Chapter II as follows:

$$8 \rightarrow U$$

$$9 \rightarrow W$$

$$10 \rightarrow S_x$$

$$11 \rightarrow S_y$$

$$12 \rightarrow Q$$

$$13 \rightarrow \theta$$

State 14 represents thrust and is a first order lag with a two second time constant.

The specification of the time constants and noise statistics of the accelerometer and pitch rate gyro noise models were used as specified in A6-1. Gusts were considered to act on States 8 and 9 and those were considered white and Gaussian, with

$$E(W_1(t)) = 0$$

$$E(W_1(t)W_1(t+\tau)) = 1. \delta(\tau)$$

This then specifies the noise model of the longitudinal axis simulation other than its initial conditions. Those conditions are zero except that:

State 2 = - 2.455
 State 3 = 1.3
 State 7 = - 2.74
 State 8 = 945.
 State 9 = 19.79775
 State 13 = .02095
 State 14 = 5699

The next consideration will be the controller. For this the matrices P_1 , R_2 , and R_1 are required. These matrices are diagonal and these diagonal values are:

P_1 Matrix

$P_1(1) = .5$	$P_1(7) = 1.$	$P_1(13) = 1.$
$P_1(2) = .25$	$P_1(8) = 1.$	$P_1(14) = .1$
$P_1(3) = .25$	$P_1(9) = 1.$	$P_1(15) = .001$
$P_1(4) = .01$	$P_1(10) = .05$	$P_1(16) = .001$
$P_1(5) = 1.$	$P_1(11) = .05$	$P_1(17) = .001$
$P_1(6) = 1.$	$P_1(12) = 1.$	$P_1(18) = .001$

R_2 Matrix

	Pitch Emphasis	Thrust Emphasis
$R_2(1)$.01	.001
$R_2(2)$	10	100

R_1 Matrix

$R_1(1) = 10$	$R_1(7) = 10$	$R_1(13) = 10$
$R_1(2) = 0$	$R_1(8) = 10$	$R_1(14) = 10$
$R_1(3) = 0$	$R_1(9) = 10$	$R_1(15) = 0$
$R_1(4) = 0$	$R_1(10) = 0$	$R_1(16) = 0$
$R_1(5) = 0$	$R_1(11) = 0$	$R_1(17) = 0$
$R_1(6) = 0$	$R_1(12) = 10$	$R_1(18) = 0$

With this designation the controller is complete. The next specification needed is the Kalman filter-estimator. As in A-6.1 the four matrices required for this specification are P_0 , $\bar{x}_0(t)$, R and Q . Also as in A-6.1 $\bar{x}_0(t)$, the initial condition of the error state vector is zero or $\bar{x}_0(t) = \bar{0}$. The other three matrices are diagonal matrices with values as follows:

P_0 Matrix

$P_0(1) = .2$	$P_0(7) = .01$	$P_0(13) = .01$
$P_0(2) = .2$	$P_0(8) = 10.$	$P_0(14) = 10.$
$P_0(3) = .2$	$P_0(9) = 10.$	$P_0(15) = .01$
$P_0(4) = .2$	$P_0(10) = 100.$	$P_0(16) = .01$
$P_0(5) = .2$	$P_0(11) = 100.$	$P_0(17) = .001$
$P_0(6) = .2$	$P_0(12) = .01$	$P_0(18) = .001$

R Matrix

	Pitch Emphasis	Airspeed Emphasis
R(1)	.5	.5
R(2)	.1	.1
R(3)	.01	.1
R(4)	.01	1.

Q Matrix

Q(1) = 1.	Q(5) = .0003
Q(2) = .001	Q(6) = .0007
Q(3) = 1.	Q(7) = .003
Q(4) = 1.	

where the individual values of Q correspond with the following model noise sources:

- Q(1) → N_1 of Figure 55
- Q(2) → N_5 of Figure 7
- Q(3) → Wind Gust Effect on U
- Q(4) → Wind Gust Effect on W
- Q(5) → Wind Gust Effect on Q
- Q(6) → N_2 of Figure 6
- Q(7) → N_4 of Figure 7

With the above specification, the only process left to be defined is the decision process. This process involves three quantities, the thresholds, the payoff for lying within threshold,

and the payoff for lying outside threshold. In the definition of the longitudinal axis simulation of Chapter V, the payoff for lying within threshold was delineated. The payoff for lying outside threshold is given by Table 3 except that since no roll is available pitch and airspeed take on values 2 and 1 respectively. The thresholds are .01 radians for pitch angle and 1.5 ft/sec for airspeed. The airspeed threshold was increased over the full aircraft model airspeed threshold to reflect more emphasis on airspeed with only the two quantities, airspeed and pitch angle, considered.

The above discussion has provided the detail to allow both insight into proper value selection for other simulations and reconstruction of this simulation.

Vita

Major Eric K. Lindberg was born 18 July 1944 in Kearney, Nebraska. He graduated from Ravenna High School, Ravenna, Nebraska, in 1962. He then attended and graduated from the United States Air Force Academy in 1966 with a Bachelor of Science degree majoring in Engineering Sciences and Astronautics. Major Lindberg graduated from Pilot Training at Williams AFB, Arizona, in 1967 and held the position of copilot on a C-124 aircraft at Dover AFB, Delaware until 1969.

He was then transferred to Danang AB, RVN, and was aircraft commander in an HH-3E, Jolly Green, helicopter. From there he spent five months at Osan AB, Korea as an HH-3E aircraft commander. Major Lindberg was then transferred to Travis AFB, California, where he was an Instructor Pilot/Flight Examiner on the C-5A and aircraft simulator. From there Major Lindberg attended the Air Force Institute of Technology, Wright-Patterson AFB, Ohio, and was awarded a Master of Science degree with Distinction in Astronautical Guidance and Control. He continued at the Air Force Institute of Technology for the Doctoral course work until 1975. Upon completion of the course work he was stationed at the Air Force Flight Dynamics Laboratory, Flight Control Division, Wright-Patterson AFB, Ohio, as a Division Systems Analyst. In July of 1977 he transferred to the Air Force Wright Aeronautical Laboratory Staff as a Test Manager, and is presently in the Air Force Flight Dynamics Laboratory as Chief, Aerodynamics and Airframe Branch.

Major Lindberg was married in 1966 to Claire A. Campbell of Ada, Oklahoma, and has two children, Hans I, and Eric K.

UNCLASSIFIED

SECURITY CLASSIFICATION OF THIS PAGE (When Data Entered)

REPORT DOCUMENTATION PAGE		READ INSTRUCTIONS BEFORE COMPLETING FORM
1. REPORT NUMBER AFIT/DS/EE/78-1	2. GOVT ACCESSION NO.	3. RECIPIENT'S CATALOG NUMBER
4. TITLE (and Subtitle) AN ADAPTIVE CONTROLLER WHICH DISPLAYS HUMAN OPERATOR LIMITATIONS FOR A FIGHTER TYPE AIRCRAFT		5. TYPE OF REPORT & PERIOD COVERED D.S. DISSERTATION
		6. PERFORMING ORG. REPORT NUMBER
7. AUTHOR(s) ERIC K. LINDBERG		8. CONTRACT OR GRANT NUMBER(s)
9. PERFORMING ORGANIZATION NAME AND ADDRESS AFIT		10. PROGRAM ELEMENT, PROJECT, TASK AREA & WORK UNIT NUMBERS
11. CONTROLLING OFFICE NAME AND ADDRESS AFFDL		12. REPORT DATE NOVEMBER 1978
		13. NUMBER OF PAGES 298
		15. SECURITY CLASS. (of this report) UNCLASSIFIED
14. MONITORING AGENCY NAME & ADDRESS (if different from Controlling Office)		15a. DECLASSIFICATION/DOWNGRADING SCHEDULE
16. DISTRIBUTION STATEMENT (of this Report) Approved for public release; distribution unlimited.		
17. DISTRIBUTION STATEMENT (of the abstract entered in Block 20, if different from Report)		
18. SUPPLEMENTARY NOTES FEB 8 1979 APPROVED FOR PUBLIC RELEASE: IAW AFR 190-17 J. P. Hipps, Maj, USAF Director of Information		
19. KEY WORDS (Continue on reverse side if necessary and identify by block number) Human Operator, Adaptive Control, Pilot Modelling		
20. ABSTRACT (Continue on reverse side if necessary and identify by block number)		

UNCLASSIFIED

SECURITY CLASSIFICATION OF THIS PAGE(When Data Entered)

Abstract

→ A general adaptive controller which displays human operation limitations is developed for a fighter type aircraft flying a dynamic trajectory by using the total airframe-control system perturbation equations. The adaptive controller is implemented using a forced separation controller with limitations. The major limitations are that it cannot actively control or observe more than one channel at a time and that there is a time delay in information processing. A decision process is necessary to choose the current channel in real-time because of the limited attention and control assumed for the controller. This attention has ⁹two effects: specification of an observation matrix, and specification of a control matrix. This specification is made using a Bayesian decision process, from a choice of possible observations and controls, each choice emphasizing different aircraft states. The mathematical outcome is an adaptive forced separation controller which is flexible enough that it can be implemented on any aircraft control problem as long as the trajectory can be specified. The stability of the closed loop system employing such a controller is demonstrated on an example using the longitudinal axis of a fighter type aircraft. Using the entire aircraft model, a detailed cause/effect analysis of the model parameters is given allowing the reader insight into the general application of the model. → Analysis and synthesis techniques for the time varying aircraft model dynamics are demonstrated. The outcome is the evolution of a method for analyzing total aircraft/controller response to perturbations on a general trajectory.

UNCLASSIFIED

SECURITY CLASSIFICATION OF THIS PAGE(When Data Entered)